
Electronic Thesis and Dissertation Repository

8-8-2017 2:00 PM

On Honey Bee Colony Dynamics and Disease Transmission

Matthew I. Betti, *The University of Western Ontario*

Supervisor: Lindi Wahl, *The University of Western Ontario*

Co-Supervisor: Mair Zamir, *The University of Western Ontario*

A thesis submitted in partial fulfillment of the requirements for the Doctor of Philosophy degree
in Applied Mathematics

© Matthew I. Betti 2017

Follow this and additional works at: <https://ir.lib.uwo.ca/etd>



Part of the [Dynamic Systems Commons](#), [Ordinary Differential Equations and Applied Dynamics Commons](#), [Other Applied Mathematics Commons](#), [Other Ecology and Evolutionary Biology Commons](#), [Partial Differential Equations Commons](#), and the [Population Biology Commons](#)

Recommended Citation

Betti, Matthew I., "On Honey Bee Colony Dynamics and Disease Transmission" (2017). *Electronic Thesis and Dissertation Repository*. 4803.

<https://ir.lib.uwo.ca/etd/4803>

This Dissertation/Thesis is brought to you for free and open access by Scholarship@Western. It has been accepted for inclusion in Electronic Thesis and Dissertation Repository by an authorized administrator of Scholarship@Western. For more information, please contact wlsadmin@uwo.ca.

Abstract

The work herein falls under the umbrella of mathematical modeling of disease transmission. The majority of this document focuses on the extent to which infection undermines the strength of a honey bee colony. These studies extend from simple mass-action ordinary differential equations models, to continuous age-structured partial differential equation models and finally a detailed agent-based model which accounts for vector transmission of infection between bees as well as a host of other influences and stressors on honey bee colony dynamics. These models offer a series of predictions relevant to the fate of honey bee colonies in the presence of disease and the nonlinear effects of disease, seasonality and the complicated dynamics of honey bee colonies. We are also able to extract from these models metrics that preempt colony failure. The analysis of disease dynamics in age-structured honey bee colony models required the study of next generation operators (NGO) and the basic reproduction number, R_0 , for partial differential equations. This led us to the development of a coherent path from the NGO to its discrete compartmental counterpart, the next generation matrix (NGM) as well as the derivation of new closed-form formulae for the NGO for specific classes of disease models.

Keywords: Honey Bee Dynamics, Colony Collapse, Basic Reproduction Number, Next Generation Operator

Co-Authorship Statement

The thesis herein has been written by Matthew Ilario Betti under the supervision of Dr. Lindi M. Wahl and Dr. Mair Zamir. Chapter 2 has been published in PLOS ONE with co-authors L.M. Wahl and M. Zamir. Chapter 3 is in press, to be published in Bulletin of Mathematical Biology with co-authors L.M. Wahl and M. Zamir. Chapter 4 has been published in Royal Society Open Science with co-authors L.M. Wahl and M. Zamir. Chapter 5 has been published in the journal Insects with co-authors J. LeClair, L.M. Wahl and M. Zamir. Chapter 6 is under review for publication in SIAM Journal of Applied Mathematics with co-authors J. LeClair, L.M. Wahl and M. Zamir. The aforementioned chapters contain models and analysis developed and carried out by M.I. Betti. The model and corresponding simulation package in Chapter 5 was co-developed with J. LeClair. The limit arguments in Chapter 6.2.1 were carried out by L.M. Wahl. All authors contributed to the writing of the respective manuscripts.

Acknowledgements

I first and foremost must thank my incredible supervisors Lindi Wahl and Mair Zamir for their continued support, insights and infinite patience. They have allowed me the freedom to travel down paths of research which did nothing more than piqued my curiosity and have been supportive the entire way. None of this would be possible without them. There are not enough words in enough languages to truly describe their influence.

I would also like to thank the Applied Mathematics department at Western University for four years of invaluable instruction, guidance and insightful discussions. In particular, I would like to thank David Dick and Josh LeClair for many thoughtful discussions.

Finally, I would like to thank Geoff Wild whose course on mathematical biology was the catalyst for everything herein.

For my parents, Elvi and Silena Betti

Handle a book as a bee does a flower, extract its sweetness but do not damage it.
- John Muir

*OH, NO! NOT THE BEES! NOT THE BEES! AAAAAHHHHH! OH, THEY'RE IN MY EYES!
MY EYES! AAAAHHHHH! AAAAAGGHHH!*

- Nicolas Cage

Contents

Co-Authorship Statement	ii
Acknowledgements	iii
Abstract	vi
List of Figures	ix
List of Tables	xi
List of Appendices	xii
1 Introduction	1
1.1 Honey Bees	1
1.1.1 Honey Bee Colony Dynamics	2
1.1.2 Honey Bee Diseases	3
1.1.3 Mathematical Models of Honey Bees	4
1.2 Basic Reproduction Number	7
2 Effects of Infection on Honey Bee Population Dynamics: A Model	22
2.1 Introduction	22
2.2 Background	24
2.2.1 Normal Demographics of a Honey Bee Colony	24
2.2.2 Nosema Infection	24
2.3 Mathematical Model	25
2.3.1 Governing Equations: Active Season	25
2.3.2 Governing Equations: Winter	27
2.3.3 Parameter Values	28
2.4 Results	29
2.5 Discussions and Conclusions	41
3 Honey Bee Reproduction Number	46
3.1 Introduction	46
3.2 Model	48
3.3 Results	51
3.3.1 Existence	51
3.3.2 Disease-free Equilibria (DFE)	53

3.3.3	Stability of DFE	56
3.3.4	Basic Reproduction Number R_0	59
3.4	Discussion	63
3.5	Appendix	65
4	Age Structure in Honey Bee Colonies	73
4.1	Introduction	73
4.2	Model	74
4.2.1	Age Structure	75
4.2.2	Winter	77
4.3	Results	79
4.4	Discussion	85
5	Bee++	90
5.1	Introduction	90
5.2	Model	91
5.2.1	Bees	92
5.2.2	Food Stores	97
5.2.3	Environment	98
5.2.4	Pathogens	99
5.3	Results	99
5.4	Discussion	114
6	The Next Generation Operator	125
6.1	Introduction	125
6.2	The limit of the Next Generation Matrix	127
6.2.1	Separable Interaction Term	128
6.2.2	Non-separable Interaction Term	131
6.3	Reaction-Diffusion System	131
6.3.1	Inversion Formula: the expected infectious occupation time	134
6.3.2	Conjecture	136
6.4	Lévy Flight	136
6.5	Approximating the Spectral Radius of the Next Generation Operator	137
6.6	Discussion	138
7	Discussion & Conclusions	147
A	Chapter 4 Supplementary Material	152
	Curriculum Vitae	166

List of Figures

1.1	The hierarchy of a colony	2
1.2	Waggle dance	3
1.3	Varroa mites	4
1.4	Basic Reproduction Number	7
1.5	Infection interaction	9
2.1	Compartmental diagram of model	27
2.2	Baseline demographic dynamics of the honey bee colony in the absence of disease.	30
2.3	Scenario 1	31
2.4	Scenario 2	32
2.5	Scenario 3	33
2.6	Average Age of Recruitment	34
2.7	Disease-induced death vs AARF	35
2.8	Scenario 4	36
2.9	The expected size of the bee population at the end of winter as influenced by the severity of the disease	37
2.10	The expected size of the bee population at the end of winter as influenced by the time interval between the onset of infection and the beginning of winter	38
2.11	Effects of environmental hazard – equal death rate	39
2.12	Effects of environmental hazard – equal average lifespan	40
3.1	The disease-free equilibrium distributions H_S^* and F_S^*	54
3.2	Total infected population after 100 days vs. R_0	62
3.3	Age-dependent R_0 vs age-independent R_0	63
4.1	Death rate distribution which match experimental results	78
4.2	Example death rates	79
4.3	Time course of total bee population in a disease-free colony.	81
4.4	Effect of age distribution on the dynamics of disease within the bee colony.	81
4.5	Time course of a diseased bee population over four years.	82
4.6	Sensitivity of honey bee populations to seasonality and disease onset	83
4.7	Most vulnerable times for the onset of disease.	84
5.1	Flow diagram of the main program loop.	93
5.2	Flow diagram of honey bee life	101
5.3	Daily temperature highs for London, Ontario, Canada	102

5.4	Sensitivity analysis; total colony size	105
5.5	Sensitivity analysis; brood size	106
5.6	Sensitivity analysis; AARF	107
5.7	Total bee population from early spring to late summer	108
5.8	Total brood population from early spring to late summer	109
5.9	Average Age of Recruitment in summer	110
5.10	Average Age of Recruitment in summer	111
5.11	Intoxication of foragers and its effect on navigation over time.	112
5.12	Map of spatial distribution of dead bees	113
6.1	R_0 in real space and Fourier space	140
6.2	Comparison of operator and NGM	141
6.3	Test functions illustrating inverse operator	142
6.4	Test functions illustrating conjecture	143
A.1	Time course of total bee population in a disease-free colony	153
A.2	Age distribution of a healthy colony at equilibrium during the active season	154
A.3	Population dynamics with increasing effects of age-dependent parameters	155
A.4	Sensitivity analysis: example Gaussian death rate	156
A.5	Sensitivity analysis: age distribution	157
A.6	Sensitivity analysis: time course of uninfected colony	158
A.7	Sensitivity analysis: time course of infected colony	159
A.8	Sensitivity analysis: time course of infected population	160
A.9	Sensitivity analysis: example linear death rate	161
A.10	Sensitivity analysis: equilibrium age distribution	162
A.11	Sensitivity analysis: time course of uninfected colony	163
A.12	Sensitivity analysis: time course of infected colony	164

List of Tables

2.1	Parameter values and references.	29
2.2	Tabulated results from the model scenarios and experimental data	41
3.1	Parameter values and source references.	55
4.1	Comparison of experimental results with model results	80
5.1	Parameter values and source references.	103
5.2	Parameters used in sensitivity analysis	104
A.1	Parameter values and source references.	152

List of Appendices

Appendix A Chapter 4 Supplementary Material	152
---	-----

Chapter 1

Introduction

1.1 Honey Bees

True honey bees, distinguished from other bees by their ability to produce honey, are any of the seven species within the genus *Apis* [45]. The most common honey bee is the Western, or European, honey bee, *Apis mellifera* [45].

Honey and wax from honey bees have been harvested by humans for at least 8,000 years [28]. There is also evidence that honey from bees provided a nutritionally dense [119] supplement for early members of the genus *Homo* [29]. While for much of human history honey bees have been cultivated and farmed for their honey and wax production [28], more recently honey bees have been used largely for their ability to pollinate commercial crops [79]. Nearly 80 years ago, the USDA recognized the need for an increase in pollinators to keep up with the increasing production of insect pollinated crops [129]. From this observation came research leading to honey bees bred specifically as pollinators for commercial crops [129].

The economic impact of insect pollinators in the U.S. in 2009 is estimated to be \$15 billion USD, with \$11.6 billion attributed to honey bees. It is worthwhile to note that these figures do not include the value of honey and wax produced by the honey bee colonies.

Due to their economic [24, 121] and ecological [35] importance, the fact that honey bee losses are increasing on a global scale [10] is of great concern. In North America alone, honey bee populations had been declining steadily since the 1960's [44].

While there are many wild pollinators who aid in the reproductive success of plants (e.g. bats, butterflies, birds, beetles, etc.) [31], it is estimated that bees pollinate roughly 70% of global crops [31, 110]. In the U.S., honey bees are estimated to pollinate 15 – 30% of commercial crops [77]. Again, the pollination of these crops is often enhanced by visitation from local, wild insect populations [52] but managed honey bee colonies remain the most economically valuable pollinator for monoculture crops [78]. While there are many pollinators who are better suited to specific crops [52, 71, 79], there are certain fruit, nut and seed plants which see a 90% decrease in crop production without honey bee pollination [121].

In [52], it is observed that managed honey bee are responsible for the majority of pollen deposition in plants yet, counter-intuitively, wild insect pollinators create higher fruit yield in the studied crops. Despite this, honey bees continue to be the most widely used commercial pollinator due to their economic viability as well as their ability to produce honey, wax, and

offer pollination services [78]. Moreover, Gaines-Day and Gratton show that in low woodland areas, there is a positive correlation between honey bee presence and crop yield [51]. In any case, a synergistic effect has been observed on crop yield when both honey bees and wild pollinators are present [21].

Of more recent concern, is the mysterious disappearance of colonies due to so-called Colony Collapse Disorder (CCD) [139]. The disorder is characterized by three symptoms: (1) the presence of brood and excessive food stores, but no adult bees, (2) the lack of dead worker bees in or surrounding the hive, and (3) delayed invasion of the abandoned hive (i.e. scavengers do not immediately pillage the hive) [132].

The current consensus is that colony collapse disorder, and in general the continual increase in number of lost colonies [80], is due to a number of factors including disease and parasites [41, 67, 101, 125], predation from competing hives [111], and environmental hazards such as pesticide exposure [64] and lack of biodiversity of plants in the local ecosystem [55]. Recently, studies have been more focused on the interactions between different combinations of stressors and their aggregate effects on honey bee colony dynamics [1, 7, 55, 95, 120, 134].

1.1.1 Honey Bee Colony Dynamics

The honey bee is a highly eusocial insect [91]. They live in female-dominated colonies [91], and are divided into castes based on sex, morphology and age [113, 116]. The major castes of honey bees are: queen, worker and drone [140]. Within the worker caste, the bees are further divided into juveniles, hive bees, and foragers [140]. Sex differentiates the queen and workers from the drones [140], morphology differentiates the queen bee from the worker bees [140], and age differentiates the subtypes of workers [108].

At the center of a honey bee colony is the queen. She is responsible for all reproduction within a hive [91]. Drones are born of unfertilized eggs, making them genetic clones of the queen [54], and workers and new queens are born of fertilized eggs [140]. The sole purpose of drones in honey bee colonies is to leave the hive to fertilize virgin queens [91].

Even though queens and workers originate from the same eggs, the care they received during their larval stages creates bees of differing morphology [116]. Worker bees are fed bee bread (a concoction of pollen and honey [133]) as larvae [140] whereas those destined to become queens are fed copious amounts of so-called royal jelly (a glandular secretion produced by worker bees) [85]. This difference in diet leads to worker bees being born functionally sterile (although a small percentage of workers can and will lay drone eggs) and smaller than a queen [46, 96, 115, 117].

The worker caste is indispensable to a functioning honey bee colony. From emergence as adults until three days of age, the workers are known as juveniles and spend most of their time eating and cleaning cells within the hive [113]. After this phase, they continue cleaning cells but take on the additional responsibility of caring for the brood [113]. After approximately

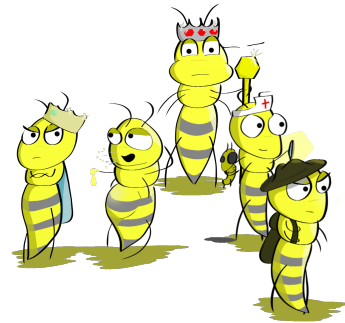


Figure 1.1: A honey bee colony functions through caste divisions based on both genetics and age.

sixteen days, the bees will move on to other hive duties (such as maintenance, security, repairs etc.) or be recruited to foraging duties [140].

Hive bees are recruited to foraging duties through the waggle dance [140]. When foragers return to the hive with food, they will pass on information such as quality of food source, distance from the hive, and direction of the source to the hive bees who will then be recruited to join the foragers [107]. There are a number of conditions surrounding this recruitment such as the age of the bee [47] (regulated by Juvenile Hormone III [108]) or the needs of the hive [69]. In order to help control the forager population within a hive, the foragers produce a pheromone ethyl oleate, which inhibits the desire to begin foraging [81]. This latter process is known as ‘social inhibition’ and reduces recruitment when the foraging population is high [81].

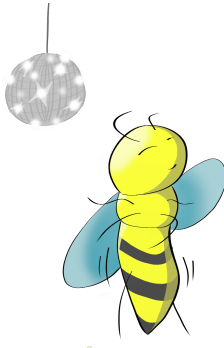


Figure 1.2: Foragers will dance upon returning to the hive if they have found a viable food source. The dance encourages other workers to begin foraging duties, as well as offers directions to the food source in question.

The foragers are responsible for exploring the nearby environment and extracting pollen and nectar from nearby flowers [140]. The flight range of a honey bee is roughly three kilometers, but has been observed up to six kilometers [43]. The nectar brought back to the hive is stored within particular cells – specifically made to hold nectar – of the hive and the water content is evaporated out through the flapping of the bees’ wings [8], producing honey.

These dynamics are confined to the spring and summer, as honey bees are dormant in the winter. As temperatures drop and food becomes scarce, honey bees halt all foraging and return to the hive [73]. Within the hive, given they are warm enough, honey bees can survive up to 6 months [116]. The egg-laying rate of the queen is also greatly reduced in the winter months and, in harsh climates, ceases completely [73]. The harsh conditions in the winter, including the lack of new bees to replace the older members of the hive and the lack of incoming food, cause considerable stress on the hive.

Honey bees are also susceptible to certain parasites, which have been found to play a role in the failure of colonies and high honey bee losses [139]. There are three major pathogens that affect honey bee colonies: *Varroa destructor*, *Nosema ceranae*, and *Nosema apis*.

1.1.2 Honey Bee Diseases

Nosema ceranae is a microsporidian introduced into the European honey bee, *Apis mellifera*, from Asia where it is a common parasite of the Asian honey bee, *Apis ceranae*. Infections by *Nosema ceranae* are thought to contribute to colony collapse [66, 67]. *Nosema ceranae* is transmitted via fecal-oral. The two major routes of transmission are through susceptible bees eating food contaminated by infected bees, or through bees ridding the hive of infected fecal matter [26, 50]. There is evidence that *N. ceranae* can also be transmitted through oral-oral transmission during feeding [120]. In 2013, it was observed that colonies that suffer from *Nosema* infection also exhibit many of the symptoms of colony collapse [122].

Nosema apis is a relative of *N. ceranae*, and is a common parasite of the European honey

bee [42]. A comparative study between *N. apis* and *N. ceranae* showed that neither has a competitive advantage at the level of individual bees [49], but *N. apis* has been observed to be less virulent than *N. ceranae* [66]. *Nosema apis* has also been observed to be less well adapted to high temperatures than its Asian counterpart [48, 90]. Furthermore, the severity of *N. ceranae* may be linked to increased energy consumption in honey bees [89]. Complicating the issue is the fact that the treatment for *N. apis* infection may suppress a bee's immune response and allows *N. ceranae* to thrive [68].

The final major parasite of honey bee colonies is *Varroa destructor*. These mites were first found in 1904, and spread globally [6]. The parasite is found in all honey bee populations except for those in Australia [5]. *Varroa* is a danger to honey bees as it acts as a vector for many viruses, including Israeli Acute Paralysis Virus [36] and Deformed Wing Virus [53]. *Varroa* mites enter brood cells before they are capped, and reproduce alongside the bee larvae [86]. A female *varroa* mite will lay up to six eggs (the majority of which are female [125]) which will then hatch and mate within the sealed brood cell and emerge with the bee [86, 87]. The female mites will then attach themselves to nearby bees and feed off of the bee for four to five days [114], between reproductive cycles [58, 86]. The mites will then insert themselves into a brood cell [114]. In addition to the viruses which are vectored by the mites, the mites themselves create wounds within the exoskeleton of the bees, which in turn increase mortality [58]. The mites themselves also lead to lower body weight of adult bees [18]. These conditions lead to reduced productivity [92] and longevity [58] at the colony level.



1.1.3 Mathematical Models of Honey Bees

Due to the complexity of honey bee colony dynamics – especially in the context of changing environments, pathogens, and pesticides – mathematical models have become an indispensable tool for exploring the underlying mechanics of these interactions. They are also powerful predictive tools that can aid in best practice decisions for colony management and protection efforts.

Early mathematical models focusing on honey bees involved broad population dynamics. Rowland and McLellan used a simple set of differential equations to model brood production in honey bee colonies [112]. Harris' model took into account only classes of adults, pupae, larvae, and eggs and was based on empirical data [61]. The foragers in this model were not distinguished from the hive bees [61]. Omholt developed a simple ordinary differential equation (ODE) model for the population size of a honey bee colony, taking into account some of the intracolony mechanics [97]. Not long after that, DeGrandi-Hoffman et al. built one of the first computer simulations for honey bee colony dynamics [32], that was able to simulate classes of drones, workers, brood and queen in a healthy colony. Other early models, such as that by Camazine and Sneyd, investigated the decision-making processes of the foragers when searching for nectar [25].

Figure 1.3: *Varroa* mites attach themselves to bees and feed off their blood for 4-5 days before inserting themselves into brood cells for reproduction.

As the global decline in honey bee populations gained notoriety in the late 20th and early 21st century [4, 16, 62, 138], new mathematical models were developed to aid in explaining these dwindling populations and to develop strategies counter-acting the observed declines. Sumpter and Martin developed models to investigate the interactions between honey bee colonies and the parasite *V. destructor*, as well as the role this parasite – and the viruses that it vectored – played in the collapse of honey bee colonies [88, 125]. In 2011, Khoury et al. developed and analyzed a simple compartmental ODE model to quantitatively predict the different sub-populations of workers in a honey bee colony: nursing bees and foragers [76]. This model was extended by the same authors in 2014 to include food stores and brood dynamics [75].

Khoury et al. developed a quantitative model for honey bee colony dynamics which focuses on the worker bees: the driving force behind a honey bee colony [76]. The ordinary differential equation model itself consists of two compartments: the hive bees (those bees that perform duties around the hive, mainly maintaining the brood), and the foragers (those that leave the hive to gather resources such as nectar and pollen). This model also quantifies the main interactions between the hive bees and foragers, mainly the effect of social inhibition [76].

A number of key insights came from the analysis of the model by Khoury et al. The authors were able to successfully determine a steady-state equilibrium of the model, as well as stability criteria for this equilibrium [76]. Also extracted from the model is a critical forager death rate above which a colony cannot survive. This insight provides evidence that foragers are integral to the success of a hive, even in the presence of sufficient food (one of the assumptions of the model) [76]. The model also proves its robustness in that, despite being a very simple representation of honey bee colony dynamics, model predictions agree well with experimental data for the Average Age of Onset of Foraging (AAOF) [76].

The same authors later extended this model to include brood dynamics and explicit food stores [75]. The extended model (building on the last) allows brood survival and recruitment to be explicitly dependent on food stores. Again, the authors derive non-zero equilibria of the model and determine the conditions for stability. Numerical analysis of the model shows the effects of a sudden increase in forager death on the colony dynamics [75]. These results suggest potential reasons for one of the symptoms of colony collapse: namely that under certain conditions colonies may go extinct while leaving behind residual food stores [75]. The authors also compare results of the model to experimental data in [60] and find good agreement with medium to large colonies [75].

In 2014, I extended the model of Khoury et al. to include the effects of infection [14]. The proposed model continued to account for basic honey bee colony dynamics (such as recruitment based on food and regulatory mechanisms, brood survival explicitly dependent on food and number of hive bees, etc.) but also included the dynamics of infection motivated by the prevalence of *N. ceranae*. The novel aspect of this model was the introduction of seasonality into the mathematical model, which allowed analysis of the interplay between infection and wintering [14]. This model is described in depth in Chapter 2, and led to seasonality being incorporated into later models.

Concurrently, many other mathematical treatments of honey bee colonies were developed. One such model, developed in 2013 by Ratti et al. and later extended in 2015 by the same group, focused on honey bee dynamics and the interactions with the parasite *V. destructor* [105, 106] that can transmit Acute Paralysis Virus (APV).

The first paper [105] introduces the four-dimensional system of ordinary differential equations which account for healthy bees, infected bees, virus-free mites, and mites who are carriers of APV. Most notably, the authors develop threshold conditions which determine the survival of a colony infested with mites [105].

The second study in this series builds upon the first and investigates the long-term behaviour of a colony that is infested with varroa mites and treated with a varroacide [106]. The effects of over-wintering are also considered, and the time to collapse is estimated based on the initial infection [106].

Other mathematical models were developed at the time that were not related to infection or pesticide exposure. The focus of these models is to generate more realistic dynamics of wild and farmed honey bee colonies. A model developed by Pereira et al. in 2016 [99] was used to show the effects of artificial feeding on honey bee colony dynamics. The model is an extension of that developed in [75], and is consistent with both the results in [75] and validated against experimental data from the literature [99].

A model developed by Dennis & Kemp describes the interplay between a strong Allee effect – a critical population size, below which the population growth rate is negative [27]– and environmental hazards on honey bee colony dynamics [34]. The results of this study show that there is a minimum critical population size as well as a stable population size in the neighbourhood of the carrying capacity of the hive [34]. One major result from this paper is the observation that environmental stresses can intensify the Allee effect leading to an increase in both the stable population size as well as the critical minimum population size, thus creating an environment in which a honey bee colony cannot survive [34].

In 2016, we extended our generalized disease model to include the age-structure of honey bee colonies [13, 15]. The worker castes (Juvenile, Nurse, Maintenance, and Forager) are divided mainly based on age [108]. Aside from determining the duties of a worker bee, the age polyethism inherent in the hive contributes to two major factors relating to honey bee colony dynamics: the death of honey bees and the recruitment of honey bees away from nursing duties and to foraging duties [108]. In [15], we develop a threshold condition (particularly the basic reproduction number, R_0) for an epidemic outbreak in a honey bee colony. We also show that in the absence of a disease, our model predicts an asymptotically stable colony, given sufficient nurse bees to seed the population [15]. A secondary study shows the long-term effects of seasonality and infection on a honey bee colony [13]. The major results of this study are the peaks of infection seen in early spring, as well as the ability of the model to capture, and offer an explanation for, ‘spring dwindle’ [141], a phenomenon in which a colony suffers major losses in early spring. The model also predicts times of disease onset during the year which would result in quantifiably significant long-term colony losses [13]. This model and its implications are discussed in Chapters 3 & 4.

While all the models described above focus on particular aspects of colony dynamics, great strides were also made to develop computational models that capture realistic colony dynamics in heterogeneous environments. Of note is the simulation package BEEHAVE developed by Becher et al. which uses an Agent-Based Model (ABM) to simulate the interactions between *V. destructor* and a honey bee colony in an environment that incorporates both spatial and temperature heterogeneity [9]. Each agent within BEEHAVE represents a group of 100 bees [9]. The model is implemented in NetLogo, and shows good agreement with experimental results from the literature [9]. The simulation package was used by Thorbek et al. to explore

the effects of pesticide exposure on a honey bee colony [128] in the context of protection goals set out by the European Food Safety Authority (EFSA) [128]. In this study, pesticide exposure is simulated via an increase in forager mortality [128].

Seeing a need for a comprehensive, robust simulation package for honey bee colony dynamics, we set out to develop Bee++ [12]. This model is implemented in C++, is object-oriented in nature, and freely available to use and modify. One of the novel features of this ABM is its ability to model and track pesticide exposure for individual bees within a colony. Each bee is able to ingest and metabolize toxins according to mechanisms derived from observations in the primary literature such as [123, 124]. Known interactions between toxins [72] are also accounted for in Bee++. The model, its components and implementation are discussed in Chapter 5.

1.2 Basic Reproduction Number

Mathematical treatments of disease progression in human populations has its beginnings in the latter half of the 18th century as Bernoulli used mathematics to model the effectiveness of inoculation against smallpox [11]. It was another 150 years before Hamer developed a discrete epidemiological model for measles epidemics [59]. This is the first evidence of the use of mass action – the idea that the number of new infections is dependent on the product of infected individuals and susceptible individuals [65]. Five years later, the first vector-borne infection model was developed for malaria in which disease transmission between humans occurred via mosquitoes [109]. Throughout the 20th century and into the present, the body of literature on epidemiological modeling has continued to grow steadily.

Central to these concepts are threshold values for epidemic outbreaks. An epidemic is said to occur when an infected population, $I(t)$, grows from its initial condition [19]. In other words, an epidemic occurs when $I'(t) \Big|_{t=t_0} > 0$. In 1927, Kermack and McKendrick developed the first epidemic model which could predict an epidemic outbreak via a threshold value made up of model parameters, and the number of susceptible individuals in a population [74].

Parallel studies in demography around the turn of the 20th century introduced the notion of the net (or later: basic) reproduction rate (number). This is said to be the number of new individuals created by a single individual in a population [30]. The notion was first introduced by Böckh in 1886 during his tenure as the head of the Statistical Office of Berlin [17, 40]. Böckh determined that there were 2.172 new females produced for each woman in the population [40]. A general formula (without a symbol or name) was first given by Sharpe and Lotka in 1911 [118]. The first evidence for the notation R_0 and the name ‘net reproduction rate’ seem to be given by Lotka,



Figure 1.4: The basic reproduction number, R_0 , determines how many new infections a single infected individual creates over its infected lifetime; in this case: $R_0 = 2$.

in French (la reproductivité nette), in 1939 [83].

The modern usage of R_0 – the number of secondary infections created by a single infected individual over its lifetime – was coined in 1952 by MacDonald as he analyzed malaria outbreaks in the tropics [84]. In this context, R_0 can predict an epidemic outbreak as well as allow for quantitative predictions on effective control measures [63, 94].

The next generation matrix (NGM) is a technique which offers both an intuitive biological basis and algorithmic mathematical framework for deriving R_0 for compartmental disease models [38, 130]. The method of the next generation matrix applies to a system of N ordinary differential equations of which M define infected classes. The equations for the infected classes are then linearized about the disease-free equilibrium and divided into two matrix components: the terms which define the influx into the infected classes from uninfected classes are put into a matrix F . The remaining terms (all other influx terms, say, between infected classes and outflux from each class) are used to generate a separate matrix, $-V$. The next generation matrix is then given by $NGM = FV^{-1}$. We offer the following clarifying example¹ of this process.

A Clarifying Example

Consider a standard SEIR model in which susceptible members, S , of a population become exposed² to an infection, E , who after a period of time then become infectious, I , and finally either die or recover from the disease and join the removed class, R . Exposed in this sense means that the individual has the disease, but is not contagious. A more apt name for this class would be incubator (but I is already being used, alas...). This situation is modeled by the system

$$\frac{dS}{dt} = B - \beta SI - \mu S \quad (1.1)$$

$$\frac{dE}{dt} = \beta SI - \kappa E - \mu E \quad (1.2)$$

$$\frac{dI}{dt} = p\kappa E - (d + \mu)I \quad (1.3)$$

$$\frac{dR}{dt} = (1 - p)\kappa E + dI + \mu(S + E + I) \quad (1.4)$$

where B is a constant birth rate, μ is a natural death rate of the population, β is the contact rate of individuals, $1/\kappa$ is the average period of incubation before the individual either becomes infectious or clears the infection, p is the probability the individual becomes infectious, and d is the death rate of an infectious individual due to disease.

The disease-free equilibrium, $(S, E, I, R) = (S^*, 0, 0, 0)$, is found using the equation

$$\frac{dS}{dt} = 0. \quad (1.5)$$

The linearized equations for the infected classes are then written as

$$\frac{dE}{dt} = \beta S^* I - (\kappa + \mu)E \quad (1.6)$$

$$\frac{dI}{dt} = p\kappa E - (d + \mu)I. \quad (1.7)$$

¹This model is based on those appearing in [3, 131].

²Exposed in the sense that the disease is incubating and non-infectious

From these equations we can generate the two necessary matrices F and $-V$. The only influx into the infected classes from non-infected classes is the term $\beta S^* I$. Therefore,

$$F = \begin{bmatrix} 0 & \beta S^* \\ 0 & 0 \end{bmatrix}. \quad (1.8)$$

The matrix $-V$ consists of all other terms in the equations for the infected classes. Note that the negative sign in front of V causes a sign change in all the terms (i.e. outflux is positive). The matrix $-V$ for this example is

$$-V = \begin{bmatrix} \kappa + \mu & 0 \\ -p\kappa & d + \mu \end{bmatrix}. \quad (1.9)$$

The next generation matrix is then given as

$$FV^{-1} = \begin{bmatrix} 0 & \beta S^* \\ 0 & 0 \end{bmatrix} \begin{bmatrix} (\kappa + \mu)^{-1} & 0 \\ \frac{p\kappa}{(\kappa + \mu)(d + \mu)} & (d + \mu)^{-1} \end{bmatrix} \quad (1.10)$$

$$= \begin{bmatrix} \frac{\beta S^* p\kappa}{(\kappa + \mu)(d + \mu)} & \frac{\beta S^*}{d + \mu} \\ 0 & 0 \end{bmatrix}. \quad (1.11)$$

As stated above, the primary function of the next generation matrix is to provide the basic reproduction number for a population model [63]. The basic reproduction number is given by the largest eigenvalue of the NGM, $R_0 = \rho(FV^{-1})$ [130]. In the above example, we find that

$$R_0 = \frac{\beta S^* p\kappa}{(\kappa + \mu)(d + \mu)}.$$

The number of studies that rely on this method (see [63] for review) for stability analysis of epidemic models substantiate the importance of the NGM.

In 2009, Diekmann et al. developed a method for deriving the NGM directly from model parameters in an intuitive, biologically relevant way [37]. This contribution to the scientific literature also aims to validate different definitions of the NGM namely, the decomposition described above, and the original formulation developed by Diekmann in 1990 [39]. A discrepancy often arises because the NGM can be constructed so that an infection moving from, say, a latent phase to infectious phase is considered a “new infection” [37]. This obviously can lead to discrepancies with the more biologically relevant formulations and definitions. Therefore, Diekmann et al. consolidate the approaches and prove conditions under which R_0 approximations are the same.

As biological processes are often multi-layered and complex, the systems which model them are often highly nonlinear and as a consequence, using



Figure 1.5: The term β appearing in equations (1.1) and (1.2) (and later equation (1.12)) determines the rate at which infectious individuals interact with susceptible individuals

systems of ordinary differential equations is often desired. The theory of ordinary differential systems and dynamical systems is rich with tools for approximating and analyzing nonlinear systems [102–104, 126]. Population structures, when using ODE models are often broken into discrete classes or compartments. Often times, a continuum is a more natural structure for a population model. For example, spatial spread and migration are easily modeled by a second and first derivative respectively [93]; nonlocal infection in either space and/or time can be modeled by a convolution [137]; and a Lévy flight [33] can be modeled by a fractional derivative.

Such models – whether partial differential equations, integro-differential equations, or both – are infinite dimensional and the theory of the framework provided by the next generation matrix does not directly apply when attempting to find the basic reproduction number, R_0 , for these systems. Instead a continuous operator is required.

Such an operator was first proposed in 1987 by Greenhalgh [56, 57]. Greenhalgh proposed an integral operator and conjectured that its spectral radius would act as a threshold condition for stability for an infinite-dimensional population model [56]. This result was then confirmed by Inaba two years later [70]. Contemporaneously, Diekmann defined the next generation operator (NGO) [39] for populations on a continuum.

Brauer also proposed a method for finding both a next generation operator and basic reproduction number for continuous age-structured models [20]. We may extend β in equations (1.1) and (1.2) to a continuous age structure. One susceptible of age a may then be infected by an infected individual of age a' at rate $\beta(a, a')$. Accounting for infected individuals of all possible ages leads to the interaction terms

$$F = S(a) \int_0^\infty \beta(a, a') I(a') da' \quad (1.12)$$

For a separable interaction term – one of the form

$$F = S(a, t) \int_0^\infty \beta(a, a') I(a') da' \quad (1.13)$$

$$= S(a, t) \alpha(a) \int_0^\infty \gamma(a') I(a') da' \quad (1.14)$$

– Brauer is able to derive an expression for the basic reproduction number explicitly [20]. For a general interaction term, the same methods allow for the construction of a next generation operator [20]. However, this method does not use the FV^{-1} factorization commonly associated with the equivalent discretized, compartmental model.

In 2009, Thieme proved that R_0 is the spectral radius of the next generation operator FB^{-1} for certain classes of infinite dimensional systems (e.g. systems of partial differential equations) [127]. The operators Thieme defines are analogous to F and $-V$ in the case of the next generation matrix for finite dimensional compartmental models. Another monumental conclusion in this work is Thieme’s result on the difference between the spectral radius and the growth parameter. Thieme shows that in infinite dimensional models, the exponential growth parameter of infected classes and the spectral radius of the next generation operator will have the same threshold characteristics, but may be quantitatively different [127].

Thieme’s work was extended by Wang and Zhao in 2012 to include reaction-diffusion models [136]. Aside from proving that the spectral radius of the next generation operator FB^{-1} is

indeed R_0 for reaction-diffusion systems, they offer an illustrative example for computing R_0 for an SEIR model with diffusion [136].

Based on this previous work, the operator factorization for the next generation operator is guaranteed to exist and provide the basic reproduction number for specific classes of infinite-dimensional systems [127, 136]. The importance of this cannot be understated as infinite-dimensional systems – especially reaction-diffusion systems – are ubiquitous in mathematical biology. This is ratified by the fact that such systems are covered in many introductory texts in mathematical biology [2, 22, 23, 82, 93, 98] (see [100, 135] for review). Yet, a closed-form next generation operator has yet to be determined.

While clearly analogs of one another, a direct connection between the NGM and NGO has remained elusive. Many formulations of the NGO are constructed ‘intuitively’, using the idea that the operator should provide the number of secondary infections created by one infected individual in its lifetime [38], or by developing an operator with the necessary threshold properties [127]. In Chapter 6, we discuss this connection and show that the NGO can be recovered as the limit of the NGM. Furthermore, we use this technique to find a closed-form operator for the NGO for a simple reaction-diffusion system and offer a conjecture which can extend this operator to a broader class of models.

Bibliography

- [1] ALAUX, C., BRUNET, J.-L., DUSSAUBAT, C., MONDET, F., TCHAMITCHAN, S., COUSIN, M., BRILLARD, J., BALDY, A., BELZUNCES, L. P., AND LE CONTE, Y. Interactions between *Nosema* microspores and a neonicotinoid weaken honeybees (*Apis mellifera*). *Environmental microbiology* 12, 3 (2010), 774–782.
- [2] ALLEN, L. J. *Introduction to mathematical biology*. Pearson/Prentice Hall, 2007.
- [3] ALLEN, L. J., AND VAN DEN DRIESSCHE, P. The basic reproduction number in some discrete-time epidemic models. *Journal of Difference Equations and Applications* 14, 10-11 (2008), 1127–1147.
- [4] ALLEN-WARDELL, G., BERNHARDT, P., BITNER, R., BURQUEZ, A., BUCHMANN, S., CANE, J., COX, P. A., DALTON, V., FEINSINGER, P., INGRAM, M., ET AL. The potential consequences of pollinator declines on the conservation of biodiversity and stability of food crop yields. *Conservation Biology* (1998), 8–17.
- [5] ANDERSON, D., AND EAST, I. J. The latest buzz about colony collapse disorder. *Science* 319, 5864 (2008), 724–725.
- [6] ANDERSON, D., AND TRUEMAN, J. *Varroa jacobsoni* (Acari: Varroidae) is more than one species. *Experimental and Applied Acarology* 24, 3 (2000), 165–189.
- [7] AUFAUVRE, J., BIRON, D. G., VIDAU, C., FONTBONNE, R., ROUDEL, M., DIAGON, M., VIGUÈS, B., BELZUNCES, L. P., DELBAC, F., AND BLOT, N. Parasite-insecticide interactions: a case study of *Nosema ceranae* and fipronil synergy on honeybee. *Scientific reports* 2 (2012).
- [8] BALL, D. W. The chemical composition of honey. *J. Chem. Educ* 84, 10 (2007), 1643.
- [9] BECHER, M. A., GRIMM, V., THORBEEK, P., HORN, J., KENNEDY, P. J., AND OSBORNE, J. L. BEEHAVE: a systems model of honeybee colony dynamics and foraging to explore multifactorial causes of colony failure. *Journal of Applied Ecology* 51, 2 (2014), 470–482.
- [10] BECHER, M. A., OSBORNE, J. L., THORBEEK, P., KENNEDY, P. J., AND GRIMM, V. Review: Towards a systems approach for understanding honeybee decline: a stocktaking and synthesis of existing models. *Journal of Applied Ecology* 50, 4 (2013), 868–880.

- [11] BERNOULLI, D. Essai d'une nouvelle analyse de la mortalité causée par la petite vérole et des avantages de l'inoculation pour la prévenir. *Histoire de l'Acad. Roy. Sci. (Paris) avec Mém. des Math. et Phys. and Mém* (1760), 1–45.
- [12] BETTI, M., LECLAIR, J., WAHL, L. M., AND ZAMIR, M. Bee++: An object-oriented, agent-based simulator for honey bee colonies. *Insects* 8, 1 (2017), 31.
- [13] BETTI, M., WAHL, L. M., AND ZAMIR, M. Age structure is critical to the population dynamics and survival of honeybee colonies. *Royal Society Open Science* 3, 11 (2016), 160444.
- [14] BETTI, M. I., WAHL, L. M., AND ZAMIR, M. Effects of infection on honey bee population dynamics: A model. *PLOS ONE* 9, 10 (2014), e110237.
- [15] BETTI, M. I., WAHL, L. M., AND ZAMIR, M. Reproduction number and asymptotic stability for a model with continuous age structure: An application to honey bee dynamics. *Bulletin of Mathematical Biology* (2016). submitted.
- [16] BIESMEIJER, J. C., ROBERTS, S., REEMER, M., OHLEMÜLLER, R., EDWARDS, M., PEETERS, T., SCHAFFERS, A., POTTS, S., KLEUKERS, R., THOMAS, C., ET AL. Parallel declines in pollinators and insect-pollinated plants in Britain and the Netherlands. *Science* 313, 5785 (2006), 351–354.
- [17] BÖCKH, R. *Statistisches Jahrbuch der Stadt Berlin, Zwölfter Jahrgang, Statistik des Jahres 1884*. P Stankiewicz, 1886.
- [18] BOWEN-WALKER, P. L., AND GUNN, A. The effect of the ectoparasitic mite, *Varroa destructor* on adult worker honeybee (*Apis mellifera*) emergence weights, water, protein, carbohydrate, and lipid levels. *Entomologia Experimentalis et Applicata* 101, 3 (2001), 207–217.
- [19] BRAUER, F. The Kermack–McKendrick epidemic model revisited. *Mathematical Biosciences* 198, 2 (2005), 119–131.
- [20] BRAUER, F., AND CASTILLO-CHAVEZ, C. *Mathematical models in population biology and epidemiology*, vol. 1. Springer, 2001.
- [21] BRITAIN, C., WILLIAMS, N., KREMEN, C., AND KLEIN, A.-M. Synergistic effects of non-*Apis* bees and honey bees for pollination services. *Proceedings of the Royal Society of London B: Biological Sciences* 280, 1754 (2013), 20122767.
- [22] BRITTON, N. *Essential mathematical biology*. Springer Science & Business Media, 2012.
- [23] BRITTON, N. F., ET AL. *Reaction-diffusion equations and their applications to biology*. Academic Press, 1986.
- [24] CALDERONE, N. W. Insect pollinated crops, insect pollinators and US agriculture: Trend analysis of aggregate data for the period 1992-2009. *PLOS ONE* 7, 5 (05 2012), e37235.

- [25] CAMAZINE, S., AND SNEYD, J. A model of collective nectar source selection by honey bees: self-organization through simple rules. *Journal of theoretical Biology* 149, 4 (1991), 547–571.
- [26] CHEN, Y., EVANS, J. D., SMITH, I. B., AND PETTIS, J. S. *Nosema ceranae* is a long-present and wide-spread microsporidian infection of the European honey bee (*Apis mellifera*) in the United States. *Journal of Invertebrate Pathology* 97, 2 (2008), 186–188.
- [27] COURCHAMP, F., BEREC, L., AND GASCOIGNE, J. *Allee effects in ecology and conservation*. Oxford University Press, Oxford, 2008.
- [28] CRANE, E. *The archaeology of beekeeping*. Cornell University Press, New York, 1983.
- [29] CRITTENDEN, A. N. The importance of honey consumption in human evolution. *Food and Foodways* 19, 4 (2011), 257–273.
- [30] CUSHING, J., AND DIEKMANN, O. The many guises of R_0 (a didactic note). *Journal of Theoretical Biology* 404 (2016), 295–302.
- [31] DAILY, G. C. *Natures services*. Island Press, Washington, DC, 1997.
- [32] DEGRANDI-HOFFMAN, G., ROTH, S. A., LOPER, G., AND ERICKSON, E. H. BEEPOP: a honeybee population dynamics simulation model. *Ecological modelling* 45, 2 (1989), 133–150.
- [33] DEL CASTILLO-NEGRETE, D., CARRERAS, B., AND LYNCH, V. Front dynamics in reaction-diffusion systems with Lévy flights: a fractional diffusion approach. *Physical Review Letters* 91, 1 (2003), 018302.
- [34] DENNIS, B., AND KEMP, W. P. How hives collapse: Allee effects, ecological resilience, and the honey bee. *PLOS ONE* 11, 2 (2016), e0150055.
- [35] DEVILLERS, J. The ecological importance of honey bees and their relevance to ecotoxicology. In *Honey Bees: Estimating the Environmental Impact of Chemicals*, J. Devillers and M. Pham-Delègue, Eds. Taylor and Francis London, London, 2002, pp. 1–11.
- [36] DI PRISCO, G., PENNACCHIO, F., CAPRIO, E., BONCRISTIANI JR, H. F., EVANS, J. D., AND CHEN, Y. *Varroa destructor* is an effective vector of Israeli acute paralysis virus in the honeybee, *Apis mellifera*. *Journal of General Virology* 92, 1 (2011), 151–155.
- [37] DIEKMANN, O., HEESTERBEEK, J., AND ROBERTS, M. The construction of next-generation matrices for compartmental epidemic models. *Journal of the Royal Society Interface* (2009), rsif20090386.
- [38] DIEKMANN, O., AND HEESTERBEEK, J. A. P. *Mathematical epidemiology of infectious diseases: model building, analysis and interpretation*, vol. 5. John Wiley & Sons, 2000.
- [39] DIEKMANN, O., HEESTERBEEK, J. A. P., AND METZ, J. A. On the definition and the computation of the basic reproduction ratio R_0 in models for infectious diseases in heterogeneous populations. *Journal of mathematical biology* 28, 4 (1990), 365–382.

- [40] DIETZ, K. The estimation of the basic reproduction number for infectious diseases. *Statistical methods in medical research* 2, 1 (1993), 23–41.
- [41] EBERL, H. J., FREDERICK, M. R., AND KEVAN, P. G. Importance of brood maintenance terms in simple models of the honeybee - *Varroa destructor* - Acute Bee Paralysis Virus complex. *Electronic Journal of Differential Equations (EJDE) [electronic only]* 2010 (2010), 85–98.
- [42] ECKERT, J., FRIEDHOFF, K. T., AND ZAHNER, H. *Lehrbuch der Parasitologie für die Tiermedizin*. Georg Thieme Verlag, 2008.
- [43] ECKERT, J. E. The flight range of the honeybee. *Journal of Agricultural Research* (1933).
- [44] ELLIS, J. D., EVANS, J. D., AND PETTIS, J. Colony losses, managed colony population decline, and colony collapse disorder in the United States. *Journal of Apicultural Research* 49, 1 (2010), 134–136.
- [45] ENGEL, M. S. The taxonomy of recent and fossil honey bees (*Hymenoptera: Apidae; Apis*). *Journal of Hymenoptera Research* 8, 2 (1999), 165–196.
- [46] EVANS, J. D., AND WHEELER, D. E. Differential gene expression between developing queens and workers in the honey bee, *apis mellifera*. *Proceedings of the National Academy of Sciences* 96, 10 (1999), 5575–5580.
- [47] FAHRBACH, S., AND ROBINSON, G. Juvenile hormone, behavioral maturation and brain structure in the honey bee. *Developmental Neuroscience* 18 (1996), 102–114.
- [48] FENOY, S., RUEDA, C., HIGES, M., MARTÍN-HERNÁNDEZ, R., AND DEL AGUILA, C. High-level resistance of *Nosema ceranae*, a parasite of the honeybee, to temperature and desiccation. *Applied and environmental microbiology* 75, 21 (2009), 6886–6889.
- [49] FORSGREN, E., AND FRIES, I. Comparative virulence of *Nosema ceranae* and *Nosema apis* in individual European honey bees. *Veterinary parasitology* 170, 3 (2010), 212–217.
- [50] FRIES, I. *Nosema apis* parasite in the honey bee colony. *Bee World* 74, 1 (1993), 5–19.
- [51] GAINES-DAY, H. R., AND GRATTON, C. Crop yield is correlated with honey bee hive density but not in high-woodland landscapes. *Agriculture, Ecosystems & Environment* 218 (2016), 53–57.
- [52] GARIBALDI, L. A., STEFFAN-DEWENTER, I., WINFREE, R., AIZEN, M. A., BOMMARCO, R., CUNNINGHAM, S. A., KREMEN, C., CARVALHEIRO, L. G., HARDER, L. D., AFIK, O., ET AL. Wild pollinators enhance fruit set of crops regardless of honey bee abundance. *Science* 339, 6127 (2013), 1608–1611.
- [53] GISDER, S., AUMEIER, P., AND GENERSCH, E. Deformed wing virus: replication and viral load in mites (*Varroa destructor*). *Journal of General Virology* 90, 2 (2009), 463–467.
- [54] GOULD, J. L., GOULD, C. G., ET AL. *The honey bee*. Scientific American Library, 1988.

- [55] GOULSON, D., NICHOLLS, E., BOTÍAS, C., AND ROTHERAY, E. L. Bee declines driven by combined stress from parasites, pesticides, and lack of flowers. *Science* 347, 6229 (2015), 1255957.
- [56] GREENHALGH, D. Analytical results on the stability of age-structured recurrent epidemic models. *Mathematical Medicine and Biology* 4, 2 (1987), 109–144.
- [57] GREENHALGH, D. Threshold and stability results for an epidemic model with an age-structured meeting rate. *Mathematical Medicine and Biology* 5, 2 (1988), 81–100.
- [58] GREGORY, P. G., EVANS, J. D., RINDERER, T., AND DE GUZMAN, L. Conditional immune-gene suppression of honeybees parasitized by *Varroa* mites. *Journal of Insect Science* 5, 7 (2005), 1–5.
- [59] HAMER, W. H. Epidemic disease in England. *Lancet* 1 (1906), 733–739.
- [60] HARBO, J. R. Effect of population size on brood production, worker survival and honey gain in colonies of honeybees. *Journal of Apicultural Research* 25, 1 (1986), 22–29.
- [61] HARRIS, J. A model of honeybee colony population dynamics. *Journal of Apicultural Research* 24, 4 (1985), 228–236.
- [62] HAUKE, G. *Toward Saving the Honeybee*. Steiner Books, Oregon, 2002.
- [63] HEFFERNAN, J., SMITH, R., AND WAHL, L. M. Perspectives on the basic reproductive ratio. *Journal of the Royal Society Interface* 2, 4 (2005), 281–293.
- [64] HENRY, M., BEGUIN, M., REQUIER, F., ROLLIN, O., ODOUX, J.-F., AUPINEL, P., APTEL, J., TCHAMITCHIAN, S., AND DECOURTYE, A. A common pesticide decreases foraging success and survival in honey bees. *Science* 336, 6079 (2012), 348–350.
- [65] HETHCOTE, H. W. The mathematics of infectious diseases. *SIAM review* 42, 4 (2000), 599–653.
- [66] HIGES, M., MARTIN-HERNANDEZ, R., BOTIAS, C., BAILON, E. G., GONZALEZ-PORTO, A. V., AND BARRIOS, L. How natural infection by *Nosema ceranae* causes honeybee colony collapse. *Environmental microbiology* 10, 10 (2008), 2659–2669.
- [67] HIGES, M., MARTIN-HERNANDEZ, R., GARRIDO-BAILON, E., GONZALEZ-PORTO, A. V., GARCIA-PALENCIA, P., AND MEANA, A. Honeybee colony collapse due to *Nosema ceranae* in professional apiaries. *Environmental Microbiology Reports* 1, 2 (2009), 110–113.
- [68] HUANG, W.-F., SOLTER, L. F., YAU, P. M., AND IMAI, B. S. *Nosema ceranae* escapes fumagillin control in honey bees. *PLOS Pathog* 9, 3 (2013), e1003185.
- [69] HUANG, Z.-Y., AND ROBINSON, G. E. Regulation of honey bee division of labor by colony age demography. *Behavioral Ecology and Sociobiology* 39 (1996), 147–158.
- [70] INABA, H. Threshold and stability results for an age-structured epidemic model. *Journal of mathematical biology* 28, 4 (1990), 411–434.

- [71] JAVOREK, S., MACKENZIE, K., AND VANDER KLOET, S. Comparative pollination effectiveness among bees (*Hymenoptera: Apoidea*) on lowbush blueberry (*Ericaceae: Vaccinium angustifolium*). *Annals of the Entomological Society of America* 95, 3 (2002), 345–351.
- [72] JOHNSON, R. M., DAHLGREN, L., SIEGFRIED, B. D., AND ELLIS, M. D. Acaricide, fungicide and drug interactions in honey bees (*Apis mellifera*). *PLOS ONE* 8, 1 (2013), e54092.
- [73] KAUFFELD, N. M. *Beekeeping in the United States Agriculture Handbook Number 335*. U.S. Department of Agriculture, 1980.
- [74] KERMACK, W. O., AND MCKENDRICK, A. G. A contribution to the mathematical theory of epidemics. *Proceedings of the Royal Society of London A: mathematical, physical and engineering sciences* 115, 772 (1927), 700–721.
- [75] KHOURY, D. S., BARRON, A. B., AND MYERSCOUGH, M. R. Modelling food and population dynamics in honey bee colonies. *PLOS ONE* 8, 5 (05 2013), e59084.
- [76] KHOURY, D. S., MYERSCOUGH, M. R., AND BARRON, A. B. A quantitative model of honey bee colony population dynamics. *PLOS ONE* 6, 4 (04 2011), e18491.
- [77] KLATT, B. K., HOLZSCHUH, A., WESTPHAL, C., CLOUGH, Y., SMIT, I., PAWELZIK, E., AND TSCHARNTKE, T. Bee pollination improves crop quality, shelf life and commercial value. *Proc. R. Soc. B* 281, 1775 (2014), 20132440.
- [78] KLEIN, A.-M., VAISSIERE, B. E., CANE, J. H., STEFFAN-DEWENTER, I., CUNNINGHAM, S. A., KREMEN, C., AND TSCHARNTKE, T. Importance of pollinators in changing landscapes for world crops. *Proceedings of the Royal Society of London B: Biological Sciences* 274, 1608 (2007), 303–313.
- [79] KREMEN, C., WILLIAMS, N. M., AND THORP, R. W. Crop pollination from native bees at risk from agricultural intensification. *Proceedings of the National Academy of Sciences* 99, 26 (2002), 16812–16816.
- [80] KULHANEK, K., STEINHAEUER, N., RENNICH, K., CARON, D. M., SAGILI, R. R., PETTIS, J. S., ELLIS, J. D., WILSON, M. E., WILKES, J. T., TARPY, D. R., ET AL. A national survey of managed honey bee 2015–2016 annual colony losses in the usa. *Journal of Apicultural Research* (2017), 1–13.
- [81] LEONCINI, I., LE CONTE, Y., COSTAGLIOLA, G., PLETTNER, E., TOTH, A. L., AND WANG, M. Regulation of behavioral maturation by a primer pheromone produced by adult worker honey bees. *Proceedings of the National Academy of Sciences of the United States of America* 101, 50 (2004), 17559–17564.
- [82] LI, J., AND BRAUER, F. Continuous-time age-structured models in population dynamics and epidemiology. In *Mathematical Epidemiology*, F. Brauer, P. van den Driessche, and J. Wu, Eds. Springer, 2008, pp. 205–227.
- [83] LOTKA, A. J. *Théorie analytique des associations biologiques: analyse démographique avec application particulière à l'espèce humaine*. Hermann, 1939.

- [84] MACDONALD, G. The analysis of equilibrium in malaria. *Tropical diseases bulletin* 49, 9 (1952), 813–829.
- [85] MALESZKA, R. Epigenetic integration of environmental and genomic signals in honey bees: the critical interplay of nutritional, brain and reproductive networks. *Epigenetics* 3, 4 (2008), 188–192.
- [86] MARTIN, S. Hygienic behaviour: an alternative view. *Bee Improvement* 7 (2000), 6–7.
- [87] MARTIN, S. Biology and life-history of *Varroa* mites. *Mites of the honey bee*. Dadant & Sons, Hamilton, IL (2001), 131–148.
- [88] MARTIN, S. J. The role of *Varroa* and viral pathogens in the collapse of honeybee colonies: a modelling approach. *Journal of Applied Ecology* 38, 5 (2001), 1082–1093.
- [89] MARTÍN-HERNÁNDEZ, R., BOTÍAS, C., BARRIOS, L., MARTÍNEZ-SALVADOR, A., MEANA, A., MAYACK, C., AND HIGES, M. Comparison of the energetic stress associated with experimental *Nosema ceranae* and *Nosema apis* infection of honeybees (*Apis mellifera*). *Parasitology research* 109, 3 (2011), 605–612.
- [90] MARTÍN-HERNÁNDEZ, R., MEANA, A., GARCÍA-PALENCIA, P., MARÍN, P., BOTÍAS, C., GARRIDO-BAILÓN, E., BARRIOS, L., AND HIGES, M. Effect of temperature on the biotic potential of honeybee microsporidia. *Applied and Environmental Microbiology* 75, 8 (2009), 2554–2557.
- [91] MICHENER, C. D. *The bees of the world*. JHU press, Maryland, 2000.
- [92] MURILHAS, A. M., ET AL. *Varroa destructor* infestation impact on *Apis mellifera carnica* capped worker brood production, bee population and honey storage in a Mediterranean climate. *Apidologie* 33, 3 (2002), 271–282.
- [93] MURRAY, J. D. *Mathematical Biology II: Spatial Models and Biomedical Applications*. Springer-Verlag New York Incorporated, 2001.
- [94] MURRAY, J. D. *Mathematical Biology I: An Introduction*. Springer, New York, NY, USA,, 2002.
- [95] NAZZI, F., BROWN, S. P., ANNOSCIA, D., DEL PICCOLO, F., DI PRISCO, G., VARRICCHIO, P., DELLA VEDOVA, G., CATTONARO, F., CAPRIO, E., AND PENNACCHIO, F. Synergistic parasite-pathogen interactions mediated by host immunity can drive the collapse of honeybee colonies. *PLOS Pathog* 8, 6 (2012), e1002735.
- [96] OLDROYD, B. P., AND RATNIEKS, F. L. Evolution of worker sterility in honey-bees (*apis mellifera*): how anarchistic workers evade policing by laying eggs that have low removal rates. *Behavioral Ecology and Sociobiology* 47, 4 (2000), 268–273.
- [97] OMHOLT, S. W. A model for intracolony population dynamics of the honeybee in temperate zones. *Journal of Apicultural Research* 25, 1 (1986), 9–21.

- [98] OTTO, S. P., AND DAY, T. *A biologist's guide to mathematical modeling in ecology and evolution*, vol. 13. Princeton University Press, 2007.
- [99] PAIVA, J. P. L. M., PAIVA, H. M., ESPOSITO, E., AND MORAIS, M. M. On the effects of artificial feeding on bee colony dynamics: A mathematical model. *PLOS ONE* 11, 11 (2016), e0167054.
- [100] PASTOR-SATORRAS, R., CASTELLANO, C., VAN MIEGHEM, P., AND VESPIGNANI, A. Epidemic processes in complex networks. *Reviews of modern physics* 87, 3 (2015), 925.
- [101] PAXTON, R. J., KLEE, J., KORPELA, S., AND FRIES, I. *Nosema ceranae* has infected *Apis mellifera* in Europe since at least 1998 and may be more virulent than *Nosema apis*. *Apidologie* 38, 6 (2007), 558–565.
- [102] PERKO, L. *Differential equations and dynamical systems*, vol. 7. Springer Science & Business Media, 2013.
- [103] POLYANIN, A. D., AND ZAITSEV, V. F. Exact solutions for ordinary differential equations. *Campman and Hall/CRC* 2 (1995).
- [104] PROTTER, P. Stochastic differential equations. In *Stochastic Integration and Differential Equations*. Springer, 1990, pp. 187–284.
- [105] RATTI, V., KEVAN, P. G., AND EBERL, H. J. A mathematical model for population dynamics in honeybee colonies infested with *Varroa destructor* and the Acute Bee Paralysis Virus. *Canadian Applied Mathematics Quarterly* 21, 1 (2013), 63–93.
- [106] RATTI, V., KEVAN, P. G., AND EBERL, H. J. A mathematical model of the honeybee-*Varroa destructor*-Acute Bee Paralysis Virus complex with seasonal effects. *Bulletin of Mathematical Biology* (2015).
- [107] RILEY, J. R., GREGGERS, U., SMITH, A. D., REYNOLDS, D. R., AND MENZEL, R. The flight paths of honeybees recruited by the waggle dance. *Nature* 435, 7039 (2005), 205–207.
- [108] ROBINSON, G. E., PAGE, R. E., STRAMBI, C., AND STRAMBI, A. Colony integration in honey bees: mechanisms of behavioral reversion. *Ethology* 90, 4 (1992), 336–348.
- [109] ROSS, R. *The prevention of malaria*. Dutton, 1910.
- [110] ROUBIK, D. W. *Pollination of cultivated plants in the tropics*. No. 118. Food & Agriculture Org., 1995.
- [111] ROUBIK, D. W., AND WOLDA, H. Do competing honey bees matter? dynamics and abundance of native bees before and after honey bee invasion. *Population Ecology* 43, 1 (2001), 53–62.
- [112] ROWLAND, C., AND McLELLAN, A. A simple mathematical model of brood production in honeybee colonies. *Journal of Apicultural Research* 21, 3 (1982), 157–160.

- [113] SAKAGAMI, S., AND FUKUDA, H. Life tables for worker honeybees. *Researches on Population Ecology* 10, 2 (1968), 127–139.
- [114] SAMMATARO, D., GERSON, U., AND NEEDHAM, G. Parasitic mites of honey bees: life history, implications, and impact. *Annual review of entomology* 45, 1 (2000), 519–548.
- [115] SEEHUUS, S.-C., NORBERG, K., GIMSA, U., KREKLING, T., AND AMDAM, G. V. Reproductive protein protects functionally sterile honey bee workers from oxidative stress. *Proceedings of the National Academy of Sciences of the United States of America* 103, 4 (2006), 962–967.
- [116] SEELEY, T. D. *Honeybee Democracy*. Princeton University Press, 2010.
- [117] SEELEY, T. D., AND VISSCHER, P. K. Survival of honeybees in cold climates: the critical timing of colony growth and reproduction. *Ecological Entomology* 10, 1 (1985), 81–88.
- [118] SHARPE, F. R., AND LOTKA, A. J. A problem in age-distribution. *The London, Edinburgh, and Dublin Philosophical Magazine and Journal of Science* 21, 124 (1911), 435–438.
- [119] SKINNER, M. Bee brood consumption: an alternative explanation for hypervitaminosis A in KNM-ER 1808 (*Homo erectus*) from Koobi Fora, Kenya. *Journal of Human Evolution* 20, 6 (1991), 493–503.
- [120] SMITH, M. L. The honey bee parasite *Nosema ceranae*: Transmissible via food exchange? *PLOS ONE* 7, 8 (08 2012), e43319.
- [121] SOUTHWICK, E. E., AND SOUTHWICK JR, L. Estimating the economic value of honey bees (*Hymenoptera: Apidae*) as agricultural pollinators in the United States. *Journal of Economic Entomology* 85, 3 (1992), 621–633.
- [122] STEVANOVIC, J., SIMEUNOVIC, P., GAJIC, B., LAKIC, N., RADOVIC, D., FRIES, I., AND STANIMIROVIC, Z. Characteristics of *Nosema ceranae* infection in Serbian honey bee colonies. *Apidologie* 44, 5 (2013), 522–536.
- [123] SUCHAIL, S., DE SOUSA, G., RAHMANI, R., AND BELZUNCES, L. P. In vivo distribution and metabolisation of ¹⁴C-imidacloprid in different compartments of *Apis mellifera* L. *Pest management science* 60, 11 (2004), 1056–1062.
- [124] SUCHAIL, S., DEBRAUWER, L., AND BELZUNCES, L. P. Metabolism of imidacloprid in *Apis mellifera*. *Pest management science* 60, 3 (2004), 291–296.
- [125] SUMPTER, D. J. T., AND MARTIN, S. J. The dynamics of virus epidemics in *Varroa*-infested honey bee colonies. *Journal of Animal Ecology* 73, 1 (2004), 51–63.
- [126] TESCHL, G. *Ordinary differential equations and dynamical systems*, vol. 140. American Mathematical Society Providence, 2012.
- [127] THIEME, H. R. Spectral bound and reproduction number for infinite-dimensional population structure and time heterogeneity. *SIAM Journal on Applied Mathematics* 70, 1 (2009), 188–211.

- [128] THORBEK, P., CAMPBELL, P. J., SWEENEY, P. J., AND THOMPSON, H. M. Using BEEHAVE to explore pesticide protection goals for European honeybee (*Apis mellifera* L.) worker losses at different forage qualities. *Environmental Toxicology and Chemistry* (2016).
- [129] TORCHIO, P. F. Diversification of pollination strategies for US crops. *Environmental Entomology* 19, 6 (1990), 1649–1656.
- [130] VAN DEN DRIESSCHE, P., AND WATMOUGH, J. Reproduction numbers and sub-threshold endemic equilibria for compartmental models of disease transmission. *Mathematical biosciences* 180, 1 (2002), 29–48.
- [131] VAN DEN DRIESSCHE, P., AND WATMOUGH, J. Further notes on the basic reproduction number. In *Mathematical Epidemiology*. Springer, 2008, pp. 159–178.
- [132] VAN ENGELSDORP, D., EVANS, J. D., SAEGERMAN, C., MULLIN, C., HAUBRUGE, E., NGUYEN, B. K., FRAZIER, M., FRAZIER, J., COX-FOSTER, D., CHEN, Y., UNDERWOOD, R., TARPY, D. R., AND PETTIS, J. S. Colony collapse disorder: A descriptive study. *PLOS ONE* 4, 8 (08 2009), e6481.
- [133] VÁSQUEZ, A., AND OLOFSSON, T. C. The lactic acid bacteria involved in the production of bee pollen and bee bread. *Journal of apicultural research* 48, 3 (2009), 189–195.
- [134] VIDAU, C., DIOGON, M., AUFAUVRE, J., FONTBONNE, R., VIGUÈS, B., BRUNET, J.-L., TEXIER, C., BIRON, D. G., BLOT, N., EL ALAOU, H., ET AL. Exposure to sublethal doses of fipronil and thiacloprid highly increases mortality of honeybees previously infected by *Nosema ceranae*. *PLOS ONE* 6, 6 (2011), e21550.
- [135] VOLPERT, V., AND PETROVSKII, S. Reaction–diffusion waves in biology. *Physics of life reviews* 6, 4 (2009), 267–310.
- [136] WANG, W., AND ZHAO, X.-Q. Basic reproduction numbers for reaction-diffusion epidemic models. *SIAM Journal on Applied Dynamical Systems* 11, 4 (2012), 1652–1673.
- [137] WANG, Z.-C., AND WU, J. Travelling waves of a diffusive Kermack–McKendrick epidemic model with non-local delayed transmission. In *Proceedings of the Royal Society of London A: Mathematical, Physical and Engineering Sciences* (2009), The Royal Society, p. rspa20090377.
- [138] WATANABE, M. E. Pollination worries rise as honey bees decline. *Science* 265, 5176 (1994), 1170–1171.
- [139] WATANABE, M. E. Colony collapse disorder: Many suspects, no smoking gun. *BioScience* 58, 5 (2008), 384–388.
- [140] WINSTON, M. *The biology of the honey bee*. Harvard University Press, 1987.
- [141] YAMADA, T., ET AL. Honeybee colony collapse disorder. *Emerging Biological Threats: A Reference Guide* 13 (2009), 141.

Chapter 2

Effects of Infection on Honey Bee Population Dynamics: A Model

Abstract

We propose a model which combines the dynamics of the spread of disease within a bee colony with the underlying demographic dynamics of the colony to determine the ultimate fate of the colony under different scenarios. The model suggests that key factors in the survival or collapse of a honey bee colony in the face of an infection are the rate of transmission of the infection and the disease-induced death rate. An increase in the disease-induced death rate, which can be thought of as an increase in the severity of the disease, may actually help the colony overcome the disease and survive through winter. By contrast, an increase in the transmission rate, which means that bees are being infected at an earlier age, has a drastic deleterious effect. Another important finding relates to the timing of infection in relation to the onset of winter, indicating that in a time interval of approximately 20 days before the onset of winter the colony is most affected by the onset of infection. The results suggest further that the age of recruitment of hive bees to foraging duties is a good early marker for the survival or collapse of a honey bee colony in the face of infection, which is consistent with experimental evidence but the model provides insight into the underlying mechanisms. The most important result of the study is a clear distinction between an exposure of the honey bee colony to an environmental hazard such as pesticides or insecticides, or an exposure to an infectious disease. The results indicate unequivocally that in the scenarios which we have examined, and perhaps more generally, an infectious disease is far more hazardous to the survival of a bee colony than an environmental hazard which causes an equal death rate in foraging bees.

2.1 Introduction

The widespread collapse of honey bee colonies has been the subject of much discussion and research in recent years [15, 34, 35]. Aside from their ecological importance [5], honey bee populations have a large economical impact on agriculture in North America, Europe, the Middle East, and Japan [2, 23, 31].

The focus of research has been largely on environmental factors outside the hive, such as pesticides or insecticides, which may cause death or injury to foraging bees and jeopardize

their return to the hive. The reduced number of foraging bees then leads to younger hive bees being recruited prematurely to perform foraging duties and this chain reaction ultimately leads to a disruption in the dynamics of the colony as a whole. Examples of this scenario would be produced by the effects of various pesticides to which foraging bees are exposed in the course of their duties [12, 35]. Other factors in the same category include possible disruptions to the bees' navigation system by mobile phones or other electronic devices, again to the effect of jeopardizing their return to the hive and thereby reducing their numbers [8].

A key element in this category of disruption to honey bee population dynamics is the untimely *death* of a certain proportion of foraging bees outside the hive and the consequences of this on the colony as a whole. An important question here concerns the threshold in the death rate of foraging bees that would determine the survival or collapse of the bee colony. This was examined recently in two papers by Khoury et al. [20, 21].

In the present paper we consider a different category of disruption to the healthy dynamics of a bee colony, namely one in which the key hazard is an *infection* by a communicable disease acquired by foraging bees outside the hive. The key difference here is that foraging bees that have been infected would then transport the disease into the hive and go on to infect other members of the colony *within the hive*. Here too the affected bees will ultimately suffer an untimely death, but the effects on the dynamics of the colony are clearly more complex because the infection in this case may now involve all members of the colony. We sought a model that would allow a comparison between the effects of these two categories of hazards (pesticide versus infection) on the ultimate fate of the bee colony.

Disease in honey bee colonies has been studied previously by Sumpter et al. [33] who modeled the effects of Varroa mites on the brood and on the adult worker bees. The focus of the model was on the relationship between the mite population within a hive and its role in virus transmission within the hive. A study by Ratti et al. [24] examined the transmission of viruses via Varroa mites, using an SIR-framework with the mites as vectors for transmission.

In the present paper we propose a more general model which combines the normal dynamics of a honey bee colony with the dynamics of an infectious disease which is acquired outside the hive but ultimately spreads to the rest of the colony. As a working example, we use a disease known as *Nosema* which is a common disease affecting both hive bees and foraging bees [9]. *Nosema* is caused by a microsporidian with two common species: *Nosema ceranae* and *Nosema apis*. The former was first discovered in Asian honey bees (*Apis ceranae*) and the latter is common among European honey bees (*Apis mellifera*). A key factor in the collapse of honey bee colonies in recent years is thought to be the introduction of *Nosema ceranae* to *Apis mellifera* [14].

The main aim of the model is to provide a general tool for determining the ultimate fate of a honey bee colony under this fairly common hazard. In particular, we identify key variables that determine the collapse or survival of the bee colony, namely the severity of the disease and the rate of transmission, and examine different scenarios using different combinations of these variables. Winter is an important phase in the normal demographic dynamics of a bee colony; the queen lays fewer eggs and foraging bees return to and remain within the hive [19, 29]. Therefore, the time interval between the onset of disease and the onset of winter may play a critical role in the ultimate survival or collapse of the colony in the face of an infection. We show that the model can be used to explore potential markers of the presence of the disease within the bee colony and of the ultimate fate of the colony under different scenarios.

2.2 Background

2.2.1 Normal Demographics of a Honey Bee Colony

Honey bee colonies are complex societies in which different members of the colony have specialized functions that serve the entire colony, thus making members of the colony highly dependent on each other.

The queen can live up to three years, is responsible for laying eggs, and during peak season may lay up to 2000 eggs per day [4]. In this function the queen is dependent on worker bees [36]. The worker bees emerge from fertilized eggs of the queen and consist of females who maintain the hive and gather resources, and males who mate with the queen to produce more eggs [28]. Drones are born from unfertilized eggs of the queen [28] and typically making up less than 5% of the hive population [17, 28]. Because they do not contribute to the colony work force, and because of their small numbers, they are generally neglected when considering the dynamics of the colony as a whole.

Female hive bees, following a transition period, leave the hive to start foraging duties and usually forage until their death. The age at which they start foraging duties is variable, depending on the state of the colony and its needs. If the number of forager bees is lower than is required for meeting the colony needs, hive bees will begin foraging duties at a younger age [16]. If the number of forager bees is higher than required, behavioural maturation of hive bees will be regulated by a pheromone, ethyl oleate, produced by the foragers. This process is usually referred to as “social inhibition” [22]. Similarly, if the number of hive bees is too low, it is possible for foragers to revert back to hive bee duties [16].

As the temperature drops outside the hive, foraging becomes less frequent, the queen begins to lay fewer eggs [36], and drones are expelled from the hive to save hive resources [28]. When the temperature drops below a certain threshold, the colony enters a winter phase in which the queen will cease to lay eggs [19] and any remaining foraging bees will return to the hive. During winter the entire hive population surrounds the queen in order to maintain a temperature of 34 – 36°C within the hive [28].

2.2.2 Nosema Infection

Nosema, also known as “Nosemosis”, is an infection affecting honey bees that is spread by the microsporidian parasites in the *Nosema* family. *Nosema ceranae* is of particular interest, as it is thought to be linked to colony collapse incidents [13, 14]. We use this disease only as an example to illustrate the utility of the model. The choice was motivated by the availability of parameter values which allowed us to examine some realistic scenarios of the dynamics of the bee colony in the presence of infection.

Within the bee colony, *Nosema* is typically spread via fecal-oral transmission. Adult bees will contract *Nosema* either from eating food contaminated by infected bees, or while ridding the hive of infected fecal matter [3]. There is also evidence that *Nosema* can be spread via oral-oral transmission, through feeding [30].

While it is typically asymptomatic at the level of individual bees, *Nosema* has some symptoms that can be observed at the colony level [9, 32]. Stevanovic et al. [32] observed in 2013

that colonies infected by the parasite *Nosema ceranae* exhibited many of the classic signs that precede colony collapse.

Much of the experimental research linking *Nosema* infection to colony collapse is based on correlated observations, but direct cause and effect evidence is lacking [9]. Our model aims to provide a possible mechanism for this linkage in terms of the interplay between the dynamics of the infection and the normal dynamics of the honey bee colony.

2.3 Mathematical Model

In what follows we present a mathematical model that combines the normal demographic dynamics of a honey bee colony with the dynamics of an infection affecting foraging bees outside the hive at first and then spreading to the rest of the colony. We follow a model for the basic dynamics of a bee colony in the absence of disease presented recently by Khoury et al. [20, 21], in which the adult bee population is divided into a number of hive bees H , and a number of foraging bees F . In the model to be described below we extend this division into four categories, namely susceptible hive bees H_S , infected hive bees H_I , susceptible foraging bees F_S , and infected foraging bees F_I . Equations governing each of these four populations during the active and winter seasons are presented in the following section.

2.3.1 Governing Equations: Active Season

The rate of change in time t (days) of the susceptible hive bee population H_S during the active season is assumed to be governed by

$$\frac{dH_S}{dt} = LS - H_S R - (\beta_{HH} H_I + \beta_{HF} F_I) H_S. \quad (2.1)$$

In the first term on the right L is the queen's egg laying rate per day and S is the proportion of those eggs that survive both larval and pupal stages to yield mature bees. This proportion is a function of the total number of hive bees and of the amount of food f available within the hive because the brood requires food as well as a sufficient number of supporting hive bees in order to survive [18]. Following [20] we take

$$S = \left(\frac{H_S + H_I}{w + H_S + H_I} \right) \left(\frac{f}{b + f} \right). \quad (2.2)$$

This function is constructed such that the value of S saturates at 1.0 in the limiting case when the amount of food f and the total number of hive bees $H_S + H_I$ are sufficiently large to ensure the survival of 100% of the eggs laid by the queen. The parameters b and w determine at what values of f and $H_S + H_I$ this saturation occurs and they will be discussed later.

In the second term on the right of Eq. 2.1, R is the proportion of maturing hive bees H_S that are being recruited to foraging duties. As discussed earlier, and following [20], we assume that recruitment is increased when either food stores or forager populations are low and recruitment is reduced when food stores and forager populations are in excess. Note that in an overabundance of foragers, R may become negative, which implies that foragers are reverting to hive

duties.

$$R = R_b + \alpha_f \left(\frac{b}{b+f} \right) - \alpha_F \left(\frac{F_I + F_S}{N} \right) \quad (2.3)$$

where R_b is the baseline recruitment rate in the absence of foragers but sufficient food stores, α_f is a weighting of the effect of low food, α_F is a weighting of the effect of excess foragers on recruitment, and $N = F_I + F_S + H_S + H_I$ is the colony adult population size. The Average Age of Recruitment to Foraging (AARF) at any point in time is equal to $1/R$.

The last term in Eq. 2.1 determines the rate at which susceptible hive bees become infected. The transmission rate per day per susceptible hive bee is given by $(\beta_{HH}H_I + \beta_{HF}F_I)$, where β_{HH} is the contact rate between hive bees and β_{HF} is that between hive bees and foraging bees.

Hive bees are safe within the hive environment under normal circumstances, surviving up to 6 months over winter [21, 28]. It is therefore assumed that the natural death rate of hive bees is negligible compared to their recruitment rate to foraging duties.

For the rate of change of the infected hive bee population, we take

$$\frac{dH_I}{dt} = (\beta_{HH}H_I + \beta_{HF}F_I)H_S - H_I R - d_H H_I. \quad (2.4)$$

Infected hive bees continue to be recruited to foraging duties but, unlike their healthy counterparts, they are at risk of dying from the disease before they do so; d_H is the rate at which this occurs.

Susceptible foragers are recruited from susceptible hive bees and may subsequently suffer natural death, at a rate m , or become infected. Their rate of change is therefore governed by

$$\frac{dF_S}{dt} = H_S R - m F_S - (\beta_{HF}H_I + \beta_{FF}F_I) F_S. \quad (2.5)$$

Infected foragers are recruited from infected hive bees or are susceptible foragers that have become infected. If the death rate from the infection is assumed to be d_F then their rate of change is governed by

$$\frac{dF_I}{dt} = H_I R + (\beta_{HF}H_I + \beta_{FF}F_I) F_S - (m + d_F) F_I. \quad (2.6)$$

Food is brought into the hive by foragers, either healthy or infected. Although infected foragers may forage less efficiently, for simplicity we assume the same foraging rate, c (gm/day) per forager. The collected food is then consumed by both foragers and hive bees and for simplicity again we assume the same consumption rate, γ_A (gm/day). The amount of food consumed by the larvae is substantial. We assume that the number of larvae is proportional to the number of surviving eggs and that the larvae consume food at a rate of γ_L (gm/day). The amount of food available at time t is thus given by

$$\frac{df}{dt} = c(F_S + F_I) - \gamma_A N - \gamma_L L S. \quad (2.7)$$

The full dynamics of the bee colony are thus governed by Eqs. 2.1, 2.4, 2.5, 2.6 and 2.7 to be solved simultaneously. A compartmental diagram of these dynamics is shown in Figure 2.3.1.

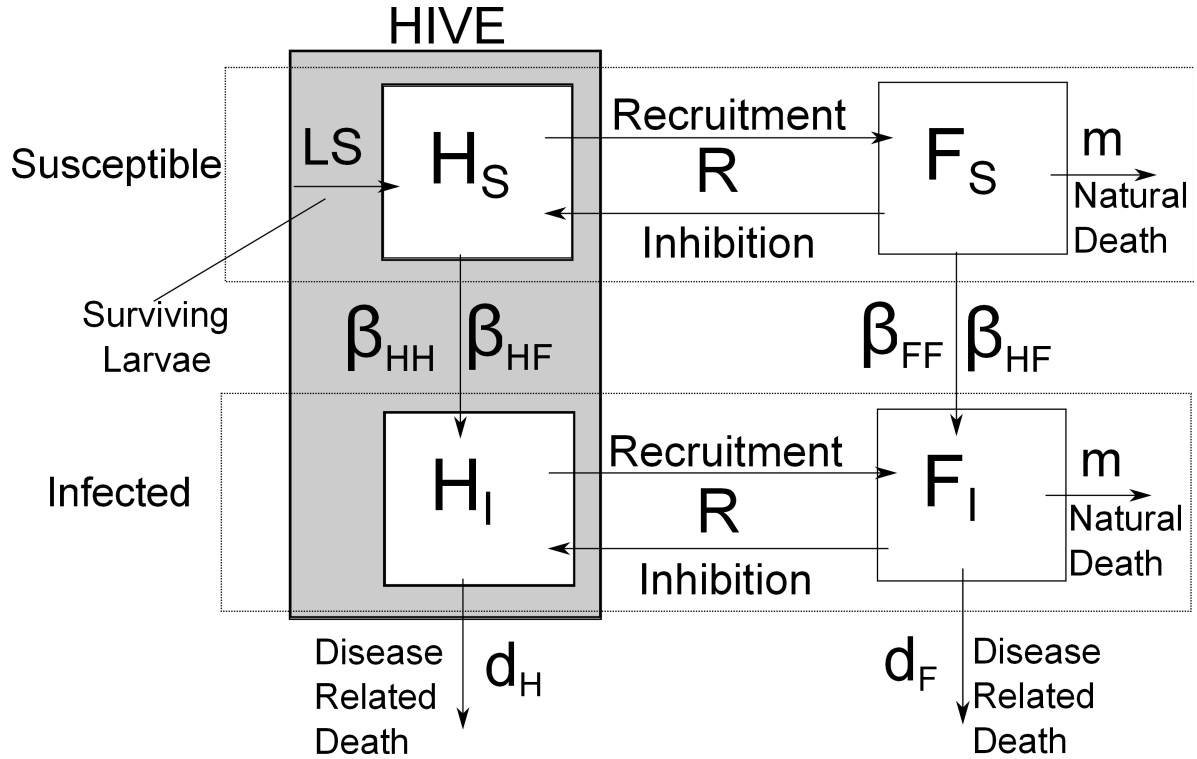


Figure 2.1: A compartmental diagram of the dynamics of the honey bee colony combined with the dynamics of an infectious disease. The susceptible and infected hive bees, H_S and H_I live within the hive. New susceptible hive bees are generated by surviving brood through the survival function, S . New infected hive bees are generated through interactions of susceptible hive bees with infected hive bees and infected foragers at rates β_{HH} and β_{HF} . Hive bees are recruited to foraging duties through the recruitment function R , which also allows for the reversal of duties, from foraging to hive duties. Foragers move into the infected compartment via interactions with infected hive bees and infected foragers at rates β_{HF} and β_{FF} . All infected bees die at rates d_H or d_F , and foragers die naturally at rate m .

2.3.2 Governing Equations: Winter

During winter the rate of egg laying by the queen is considerably diminished, and in harsh climates the queen may cease laying eggs completely [19]. For simplicity, in our model simulations therefore we take $L = 0$ for the winter season.

Foraging resources become scarce in winter and foraging bees return to the hive to join hive bees in their effort to keep the hive warm [19]. The two groups thus perform the same duties in winter and there is no longer any recruitment from hive to foraging duties. We therefore set $R = 0$, although we maintain the separate identities of the two groups in the model in order to track the behaviors of bees that were foraging before winter against those that were hive bees.

Since there is no foraging in winter, food production halts and we set $c = 0$. Also, bees are able to survive longer in winter than they do outside the hive during the active season [26]. Thus the new natural death rate for both hive bees and foraging bees during the winter season

is set to be m_W .

Introducing these changes into the equations governing the dynamics of the colony (Eqs. 2.1, 2.4, 2.5, 2.6, 2.7) we obtain the corresponding equations for the winter season:

$$\frac{dH_S}{dt} = -m_W H_S - (\beta_{HH} H_I + \beta_{HF} F_I) H_S \quad (2.8)$$

$$\frac{dF_S}{dt} = -m_W F_S - (\beta_{HF} H_I + \beta_{FF} F_I) F_S \quad (2.9)$$

$$\frac{dH_I}{dt} = (\beta_{HH} H_I + \beta_{HF} F_I) H_S - (m_W + d_H) H_I \quad (2.10)$$

$$\frac{dF_I}{dt} = (\beta_{HF} H_I + \beta_{FF} F_I) F_S - (m_W + d_F) F_I \quad (2.11)$$

$$\frac{df}{dt} = -\gamma_A N - \gamma_L LS \quad (2.12)$$

2.3.3 Parameter Values

The model presented in Section 2.3 contains a total of 13 parameters. Of these, 10 parameters relate to the baseline demographic dynamics of a honey bee colony, in the absence of disease, for which empirical estimates are available in the literature. In particular, we consider a bee colony in which the maximum rate (L in Eq. 4.10) of egg laying by the queen is 2000 eggs/day and take $w = 5000$ [21]. Hive bees spend, on average, a minimum of 4 days in the hive before being recruited to foraging duties [7], and foragers will not revert to hive duties unless one-third of the bee population is foraging [21]. Based on these values, and following [21], we take $R_b = 0.25$ and $\alpha_f = 0.75$. In the complete absence of food, recruitment of foragers will double [27], thus we take $\alpha_F = 0.25$. Foraging bees are estimated to live approximately 6.76 days outside the hive [6], thus we set $m = 0.14$ deaths per bee per day.

The parameter b in Eq. 4.10 is the amount of food required to ensure the survival of half of the eggs to maturation. Based on the observation that the effects of low food stores become evident when there is less than 1 kg of stored food [21], we take $b = 500$. It is estimated that as long as the hive is in an environment that provides sufficient food resources, a forager will return with $c = 0.1$ g of food per day [11, 25]. It is also estimated that the daily food requirement of each member of the brood is $\gamma_L = 0.018$ g and that of an adult hive or foraging bee is $\gamma_A = 0.007$ g [11, 20, 21].

We assume that both the rate of food consumption and the transmission rate of the disease remain the same during the active and winter seasons. However, empirical evidence indicates that bees live longer in winter, surviving up to six months [26], and on that basis we take the natural death rate in winter, $m_W = 1/180$ deaths per bee per day.

The remaining parameters relate to the dynamics of the disease and, as stated earlier, we have chosen *Nosema ceranae* particularly because of the availability of parameter values. The effect of *Nosema ceranae* infection is estimated to double the mortality rate of adult foragers [10]. On that basis we take $d_H = d_F = m = 0.14$ deaths per bee per day. For the rates of transmission at first we considered different values of β_{HH} , β_{HF} , β_{FF} . Following some preliminary simulations, however, we found these different values have only a marginal qualitative effect on the overall dynamics of the disease. Accordingly, and in the absence of any field values on which to base a meaningful examination of this issue, the simulations which we

present in this paper are based on taking $\beta_{HH} = \beta_{HF} = \beta_{FF} = \beta$. Generally, transmission of the disease is mediated via the food stores [30], which makes it difficult in practice to measure the rate of transmission from an infected bee to a susceptible bee.

A summary of all the parameter values we used is provided in Table 2.1.

L	maximum rate of egg laying	2000 eggs/day	[21]
w	number of hive bees for 50% egg survival	5000 bees	[21]
R_b	baseline recruitment rate	25%/day	[7]
α_f	maximum additional recruitment in absence of food	25%/day	[27]
α_F	effect of excess foragers on recruitment	75%/day	[21]
m	natural death rate of foragers (active season)	14%/day	[6]
m_w	natural death rate of foragers and hive bees (winter)	0.56%/day	[26]
b	mass of food stored for 50% egg survival	500 g	[20]
c	food gathered per day per forager	0.1 g /day	[25]
γ	daily food requirement per adult bee	0.007 g	[20]
d_H	death rate of hive bees due to infection	14%/day	[10]
d_F	death rate of foragers due to infection	14%/day	[10]
β_{HH}	disease transmission rate: hive bee to hive bee	variable	
β_{HF}	disease transmission rate: hive bee to forager	variable	
β_{FH}	disease transmission rate: forager to hive bee	variable	
β_{FF}	disease transmission rate: forager to forager	variable	

Table 2.1: Parameter values and references.

2.4 Results

In what follows we present the results of numerical simulations of key scenarios that illustrate the main dynamics of the bee colony in the presence of disease.

To simulate the dynamics of the bee colony, we integrate the governing equations (Eqs. 2.1, 2.4, 2.5, 2.6, 2.7) numerically, with initial conditions $H_I(0) = F_I(0) = 0$ and $H_S(0), F_S(0)$ based on steady state values for the disease free equilibrium which can be determined analytically. The food stores, f , continue to grow throughout the active season, and we have found that the results are not sensitive to the initial value of food in the hive. We present scenarios in which the dynamics of the disease begin at day 100. The initial onset of infection is simulated by turning 10% of the susceptible foragers into infected foragers.

Scenario 0: In this scenario we illustrate the baseline demographic dynamics of the colony in the absence of disease, particularly to highlight the natural seasonal variations. Thus, for this purpose, in this case we introduce winter after the initial 100 days of integration. The results are shown in Figure 6.2. The figure shows that both the hive and the foraging bee populations decrease (from natural death) over winter, but sufficient numbers remain (because of a lower death rate within the safety of the hive) after a fairly long winter of 100 days. At day 200, the active season resumes and the colony rebounds to the pre-winter equilibrium.

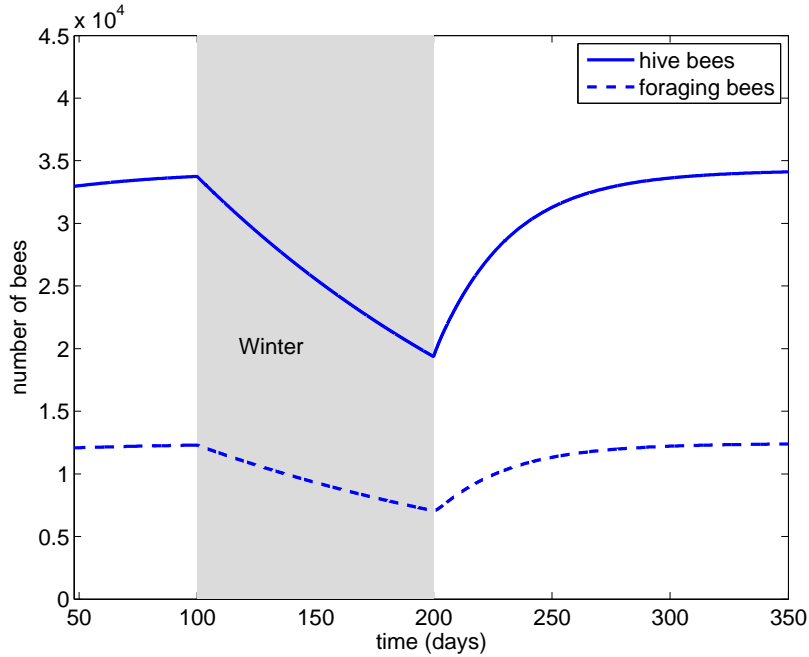


Figure 2.2: Baseline demographic dynamics of the honey bee colony in the absence of disease.

Scenario 1: In this scenario, after the initial 100 days we introduce infected foragers into the system, followed by winter 100 days later. The results are shown in Figure 2.3 based on $\beta = 5 \times 10^{-5}$ and $d_H = d_F = m = 0.14$. The figure shows that within about 5 days the susceptible bee population suffers a drastic drop and the majority of the hive bees have become infected. The infection greatly reduces the overall size of the colony but a new equilibrium is reached, with about 65% of the total population sustaining the infection. At the onset of winter, the size of the colony is not sustainable and within 50 days of winter the colony has collapsed.

Scenario 2: In this scenario we examine the effect of a more severe infection in which the transmission rate is unchanged but the mortality rates from the disease are increased to $d_H = d_F = 4m = 0.56$. The results, in Figure 2.4, show that after an initial drastic drop, the population of susceptible bees begins to recover approximately 10 days after the onset of the infection. The small numbers of infected hive and forager bees lead to their quick demise soon after the onset of winter, and the disease is eradicated from the hive within 25 days of the onset of winter. Thus, in this case while the colony has sustained heavy losses from the infection, it survives winter with a viable number of bees and no disease. A more severe infection, in the sense that it kills faster, can therefore lead to the survival of the colony as a whole.

Scenario 3: In this scenario we examine the effect of an increased rate of transmission, setting $\beta = 5 \times 10^{-3}$ and $d_H = d_F = 2m = 0.28$. The results are shown in Figure 2.5. The infection spreads quickly through the colony, the susceptible population is almost immediately

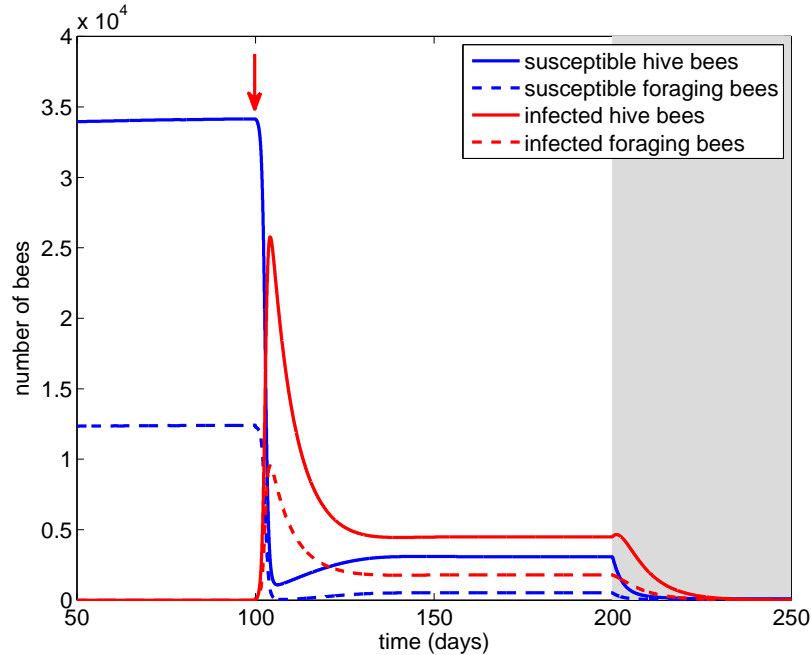


Figure 2.3: Scenario 1: Colony dynamics in the presence of disease with $\beta = 5 \times 10^{-5}$, $d_H = d_F = 0.14$. Red arrow = onset of infection, grey shading = winter.

eradicated, and within 30 days the colony drops drastically to $< 10\%$ of its size before infection. Thereafter, the colony population continues to dwindle slowly, and at the onset of winter it collapses within 10 days. For comparison, with the same natural death rate but in the absence of infection, the colony survives through winter and rebounds to its pre-winter level at the onset of the next active season as seen in Figure 2.2.

Age of Recruitment to Foraging Duties: The average age at which hive bees are recruited to foraging duties (AARF) under the three scenarios is shown in Figure 2.6. The figure shows that AARF is an important marker of the health of the colony in the sense that a colony with a younger workforce can be taken as a sign of disease within the colony. In Scenario 1, AARF is reduced from 19.6 days before the onset of infection to 13.16 after the infection. In Scenario 2, with a more severe infection, AARF is reduced to about 14.6 days, though fluctuating between 10 days and 16 days at first. In Scenario 3, with a higher rate of transmission of the infection, AARF is reduced drastically to 9.7 days. This value is determined from the inverse of the recruitment function, R .

Figure 2.7 shows the complex relationship between the rate of transmission β and disease-induced the death rates d_H, d_F in their effects on the AARF. The figure shows that a combination of small β and large d_H is favorable in that it leads to higher value of the AARF. At higher values of β , however, the AARF becomes less sensitive to the value of β (as indicated by the clumping of the curves in that region). The position of the three scenarios in this relationship as shown in the figure, and their ultimate fate as described earlier, shows again that AARF is an early marker of colony collapse, which has been supported by experimental evidence [1].

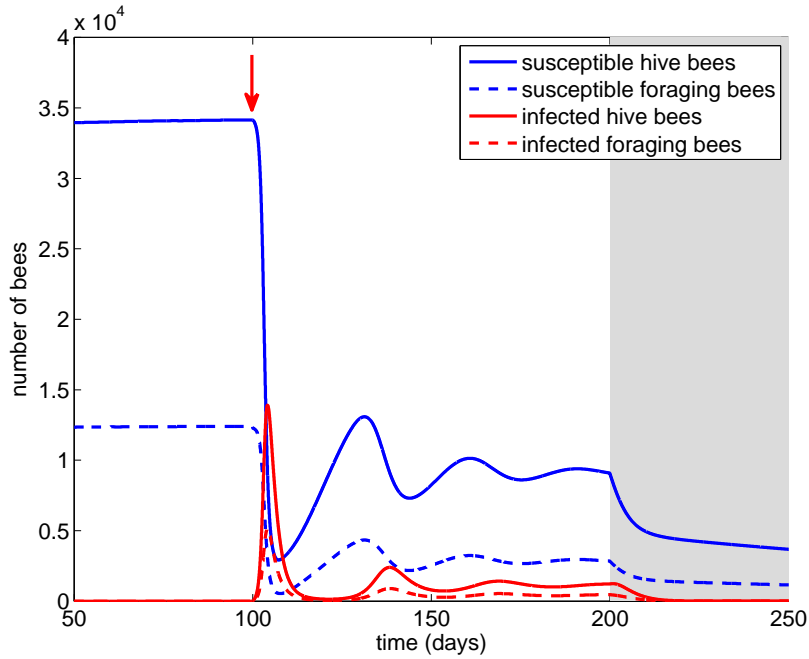


Figure 2.4: Scenario 2: Colony dynamics under a more severe infection represented by a higher death rates from the disease, with $\beta = 5 \times 10^{-5}$, $d_H = d_F = 0.56$. Red arrow = onset of infection, grey shading = winter.

Scenario 4: In this scenario, finally, we examine the effect of the timing of the infection in relation to the onset of winter. Figure 2.8 shows the effect of infection occurring only 10 days before the onset of winter, compared with 100 days in earlier scenarios. The results, compared with those in Scenario 2, show that the disease is eradicated sooner by early winter. This is clearly because healthy bees live longer in the safety of the hive in winter, while the death rate from infection is unchanged.

Another important indicator of the ultimate fate of the bee colony is the size of the bee population at the end of winter. While under all scenarios winter is taken to last 100 days, the size of the bee population at the end of winter is influenced by the severity of the disease (d_H, d_F), the transmission rate (β), and the time interval between the onset of infection and the beginning of winter which we shall denote Δt . This complex relationship is shown first in Figure 2.9 for Scenarios 1, 2, 3 where $\Delta t = 100$ days in all three cases. Again, we see a decrease in sensitivity to β at higher values of β . Furthermore, an increase in the value of d_H initially has an unfavorable effect on the colony size at end of winter, but at high values of d_H this effect is reversed. The region of fractional values is included in Figure 2.9 only for (mathematical) completeness of the figure. Biologically, the region represents colonies that do not survive. By comparison, in Scenario 4 where $\Delta t = 10$ the size of the bee population at end of winter is reduced by 38% from that in Scenario 2 where the values of other parameters are the same. A more general indication of the dependence of the size of the bee population

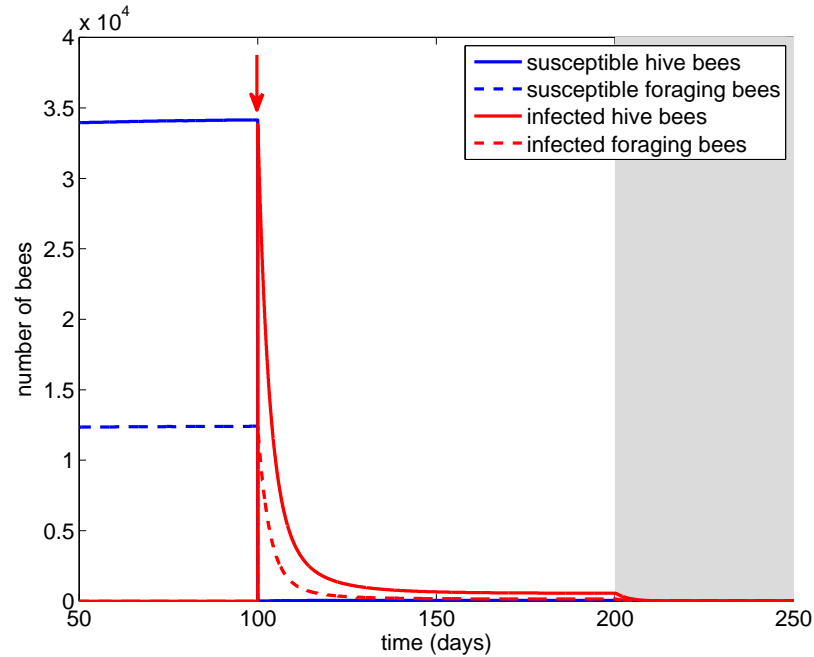


Figure 2.5: Scenario 3: Colony dynamics under a higher rate of transmission of the disease, with $\beta = 5 \times 10^{-3}$, $d_H = d_F = 0.56$. Red arrow = onset of infection, grey shading = winter.

at end of winter on Δt is shown in Figure 2.10. The figure shows that for $\Delta t < 20$ days or so, there is very high sensitivity to the value of Δt , but for $\Delta t > 20$ days or so this sensitivity is considerably diminished. This indicates that in the three weeks or so before winter the bee colony is most vulnerable to the risk of infection.

Finally, in Figure 2.11 we compare the effects of two major types of hazards faced by a honey bee colony, one in which there is a simple increase in the death rate of foragers because of exposure to an environmental hazard and another in which the bees are exposed to an infectious disease. Specifically, in this figure we contrast the dynamics of Scenario 3 with the dynamics of an environmental hazard scenario in which the hive is disease-free but the death rate from the environmental hazard is *the same as the total death rate in Scenario 3*. Specifically, in Scenario 3 we had $d_F = 0.28$, $d_H = 0.28$, $m = 0.14$ for a total death rate of 0.7, thus, for a comparable environmental hazard scenario we take $m = 0.7$ and $d_F = d_H = 0$. The figure shows clearly that the survival of the colony is almost guaranteed in the environmental hazard scenario, while the collapse of the colony is almost guaranteed in the disease scenario.

This comparison is clearly approximate because the three components of death rate in the infectious disease case (d_F, d_H, m) are independent of each other and therefore their sum is not accurately comparable to the total death rate in the environmental hazard case. For this reason, in Figure 2.12 we consider another comparison in which the dynamics of the two hazards are such that the *average lifespan of bees is the same in both cases*. The results again show that the colony survives under the environmental hazard.

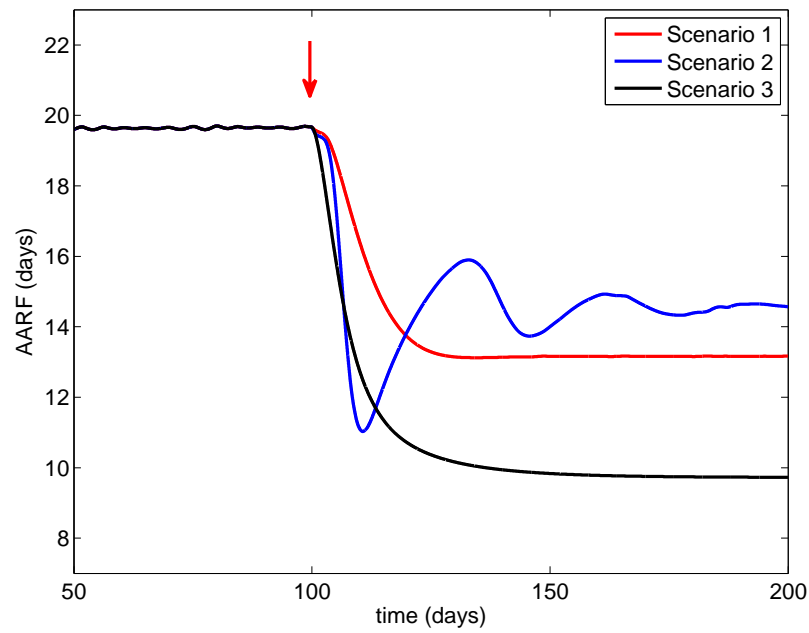


Figure 2.6: Average age of recruitment to foraging duties (AARF) under the three scenarios in Figures 2.3, 2.4, 2.5. Red arrow = onset of infection.

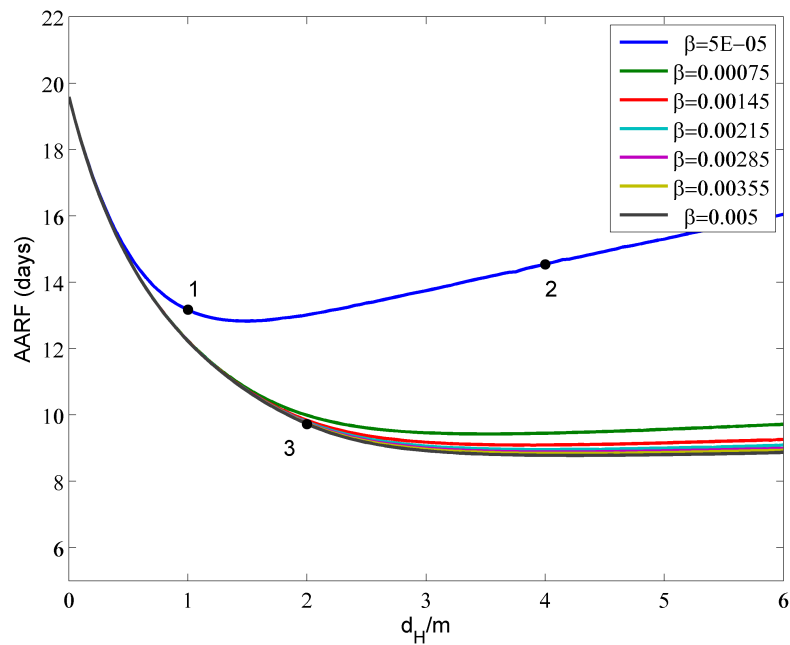


Figure 2.7: Relationship between the rate of transmission β and disease-induced death rates $d_H = d_F$ in their effects on the Average Age of Recruitment to Foraging (AARF). The figure shows the effects of an increase of β and d_H on the AARF. Note that the AARF becomes less sensitive to changes in β as β is increased. Meanwhile, for small β , an increase in d_H can have a favourable effect on the AARF.

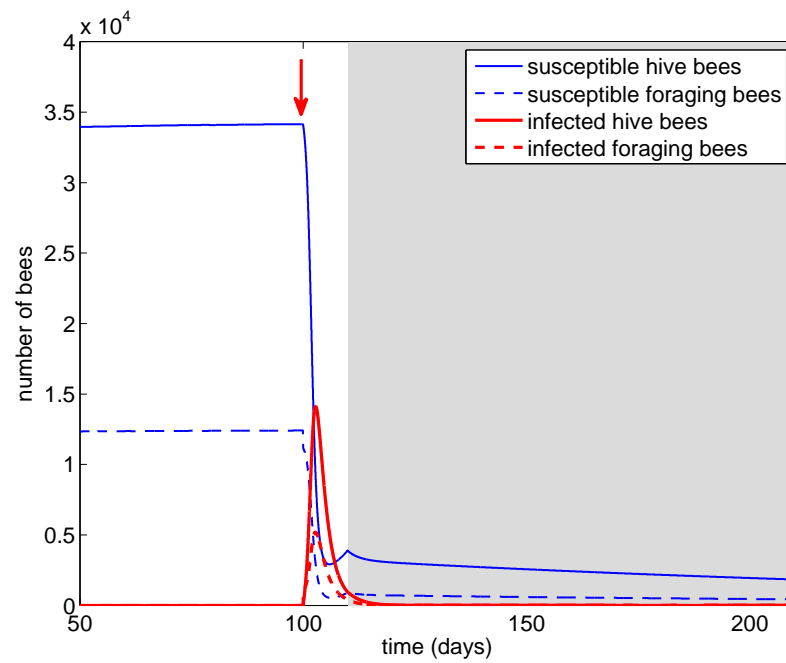


Figure 2.8: Scenario 4: $\beta = 5 \times 10^{-5}$, $d_H = d_F = 0.56$. Effect of the proximity of the onset of infection to the onset of winter. Red arrow = onset of infection, grey shading = winter.

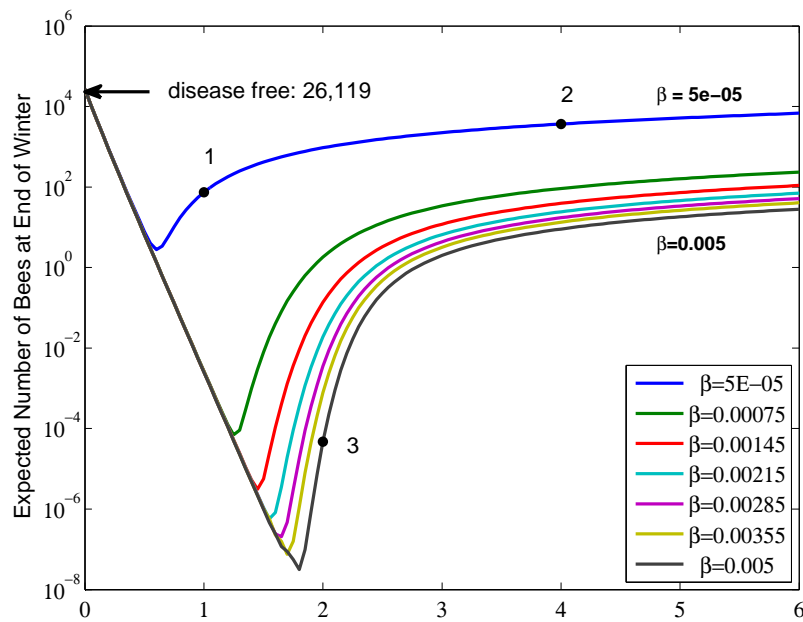


Figure 2.9: The expected size of the bee population at the end of winter as influenced by the severity of the disease ($d_H = d_F$) and the transmission rate of the disease (β). For comparison, the black arrow indicates the population size at end of winter in the absence of disease (Figure 2.2). The figure illustrates the different sensitivity to β and d_H . Note that d_H has a favourable effect for small β and d_H large enough.

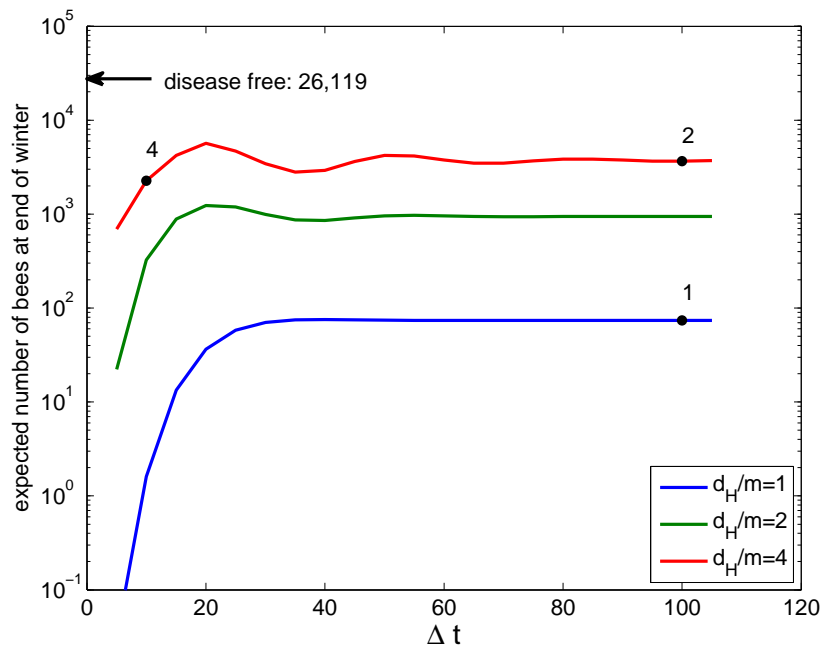


Figure 2.10: The expected size of the bee population at the end of winter as influenced by the time interval between the onset of infection and the beginning of winter (Δt), with $\beta = 5 \times 10^{-5}$. For comparison, the black arrow indicates the population size at end of winter in the absence of disease (Figure 6.2).

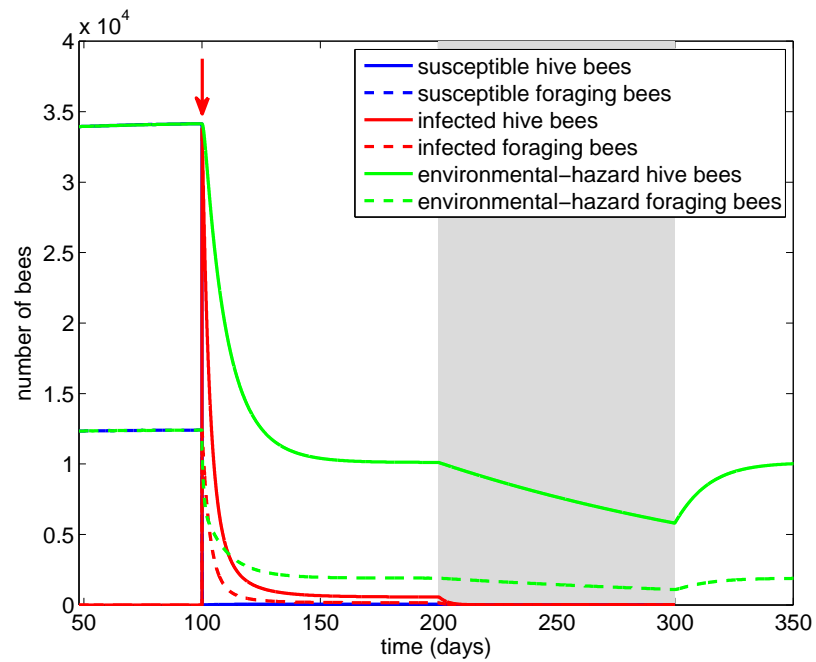


Figure 2.11: The stark difference between the dynamics of Scenario 3 with an environmental hazard scenario in which the death rate is increased (by the effects of pesticides, for example) *to equal the total death rate in Scenario 3*. The survival of the colony is almost guaranteed in the environmental hazard scenario while the collapse of the colony is almost guaranteed in the disease scenario.

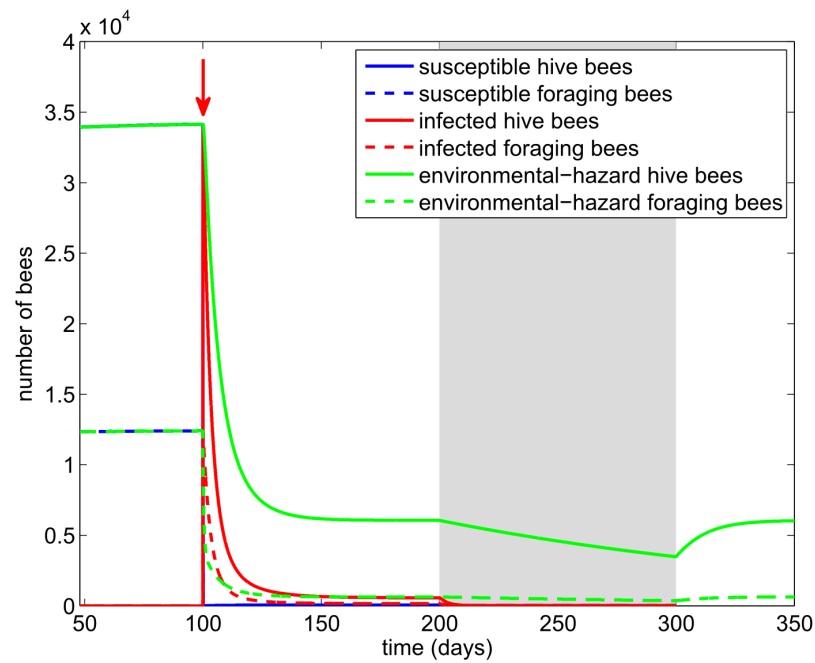


Figure 2.12: An alternative comparison of the dynamics of Scenario 3 with an environmental hazard scenario in which the comparison between the two hazards is based not on the total death rate as in Figure 2.11 but on the average lifespan of bees being the same in both cases.

2.5 Discussions and Conclusions

The main aim of this study was to construct a model for examining the way in which the dynamics of a honey bee colony are affected by an infection. We present this model in terms of a set of governing equations representing the interplay between the dynamics of the spread of the disease and the demographic dynamics of the bee colony. Up to this point the model is fairly general in regard to the specific characteristics of the colony or the disease and can thus be adapted to a variety of specific cases by an appropriate choice of parameter values. To illustrate the utility of the model, we chose parameter values associated with *Nosema ceranae* which has been well studied experimentally. Our findings, compared with those found experimentally are summarized in Table 2.2.

	Exp.	1	2	3
AARF- Healthy	14-21	19.6	19.6	19.6
AARF- Infected	7-16	13.1	14.6	9.7
$(H_I + F_I)/N$	45%	64%	12.2%	92%

Table 2.2: Tabulated results from the model scenarios 1, 2, and 3 and experimental data from [1] and [10]. The last row shows the percentage of the population infected at the endemic equilibrium, and the experimental value is the threshold value which leads to over-winter colony collapse.

The model suggests that key factors in the survival or collapse of a honey bee colony in the face of an infection are the rate of transmission of the infection β and the disease-induced death rates, d_H and d_F . An increase in the disease-induced death rates, which can be thought of as an increase in the severity of the disease, may actually help the colony overcome the disease and survive through winter (Scenario 2), which is consistent with SIR models of epidemics. By contrast, an increase in the transmission rate, which means that bees are being infected at an earlier age, has a drastic deleterious effect (Scenario 3).

Another important finding relates to the timing of infection in relation to the onset of winter. The results (Figure 2.10) suggest that in a time interval of approximately 20 days before the onset of winter the colony is most affected by the onset of infection. An infection during this “dangerous” time period is more likely to lead to colony collapse because the number of bees surviving through winter becomes unviable for a rebound of the colony in the new active season. Outside this dangerous time period, i.e. for $\Delta t > 20$ days, the survival of the colony is no longer critically affected by the timing of infection. It must be emphasized that the numerical value of 20 days for this dangerous time period is likely not a “universal” value but one that is specific to the choice of parameter values we used both for the colony and the disease. With other combinations of colony and disease parameters, the model can be used to find the corresponding critical time period.

Our results (Figures 2.6 and 2.7) suggest that AARF is a good early marker for the survival or collapse of a honey bee colony in the face of infection. This is consistent with experimental evidence in [1] but the model and the results in Figures 2.6 and 2.7 provide an insight into the underlying mechanisms for this.

Finally, an important result of this study is the clear distinction between two major types of hazards faced by a honey bee colony, namely, one in which there is a simple increase in

the death rate of bees because of exposure to an environmental hazard such as pesticides or insecticides, and another in which the bees are exposed to an infectious disease. The results in Figure 2.11 show that an exposure to an infectious disease is almost guaranteed to lead to colony collapse while under an environmental hazard the colony has a good chance of survival. This conclusion is confirmed by the results of Figure 2.12 in which the comparison between the two hazards is based not on the total death rate but on the average lifespan of bees being the same in both cases. Since an environmental hazard in the first place affects only forager bees, the comparison in this case is equivalent to considering a more severe environmental hazard than that in Figure 2.11, or to considering the long term consequences of an environmental hazard as it affects the demographics of the colony. Together, the two comparisons lead us to suspect that, under comparable death rates and the range of disease transmission rates which we have considered, an infectious disease may typically be more hazardous to the survival of a bee colony than an exposure to pesticide or insecticide.

Acknowledgment

This work was supported by the Natural Sciences and Engineering Research Council of Canada. We thank Mary Myerscough and Gloria DeGrandi-Hoffman for insightful comments.

Bibliography

- [1] BOTIAS, C., MARTIN-HERNANDEZ, R., BARRIOS, L., MEANA, A., AND HIGES, M. *Nosema* spp. infection and its negative effects on honey bees (*Apis mellifera iberiensis*) at the colony level. *Veterinary research* 44, 1 (2013), 1–15.
- [2] CALDERONE, N. W. Insect pollinated crops, insect pollinators and US agriculture: Trend analysis of aggregate data for the period 1992-2009. *PLOS ONE* 7, 5 (05 2012), e37235.
- [3] CHEN, Y., EVANS, J. D., SMITH, I. B., AND PETTIS, J. S. *Nosema ceranae* is a long-present and wide-spread microsporidian infection of the European honey bee (*Apis mellifera*) in the United States. *Journal of Invertebrate Pathology* 97, 2 (2008), 186–188.
- [4] CRAMP, D. *A Practical Manual of Beekeeping*. How To Books, London, 2008.
- [5] DEVILLERS, J. The ecological importance of honey bees and their relevance to ecotoxicology. In *Honey Bees: Estimating the Environmental Impact of Chemicals*, J. Devillers and M. Pham-Delègue, Eds. Taylor and Francis London, London, 2002, pp. 1–11.
- [6] DUKAS, R. Mortality rates of honey bees in the wild. *Insectes Sociaux* 55, 3 (2008), 252–255.
- [7] FAHRBACH, S., AND ROBINSON, G. Juvenile hormone, behavioral maturation and brain structure in the honey bee. *Developmental Neuroscience* 18 (1996), 102–114.
- [8] FAVRE, D. Mobile phone-induced honeybee worker piping. *Apidologie* 42, 3 (2011), 270–279.
- [9] FRIES, I. *Nosema ceranae* in European honey bees (*Apis mellifera*). *Journal of invertebrate pathology* 103 (2010), S73–S79.
- [10] GOBLIRSCH, M., HUANG, Z. Y., AND SPIVAK, M. Physiological and behavioral changes in honey bees (*Apis mellifera*) induced by *Nosema ceranae* infection. *PLOS ONE* 8, 3 (03 2013), e58165.
- [11] HARBO, J. R. Effect of brood rearing on honey consumption and the survival of the worker honey bees. *Journal of Apicultural Research* 32, 1 (1993), 11–17.
- [12] HENRY, M., BEGUIN, M., REQUIER, F., ROLLIN, O., ODOUX, J.-F., AUPINEL, P., APTEL, J., TCHAMITCHIAN, S., AND DECOURTYE, A. A common pesticide decreases foraging success and survival in honey bees. *Science* 336, 6079 (2012), 348–350.

- [13] HIGES, M., MARTIN-HERNANDEZ, R., BOTIAS, C., BAILON, E. G., GONZALEZ-PORTO, A. V., AND BARRIOS, L. How natural infection by *Nosema ceranae* causes honeybee colony collapse. *Environmental microbiology* 10, 10 (2008), 2659–2669.
- [14] HIGES, M., MARTIN-HERNANDEZ, R., GARRIDO-BAILON, E., GONZALEZ-PORTO, A. V., GARCIA-PALENCIA, P., AND MEANA, A. Honeybee colony collapse due to *Nosema ceranae* in professional apiaries. *Environmental Microbiology Reports* 1, 2 (2009), 110–113.
- [15] HO, M.-W., AND CUMMINS, J. Mystery of disappearing honeybees. *Science in Society* 34 (2007), 35–36.
- [16] HUANG, Z.-Y., AND ROBINSON, G. E. Regulation of honey bee division of labor by colony age demography. *Behavioral Ecology and Sociobiology* 39 (1996), 147–158.
- [17] JAY, S. Seasonal development of honeybee colonies started from package bees. *Journal of Apicultural Research* 13 (1974), 149–152.
- [18] JONES, J. C., HELLIWELL, P., BEEKMAN, M., MALESZKA, R., AND OLDROYD, B. The effects of rearing temperature on developmental stability and learning and memory in the honey bee, *Apis mellifera*. *Journal of Comparative Physiology A* 191, 12 (2005), 1121–1129.
- [19] KAUFFELD, N. M. *Beekeeping in the United States Agriculture Handbook Number 335*. U.S. Department of Agriculture, 1980.
- [20] KHOURY, D. S., BARRON, A. B., AND MYERSCOUGH, M. R. Modelling food and population dynamics in honey bee colonies. *PLOS ONE* 8, 5 (05 2013), e59084.
- [21] KHOURY, D. S., MYERSCOUGH, M. R., AND BARRON, A. B. A quantitative model of honey bee colony population dynamics. *PLOS ONE* 6, 4 (04 2011), e18491.
- [22] LEONCINI, I., LE CONTE, Y., COSTAGLIOLA, G., PLETTNER, E., TOTH, A. L., AND WANG, M. Regulation of behavioral maturation by a primer pheromone produced by adult worker honey bees. *Proceedings of the National Academy of Sciences of the United States of America* 101, 50 (2004), 17559–17564.
- [23] NEUMANN, P., AND CARRECK, N. L. Honey bee colony losses. *Journal of Apicultural Research* 49, 1 (2010), 1–6.
- [24] RATTI, V., KEVAN, P. G., AND EBERL, H. J. A mathematical model for population dynamics in honeybee colonies infested with *Varroa destructor* and the Acute Bee Paralysis Virus. *Canadian Applied Mathematics Quarterly* 21, 1 (2013), 63–93.
- [25] RUSSELL, S., BARRON, A. B., AND HARRIS, D. Dynamic modelling of honey bee (*Apis mellifera*) colony growth and failure. *Ecological Modelling* 265, 0 (2013), 158 – 169.
- [26] SAKAGAMI, S., AND FUKUDA, H. Life tables for worker honeybees. *Researches on Population Ecology* 10, 2 (1968), 127–139.

- [27] SCHULZ, D. J., HUANG, Z.-Y., AND ROBINSON, G. E. Effects of colony food shortage on behavioral development in honey bees. *Behavioral Ecology and Sociobiology* 42, 5 (1998), 295–303.
- [28] SEELEY, T. D. *Honeybee Democracy*. Princeton University Press, 2010.
- [29] SEELEY, T. D., AND VISSCHER, P. K. Survival of honeybees in cold climates: the critical timing of colony growth and reproduction. *Ecological Entomology* 10, 1 (1985), 81–88.
- [30] SMITH, M. L. The honey bee parasite *Nosema ceranae*: Transmissible via food exchange? *PLOS ONE* 7, 8 (08 2012), e43319.
- [31] SOUTHWICK, E. E., AND SOUTHWICK JR, L. Estimating the economic value of honey bees (*Hymenoptera: Apidae*) as agricultural pollinators in the United States. *Journal of Economic Entomology* 85, 3 (1992), 621–633.
- [32] STEVANOVIC, J., SIMEUNOVIC, P., GAJIC, B., LAKIC, N., RADOVIC, D., FRIES, I., AND STANIMIROVIC, Z. Characteristics of *Nosema ceranae* infection in Serbian honey bee colonies. *Apidologie* 44, 5 (2013), 522–536.
- [33] SUMPTER, D. J. T., AND MARTIN, S. J. The dynamics of virus epidemics in *Varroa*-infested honey bee colonies. *Journal of Animal Ecology* 73, 1 (2004), 51–63.
- [34] VANENGELSDORP, D., EVANS, J. D., SAEGERMAN, C., MULLIN, C., HAUBRUGE, E., NGUYEN, B. K., FRAZIER, M., FRAZIER, J., COX-FOSTER, D., CHEN, Y., UNDERWOOD, R., TARPY, D. R., AND PETTIS, J. S. Colony collapse disorder: A descriptive study. *PLOS ONE* 4, 8 (08 2009), e6481.
- [35] WATANABE, M. E. Colony collapse disorder: Many suspects, no smoking gun. *BioScience* 58, 5 (2008), 384–388.
- [36] WINSTON, M. *The biology of the honey bee*. Harvard University Press, 1987.

Chapter 3

Reproduction Number And Asymptotic Stability For The Dynamics of a Honey Bee Colony with Continuous Age Structure

Abstract

A system of partial differential equations is derived as a model for the dynamics of a honey bee colony with a continuous age distribution, and the system is then extended to include the effects of a simplified infectious disease. In the disease-free case we analytically derive the equilibrium age distribution within the colony and propose a novel approach for determining the global asymptotic stability of a reduced model. Furthermore, we present a method for determining the basic reproduction number R_0 of the infection; the method can be applied to other age-structured disease models with interacting susceptible classes. The results of asymptotic stability indicate that a honey bee colony suffering losses will recover naturally so long as the cause of the losses is removed before the colony collapses. Our expression for R_0 has potential uses in the tracking and control of an infectious disease within a bee colony.

3.1 Introduction

Honey bee populations continue to decline on a global scale [3], and as research efforts to identify the underlying cause or causes continue [23, 63, 65], there is as yet no clear resolution of the problem. While the consequences of the decline are usually discussed in the context of agriculture and economics [9, 37, 54], the key question clearly hinges on the stability of a honey bee colony as a population dynamical system. Mathematical models thus provide critically important tools for studying honey bee populations as they can both simulate many different environments as well as suggest potential sensitivities a colony may have to environmental hazards such as pesticides and climate change, or microbial hazards such as parasites and disease.

Mathematical models have been used in recent years to shed light on the effects of pesticides on the lifespan of foraging bees [29, 30]. Other models have focused on the changing

dynamics of a colony under changing environmental conditions [58], or the interactions between colonies [49]. Recent work has also investigated the effects of infection on honey bee colony dynamics, including Varroa mites [17, 44, 45] and nosema [5], the latter approximating infection through mass action. An approach from systems biology has been used to explore the multifactorial causes of colony failure [2].

One of the complicating factors in the dynamics of a honey bee colony is the age distribution (structure) within the colony since age groups may differ in their expected lifespans, foraging behaviour or susceptibility to a given hazard. While age-independent models have provided a number of key insights into the properties of colony dynamics [5, 30, 44], the ultimate conditions for the survival or collapse of a honey bee colony must take into account this added dimension of the problem.

From a mathematical standpoint, incorporating the age structure of a honey bee colony into the equations governing the population dynamics leads to a set of partial differential equations instead of the ordinary differential equations obtained when age structure is not included. The problem of finding stability and equilibrium conditions for the dynamics of the colony becomes correspondingly more complex. When considering disease dynamics, the problem of finding the basic reproduction number (R_0) at which the fate of the colony is at a bifurcation becomes particularly difficult.

We propose a method of resolving these mathematical difficulties by transforming the problem from the real space (age, time) into the Laplace space such that the governing equations become ordinary differential equations, and from the solution of these equations it is then possible to deduce the asymptotic behavior of the dynamical system in the real space. In particular, in the absence of disease we show that the system has an asymptotically stable equilibrium, which implies that the bee population will rebound from losses when hazards are removed, provided they are removed before the complete demise of the colony. In the presence of disease we use a linearized form of the system to obtain a closed form expression for the basic reproduction number R_0 . The expression thus provides a measurable threshold for whether the disease will decay or persist.

Determining R_0 for age-structured models has been previously studied for general disease models with one infected class [25, 32, 59]. Our model has the added complexity of having two interacting infected classes, namely infected hive bees (H_I) and infected foragers (F_I), that cannot be transformed into a single infected class for analysis. Moreover, work on the asymptotic stability of disease models with age structure is sparse. Several studies use Lyapunov functions and semi-group analysis to prove persistence of solutions [21, 33], while perturbation analysis has also proved useful [26]. Other work has made use of properties of the particular model at hand to show stability [11].

In the present study, we take advantage of detailed experimental work elucidating the distinct roles that honey bees of different ages play within a honey bee colony, and use this information to develop a model of honey bee demographics with continuous age structure (Section 3.2). This model is then extended to include the dynamics of an infectious disease within the colony. In particular, we find a stability threshold criterion which corresponds to the basic reproduction number R_0 . In Section 3.3.1, we use a steady-state approximation to derive the equilibrium age distribution of the disease-free hive. In 3.3.2, we develop a novel Laplace transform approach to prove global stability of this disease-free distribution in a reduced model, implying local stability in the full model. In 3.3.3, we again develop a novel approach to find a

threshold criterion at which this equilibrium state becomes unstable, and an infection will invade; this threshold corresponds to the basic reproductive number, R_0 . In Section 4, we discuss the implications of these results and suggest possible applications of the new approaches we have developed to other problems in population dynamics.

3.2 Model

The proposed model combines the normal demographics of a honey bee colony with a disease that at first infects foragers and then spreads to the rest of the colony. As in previous studies, to keep the problem tractable, we focus on hive bees, H , which are primarily responsible for maintenance of the brood, and foragers, F , which are responsible for bringing food, f , into the hive. Although hive bees can take on other duties such as guarding or hive maintenance, for simplicity we do not model these roles explicitly, but assume all hive bees contribute either directly or indirectly to the survival of the brood. Male honey bees, known as drones, do not contribute to the maintenance of the hive, so this population is not included in the model.

Generally, bees emerge from the brood as hive bees and are later recruited to foraging duties. These two classes are further divided, in the presence of disease, into susceptible populations, H_S and F_S , and infected populations, H_I and F_I . The following sections present the governing equations for each of these sub-populations. The total size of the colony to be modeled in age, a (days), and time, t (days), is thus,

$$N(t) = \int_0^{\infty} (H_S(a, t) + H_I(a, t) + F_S(a, t) + F_I(a, t)) da, \quad (3.1)$$

while the total infected population of the hive, denoted I , is

$$I(t) = \int_0^{\infty} (H_I(a, t) + F_I(a, t)) da. \quad (3.2)$$

Susceptible Hive Bees: For the susceptible hive bee population $H_S(a, t)$, incorporating age using the standard approach of McKendrick [36] into our earlier formulation of the problem [5], the governing equation becomes

$$\frac{\partial H_S(a, t)}{\partial t} + \frac{\partial H_S(a, t)}{\partial a} = -u(a, t)H_S(a, t) - \beta I(t)H_S(a, t). \quad (3.3)$$

Here, the first term on the right-hand side represents the recruitment of hive bees to foraging duties, as described below, where $u(a, t)$ denotes the age-dependent rate of recruitment. The second term on the right governs the disease dynamics within the colony, as described in the next subsection. It is assumed that the hive provides sufficient safety for bees that remain within it [30, 51] such that the natural death rate of healthy hive bees is negligible compared to the rate of recruitment to foraging.

Research has shown that juvenile hormone III regulates the age at which honey bees begin foraging [46], and there is a minimum age, a_R , at which hive bees are normally recruited to foraging duties [18]. If the foraging needs of the colony are not being met, however, hive

bees will be recruited to foraging duties at a younger age [24]. Conversely, if the foraging bee population exceeds the needs of the colony, foragers produce a pheromone, ethyl oleate, to reduce recruitment [31]. We incorporate these regulatory mechanisms by taking

$$u(a, t) = \alpha \left(\frac{a}{a+k} \right)^2 \left(1 - \frac{\sigma}{N(t)} \int_0^\infty (F_S + F_I) da \right) H_v(a - a_R) \quad (3.4)$$

where α is a free parameter representing the base rate of recruitment, $H_v(a - a_R)$ is the Heaviside function, and $1/\sigma$ is the maximum allowable fraction of foragers in the colony size. Thus recruitment begins at age a_R and increases sigmoidally with age thereafter where k is the age at which recruitment is at a quarter of its maximal rate. The form of this sigmoidal function, $(a/(a+k))^2$, was chosen as it yielded the best fit to available data describing the age distribution of a healthy honey bee colony [4].

Disease dynamics: To retain analytical tractability when both age- and caste-structure have been added to the model, we use the simplest possible approximation for disease dynamics. In particular, we assume the infection is transmitted via mass action at a constant rate β , and infection can be transferred from hive bees to foragers or vice versa. While mass action kinetics, with no time delay, are unlikely to be the best possible model for any particular disease of honey bees, this model allows us to gain analytical insight into key broad features of infection in the colony. Mass action kinetics provide a reasonable approximation for certain modes of transmission; for example, in the case of nosema, fecal-oral transmission [55], and contamination of food stores [53] can be modeled by mass action under the assumptions that food is well-mixed and infected food is proportional to infected foragers. Of course, nosema infects food stores and bees via the microsporidian *Nosema ceranae* [6, 53]. The microsporidian population within the hive fluctuates seasonally and adds a further complexity to nosema infection in colonies. The simple transmission terms we assume will clearly not capture the complete pathogenesis of nosema infections [42].

Three important simplifying assumptions underpin disease transmission in the model. The first is that hive bees and foragers are both infected (and infect) at the same rate, while the second is that the disease affects both equally (i.e. same disease-induced death rate for both classes). Both of these assumptions have been chosen to allow for a simple, general model. The methods described here, however, remain valid if the second assumption is relaxed, that is, the approach can also be used to describe a disease which affects the lifespan of hive bees and foragers differently. Lastly, we assume infected bees are recruited to foraging at the same rate as healthy bees. We have previously demonstrated that despite this simplifying assumption, a related model [5] is able to capture reductions caused by infection in the average age at which bees are recruited to foraging.

Infected Hive Bees: Infected hive bees are at risk of dying due to disease at an age-dependent rate $d(a)$. The equation governing their dynamics is then

$$\frac{\partial H_I(a, t)}{\partial t} + \frac{\partial H_I(a, t)}{\partial a} = \beta I(t) H_S(a, t) - [u(a, t) + d(a)] H_I(a, t). \quad (3.5)$$

Susceptible Foragers: Susceptible foragers are recruited from susceptible hive bees and are subject to age-dependent natural death at rate $\mu(a)$. The equation governing their dynamics

is thus given by

$$\frac{\partial F_S(a, t)}{\partial t} + \frac{\partial F_S(a, t)}{\partial a} = u(a, t)H_S(a, t) - [\mu(a) + \beta I(t)]F_S(a, t). \quad (3.6)$$

In all of the analytical work to follow (Sections 3.3.1, 3.3.2, 3.3.3 and 3.3.4), the function $\mu(a)$ is completely general. For illustrative purposes (in the figures only), a quadratic function has been used to match qualitative observations of forager mortality. In particular, precocious foraging has been shown to have deleterious effects on forager lifespan [27, 62], while mortality has been observed to increase with chronological age [16]. Given these two observations, the simplest smooth function that agrees qualitatively would be a quadratic with a central age at which mortality is at a minimum. The function used for numerical illustrations in this study is provided in Table A.1.

Infected Foragers: Infected foragers can be either (i) infected hive bees that have been recruited to foraging duties or (ii) susceptible foragers that have become infected by either infected foragers or infected hive bees. They are subject to a disease-related death rate, $d(a)$, and their dynamics are governed by

$$\frac{\partial F_I(a, t)}{\partial t} + \frac{\partial F_I(a, t)}{\partial a} = u(a, t)H_I(a, t) + \beta I(t)F_S(a, t) - [\mu(a) + d(a)]F_I(a, t). \quad (3.7)$$

Food stores: Food, f , is brought into the hive by both susceptible and infected foragers. For simplicity, we assume that all foragers bring in food at the same rate c (g/day), although it is likely that infected foragers would be less efficient at the task. Food is consumed by foragers and hive bees at, again for simplicity, the same rate, γ . The amount of food available at time t is therefore given by

$$\frac{df}{dt} = c \int_0^{\infty} (F_S + F_I) da - \gamma N. \quad (3.8)$$

Boundary Conditions: The system of equations (3.3),(3.5),(3.6),(3.7) is subject to the following boundary conditions:

$$\begin{cases} H_S(0, t) = LV(t) \\ H_I(0, t) = F_S(0, t) = F_I(0, t) = 0. \end{cases} \quad (3.9)$$

The first condition represents the birth of new bees where L is the daily egg laying rate by the queen and V is a survivability function which determines how many of the brood survive to become viable hive bees. The brood needs both sufficient food and sufficient care from the hive bees in order to survive [28]. Moreover, it has been shown that there is a range of ages within which hive bees will care for the brood. Field data suggest that hive bees take on nursing duties at a minimum age a_{mn} and complete these duties at a maximum age a_{mx} . After this age, hive bees tend to either transition to foraging duties or take on hive security or maintenance duties [66]. On this basis, we define the survivability function $V(t)$ as

$$V(t) = \mathcal{W} \left(\frac{f}{b + f} \right) \left(\frac{\int_{a_{mn}}^{a_{mx}} H_S(a, t) da}{w + \int_{a_{mn}}^{a_{mx}} H_S(a, t) da} \right), \quad (3.10)$$

where b is the amount of food required for half the brood to survive to adulthood in the presence of sufficient care from hive bees, and w is the number of nursing hive bees necessary to ensure survival of half the brood in the presence of sufficient food stores. The term \mathcal{W} provides a ‘conversion’ of eggs to bees with a fixed value of $\mathcal{W} = 1$ bee per egg, and can be interpreted as the maximum number of bees produced by a single egg. The number of new hive bees created from L eggs is dependent on the amount of food available as well as the amount of care available. The boundary conditions for the infected classes assume that bees cannot emerge infected.

Equations (3.3), (3.5), (3.6), (3.7), (3.8) form a system of integro-partial differential equations to be solved simultaneously subject to the boundary conditions (3.9).

Numerical Treatment: For illustrative purposes (the figures only), the full system was solved numerically using a finite difference scheme [20], using parameter values provided in Table 3.1. Age was divided into N classes, each of size Δa , and the first derivative was approximated by using a backward difference [52]. Time integration used Forward Euler [12] from an initial condition of $H(a, 0) = 10^4 e^{-a}$, $F(a, 0) = 0$ with step size of $\Delta t = 10^{-3}$. The limit as $a \rightarrow \infty$ was approximated by using a maximum value $A_{max} \gg \Delta a$. Solutions were considered to be at steady state when $\|(F_S(a, t_n) + H_S(a, t_n)) - (F_S(a, t_{n-1}) + H_S(a, t_{n-1}))\|_2 < 10^{-10} \Delta t$.

3.3 Results

3.3.1 Existence

We use the method of characteristics [39], with characteristics given by

$$\frac{da}{dt} = 1, \quad a(0) = 0 \quad (3.11)$$

$$\frac{dt}{da} = 1, \quad t(0) = t_0. \quad (3.12)$$

The latter equations lead to parallel characteristics of the form $t(a) = a + t_0$. Along these characteristics, the populations $H_S(a, t(a))$, $F_S(a, t(a))$, $H_I(a, t(a))$, and $F_I(a, t(a))$ satisfy the

equations

$$\begin{aligned} \frac{dH_S}{da} = & -u(a, t(a))H_S(a, t(a)) \\ & - \beta H_S(a, t(a)) \int_0^\infty H_I(a^*, t(a^*)) + F_I(a^*, t(a^*)) da^* \end{aligned} \quad (3.13)$$

$$\begin{aligned} \frac{dF_S}{da} = & u(a, t(a))H_S(a, t(a)) - \mu(t(a))F_S(a, t(a)) \\ & - \beta F_S(a, t(a)) \int_0^\infty H_I(a^*, t(a^*)) + F_I(a^*, t(a^*)) da^* \end{aligned} \quad (3.14)$$

$$\begin{aligned} \frac{dH_I}{da} = & -(u(a, t(a)) - d(t(a)))H_I(a, t(a)) \\ & + \beta H_S(a, t(a)) \int_0^\infty H_I(a^*, t(a^*)) + F_I(a^*, t(a^*)) da^* \end{aligned} \quad (3.15)$$

$$\begin{aligned} \frac{dF_I}{da} = & u(a, t(a))H_I(a, t(a)) - (\mu(t(a)) + d(t(a)))F_I(a, t(a)) \\ & + \beta F_S(a, t(a)) \int_0^\infty H_I(a^*, t(a^*)) + F_I(a^*, t(a^*)) da^* \end{aligned} \quad (3.16)$$

with initial values

$$H_S(a, t_0) = LV(t_0)e^{-a} \quad (3.17)$$

$$F_S(a, t_0) = H_I(a, t_0) = F_I(a, t_0) = 0. \quad (3.18)$$

Due to the discontinuity in $u(a, t)$, we cannot find a unique differentiable solution to equations (13), (14), (15), and (16). We can however split the problem at the discontinuity and solve the system in two parts. Patching together these two solutions allows us to infer the existence of a continuous, but not differentiable, weak solution to the governing PDEs.

The first-order integro-differential equations (13), (14), (15), and (16) – which define the steady-state distribution of bees – can be reduced to a finite set of ordinary differential equations through methods developed in [14, 15, 19]. The approach described therein creates a map between a system of integro-differential equations with a degenerate kernel (i.e. $K(x, y) = K_1(x)K_2(y)$), and an equivalent system of ordinary differential equations which are guaranteed to have a unique solution on $a \in (0, a_R)$ [7]. We denote these solutions as $Hj_S(a, t)$, $Fj_S(a, t)$, $Hj_I(a, t)$, and $Fj_I(a, t)$ (j for ‘juvenile’). As well, we appeal to the same theoretical framework to guarantee a solution in the interval $a \in (a_R, \infty)$, denoted $Hm_S(a, t)$, $Fm_S(a, t)$, $Hm_I(a, t)$, and $Fm_I(a, t)$ (m for ‘mature’), provided $Hm_I(a, t)$ and $Fm_I(a, t)$ are bounded and decay as $a \rightarrow \infty$. The full solution is continuous on $a \in (0, \infty)$ under the conditions

$$Hm_S(a_R, a_R + t_0) = Hj_S(a_R, a_R + t_0) \quad (3.19)$$

$$Fm_S(a_R, a_R + t_0) = Fj_S(a_R, a_R + t_0) \quad (3.20)$$

$$Hm_I(a_R, a_R + t_0) = Hj_I(a_R, a_R + t_0) \quad (3.21)$$

$$Fm_I(a_R, a_R + t_0) = Fj_I(a_R, a_R + t_0). \quad (3.22)$$

These conditions act as initial conditions for equations (13), (14), (15), and (16) on the interval $a \in (a_R, \infty)$. As the characteristics are parallel, the solution is unique in the entirety of at -space.

3.3.2 Disease-free Equilibria (DFE)

One equilibrium for the disease-free system is the trivial equilibrium

$$H_S(a) = F_S(a) = f(t) = 0. \quad (3.23)$$

A second equilibrium exists, and is the solution to the ODE system,

$$\frac{dH_S^{**}}{da} = -u(a)H_S^{**}(a) \quad (3.24)$$

$$\frac{dF_S^{**}}{da} = u(a)H_S^{**}(a) - \mu(a)F_S^{**}(a) \quad (3.25)$$

$$\gamma N(t) = c \int_0^\infty F_S^{**}(a) da \quad (3.26)$$

where H_S^{**} and F_S^{**} denote the steady state solutions. We may relax condition (3.26) by setting $\frac{df}{dt} \geq 0$ as opposed to $\frac{df}{dt} = 0$, and instead seek a *quasi-steady state* under which food may be bounded, or may grow unbounded. Note that the quasi-steady state conditions include the true equilibrium as well.

Equations (3.3) and (3.6) are non-linear, and coupled in such a way as to make an analytical expression for their equilibrium evasive. The nonlinearities for the system all appear in the term $u(a)$, given by equation (3.4), which also depends on H_S and F_S in the disease-free case through the integrals $\int F_S da/N$. At equilibrium, this term will reduce to a constant. In other words, we can rewrite the term

$$\frac{\int F_S da}{N} = K_1$$

at equilibrium. In the case of bounded food stores, as in equation (3.26),

$$K_1 = \frac{\gamma}{c}$$

but in the case of unbounded food stores,

$$K_1 \geq \frac{\gamma}{c}.$$

We write the recruitment function at equilibrium, $u_{eq}(a)$ as

$$u_{eq}(a) = \alpha \left(\frac{a}{k+a} \right)^2 (1 - \sigma K_1) H_v \left(\frac{\hat{a} - \hat{a}_R}{K} \right) \quad (3.27)$$

$$= K \left(\frac{a}{k+a} \right)^2 H_v \left(\frac{\hat{a} - \hat{a}_R}{K} \right) \quad (3.28)$$

where $K = \alpha(1 - \sigma K_1)$. We may then rescale the time variables of the system ($\hat{t} = Kt$ and $\hat{a} = Ka$) to obtain the scaled system,

$$K \frac{dH_S^*}{d\hat{a}} = -K \left(\frac{\hat{a}/K}{\hat{a}/K + \hat{k}/K} \right)^2 H_v \left(\frac{\hat{a} - \hat{a}_R}{K} \right) H_S^*(\hat{a}) \quad (3.29)$$

$$K \frac{dF_S^*}{d\hat{a}} = K \left(\frac{\hat{a}/K}{\hat{a}/K + \hat{k}/K} \right)^2 H_v \left(\frac{\hat{a} - \hat{a}_R}{K} \right) H_S^*(\hat{a}) - \mu(\hat{a})F_S^*(\hat{a}) \quad (3.30)$$

We can then simplify the system to

$$\frac{dH_S^*}{d\hat{a}} = -\left(\frac{\hat{a}}{\hat{a} + \hat{k}}\right)^2 H_v \left(\frac{\hat{a} - \hat{a}_R}{K}\right) H_S^*(\hat{a}) \quad (3.31)$$

$$\frac{dF_S^*}{d\hat{a}} = \left(\frac{\hat{a}}{\hat{a} + \hat{k}}\right)^2 H_v \left(\frac{\hat{a} - \hat{a}_R}{K}\right) H_S^*(\hat{a}) - \hat{\mu}(\hat{a}) F_S^*(\hat{a}) \quad (3.32)$$

where $\hat{\mu}(a) = \mu(a)/K$. The solutions of equations (3.31) and (3.32) in scaled variables are independent of K (shown below).

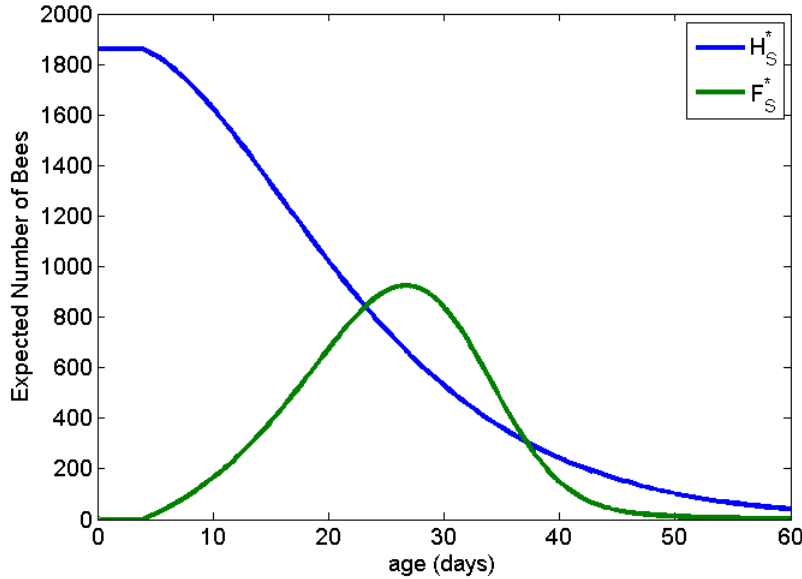


Figure 3.1: The disease-free equilibrium distributions H_S^* and F_S^* . The equilibrium plotted here is found by running the full, time dependent equations (3.3), (3.6), (3.8) and (3.9) until the pointwise solution was no longer changing (below threshold $O(10^{-13})$), as well as by plotting equations (3.33) and (3.34). The two are indistinguishable. All parameter values used in this simulation, with references to the literature, are found in Table 1. Total hive bee population is $\int_0^\infty H_S(a)da = 44839$ bees and the total forager population is $\int_0^\infty F_S(a)da = 18312$ bees.

Equation (3.31) is decoupled from equation (3.32) and is linear. It can be integrated directly. Using the results, equation (3.32) can then be solved by variation of parameters, as it is a linear, non-homogeneous equation. The full solution to equations (3.31) and (3.32) is finally given by

$$H_S^*(\hat{a}) = \begin{cases} H_{S0}, & \text{if } \hat{a} < \hat{a}_R \\ H_{S0} \frac{(\hat{a} + \hat{k})^{2\hat{k}} \exp\left(-\frac{\hat{a}^2 + \hat{a}\hat{k} - \hat{k}^2}{\hat{a} + \hat{k}}\right)}{\left((\hat{a}_R + \hat{k})^{2\hat{k}}\right) \exp\left(-\frac{\hat{a}_R^2 + \hat{a}_R\hat{k} - \hat{k}^2}{\hat{a}_R + \hat{k}}\right)}, & \text{if } \hat{a} \geq \hat{a}_R \end{cases} \quad (3.33)$$

Table 3.1: Parameter values and source references.

L	maximum rate of egg laying	2000 eggs/day	[30]
w	number of hive bees for 50% egg survival	5000 bees	[30]
b	mass of food stored for 50% egg survival	500g	[29]
a_{mn}	age at which hive bees begin brood care	3 days	[24]
a_{mx}	age at which hive bees end brood care	16 days	[24]
a_R	minimum recruitment age	4 days	[18]
k	age at which rate of recruitment is 25% of max.	10 days	
α	maximum rate of recruitment	1 /day	
$\frac{1}{\sigma}$	maximum fraction of colony that can be foraging	1/3	[30]
$\mu(a)$	natural death rate of foragers (summer)	$(a-20)^2/400$	[16, 27, 62]
c	food gathered per day per forager	0.1 g /day /bee	[47]
γ	daily food requirement per adult bee	0.007 g /day /bee	[29]

and

$$F_S^*(\hat{a}) = \begin{cases} F_{S0} \exp\left(\int_0^{\hat{a}} -\hat{\mu}(\hat{a}^*) d\hat{a}^*\right), & \text{if } \hat{a} < \hat{a}_R \\ (A(\hat{a}) + F_{S0}) \exp\left(\int_{\hat{a}_R}^{\hat{a}} -\hat{\mu}(\hat{a}^*) d\hat{a}^*\right), & \text{if } \hat{a} \geq \hat{a}_R \end{cases} \quad (3.34)$$

where

$$\begin{cases} H_{S0} = H_S^*(0) \\ F_{S0} = F_S^*(0) \end{cases}, \quad (3.35)$$

$$A(a) = \int_{a_R}^a \left(\frac{a^*}{a^* + k}\right)^2 H_S^*(a^*) e^{\int_{a_R}^{a^*} \hat{\mu}(s) ds} da^* \quad (3.36)$$

The conditions on variable \hat{a} stem from the Heaviside term in the definition of $u(a)$ in equation (3.4). The age distributions of susceptible hive and foraging bees in equations (3.33) and (3.34) are shown in Figure 3.1.

In order to recover the equilibrium for unscaled variables, one is required to solve the implicit, nonlinear equation for K ,

$$K = \alpha \left(1 - \sigma \frac{\int_0^\infty F_S^*(Ka) da}{\int_0^\infty H_S^*(Ka) + F_S^*(Ka) da} \right) \quad (3.37)$$

which can then be used to recover the equilibrium distributions in unscaled time, $H_S^{**}(a) = H_S^*(Ka)$ and $F_S^{**}(a) = F_S^*(Ka)$.

Using equations (4.9) and (3.31), this steady-state exists so long as

$$\int_{a_{mn}}^{a_{mx}} H^*(a) da > \frac{w}{L\mathcal{W}(f/f+b)}. \quad (3.38)$$

3.3.3 Stability of DFE

If the Laplace transform of $H(a, t)$ is denoted by $\mathcal{L}\{H(a, t)\} = \mathcal{H}(a, s)$ and $\lim_{t \rightarrow \infty} H(a, t)$ is finite, then by the Final Value Theorem [40],

$$\lim_{t \rightarrow \infty} H(a, t) = \lim_{s \rightarrow 0} s \mathcal{H}(a, s) \quad (3.39)$$

under two conditions [10]:

- i) There is at most one simple pole at the origin in s -space.
- ii) Any roots of the denominator of $\mathcal{H}(a, s)$ are negative.

In what follows we use this theorem to analyze the asymptotic behaviour of the PDE system given by equations (3.3), (3.5), (3.6), (3.7) and (3.8) expressed in scaled variables \hat{a} and \hat{t} , and ultimately show that the disease-free equilibrium is locally asymptotically stable.

To begin, we approximate the recruitment function $u(a, t)$ as

$$u(a, t) = u_{eq}(a) + \epsilon(a, t) \quad (3.40)$$

where $u_{eq}(a)$ is defined as in equation (3.28) as the rate of recruitment at equilibrium and $\epsilon(a, t)$ is a small perturbation in this function near the equilibrium.

We then take the Laplace Transform in \hat{t} of equation (3.3) near the disease-free equilibrium, ignoring the term βIH_S since here we are interested in the disease-free case, which yields

$$s \mathcal{H}(\hat{a}, s) - H_S(\hat{a}, 0) + \frac{\partial \mathcal{H}(\hat{a}, s)}{\partial \hat{a}} = -u_{eq}(\hat{a}) \mathcal{H}(\hat{a}, s) + \int_0^s \epsilon(\hat{a}, r - s) \mathcal{H}(\hat{a}, r) dr \quad (3.41)$$

where

$$\mathcal{H}(\hat{a}, s) = \mathcal{L}\{H_S(\hat{a}, t)\} \quad (3.42)$$

$$\epsilon(\hat{a}, s) = \mathcal{L}\{\epsilon(\hat{a}, t)\}. \quad (3.43)$$

The corresponding boundary condition is then given by taking the Laplace transform of condition (4.9) but this is not easy because of the time dependence of that boundary condition. We simplify this problem by noting that when food stores are unbounded and we are interested in the behaviour as $t \rightarrow \infty$, the term involving food will saturate. On this basis we use the approximation

$$\lim_{t \rightarrow \infty} \frac{f}{b + f} \approx 1. \quad (3.44)$$

As well, the second factor in the function V (equation (3.10)) can be expressed at equilibrium as

$$0 \leq \kappa = \frac{\int_{a_{mn}}^{a_{mx}} H_S^*(a) da}{w + \int_{a_{mn}}^{a_{mx}} H_S^*(a) da} \leq 1. \quad (3.45)$$

We can linearize about the equilibrium, $\int H_S^*(a)da$ (note we have suppressed the limits of integration for readability) using the Taylor series

$$H_S(0, t) \approx L\kappa + L \frac{dV}{d \int H_S da} \Big|_{H_S=H_S^*} \left(\int H_S(a, t) da - \int H_S^*(a) da \right) \quad (3.46)$$

where $\frac{dV}{d \int H_S(a, t) da}$ is the derivative of V with respect to $\int H_S(a, t) da$ here defined as

$$\frac{dV}{d \int H_S(a, t) da} = \frac{w}{\left(w + \int H_S(a, t) da\right)^2}. \quad (3.47)$$

Using these approximations, the boundary condition for \mathcal{H} becomes

$$\begin{aligned} \mathcal{H}(0, s) &= \frac{L\kappa}{s} + L \left(\frac{w}{\left(w + \int_{a_{mn}}^{a_{mx}} H_S^*(a) da\right)^2} \right) \left(\int \mathcal{H}(a, s) da - \frac{\int H_S^*(a) da}{s} \right) \\ &= \frac{L\kappa^2}{s} + L \frac{dV}{d \int_{a_{mn}}^{a_{mx}} H_S da} \int_{a_{mn}}^{a_{mx}} \mathcal{H}(a, s) da \end{aligned} \quad (3.48)$$

and the limit of $s\mathcal{H}(0, s)$ becomes

$$\lim_{s \rightarrow 0} s\mathcal{H}(0, s) = L\kappa^2 \quad (3.49)$$

which we note is constant.

Solving the ODE (3.41) with initial condition $H_S(\hat{a}, 0) = g(\hat{a}) \geq 0$ (bounded, analytic, and satisfying the two aforementioned conditions) yields,

$$\mathcal{H}(\hat{a}, s) = \begin{cases} \left(\int_0^{\hat{a}} g(\tilde{a}) e^{s\tilde{a}} d\tilde{a} + \mathcal{H}(0, s) \right) e^{-s\hat{a}} & \hat{a} < \hat{a}_R \\ (x(\hat{a}, s) + C(s)) y(\hat{a}, s) & \hat{a} \geq \hat{a}_R \end{cases} \quad (3.50)$$

where

$$y(a, s) = (a + \hat{k})^{2\hat{k}} \exp\left(-\frac{sa^2 + sa\hat{k} + a^2 + a\hat{k} - \hat{k}^2}{a + \hat{k}}\right) \quad (3.51)$$

$$x(a, s) = \int_{\hat{a}_R}^a \left(g(\tilde{a}) + \int_0^s \varepsilon(\tilde{a}, s-r) \mathcal{H}(\tilde{a}, r) dr \right) \frac{1}{y(\tilde{a})} d\tilde{a} \quad (3.52)$$

and

$$C(s) = \mathcal{H}(0, s) \left((\hat{a}_R + \hat{k})^{2\hat{k}} \right)^{-1} \left(\exp\left(-\frac{s\hat{a}_R^2 + s\hat{a}_R\hat{k} + \hat{a}_R^2 + \hat{a}_R\hat{k} - \hat{k}^2}{\hat{a}_R + \hat{k}}\right) \right)^{-1}. \quad (3.53)$$

The tilde sign signifies dummy variables.

We examine this result in two parts:

(i) $\hat{a} > \hat{a}_R$: Here we observe that

$$s y(\hat{a}) x(\hat{a}) \geq 0 \quad (3.54)$$

and note that

$$\lim_{s \rightarrow 0} s \int_0^s \varepsilon(\hat{a}, s-r) \mathcal{H}(\hat{a}, r) dr = 0. \quad (3.55)$$

Since $g(\hat{a})$ is bounded, and

$$0 \leq \frac{\exp\left(-\frac{\hat{k}^2}{\hat{a} + \hat{k}}\right)}{(\hat{a} + \hat{k})^{2\hat{k}}} \leq 1$$

we find

$$\begin{aligned} s y(\hat{a}) x(\hat{a}) &\leq s y(\hat{a}) \left(\max_{\hat{a} \in [0, \infty)} g(\hat{a}) \right) \int_{\hat{a}_R}^{\hat{a}} e^{-\hat{a}(\hat{s}+1)} d\hat{a} \\ &= s y(\hat{a}) \left(\max_{\hat{a} \in [0, \infty)} g(\hat{a}) \right) \frac{e^{-(s+1)\hat{a}_R} - e^{-(s+1)\hat{a}}}{s+1}. \end{aligned} \quad (3.56)$$

We also note that

$$\lim_{s \rightarrow 0} s y(\hat{a}) \left(\max_{\hat{a} \in [0, \infty)} g(\hat{a}) \right) \frac{e^{-(s+1)\hat{a}_R} - e^{-(s+1)\hat{a}}}{s+1} = 0. \quad (3.57)$$

Using conditions (3.54), (3.56), (3.57) and the Squeeze Theorem [56] we conclude that

$$\lim_{s \rightarrow 0} s y(\hat{a}) x(\hat{a}) = 0 \quad (3.58)$$

As well,

$$\begin{aligned} \lim_{s \rightarrow 0} s C &= \lim_{s \rightarrow 0} \left\{ s \mathcal{H}(0, s) \left((\hat{a}_R + \hat{k})^{2\hat{k}} \right)^{-1} \cdot \right. \\ &\quad \left. \left(\exp\left(-\frac{s\hat{a}_R^2 + s\hat{a}_R\hat{k} + \hat{a}_R^2 + \hat{a}_R\hat{k} - \hat{k}^2}{\hat{a}_R + \hat{k}}\right) \right)^{-1} \right\} \\ &= L\kappa^2 \left((\hat{a}_R + \hat{k})^{2\hat{k}} \right)^{-1} \exp\left(\frac{\hat{a}_R^2 + \hat{a}_R\hat{k} - \hat{k}^2}{\hat{a}_R + \hat{k}}\right) \end{aligned} \quad (3.59)$$

Using the above, we find

$$\lim_{s \rightarrow 0} s \mathcal{H}(\hat{a}, s) = L\kappa^2 (\hat{a} + \hat{k})^{2\hat{k}} \exp\left(-\frac{s\hat{a}^2 + s\hat{a}\hat{k} + \hat{a}^2 + \hat{a}\hat{k} - \hat{k}^2}{\hat{a} + \hat{k}}\right) \quad (3.60)$$

$$= H_S^*(\hat{a}), \quad (3.61)$$

and applying the Final Value Theorem we find

$$\lim_{t \rightarrow \infty} H_S(\hat{a}, t) = H_S^*(\hat{a}), \quad \hat{a} \geq \hat{a}_R \quad (3.62)$$

(ii) $\hat{a} < \hat{a}_R$: Here we note simply that

$$\lim_{s \rightarrow 0} s \left(\int_0^{\hat{a}} g(\tilde{a}) e^{s\tilde{a}} d\tilde{a} + \mathcal{H}(0, s) \right) e^{-s\hat{a}} \quad (3.63)$$

$$= \left(\int_0^{\hat{a}} \lim_{s \rightarrow 0} s g(\tilde{a}) e^{s\tilde{a}} d\tilde{a} + \lim_{s \rightarrow 0} L\kappa^2 \right) e^{-s\hat{a}} \quad (3.64)$$

$$= L\kappa^2 = H_S^*(\hat{a}). \quad (3.65)$$

This completes the stability analysis of the DFE for H_S . Similar analysis applies to the DFE for F_S , though with considerably more tedious algebra, therefore we omit the details.

The above analysis determines the global stability of the linearized model in which we have sufficient food stores, brood care and time-independent recruitment. This linearized model is in fact an approximation to the full model governed by equations (3.3), (3.5), (3.6), (3.7) and (3.8) near the quasi-steady state distribution given by equations (3.33) and (3.34). Note that, rather than linearizing the full system by using first order approximations (the Jacobian) in the neighbourhood of the equilibrium, here we need only consider the functional forms of the recruitment and survival terms. At any equilibrium, factors in these terms that vary with the population size of a certain class will be constant. Imposing only this assumption, along with equation 3.44, produces a linearized model that is valid in some neighbourhood of the disease-free equilibrium. Therefore, the global stability of the linearized model implies local stability of the full model.

The significance of these results is that starting from any initial age distribution $g(a)$ such that equation (3.38) is satisfied, given sufficient food stores and brood care, a colony will rebound toward the distributions in equations (3.33) and (3.34), shown numerically in Figure 3.1. While the analysis does not provide a time frame in which the rebound will occur, numerical experiments suggest that the rebound is relatively fast. More specifically, within months of an environmental hazard being removed, the colony returns to its quasi-steady state distribution. Of course, this applies only to the active season, when temperatures are amenable to optimal colony function. The effects of seasonal changes with age structure are explored separately elsewhere [4], while an exploration of the effects of seasonal changes with an age-independent model have been previously studied [45, 47].

3.3.4 Basic Reproduction Number R_0

The basic reproduction number, R_0 , for a system of partial differential equations has been explored previously in [25, 32, 59]. The main difficulty in finding an expression for R_0 is that a system of partial differential equations has infinite dimensions and is therefore not amenable to standard methods such as the next generation matrix [13, 60]. In the present case the situation is further compounded because there are two susceptible classes, namely H_S and F_S , and they interact with each other. In what follows we propose techniques similar to those introduced by [32] and [25] to determine the basic reproduction number in the face of these complications.

We begin by linearizing the system (equations (3.3),(3.5),(3.6),(3.7),(3.8)) about the DFE given by equations (3.33) and (3.34). Again, since we are near the disease free equilibrium, we use $u_{eq}(a)$ to approximate the recruitment function, and rescale time as described previously. For the basic reproduction number, we are concerned with the growth of only the infected classes, governed by the following linearized equations in scaled variables:

$$\begin{aligned} \frac{\partial H_I}{\partial \hat{t}} + \frac{\partial H_I}{\partial \hat{a}} = & - \left(\left(\frac{\hat{a}}{\hat{a} + \hat{k}} \right)^2 H_v(\hat{a} - \hat{a}_R) + \hat{d}(\hat{a}) \right) H_I \\ & + \hat{\beta} H_S^* \int (H_I + F_I) d\hat{a} \end{aligned} \quad (3.66)$$

$$\begin{aligned} \frac{\partial F_I}{\partial \hat{t}} + \frac{\partial F_I}{\partial \hat{a}} &= \left(\frac{\hat{a}}{\hat{a} + \hat{k}} \right)^2 H_v(\hat{a} - \hat{a}_R) H_I - (\hat{d}(\hat{a}) + \hat{\mu}(\hat{a})) F_I(\hat{a}) \\ &+ \hat{\beta} F_S^* \int (H_I + F_I) d\hat{a} \end{aligned} \quad (3.67)$$

where H_S^* and F_S^* are the distributions of the disease-free equilibrium found in Section 3.1. We then use the ansatz that at least for a short time after the infection begins, the two infected populations have fixed age distributions that grow or decay exponentially in time [8, 64], that is

$$H_I(\hat{a}, \hat{t}) = h_I(\hat{a}) e^{\rho \hat{t}} \quad (3.68)$$

$$F_I(\hat{a}, \hat{t}) = f_I(\hat{a}) e^{\rho \hat{t}}. \quad (3.69)$$

The set of all values of the exponent ρ is thus viewed as the growth parameters of the linearized system, equations (3.66),(3.67). For $\rho < 0$ the solutions will decay to zero, and the DFE will be asymptotically stable. For $\rho > 0$ the solutions will lead to an epidemic outbreak, and we now proceed to determine conditions under which this occurs.

Substituting (3.68) and (3.69) into (3.66) and (3.67) gives a system of integro-differential equations:

$$\frac{dh_I}{d\hat{a}} = - \left[\left(\frac{\hat{a}}{\hat{a} + \hat{k}} \right)^2 H_v(\hat{a} - \hat{a}_R) + \hat{d}(\hat{a}) + \rho \right] h_I + b(\hat{a}) W \quad (3.70)$$

$$\frac{df_I}{d\hat{a}} = \left(\frac{\hat{a}}{\hat{a} + \hat{k}} \right)^2 H_v(\hat{a} - \hat{a}_R) h_I - \left[(\hat{d}(\hat{a}) + \hat{\mu}(\hat{a}) + \rho) \right] f_I + B(\hat{a}) W \quad (3.71)$$

where

$$W = \int (h_I + f_I) d\hat{a}, \quad (3.72)$$

$$b(a) = \hat{\beta} H_S^*(a) \quad (3.73)$$

and

$$B(a) = \hat{\beta} F_S^*(a). \quad (3.74)$$

The above system has the solution,

$$h_I(\hat{a}) = W e^{-\rho \hat{a}} e^{-\hat{\Gamma}_1(\hat{a})} \int_0^{\hat{a}} e^{\rho \tilde{s}} b(\tilde{s}) e^{\hat{\Gamma}_1(\tilde{s})} d\tilde{s} \quad (3.75)$$

$$f_I(\hat{a}) = W e^{-\rho \hat{a}} e^{-\hat{\Gamma}_2(\hat{a})} \int_0^{\hat{a}} e^{\rho \tilde{s}} e^{\hat{\Gamma}_2(\tilde{s})} (B(\tilde{s}) + \hat{u}(\tilde{s}) h_I^W(\tilde{s})) d\tilde{s} \quad (3.76)$$

where

$$\hat{u}(a) = \left(\frac{a}{a + k} \right)^2 H_v(a - \hat{a}_R) \quad (3.77)$$

$$\hat{\Gamma}_1(a) = \int_0^a \hat{u}(\tilde{a}) + \hat{d}(\tilde{a}) d\tilde{a} \quad (3.78)$$

$$\hat{\Gamma}_2(a) = \int_0^a \hat{d}(\tilde{a}) + \hat{\mu}(\tilde{a}) d\tilde{a} \quad (3.79)$$

$$h_I^W(a) = e^{-\rho a} e^{-\hat{\Gamma}_1(a)} \int_0^a e^{\rho \tilde{s}} b(\tilde{s}) e^{\hat{\Gamma}_1(\tilde{s})} d\tilde{s}. \quad (3.80)$$

Substituting equations (3.75) and (3.76) into equation (6.73), we find

$$W = WR(\rho) \quad (3.81)$$

where

$$R(\rho) = \int_0^\infty e^{-\rho \hat{a}} \left\{ e^{-\hat{\Gamma}_1(\hat{a})} \int_0^{\hat{a}} e^{\rho s} b(s) e^{\hat{\Gamma}_1(s)} ds \right. \\ \left. + e^{-\hat{\Gamma}_2(\hat{a})} \int_0^{\hat{a}} e^{\rho s} e^{\hat{\Gamma}_2(s)} (B(s) + \hat{u}(s) h_I^W(s)) ds \right\} d\hat{a}. \quad (3.82)$$

To determine if a non-zero solution of equation (6.75) exists, we seek a ρ_c such that

$$R(\rho_c) = 1. \quad (3.83)$$

We use the Mean Value Theorem to simplify equation (3.82) and rewrite equation (3.82) as

$$R(\rho) = \int_0^\infty e^{\rho(c_1 - \hat{a})} e^{-\hat{\Gamma}_1(\hat{a})} \int_0^{\hat{a}} b(s) e^{\hat{\Gamma}_1(s)} ds \\ + e^{\rho(c_2 - \hat{a})} e^{-\hat{\Gamma}_2(\hat{a})} \int_0^{\hat{a}} e^{\hat{\Gamma}_2(s)} B(s) ds \\ + e^{\rho(c_3 - c_4 - \hat{a})} e^{-\hat{\Gamma}_2(\hat{a})} \int_0^{\hat{a}} \hat{u}(s) \tilde{h}_I^W(s) e^{\hat{\Gamma}_2(s)} ds d\hat{a} \quad (3.84)$$

where

$$\{c_1, c_2, c_3, c_4\} \in [0, \hat{a}] \quad (3.85)$$

and, as a consequence,

$$c_i - \hat{a} \leq 0 \quad \text{for } i = 1, 2, 3, 4. \quad (3.86)$$

Taking the derivative of equation (3.84) with respect to ρ yields

$$R'(\rho) = - \rho \int_0^\infty \left\{ |c_1 - \hat{a}| e^{\rho(c_1 - \hat{a})} e^{-\hat{\Gamma}_1(\hat{a})} \int_0^{\hat{a}} b(s) e^{\hat{\Gamma}_1(s)} ds \right. \\ + |c_2 - \hat{a}| e^{\rho(c_2 - \hat{a})} e^{-\hat{\Gamma}_2(\hat{a})} \int_0^{\hat{a}} e^{\hat{\Gamma}_2(s)} B(s) ds \\ \left. + |c_3 - c_4 - \hat{a}| e^{\rho(c_3 - c_4 - \hat{a})} e^{-\hat{\Gamma}_2(\hat{a})} \int_0^{\hat{a}} \hat{u}(s) \tilde{h}_I^W(s) e^{\hat{\Gamma}_2(s)} ds \right\} d\hat{a}. \quad (3.87)$$

Recall that for a disease to persist, a value of $\rho_c > 0$ is required such that $R(\rho_c) = 1$. Since each integral in equation (3.87) is positive (because each integrand is positive), then $R(\rho)$ is a non-increasing function of ρ . Therefore, if $R(0) < 1$ then $R(\rho) \neq 1$ for any $\rho > 0$. On the other hand, if $R(0) > 1$ then by continuity of $R(\rho)$, there must exist a ρ_c such that $R(\rho_c) = 1$. This then implies there is a solution to equation (6.75) such that $W \neq 0$ which then in turn implies that h_I and f_I are nonzero. Under these conditions an infection will persist.

The above analysis provides the basis for taking $R(0)$ as our basic reproduction number, that is for setting $R(0) = R_0$. For $R_0 < 1$ the infection will decay, whereas for $R_0 > 1$ the infection will grow.

The basic reproduction number for this model is thus given by

$$R_0 = \hat{\beta} \int_0^\infty \left\{ e^{-\hat{\Gamma}_1(\hat{a})} \int_0^{\hat{a}} H_S^*(s) e^{\hat{\Gamma}_1(s)} ds \right. \\ \left. + e^{-\hat{\Gamma}_2(\hat{a})} \int_0^{\hat{a}} \left(F_S^*(s) + \hat{u}(s) \int_0^s H_S^*(\tilde{s}) e^{\hat{\Gamma}_1(\tilde{s})} d\tilde{s} \right) e^{\hat{\Gamma}_2(s)} ds \right\} d\hat{a}. \quad (3.88)$$

Transforming back to the unscaled variables, R_0 can be written:

$$R_0 = \beta \int_0^\infty \left\{ \int_0^a H_S^{**}(s) e^{-(\Gamma_1(a)-\Gamma_1(s))} ds \right\} da \\ + \beta \int_0^\infty \left\{ \int_0^a F_S^{**}(s) e^{-(\Gamma_2(a)-\Gamma_2(s))} ds \right\} da \\ + \beta \int_0^\infty \left\{ u_{eq}(s) e^{-\Gamma_2(a)} \int_0^s H_S^{**}(\tilde{s}) e^{-(\Gamma_2(s)-\Gamma_1(\tilde{s}))} d\tilde{s} ds \right\} da, \quad (3.89)$$

recalling that $H_S^{**}(a)$ and $F_S^{**}(a)$ are the disease-free equilibrium distributions in unscaled time. This value of R_0 defines a bifurcation point at which the disease-free equilibrium loses stability and gives rise to an epidemic. The appendix relates this expression for R_0 to the expression in the age independent case, \hat{R}_0 .

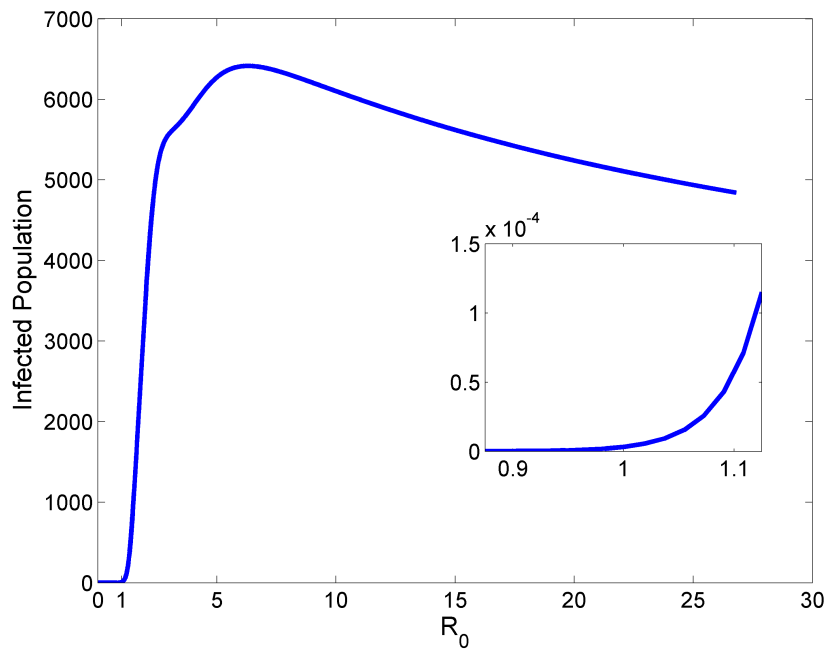


Figure 3.2: The total infected population in the hive after integrating equations (3.3),(3.5),(3.6) and (3.7) for 100 days vs. R_0 computed by numerical integration of equation (3.89). We see that the infection cannot infiltrate the colony for $R_0 < 1$.

Figure 6.1 shows the total infected population, computed numerically and plotted against values of the basic reproduction number R_0 . The figure confirms numerically the bifurcation

value of R_0 at 1 as predicted by the analysis. The reduction in I seen as R_0 increases shows the slow collapse of the colony as the bee population becomes more afflicted by the disease.

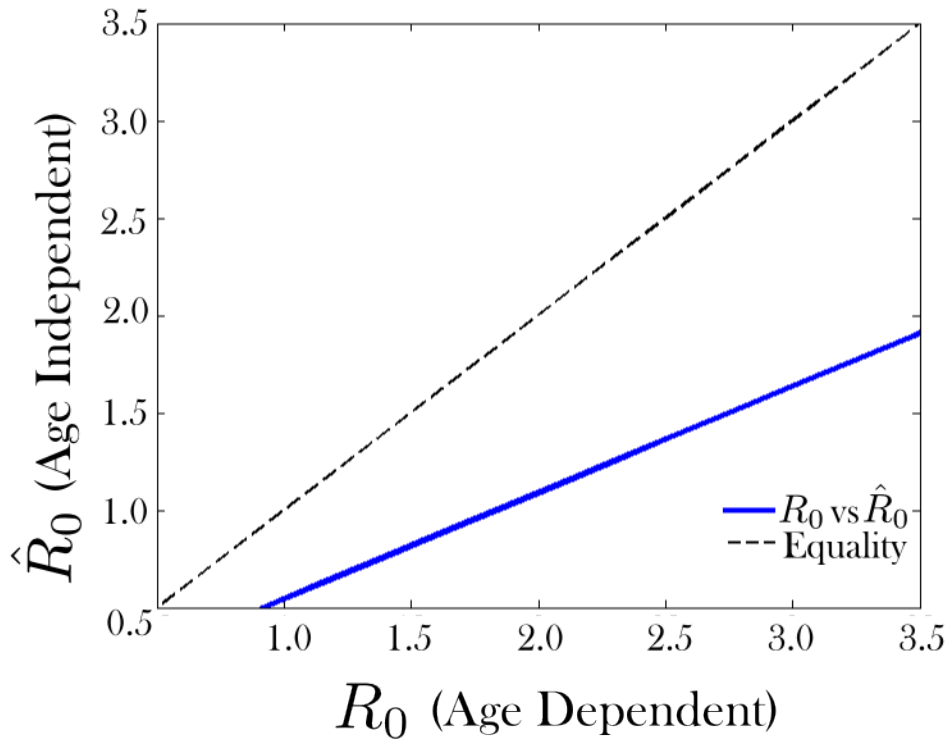


Figure 3.3: R_0 as calculated using equation (3.89) plotted against the basic reproduction number in the age-independent case, \hat{R}_0 calculated using the next generation matrix (see Appendix). The dashed black line represents equality, while the data are shown in blue. The age-independent model consistently under estimates the value of R_0 .

Figure 6.2 shows that the corresponding age-independent R_0 (where the parameter values are taken to be the average over all ages) significantly under-estimates the basic reproduction number.

3.4 Discussion

Considerable research has highlighted the importance of age structure to a honey bee colony. Recently Perry *et al.* have shown experimentally that various stressors can cause rapid behavioural maturation, which in turn will accelerate colony failure [41]. Models have also predicted that earlier recruitment to foraging can be a marker for potential colony collapse [5, 29, 30]. Modelling age structure explicitly can help us better understand the mechanisms driving such earlier maturation. Moreover, as seen in [4], an explicit age structure allows the model to capture behaviours that have been missed by simpler ordinary differential equation models, including spring dwindle, the loss of bees in early spring. Furthermore, since parasites and diseases often target, and affect differently, bees of particular age classes [34, 57], an age-structured model can aid in understanding and predicting the effects of these pathogens. The

differences between an age-structured model and age-independent model are explored further in [4], where we found that the age-structured model provides much richer dynamics, which sometimes contrast the predictions of simpler models.

Equation (3.38) implies that the less food available, the more care is required in order for an acceptable fraction of the brood to survive. Moreover, if the hive bees begin nursing duties substantially late, or leave nursing duties early, the equilibrium may disappear, leaving only the trivial equilibrium (i.e. extinction). This gives insights into the sensitivity of a honey bee colony to the age polyethism inherent in their social structure.

An important prediction of this study is that if a hazard (environmental, parasitic, etc.) causes a bee colony to decline, the colony can recover if the hazard is removed in a timely fashion (given there are still sufficient food stores and brood care). This prediction is further examined in the sister study [4], where we explore the same model in the context of changing seasons. This general stability result for honey bee dynamics is consistent with the fact that honey bee colonies experience annual cycles in population size. Colonies typically suffer great losses in the late fall and early winter [66], and recover to peak colony population size by late spring to mid-summer [1, 38]. In this context, winter itself can be seen as a stressor on the colony, and its end allows the colony to once again reach equilibrium. Moreover, consistent again with experimental results, this is only possible if there are sufficient bees at the end of winter (Becher et al. estimate this number to be approximately 4000 bees [3]) and sufficient food stores (honey bees typically require at least 20kg of stored honey to survive winter [50]). This of course depends on the length of winter.

Given the parameter set in Table A.1, we are able to predict an age distribution for the population of a healthy colony. The total colony size predicted here is consistent within ranges reported by [3, 30, 43]. The age distribution is also consistent with the demography reported by [48, 49, 61]. This agreement suggests that the simple death rate used in this model is a reasonable approximation.

In [5, 29, 30, 44], the average age of recruitment to foraging (AARF) is found to be a good indicator of colony health. Lack of food [29], pesticide exposure [30, 41] and disease [5, 44] have all been predicted to lower the average age of recruitment to foraging. In our age-dependent model, this average age can be further refined as we can keep track of the age of bees explicitly. In particular, at any time, we have an age-dependent recruitment function, $u(a, t)$, which (in the full model) depends on the populations of hive bees and foragers. Thus the age-dependent model can recover a full distribution of the age at which bees are recruited to foraging, not simply the average value. This distribution is an interesting focus for future work. For example, a reduction in the AARF could be caused by a reduction in the number of older bees becoming foragers, or potentially an increase in the number of young bees becoming foragers. While [41] shows that pesticides would cause the latter situation, our model allows for differentiation between these two scenarios; exploring the possible causes underlying each case could be of interest.

The work we present here also provides some interesting mathematical techniques, which can be adapted to other PDE models. The results of this study determine the necessary conditions under which the introduction of an infection will lead to an epidemic outbreak within a bee colony by determining the basic reproduction number, R_0 . In theory, the formulation of R_0 can be verified using an infinite dimensional analog of the next generation matrix [59]. We confirm our derived expression of R_0 numerically and via reduction to an age-independent

model, analyzed using the next generation matrix. Although many models have been proposed for disease dynamics within a honey bee colony [5, 35, 44, 57] and several provide stability criteria for the disease-free equilibrium, none have provided an expression for R_0 . Here, we provide a closed-form expression for R_0 , admittedly for a simplified disease model, in both the age-independent case and for the continuous age-structured model. In theory, this should provide an upper and lower bound for R_0 for a model of N age classes.

Moreover, R_0 , although complicated in its formulation, can be used to determine whether a disease will be detrimental to a colony's health if the transmission rate and death rate associated with that disease are known. In practice, it is often easier to obtain an estimate of R_0 itself, in which case our formula can be used to determine the rate of transmission between bees or the distribution of the death rate. This knowledge may help in determining strategies for saving the colony or estimating death rates to be used to more accurately simulate disease transmission in a colony.

As we demonstrated, the basic reproduction number scales linearly with a constant transmission rate β , as expected. With similar analysis this result can be generalized to an age-dependent $\beta(a)$. Also, the rate of recruitment plays a role in the spread of infection to the extent that a change in rate of recruitment may have the potential to either increase or decrease R_0 . In the case of the linearized, age-independent expression, \hat{R}_0 , we find that an increase in recruitment lowers R_0 (see appendix). We also observe that by omitting age-structure from a model of honey bee colony dynamics, R_0 is under-estimated.

Finally, we note that using the Laplace transform to determine asymptotic stability may be applied more generally to time-dependent systems of partial differential equations, when the boundary conditions are constant. Also, the computation of R_0 is applicable to many biological models with interacting susceptible classes. For example, age-dependent models of many sexually transmitted diseases may have interacting susceptible classes and could benefit from the approach we develop here. Future plans involve describing the methods more rigorously to determine exactly when they can be applied to a more general class of PDE systems.

3.5 Appendix

Test: Uniform age distribution. We test the validity of this bifurcation parameter by reducing equations (3.70) and (3.71) to a system in which all parameters are constant with respect to age. In doing so, we find from equation (3.89) that

$$\hat{R}_0 = \beta \frac{H_S^*}{u + d} + \beta \frac{uH_S^*}{(\mu + d)(u + d)} + \beta \frac{F_S^*}{\mu + d}. \quad (3.90)$$

This can be verified by using the next generation matrix on the infected classes of the following reduced model

$$\frac{dH_S}{dt} = -uH_S + \beta(H_I + F_I)H_S \quad (3.91)$$

$$\frac{dF_S}{dt} = uH_S + \beta(H_I + F_I)F_S - \mu F_S \quad (3.92)$$

$$\frac{dH_I}{dt} = -uH_I + \beta(H_I + F_I)H_S - dH_I \quad (3.93)$$

$$\frac{dF_I}{dt} = uH_I + \beta(H_I + F_I)F_S - (d + \mu)F_I \quad (3.94)$$

which are a reduced form of equations (4.5) and (4.7). The ratio of the disease-free equilibrium values of F_S, H_S will always be such that

$$\frac{H_S^*}{F_S^*} = \frac{\mu}{u}. \quad (3.95)$$

This ratio is found by setting $H_I = F_I = \frac{dH_S}{dt} = \frac{dF_S}{dt} = 0$ in equations (3.91), (3.92), (3.93) and (3.94).

From these reduced equations we find the matrices,

$$F = \begin{bmatrix} \beta H_S^* & \beta H_S^* \\ \beta F_S^* & \beta F_S^* \end{bmatrix} \quad (3.96)$$

$$V = \begin{bmatrix} d + u & 0 \\ -u & d + \mu \end{bmatrix} \quad (3.97)$$

which yield the next generation matrix

$$FV^{-1} = \begin{bmatrix} \frac{\beta H_S^*}{u + d} + \frac{\beta u H_S^*}{(u + d)(\mu + d)} & \frac{\beta H_S^*}{\mu + d} \\ \frac{\beta F_S^*}{u + d} + \frac{\beta u F_S^*}{(u + d)(\mu + d)} & \frac{\beta F_S^*}{\mu + d} \end{bmatrix} \quad (3.98)$$

Each term in this matrix has a biological interpretation which is the expected number of infections in each class (H or F) caused by a single infected individual in each class. For example, the term

$$\frac{\beta H_S^*}{u + d} \quad (3.99)$$

gives the expected number of susceptible hive bees that an infected hive bee will infect while it is still a hive bee. The term

$$\frac{\beta u H_S^*}{(u + d)(\mu + d)} \quad (3.100)$$

represents the probability that an infected hive bee will be recruited to foraging duties during its life time, multiplied by the expected number of susceptible hive bees that would then become infected. The expected number of susceptible hive bees infected by a single forager is given by

$$\frac{\beta H_S^*}{\mu + d} \quad (3.101)$$

The interpretations for the second row of matrix (3.98) are similar, but give the expected numbers of susceptible foragers that will become infected.

The basic reproduction number for this uniform age distribution model is then determined by the largest eigenvalue of the matrix FV^{-1} . Since we have the relation (3.95), matrix (3.98) is rank 1. Therefore, one of its eigenvalues is zero and the other is given by its trace. We can see that the trace of matrix (3.98) gives the same expression for the basic reproduction number as (3.90).

The three terms that appear in (3.89) are analogous to the three terms that appear in equation (3.90). This suggests that (3.89) correctly determines not only the threshold for disease persistence but also correctly estimates the number of secondary infections subsequent to one primary infection [22].

Bibliography

- [1] BALL, B., AND ALLEN, M. The prevalence of pathogens in honey bee (*Apis mellifera*) colonies infested with the parasitic mite *Varroa jacobsoni*. *Annals of applied biology* 113, 2 (1988), 237–244.
- [2] BECHER, M. A., GRIMM, V., THORBEC, P., HORN, J., KENNEDY, P. J., AND OSBORNE, J. L. BEEHAVE: a systems model of honeybee colony dynamics and foraging to explore multifactorial causes of colony failure. *Journal of applied ecology* 51, 2 (2014), 470–482.
- [3] BECHER, M. A., OSBORNE, J. L., THORBEC, P., KENNEDY, P. J., AND GRIMM, V. Review: Towards a systems approach for understanding honeybee decline: a stocktaking and synthesis of existing models. *Journal of Applied Ecology* 50, 4 (2013), 868–880.
- [4] BETTI, M., WAHL, L. M., AND ZAMIR, M. Age structure is critical to the population dynamics and survival of honeybee colonies. *Royal Society Open Science* 3, 11 (2016), 160444.
- [5] BETTI, M. I., WAHL, L. M., AND ZAMIR, M. Effects of infection on honey bee population dynamics: A model. *PLOS ONE* 9, 10 (2014), e110237.
- [6] BOTIAS, C., MARTIN-HERNANDEZ, R., BARRIOS, L., MEANA, A., AND HIGES, M. *Nosema* spp. infection and its negative effects on honey bees (*Apis mellifera iberiensis*) at the colony level. *Veterinary research* 44, 1 (2013), 1–15.
- [7] BOYCE, W., AND DIPRIMA, R. *Differential Equations and Boundary Value Problems*. Wiley New York, 2008.
- [8] BRAUER, F., CASTILLO-CHAVEZ, C., AND CASTILLO-CHAVEZ, C. *Mathematical models in population biology and epidemiology*, vol. 1. Springer, 2001.
- [9] CALDERONE, N. W. Insect pollinated crops, insect pollinators and US agriculture: Trend analysis of aggregate data for the period 1992-2009. *PLOS ONE* 7, 5 (05 2012), e37235.
- [10] CANNON, R. H. *Dynamics of physical systems*. Courier Corporation, 2003.
- [11] CASTILLO-CHAVEZ, C., AND FENG, Z. Global stability of an age-structure model for TB and its applications to optimal vaccination strategies. *Mathematical biosciences* 151, 2 (1998), 135–154.

- [12] CORLESS, R. M., AND FILLION, N. A graduate introduction to numerical methods. *AMC 10* (2013), 12.
- [13] DIEKMANN, O., HEESTERBEEK, J., AND METZ, J. A. On the definition and the computation of the basic reproduction ratio R_0 in models for infectious diseases in heterogeneous populations. *Journal of mathematical biology* 28, 4 (1990), 365–382.
- [14] DOMOSHNIISKY, A. Exponential stability of convolution integro-differential equations. *Functional Differential Equations* 5, 3-4 (2004), p–297.
- [15] DOMOSHNIISKY, A., AND GOLTSEY, Y. One approach to study of stability of integro-differential equations. *Nonlinear Analysis: Theory, Methods & Applications* 47, 6 (2001), 3885–3896.
- [16] DUKAS, R. Mortality rates of honey bees in the wild. *Insectes Sociaux* 55, 3 (2008), 252–255.
- [17] EBERL, H. J., FREDERICK, M. R., AND KEVAN, P. G. Importance of brood maintenance terms in simple models of the honeybee - *Varroa destructor* - Acute Bee Paralysis Virus complex. *Electronic Journal of Differential Equations (EJDE) [electronic only]* 2010 (2010), 85–98.
- [18] FAHRBACH, S., AND ROBINSON, G. Juvenile hormone, behavioral maturation and brain structure in the honey bee. *Developmental Neuroscience* 18 (1996), 102–114.
- [19] GOLTSEY, Y., AND LITSYN, E. Volterra integro-differential equations and infinite systems of ordinary differential equations. *Mathematical and computer Modelling* 42, 1-2 (2005), 221–233.
- [20] GROSSMANN, C., ROOS, H.-G., AND STYNES, M. *Numerical treatment of partial differential equations*. Springer, 2007.
- [21] HALE, J. K., AND WALTMAN, P. Persistence in infinite-dimensional systems. *SIAM Journal on Mathematical Analysis* 20, 2 (1989), 388–395.
- [22] HEFFERNAN, J., SMITH, R., AND WAHL, L. M. Perspectives on the basic reproductive ratio. *Journal of the Royal Society Interface* 2, 4 (2005), 281–293.
- [23] HO, M.-W., AND CUMMINS, J. Mystery of disappearing honeybees. *Science in Society* 34 (2007), 35–36.
- [24] HUANG, Z.-Y., AND ROBINSON, G. E. Regulation of honey bee division of labor by colony age demography. *Behavioral Ecology and Sociobiology* 39 (1996), 147–158.
- [25] HYMAN, J. M., AND LI, J. An intuitive formulation for the reproductive number for the spread of diseases in heterogeneous populations. *Mathematical biosciences* 167, 1 (2000), 65–86.
- [26] INABA, H. Threshold and stability results for an age-structured epidemic model. *Journal of mathematical biology* 28, 4 (1990), 411–434.

- [27] JAYCOX, E. R., SKOWRONEK, W., AND GUYNN, G. Behavioral changes in worker honey bees (*apis mellifera*) induced by injections of a juvenile hormone mimic. *Annals of the Entomological Society of America* 67, 4 (1974), 529–534.
- [28] JONES, J. C., HELLIWELL, P., BEEKMAN, M., MALESZKA, R., AND OLDROYD, B. The effects of rearing temperature on developmental stability and learning and memory in the honey bee, *Apis mellifera*. *Journal of Comparative Physiology A* 191, 12 (2005), 1121–1129.
- [29] KHOURY, D. S., BARRON, A. B., AND MYERSCOUGH, M. R. Modelling food and population dynamics in honey bee colonies. *PLOS ONE* 8, 5 (05 2013), e59084.
- [30] KHOURY, D. S., MYERSCOUGH, M. R., AND BARRON, A. B. A quantitative model of honey bee colony population dynamics. *PLOS ONE* 6, 4 (04 2011), e18491.
- [31] LEONCINI, I., LE CONTE, Y., COSTAGLIOLA, G., PLETTNER, E., TOTH, A. L., AND WANG, M. Regulation of behavioral maturation by a primer pheromone produced by adult worker honey bees. *Proceedings of the National Academy of Sciences of the United States of America* 101, 50 (2004), 17559–17564.
- [32] LI, J., AND BRAUER, F. Continuous-time age-structured models in population dynamics and epidemiology. In *Mathematical Epidemiology*, F. Brauer, P. van den Driessche, and J. Wu, Eds. Springer, 2008, pp. 205–227.
- [33] MAGAL, P., McCLUSKEY, C., AND WEBB, G. Lyapunov functional and global asymptotic stability for an infection-age model. *Applicable Analysis* 89, 7 (2010), 1109–1140.
- [34] MARTIN, S. Hygienic behaviour: an alternative view. *Bee Improvement* 7 (2000), 6–7.
- [35] MARTIN, S. J. The role of *Varroa* and viral pathogens in the collapse of honeybee colonies: a modelling approach. *Journal of Applied Ecology* 38, 5 (2001), 1082–1093.
- [36] McKENDRICK, A., AND PAI, M. K. The rate of multiplication of microorganisms: a mathematical study. vol. 31, pp. 649–655.
- [37] NEUMANN, P., AND CARRECK, N. L. Honey bee colony losses. *Journal of Apicultural Research* 49, 1 (2010), 1–6.
- [38] ODOUX, J.-F., AUPINEL, P., GATEFF, S., REQUIER, F., HENRY, M., AND BRETAGNOLLE, V. ECOBEE: a tool for long-term honey bee colony monitoring at the landscape scale in West European intensive agroecosystems. *Journal of Apicultural Research* 53, 1 (2014), 57–66.
- [39] OLVER, P. J. *Introduction to partial differential equations*. Springer, 2014.
- [40] PARKER, S. *McGraw-Hill dictionary of scientific and technical terms*. McGraw-Hill, 2003.
- [41] PERRY, C. J., SØVIK, E., MYERSCOUGH, M. R., AND BARRON, A. B. Rapid behavioral maturation accelerates failure of stressed honey bee colonies. *Proceedings of the National Academy of Sciences* 112, 11 (2015), 3427–3432.

- [42] PETRIC, A. T. *A Mathematical Model for a *N. ceranae* Infection in an *A. mellifera* Colony*. PhD thesis, 2016.
- [43] RATNIEKS, F. L., AND KELLER, L. Queen control of egg fertilization in the honey bee. *Behavioral Ecology and Sociobiology* 44, 1 (1998), 57–61.
- [44] RATTI, V., KEVAN, P. G., AND EBERL, H. J. A mathematical model for population dynamics in honeybee colonies infested with *Varroa destructor* and the Acute Bee Paralysis Virus. *Canadian Applied Mathematics Quarterly* 21, 1 (2013), 63–93.
- [45] RATTI, V., KEVAN, P. G., AND EBERL, H. J. A mathematical model of the honeybee-*Varroa destructor*-Acute Bee Paralysis Virus complex with seasonal effects. *Bulletin of Mathematical Biology* (2015).
- [46] ROBINSON, G. E., PAGE, R. E., STRAMBI, C., AND STRAMBI, A. Colony integration in honey bees: mechanisms of behavioral reversion. *Ethology* 90, 4 (1992), 336–348.
- [47] RUSSELL, S., BARRON, A. B., AND HARRIS, D. Dynamic modelling of honey bee (*Apis mellifera*) colony growth and failure. *Ecological Modelling* 265, 0 (2013), 158 – 169.
- [48] SAKAGAMI, S., AND FUKUDA, H. Life tables for worker honeybees. *Researches on Population Ecology* 10, 2 (1968), 127–139.
- [49] SCHMICKL, T., AND CRAILSHEIM, K. Hopomo: A model of honeybee intracolony population dynamics and resource management. *Ecological modelling* 204, 1 (2007), 219–245.
- [50] SEELEY, T. D. *The wisdom of the hive: the social physiology of honey bee colonies*. Harvard University Press, 2009.
- [51] SEELEY, T. D. *Honeybee Democracy*. Princeton University Press, 2010.
- [52] SMITH, G. D. *Numerical solution of partial differential equations: finite difference methods*. Oxford University press, 1985.
- [53] SMITH, M. L. The honey bee parasite *Nosema ceranae*: Transmissible via food exchange? *PLOS ONE* 7, 8 (08 2012), e43319.
- [54] SOUTHWICK, E. E., AND SOUTHWICK JR, L. Estimating the economic value of honey bees (*Hymenoptera: Apidae*) as agricultural pollinators in the United States. *Journal of Economic Entomology* 85, 3 (1992), 621–633.
- [55] STEVANOVIC, J., SIMEUNOVIC, P., GAJIC, B., LAKIC, N., RADOVIC, D., FRIES, I., AND STANIMIROVIC, Z. Characteristics of *Nosema ceranae* infection in Serbian honey bee colonies. *Apidologie* 44, 5 (2013), 522–536.
- [56] STEWART, J. *Multivariable calculus*. Cengage Learning, 2011.
- [57] SUMPTER, D. J. T., AND MARTIN, S. J. The dynamics of virus epidemics in *Varroa*-infested honey bee colonies. *Journal of Animal Ecology* 73, 1 (2004), 51–63.

- [58] TERESHKO, V., AND LOENGAROV, A. Collective decision-making in honey bee foraging dynamics. *Computing and Information Systems* 9, 3 (2005), 1.
- [59] THIEME, H. R. Spectral bound and reproduction number for infinite-dimensional population structure and time heterogeneity. *SIAM Journal on Applied Mathematics* 70, 1 (2009), 188–211.
- [60] VAN DEN DRIESSCHE, P., AND WATMOUGH, J. Reproduction numbers and sub-threshold endemic equilibria for compartmental models of disease transmission. *Mathematical biosciences* 180, 1 (2002), 29–48.
- [61] VAN DER STEEN, J. J., CORNELISSEN, B., DONDEERS, J., BLACQUIÈRE, T., AND VAN DOOREMALEN, C. How honey bees of successive age classes are distributed over a one storey, ten frames hive. *Journal of Apicultural Research* 51, 2 (2012), 174–178.
- [62] VANCE, J. T., WILLIAMS, J. B., ELEKONICH, M. M., AND ROBERTS, S. P. The effects of age and behavioral development on honey bee (*Apis mellifera*) flight performance. *Journal of Experimental Biology* 212, 16 (2009), 2604–2611.
- [63] VANENGELSDORP, D., EVANS, J. D., SAEGERMAN, C., MULLIN, C., HAUBRUGE, E., NGUYEN, B. K., FRAZIER, M., FRAZIER, J., COX-FOSTER, D., CHEN, Y., UNDERWOOD, R., TARPY, D. R., AND PETTIS, J. S. Colony collapse disorder: A descriptive study. *PLOS ONE* 4, 8 (08 2009), e6481.
- [64] WANG, W., AND ZHAO, X.-Q. Basic reproduction numbers for reaction-diffusion epidemic models. *SIAM Journal on Applied Dynamical Systems* 11, 4 (2012), 1652–1673.
- [65] WATANABE, M. E. Colony collapse disorder: Many suspects, no smoking gun. *BioScience* 58, 5 (2008), 384–388.
- [66] WINSTON, M. *The biology of the honey bee*. Harvard University Press, 1987.

Chapter 4

Age structure is Critical to the Population Dynamics and Survival of Honey Bee Colonies

Abstract

Age-structure is an important feature of the division of labour within honey bee colonies, but its effects on colony dynamics have rarely been explored. We present a model of a honey bee colony that incorporates this key feature, and use this model to explore the effects of both winter and disease on the fate of the colony. The model offers a novel explanation for the frequently observed phenomenon of “spring dwindle”, which emerges as a natural consequence of the age-structured dynamics. Furthermore, the results indicate that a model taking age structure into account markedly affects the predicted timing and severity of disease within a bee colony. The timing of the onset of disease with respect to the changing seasons may also have a substantial impact on the fate of a honey bee colony. Finally, simulations predict that an infection may persist in a honey bee colony over several years, with effects that compound over time. Thus the ultimate collapse of the colony may be the result of events several years past.

4.1 Introduction

As honey bee populations continue to decline on a global scale [5], research efforts have been directed at identifying the underlying causes [12, 20, 43, 45]. These efforts are necessitated by the ecological [13] and economical importance of honey bee colonies worldwide [9, 29, 40].

To date, much of this research has been focused on the effects of pesticide and insecticide exposure on honey bee health and ultimately colony fitness [18, 45]. Such hazards may cause injury or death to foraging bees, forcing surviving bees to begin foraging prematurely which will then disrupt the dynamics of the colony, ultimately leading to colony collapse [18, 23, 24]. Further research has focused on the effects of parasitism and disease [6, 7, 14, 32, 33, 41], for example, the effects of *Varroa destructor* on honey bee colony dynamics [14, 32, 33, 41], the effects of the microsporidian parasite *Nosema ceranae* [19], and the effects of communicable infections more generally [6].

Recent work has also explored the combined effects of two stressors such as disease, limited biodiversity, and/or exposure to pesticides, which may create conditions detrimental to honey bee colony survival [1, 2, 17, 28, 39, 44]. Simulation packages have been developed to model these effects using realistic parameter values [4, 36]. For example, Pettis et al. explored the interplay between environmental hazards and the subsequent susceptibility to *Nosema ceranae* [31]. In previous work [6], we showed that the fate of a honey bee colony in the presence of disease is dependent on seasonality, particularly the onset of winter.

Previous mathematical models of honey bee dynamics have not considered the effects of age-structure within the hive, yet the duties of female bees, which constitute the main work force of the hive, are determined primarily by their age [34]. Specifically, the hierarchy of a colony hinges on both bee morphology and age [10, 35, 37]: caste polyethism differentiates a queen bee from a female worker bee [46], while age polyethism determines the functions of the worker bees [34].

The age distribution within a honey bee colony is an intrinsic property and this property is therefore important to colony survival because it affects two key components in the dynamics of the colony, namely ongoing recruitment and death. In the present paper, we examine how the disease-free age distribution within a colony is altered in the face of a hazard, and how these changes affect previous predictions of colony survival.

We identify periods of increased vulnerability of the colony to the effects of winter, disease, or a combination of the two, during which the colony would benefit from remedial actions (e.g. higher anti-microbial treatments, increased observation and management etc.). In addition, we use the added dimension of age-structure to explore the long standing phenomenon of “spring dwindle” whereby a drop in the number of bees within a colony occurs immediately after the end of winter [47]. While the phenomenon is generally suspected to be due to various stressors [15, 30, 38], the specific colony dynamics that lead to this phenomenon have not been established. The question of why the dwindle occurs after rather than during winter remains unanswered. The resolution of this puzzle is of particular value in the ongoing research efforts to understand and ultimately avert honey bee colony collapse, since spring dwindle leaves the colony in a particularly vulnerable state. Finally, we simulate colony dynamics in the presence of disease for multiple years to demonstrate the compounding effects of infection.

4.2 Model

We present a mathematical model that combines the disease-free demographics of a honey bee colony with the effects of seasonal changes and a disease that at first infects foragers, and then spreads to the rest of the colony. Earlier versions of this model were introduced by Khoury et al. in 2011 and 2013 [23, 24] and were developed further in 2015 [6]. Analytical details of the model, including local and global stability of the disease free equilibrium as well as a derivation of the basic reproduction number, R_0 , are presented in [7].

Briefly, the effects of the brood, guarding bees, as well as bees that work to repair the hive are neglected. The focus is solely on the hive bees, H , which are responsible for ensuring the survival of the brood, and the foragers, F , which are responsible for bringing food, f , into the hive. The male honey bees, known as drones, are also neglected since they contribute only to reproduction [46]. In the presence of disease, the two classes of bees are further divided into

the susceptible populations, H_S and F_S , and the infected populations, H_I and F_I .

4.2.1 Age Structure

We incorporate an age structure into the age-independent equations [6], using the standard approach of McKendrick [27] by writing

$$\frac{\partial H_S}{\partial t} + \frac{\partial H_S}{\partial a} = -u(a)H_S - \beta \mathcal{N} H_S, \quad (4.1)$$

where $H_S(a, t)$ is the number of susceptible hive bees of age a at time t and $u(a)$ is the age-dependent rate of recruitment to foraging. Juvenile hormone III regulates the age at which honey bees begin foraging [34], making older bees more likely to be recruited to foraging duties. As well, it has been observed that there is a minimum age, a_R , before which bees cannot be recruited [16]. Behavioural maturation of hive bees is further regulated by a pheromone, ethyl oleate, that is produced by foragers [26] and has the effect of delaying the age at which bees are recruited to foraging duties. This so-called ‘‘social inhibition’’ process reduces recruitment when the number of foragers in the colony is high [26]. We account for these biological processes by defining $u(a)$ as

$$u(a) = \alpha \left(\frac{a}{a+k} \right)^2 \left(1 - \frac{\sigma}{N} \int (F_S + F_I) da \right) H_v(a - a_R) \quad (4.2)$$

where α is the maximum rate of recruitment and $H_v(a - a_R)$ is the Heaviside function such that recruitment cannot begin before age a_R . Thereafter, the recruitment rate we are using increases sigmoidally with age. At age k , recruitment will be one quarter the maximum rate of recruitment. $1/\sigma$ is the maximum proportion of bees that are foraging at any given time and N is the total number of bees given by

$$N = \int (H_S + H_I + F_S + F_I) da. \quad (4.3)$$

The emergence of new hive bees is modeled as the left boundary condition to Equation (4.1). This, along with other boundary conditions are described at the end of this section.

The second term on the right-hand side of equation (4.1) governs the disease dynamics within the hive. We approximate the transmission of disease as a mass action process and assume that, on average, hive bees and foragers transmit infection between or within classes at rate β . The total number of infected bees is given by

$$\mathcal{N} = \int (H_I + F_I) da. \quad (4.4)$$

The hive provides substantial safety for bees that are confined to it [24, 37]. We therefore assume that the natural death rate of healthy hive bees is negligible compared to the rate of recruitment.

The equation governing the dynamics of infected hive bees is given by

$$\frac{\partial H_I}{\partial t} + \frac{\partial H_I}{\partial a} = \beta \mathcal{N} H_S - u(a)H_I - d_H(a)H_I. \quad (4.5)$$

In contrast with their healthy peers, infected hive bees are at risk of dying due to disease at an age-dependent rate $d_H(a)$.

Susceptible foragers are recruited from susceptible hive bees, and suffer age-dependent natural death at rate $\mu(a)$. Their dynamics are therefore governed by

$$\frac{\partial F_S}{\partial t} + \frac{\partial F_S}{\partial a} = u(a)H_S - \mu(a)F_S - \beta\mathcal{N}F_S \quad (4.6)$$

Infected foragers can either be recruited from infected hive bees, or from susceptible foragers that have become infected. If we assume this class is subject to a disease-related death rate of $d_F(a)$, then their dynamics are governed by

$$\frac{\partial F_I}{\partial t} + \frac{\partial F_I}{\partial a} = u(a)H_I + \beta\mathcal{N}F_S - (\mu(a) + d_F(a))F_I. \quad (4.7)$$

Food, f , is brought into the hive by both susceptible and infected foragers. Although it is likely that infected foragers would be less efficient at this task [25], for simplicity, we take an average rate of food intake, c (g/day/forager). Food is consumed by foragers and hive bees at an average rate γ . Therefore, the amount of food available at time t changes according to

$$\frac{df}{dt} = c \int (F_S + F_I) da - \gamma N. \quad (4.8)$$

The above system of equations governing the dynamics of the colony is subject to the following boundary conditions:

$$\begin{cases} H_S(0, t) = LS \\ H_I(0, t) = F_S(0, t) = F_I(0, t) = 0 \end{cases} \quad (4.9)$$

The first condition represents the emergence of new adult bees, where L is the daily egg laying rate of the queen and S is a survivability function, which determines how many eggs survive to adulthood. The brood needs both sufficient food and sufficient care from the hive bees in order to survive [22]. Moreover, it has been shown that there is a range of ages within which hive bees will take on this care for the brood, a minimum age, a_m , and a maximum age, a_T between 11 and 16 days old [35]. After this age, hive bees tend to transition to foraging duties, or possibly security or hive maintenance [46]. Therefore, we define the survivability function S as

$$S = \left(\frac{f}{b + f} \right) \left(\frac{\int_{a_m}^{a_T} H(a, t) da}{w + \int_{a_m}^{a_T} H(a, t) da} \right). \quad (4.10)$$

Here b is the amount of food required for half the eggs to survive to adulthood provided the brood has sufficient care, w is the number of care providers required for half the eggs to survive provided the brood has sufficient food, and $H(a, t) = H_S(a, t) + H_I(a, t)$.

The dynamics described in this section relate to the main active season of the bee colony, which is defined as the time interval between the end of one winter and the beginning of the next.

4.2.2 Winter

The winter season is assumed to last 155 days or roughly 5 months, roughly corresponding to a humid continental climate [3]. Over winter, no new hive bees emerge (although some eggs are still being laid by the queen) and foragers return to the hive [46]. Accordingly, in boundary conditions 4.9 we set $L = 0$ and in equations 4.1, 4.5, 4.6, 4.7 and 4.8 we set $u(a) = 0$ and $c = 0$. Due to an extended lifespan of bees over winter [46], the death rate of hive bees is no longer negligible and is set to an average rate of

$$\mu_w = \frac{1}{180}, \quad (4.11)$$

corresponding to an average lifespan over winter of 6 months [46]. All bees are performing the same function over winter (keeping the hive warm [21]), therefore we set the natural death rate of foragers equal to that of the hive bees, $\mu(a) = \mu_w$.

As winter ends, bees resume their normal age-related duties, and bees that were foraging before winter resume their roles as foragers. We assume that a 21-day transition takes place during which parameter values change linearly from end-of-winter to new active season values as follows:

$$\left. \begin{aligned} \mu_{trans}(a) &= \left(1 - \frac{t}{21}\right)\mu_w(a) + \left(\frac{t}{21}\right)\mu(a) \\ L_{trans} &= \left(\frac{t}{21}\right)L \\ S_{trans} &= \left(\frac{t}{21}\right)S + \left(1 - \frac{t}{21}\right)S^* \end{aligned} \right\} 0 \leq t \leq 21 \quad (4.12)$$

where

$$S^* = \left(\frac{f}{b+f}\right) \left(\frac{\int_{a_m}^{\infty} H_S(a,t) da}{w + \int_{a_m}^{\infty} H_S(a,t) da}\right), \quad (4.13)$$

that is, during winter hive bees of all ages may contribute to brood care. Note that new hive bees that emerge during the early spring come from eggs that were laid over the winter months, after completing phases of development to adulthood.

Equations (4.1), (4.5), (4.6), (4.7), and (4.8) form a system of integro-partial differential equations which we solved simultaneously to predict the population dynamics of a honey bee colony. The parameter values used in the solution are given in Table A.1 in the supplementary material.

In [42], the authors found that the age distribution in a colony is as follows: 41% of bees were one week old, 23% were two weeks old, 17% were three weeks old, 11% were four weeks old, and 8% were five weeks old. Accordingly, the death rate $\mu_{ex}(a)$ in our model was constructed to approximately match the experimental findings. In order to account for the whole range of ages and remain consistent with the five weeks of study in [42], we break the age range into five cohorts of ten days each. The comparison between experimental data and our model is summarized in Table 4.1. The death rate that best matched the observed data is defined by

$$\mu_{ex}(a) = \begin{cases} 1 - e^{-\frac{(a-20)^2}{10}} & a \leq 20 \\ C_{ex} \left(\frac{a-20}{20}\right)^4 & a > 20 \end{cases}. \quad (4.14)$$

where parameter values were set such that the percentage of bees in their first week of life matches the experimental data. This death rate is relatively high for very young ($\approx < 10$ days) or very old bees ($\approx > 40$ days), as shown in Figure 6.2. We see that the drop in population density after week 1, as observed in [42], can be explained by the high death rate of young foragers.

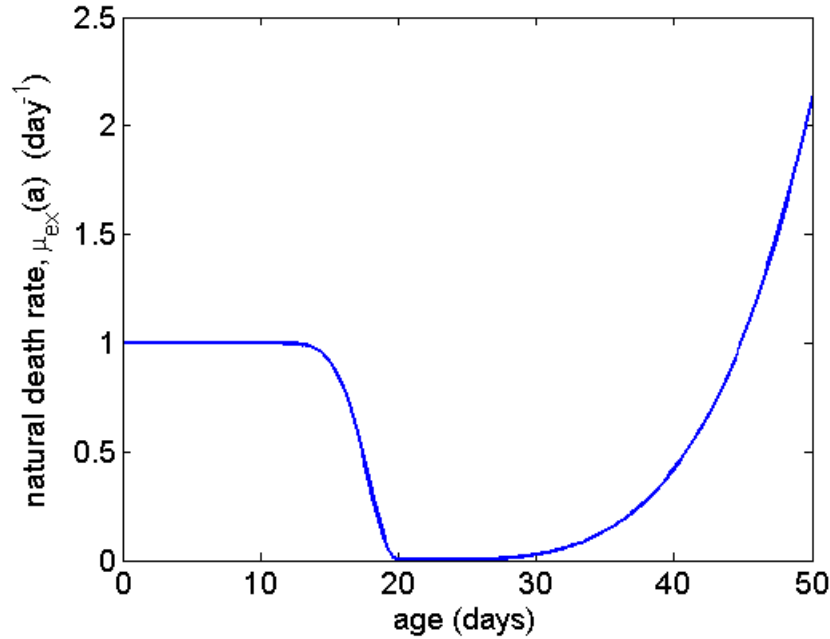


Figure 4.1: Death rate distribution which provides the best fit to experimental results observed in [42]; parameter $C_{ex} = 0.42$.

We performed sensitivity analysis (see Supplementary Material Figure A.1) and found that our results are insensitive to the details of the death rate distribution. We therefore use a simplified version of the natural death rate distribution,

$$\mu(a) = C \frac{(a - 20)^2}{400}, \quad (4.15)$$

to make the mathematics more tractable. This death rate is plotted in Figure 4.2, and also compared with the experimental results in Table 4.1, showing good agreement.

The disease-related death rate,

$$d(a) = -\frac{K_1}{\pi} \tan^{-1}(a - 10) + K_2, \quad (4.16)$$

is motivated by deformed wing virus [11] that disproportionately affects young bees. The constants C , K_1 and K_2 are chosen such that both the natural and disease-related death rates are non-negative and have an average of 0.14 per day as in [6]. In other cases, we assume the disease affects all bees uniformly, i.e. $d(a) = d$. The effects of different death rate distributions are shown in the supplementary material (Figures A.4–A.12). The results are qualitatively the same.

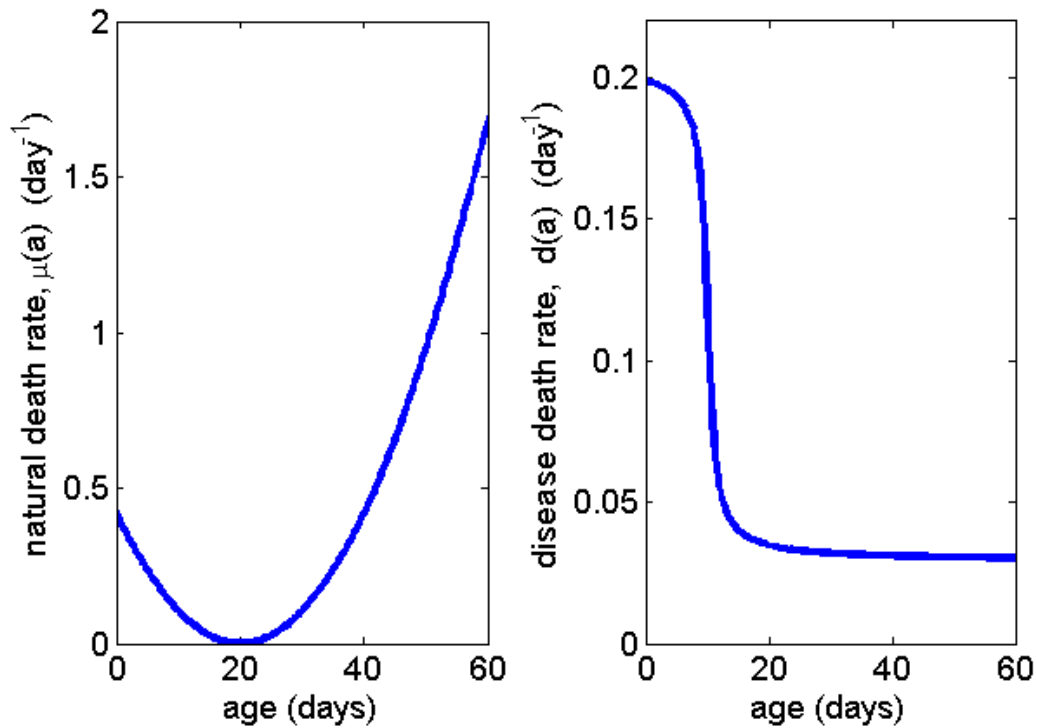


Figure 4.2: The natural death rate, $\mu(a)$, and an example of disease-related death rate, $d(a)$, motivated by deformed wing virus, which predominantly affects young bees [11]. During the active season, honey bees live an average of five to seven weeks [46], thus we define our death rates until the age of 60 days. Beyond this age few, if any, bees are still alive and we set their natural death rate as $\mu(a > 60) = \max(\mu(a))$.

Figure A.1 in the supplementary material shows the age distribution within a disease-free colony under the natural death rate $\mu(a)$ shown in Figure 4.2. This is used as a baseline distribution for all simulations that begin from equilibrium. We predict from this distribution that the mean forager age of a healthy colony is approximately 25 days [8, 46].

4.3 Results

Figure 4.3 shows the effects of changing seasons on the number of bees in a colony in the absence of disease. The seasonal shift back to normal operating conditions is seen to bring with it a drop in the bee population as the colony emerges from winter. It is obvious that a longer winter may have a fatal effect on the colony, due to winter only having deleterious effects on a colony. This is because the surviving bees are now much older and are subject to a higher natural death rate, while a new generation of younger bees has not yet emerged to replace them. This seasonal drop in the bee population, which has been referred to as “spring dwindle” [15, 30, 38, 47], is discussed further in the next section. The population dynamics that produce the phenomenon have not been fully understood in the past because these dynamics emerge only when the age distribution within the colony is considered.

Cohort	Experimental Values [42]	Model Values, $\mu_{ex}(a)$	Model Values, $\mu(a)$
1	$41 \pm 6.4\%$	41% (0)	41% (0)
2	$23 \pm 5.1\%$	25% (0.39)	30% (1.37)
3	$17 \pm 3.7\%$	18% (0.27)	16% (0.27)
4	$11 \pm 2.2\%$	11% (0)	7% (1.81)
5	$8 \pm 1.3\%$	5% (2.31)	6% (1.54)

Table 4.1: Comparison of experimental results with model results. Standard deviation for experimental results are given; z-scores computed from experimental mean and standard deviations are given in parentheses next to model values.

Our next objective is to compare the dynamics of the age-structured honey bee colony model with the dynamics of the age-independent model such as that presented in [6]. To give the comparison a measure of equivalency, the same value of the basic reproduction number is used in both cases, namely $R_0 = 1.43$, calculated using the formulas derived in [7]. Figure 5.7 shows that an age-independent model makes significantly different predictions about the timing and the severity of disease within a bee colony. This is further explored in the supplementary material (Figure A.3) where we demonstrate that an age-dependent recruitment function both lowers the severity of a disease and delays the timing of an epidemic, while age-dependent death rates, $\mu(a)$ and $d(a)$, trade-off the two effects.

The vulnerability of a bee colony in early spring is explored further in Figure 4.5 which illustrates that an infection which is endemic in a colony during one active season and one winter may pose the greatest risk to the colony during the small window in which the hive is recovering from the winter months. Moreover, the colony may suffer much greater losses after its second, third and fourth winters with disease (figure inset).

The time interval between the beginning of an infection and the onset of winter is an important determinant of the health of the colony at the end of winter, as illustrated in Figure 4.6. The figure shows that the number of bees surviving to the end of winter, N_W , depends on when the infection begins relative to winter. In the figure the infection begins from a single infected forager Δt days before winter. The time interval between the end of one winter and the beginning of the next is taken to be approximately 200 days (≈ 7 months). The timing of the infection is seen to produce a point of highest vulnerability (local minimum in population size) which depends on the severity of the disease as represented by the basic reproduction number.

The timing and depth of the points of highest vulnerability seen in Figure 4.6 are tightly coupled to the time at which an infection peaks within the colony, which in turn is related to R_0 . Figure 4.7 shows this relationship, estimating the time of greatest risk to the colony, Δt^* , with respect to the onset of winter, based on the basic reproduction number. Of course, for high values of R_0 the colony is likely to suffer substantial losses regardless of when a disease occurs. In Figure 4.6, we see for example that for $R_0 = 2.0$, Δt^* is unique, but when $R_0 = 2.2$ there are two Δt^* values producing the observed bifurcation in Figure 4.7. To measure the relative significance of these minima, we use the metric $\max(N_W) - \min(N_W)$ where the maximum and minimum are computed for each value of R_0 , over the range of possible Δt . The larger the value of this metric, the greater the significance of the time of onset of disease, Δt .

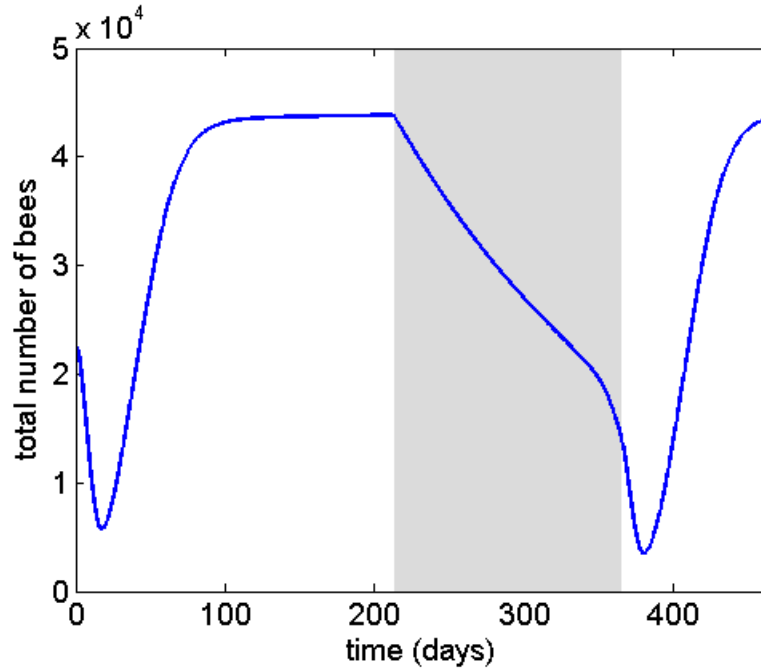


Figure 4.3: Time course of total bee population in a disease-free colony. Shaded area denotes winter, during which no brood is produced. We see that the aged bees that restart the colony post-winter create an added risk to the colony, because of their relatively high death rate, until new brood is able to hatch and contribute to population rebound. The post-winter dip seen in the figure has been referred to in the literature as “spring dwindle” but its dynamics have not been previously described.

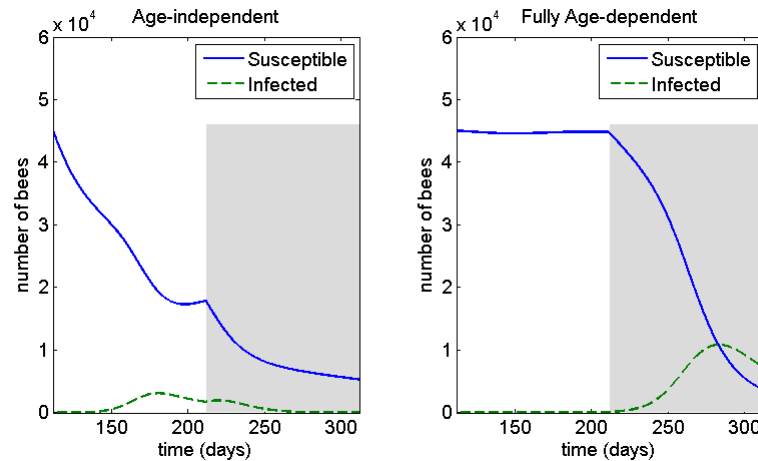


Figure 4.4: Effect of age distribution on the dynamics of disease within the bee colony. The blue line represents the total number of susceptible bees and the green dashed line represents the total infected bees. The shaded area denotes winter. Disease begins with a single infected forager at $t = 112$. We use the death rates given in Figure 4.2. The two time courses show that the two models have significant differences in their predictions when simulating disease dynamics in the colony.

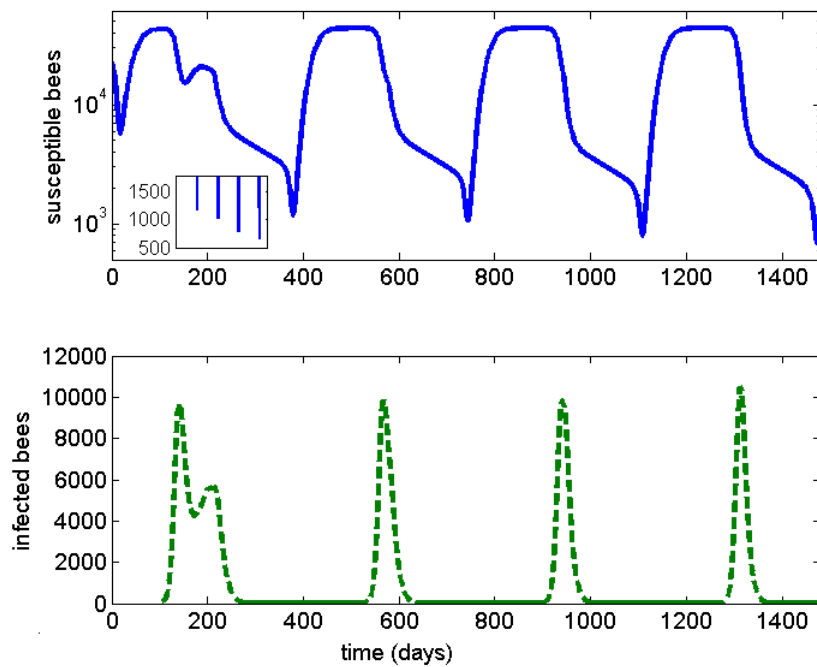


Figure 4.5: Time course of the bee population over four years. The top panel shows the total number of susceptible bees, $H_S + F_S$, and the bottom panel shows the total number of infected bees, $H_I + F_I$. An infection is introduced into a colony at equilibrium through a single infected forager at time $t = 0$. The inset shows the minimum population size of susceptible bees during the spring dwindle following each winter. There is a clear decrease in this minimum year after year, thus the risk of colony collapse increases year after year. The ultimate collapse of a bee colony may therefore be the consequence of events long past.

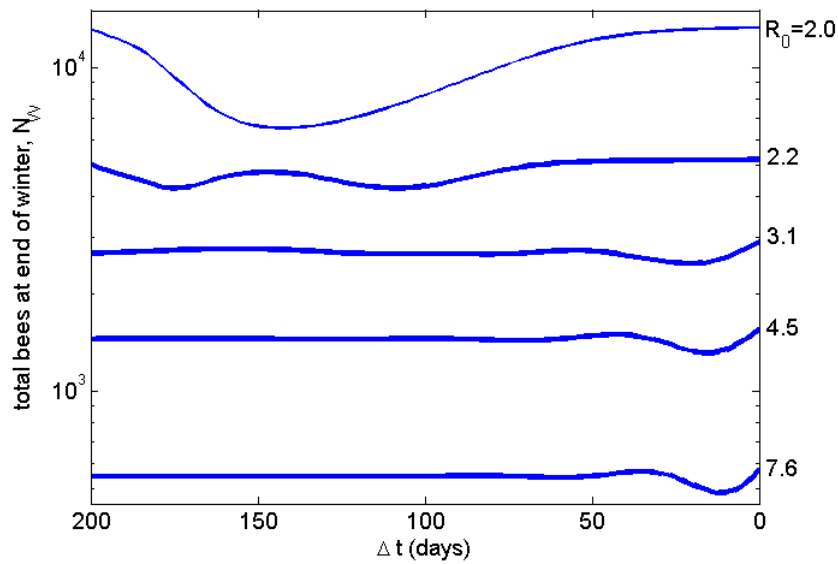


Figure 4.6: Number of bees at the end of winter as a function of the time interval, Δt between the onset of disease and the beginning of winter, based on various values of the basic reproduction number, R_0 . The minima show times during which the colony is most vulnerable due to the combined effects of winter and disease. The colony is started from the equilibrium age distribution shown in Figure A.1. Infection is introduced at time $t = 200 - \Delta t$ via one infected forager. The total number of bees is calculated at the end of winter. R_0 values are calculated using the expression derived in [7].

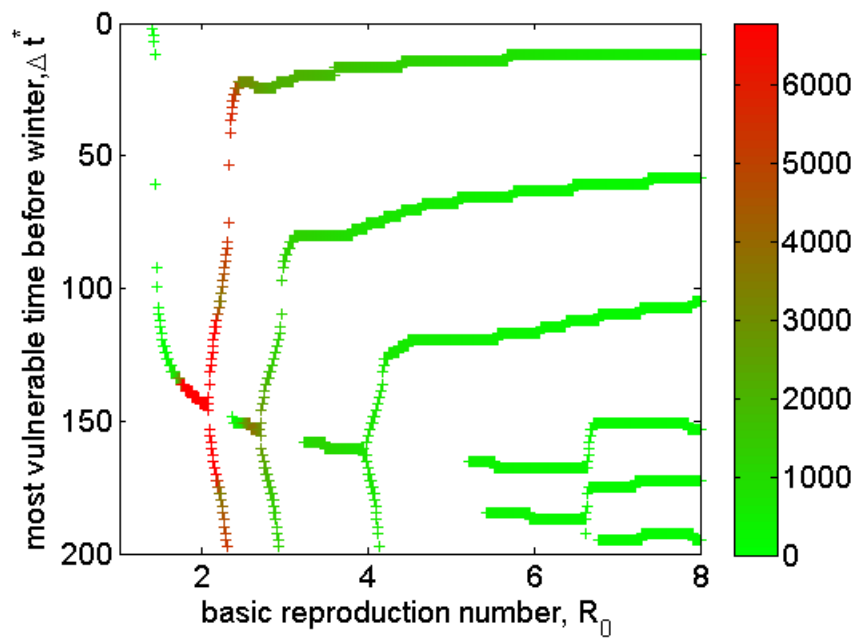


Figure 4.7: The timing and depth of points of highest vulnerability as a function of the basic reproduction number, R_0 . The colour bar reflects the depth of the minima seen in Figure 4.6 (see text for details). Red indicates the most severe combinations of R_0 and Δt^* , where Δt^* is the value of Δt in Figure 4.6 at which a local minimum occurs.

4.4 Discussion

Our results demonstrate that the age structure that is inherent to all honey bee colonies has critical effects on colony survival that are not captured by previously explored age-independent models. Most notably, an age-dependent recruitment rate has a profound impact on the dynamics, severity, and spread of an infection in a bee colony. In fact, our results predict that age polyethism in a honey bee colony has the beneficial effect of impeding the spread of infection within the colony. Thus, in practice, any disturbance in the natural age structure of a bee colony may also increase the severity of an infection within the hive. Results in the supplementary material (Figure A.3) indicate that the natural age distribution within a colony creates a delay in the speed of spread of an infection. Again, this suggests that any intervention that would alter the natural age distribution may have the adverse effect of increasing the spread of infection within a hive.

Our explicit treatment of the colony age distribution also revealed the dynamics underlying the frequently observed phenomenon of “spring dwindle” in which the total number of bees within a colony weakens rapidly immediately after the end of winter. While the phenomenon is generally suspected to be due to various stressors that occurs during winter [15, 30, 38], our results suggest that declining spring populations are a natural consequence of honey bee colony dynamics, leading to seasonal vulnerability during which the colony may be particularly susceptible to other hazards. This post-winter dip is not captured by age-independent models because the phenomenon is due predominantly to the aging of the bees over the winter months and the time required to replace them by younger bees in the early spring.

Simulations of colony dynamics over multiple winter seasons demonstrated that endemic diseases may weaken the colony year after year, increasing the risk of colony collapse during spring. Thus the eventual collapse of a bee colony may be due to the compounded effects of an infection over several years.

The time interval between the onset of an infection and the beginning of an approaching winter is a critical determinant of the ultimate course and consequence of the disease within a bee colony. As illustrated in Figures 4.6 and 4.7, this effect is most important for infections with a basic reproduction number close to 2. In this case, the colony is particularly vulnerable in the early spring, approximately 5 months before the onset of winter.

In conclusion, age structure is an inherent property of honey bee colonies, determining the division of labour and defining how age-related events such as disease and death unfold within the colony. Our results suggest that age structure should be a key consideration in future studies of honey bee population dynamics, and that accurate models of age structure will be necessary if we are to understand, and ultimately reverse, the increases in colony collapse observed in recent years.

Bibliography

- [1] ALAUX, C., BRUNET, J.-L., DUSSAUBAT, C., MONDET, F., TCHAMITCHAN, S., COUSIN, M., BRILLARD, J., BALDY, A., BELZUNCES, L. P., AND LE CONTE, Y. Interactions between *Nosema* microspores and a neonicotinoid weaken honeybees (*Apis mellifera*). *Environmental microbiology* 12, 3 (2010), 774–782.
- [2] AUFAUVRE, J., BIRON, D. G., VIDAU, C., FONTBONNE, R., ROUDEL, M., DIOGON, M., VIGUÈS, B., BELZUNCES, L. P., DELBAC, F., AND BLOT, N. Parasite-insecticide interactions: a case study of *Nosema ceranae* and fipronil synergy on honeybee. *Scientific reports* 2 (2012).
- [3] BALDWIN, D. J., DESLOGES, J. R., AND BAND, L. E. Physical geography of ontario. *Ecology of a managed terrestrial landscape: patterns and processes of forest landscapes in Ontario* (2011), 12.
- [4] BECHER, M. A., GRIMM, V., THORBEC, P., HORN, J., KENNEDY, P. J., AND OSBORNE, J. L. BEEHAVE: a systems model of honeybee colony dynamics and foraging to explore multifactorial causes of colony failure. *Journal of applied ecology* 51, 2 (2014), 470–482.
- [5] BECHER, M. A., OSBORNE, J. L., THORBEC, P., KENNEDY, P. J., AND GRIMM, V. Review: Towards a systems approach for understanding honeybee decline: a stocktaking and synthesis of existing models. *Journal of Applied Ecology* 50, 4 (2013), 868–880.
- [6] BETTI, M. I., WAHL, L. M., AND ZAMIR, M. Effects of infection on honey bee population dynamics: A model. *PLOS ONE* 9, 10 (2014), e110237.
- [7] BETTI, M. I., WAHL, L. M., AND ZAMIR, M. Reproduction number and asymptotic stability for a model with continuous age structure: An application to honey bee dynamics. *Bulletin of Mathematical Biology* (2016). submitted.
- [8] BOTIAS, C., MARTIN-HERNANDEZ, R., BARRIOS, L., MEANA, A., AND HIGES, M. *Nosema* spp. infection and its negative effects on honey bees (*Apis mellifera iberiensis*) at the colony level. *Veterinary research* 44, 1 (2013), 1–15.
- [9] CALDERONE, N. W. Insect pollinated crops, insect pollinators and US agriculture: Trend analysis of aggregate data for the period 1992-2009. *PLOS ONE* 7, 5 (05 2012), e37235.
- [10] CRAMP, D. *A Practical Manual of Beekeeping*. How To Books, London, 2008.
- [11] DE MIRANDA, J. R., AND GENERSCH, E. Deformed wing virus. *Journal of Invertebrate Pathology* 103 (2010), S48–S61.

- [12] DENNIS, B., AND KEMP, W. P. How hives collapse: Allee effects, ecological resilience, and the honey bee. *PLOS ONE* 11, 2 (2016), e0150055.
- [13] DEVILLERS, J. The ecological importance of honey bees and their relevance to ecotoxicology. In *Honey Bees: Estimating the Environmental Impact of Chemicals*, J. Devillers and M. Pham-Delègue, Eds. Taylor and Francis London, London, 2002, pp. 1–11.
- [14] EBERL, H. J., FREDERICK, M. R., AND KEVAN, P. G. Importance of brood maintenance terms in simple models of the honeybee - *Varroa destructor* - Acute Bee Paralysis Virus complex. *Electronic Journal of Differential Equations (EJDE) [electronic only]* 2010 (2010), 85–98.
- [15] EVANS, J. D., AND SCHWARZ, R. S. Bees brought to their knees: microbes affecting honey bee health. *Trends in microbiology* 19, 12 (2011), 614–620.
- [16] FAHRBACH, S., AND ROBINSON, G. Juvenile hormone, behavioral maturation and brain structure in the honey bee. *Developmental Neuroscience* 18 (1996), 102–114.
- [17] GOULSON, D., NICHOLLS, E., BOTÍAS, C., AND ROTHERAY, E. L. Bee declines driven by combined stress from parasites, pesticides, and lack of flowers. *Science* 347, 6229 (2015), 1255957.
- [18] HENRY, M., BEGUIN, M., REQUIER, F., ROLLIN, O., ODOUX, J.-F., AUPINEL, P., APTEL, J., TCHAMITCHIAN, S., AND DECOURTYE, A. A common pesticide decreases foraging success and survival in honey bees. *Science* 336, 6079 (2012), 348–350.
- [19] HIGES, M., MARTIN-HERNANDEZ, R., GARRIDO-BAILON, E., GONZALEZ-PORTO, A. V., GARCIA-PALENCIA, P., AND MEANA, A. Honeybee colony collapse due to *Nosema ceranae* in professional apiaries. *Environmental Microbiology Reports* 1, 2 (2009), 110–113.
- [20] HO, M.-W., AND CUMMINS, J. Mystery of disappearing honeybees. *Science in Society* 34 (2007), 35–36.
- [21] JAY, S. Seasonal development of honeybee colonies started from package bees. *Journal of Apicultural Research* 13 (1974), 149–152.
- [22] JONES, J. C., HELLIWELL, P., BEEKMAN, M., MALESZKA, R., AND OLDROYD, B. The effects of rearing temperature on developmental stability and learning and memory in the honey bee, *Apis mellifera*. *Journal of Comparative Physiology A* 191, 12 (2005), 1121–1129.
- [23] KHOURY, D. S., BARRON, A. B., AND MYERSCOUGH, M. R. Modelling food and population dynamics in honey bee colonies. *PLOS ONE* 8, 5 (05 2013), e59084.
- [24] KHOURY, D. S., MYERSCOUGH, M. R., AND BARRON, A. B. A quantitative model of honey bee colony population dynamics. *PLOS ONE* 6, 4 (04 2011), e18491.
- [25] KRALJ, J., AND FUCHS, S. *Nosema* sp. influences flight behavior of infected honey bee (*Apis mellifera*) foragers. *Apidologie* 41, 1 (2010), 21–28.

- [26] LEONCINI, I., LE CONTE, Y., COSTAGLIOLA, G., PLETTNER, E., TOTH, A. L., AND WANG, M. Regulation of behavioral maturation by a primer pheromone produced by adult worker honey bees. *Proceedings of the National Academy of Sciences of the United States of America* 101, 50 (2004), 17559–17564.
- [27] MCKENDRICK, A., AND PAI, M. K. The rate of multiplication of microorganisms: a mathematical study. vol. 31, pp. 649–655.
- [28] NAZZI, F., BROWN, S. P., ANNOSCIA, D., DEL PICCOLO, F., DI PRISCO, G., VARRICCHIO, P., DELLA VEDOVA, G., CATTONARO, F., CAPRIO, E., AND PENNACCHIO, F. Synergistic parasite-pathogen interactions mediated by host immunity can drive the collapse of honeybee colonies. *PLOS Pathog* 8, 6 (2012), e1002735.
- [29] NEUMANN, P., AND CARRECK, N. L. Honey bee colony losses. *Journal of Apicultural Research* 49, 1 (2010), 1–6.
- [30] OLDROYD, B. P. What’s killing American honey bees. *PLOS Biol* 5, 6 (2007), e168.
- [31] PETTIS, J. S., LICHTENBERG, E. M., ANDREE, M., STITZINGER, J., ROSE, R., VANENGELSDORP, D., ET AL. Crop pollination exposes honey bees to pesticides which alters their susceptibility to the gut pathogen *Nosema ceranae*. *PLOS ONE* 8, 7 (2013), e70182.
- [32] RATTI, V., KEVAN, P. G., AND EBERL, H. J. A mathematical model for population dynamics in honeybee colonies infested with *Varroa destructor* and the Acute Bee Paralysis Virus. *Canadian Applied Mathematics Quarterly* 21, 1 (2013), 63–93.
- [33] RATTI, V., KEVAN, P. G., AND EBERL, H. J. A mathematical model of the honeybee-*Varroa destructor*-Acute Bee Paralysis Virus complex with seasonal effects. *Bulletin of Mathematical Biology* (2015).
- [34] ROBINSON, G. E., PAGE, R. E., STRAMBI, C., AND STRAMBI, A. Colony integration in honey bees: mechanisms of behavioral reversion. *Ethology* 90, 4 (1992), 336–348.
- [35] SAKAGAMI, S., AND FUKUDA, H. Life tables for worker honeybees. *Researches on Population Ecology* 10, 2 (1968), 127–139.
- [36] SCHMICKL, T., AND CRAILSHEIM, K. Hopomo: A model of honeybee intracolony population dynamics and resource management. *Ecological modelling* 204, 1 (2007), 219–245.
- [37] SEELEY, T. D. *Honeybee Democracy*. Princeton University Press, 2010.
- [38] SMART, M. D., AND SHEPPARD, W. S. *Nosema ceranae* in age cohorts of the western honey bee (*Apis mellifera*). *Journal of invertebrate pathology* 109, 1 (2012), 148–151.
- [39] SMITH, M. L. The honey bee parasite *Nosema ceranae*: Transmissible via food exchange? *PLOS ONE* 7, 8 (08 2012), e43319.
- [40] SOUTHWICK, E. E., AND SOUTHWICK JR, L. Estimating the economic value of honey bees (*Hymenoptera: Apidae*) as agricultural pollinators in the United States. *Journal of Economic Entomology* 85, 3 (1992), 621–633.

- [41] SUMPTER, D. J. T., AND MARTIN, S. J. The dynamics of virus epidemics in *Varroa*-infested honey bee colonies. *Journal of Animal Ecology* 73, 1 (2004), 51–63.
- [42] VAN DER STEEN, J. J., CORNELISSEN, B., DONDEERS, J., BLACQUIÈRE, T., AND VAN DOOREMALEN, C. How honey bees of successive age classes are distributed over a one storey, ten frames hive. *Journal of Apicultural Research* 51, 2 (2012), 174–178.
- [43] VANENGELSDORP, D., EVANS, J. D., SAEGERMAN, C., MULLIN, C., HAUBRUGE, E., NGUYEN, B. K., FRAZIER, M., FRAZIER, J., COX-FOSTER, D., CHEN, Y., UNDERWOOD, R., TARPY, D. R., AND PETTIS, J. S. Colony collapse disorder: A descriptive study. *PLOS ONE* 4, 8 (08 2009), e6481.
- [44] VIDAU, C., DIOGON, M., AUFAUVRE, J., FONTBONNE, R., VIGUÈS, B., BRUNET, J.-L., TEXIER, C., BIRON, D. G., BLOT, N., EL ALAOU, H., ET AL. Exposure to sublethal doses of fipronil and thiacloprid highly increases mortality of honeybees previously infected by *Nosema ceranae*. *PLOS ONE* 6, 6 (2011), e21550.
- [45] WATANABE, M. E. Colony collapse disorder: Many suspects, no smoking gun. *BioScience* 58, 5 (2008), 384–388.
- [46] WINSTON, M. *The biology of the honey bee*. Harvard University Press, 1987.
- [47] YAMADA, T., ET AL. Honeybee colony collapse disorder. *Emerging Biological Threats: A Reference Guide: A Reference Guide* 13 (2009), 141.

Chapter 5

Bee++: An Object-Oriented, Agent-Based Simulator for Honey Bee Colonies

Abstract

We present a model and associated simulation package (www.beeplusplus.ca) to capture the natural dynamics of a honey bee colony in a spatially-explicit landscape, with temporally-variable, weather-dependent parameters. The simulation tracks bees of different ages and castes, food stores within the colony, pollen and nectar sources and the spatial position of individual foragers outside the hive. We track explicitly the intake of pesticides in individual bees and their ability to metabolize these toxins, such that the impact of sub-lethal doses of pesticides can be explored. Moreover, pathogen populations (in particular, *Nosema apis*, *Nosema cerenae* and *Varroa* mites) have been included in the model and may be introduced at any time or location. The ability to study interactions among pesticides, climate, biodiversity and pathogens in this predictive framework should prove useful to a wide range of researchers studying honey bee populations. To this end, the simulation package is written in open source, object-oriented code (C++) and can be easily modified by the user. Here, we demonstrate the use of the model by exploring the effects of sub-lethal pesticide exposure on the flight behaviour of foragers.

5.1 Introduction

Due to the importance of honey bees, both ecologically and agriculturally [14, 19, 51, 74], and because of their decreasing populations on a global scale, honey bees have been the focus of a large body of research [7, 24, 26, 34, 36, 43, 60, 80, 85]. The recent problem of colony collapse has led to a surge in research efforts into honey bee colony dynamics and the stresses they face. Efforts to understand the causes underlying honey bee decline are impeded by complex colony dynamics, along with the numerous interactions bees have with their local ecosystem; these factors create a system with multiple entwined variables, often confounding causality [19]. In order to gain insight into the problem of colony collapse and into the impact of honey bees as key players in their local ecosystem more generally, the suspected causes of colony collapse are often studied in isolation. In the last fifteen years, both experimental and theoretical studies have looked into the effects of factors such as competing hives [65], parasites [22, 35, 55, 80], food stores [42], and

pesticides [34]. More recently, the combined effects of parasites and pesticides have been addressed experimentally [84].

Due to the complexity of the problem, mathematical modelling has emerged as a valuable tool for exploring the dynamics of honey bee colonies; in particular, modelling approaches are well-suited for understanding the combined effects of multiple stressors on the colony. Several mathematical studies have addressed the compounding effects of pesticides and parasites on a honey bee colony [2, 22, 57, 61, 82]. In [22, 61], the effects of acute bee paralysis (vectored by the *Varroa destructor*) are studied in combination with pesticides and seasonality respectively. Pettis et al. predicted that an exposure to pesticides will increase the susceptibility of *Nosema ceranae* [57], which was shown experimentally by [2]. The effects of pesticide use in the local environment in the context of honey bee protection policy is studied, through models, in [82]. Others have further broadened the scope to account for the combined effects of pesticides and parasites, as well as a lack of biodiversity in the local environment [30]. Our previous studies have focused on the combined effects of temperature, seasonality and disease [7, 8].

These combined effects have also been synthesized into software simulation packages, studying *in silico* honey bee colonies in a wide range of environmental scenarios [5, 69]; this individual-based approach has proven useful for many ecological models [76]. The honey bee software packages are agent-based and include temperature data, stochastic behaviour, and seasonality. Also included in [5] is *Varroa* transmission, as well as possible human intervention in the context of care, or honey harvesting. Pesticide exposure is modelled as an increase in the death rate of foraging bees. In [69], the basic dynamics of a honey bee colony are modelled in depth.

We have developed a software package, Bee++, that can accurately model a honey bee colony in a spatially-explicit landscape, in which individual foragers can be tracked for the entirety of their trips away from the hive. Building on previous approaches, our model includes age, caste, food stores, temperature data and pathogens. In addition, our proposed model relaxes the typical simplification that pesticides can only affect the death rate of bees and allows for explicit tracking of toxin levels within individual bees. As a consequence, our model also allows individual bees to detoxify over time by modelling known mechanisms [39, 40]. This allows Bee++ to be used to simulate and study the long-term effects of pesticide exposure at non-lethal doses, as well as to simulate the compounding effects of different pesticides or prolonged exposure on honey bee physiology. The software package is highly configurable and developed on an open source platform. The individual parameters within the model may be varied by the user, and moreover, the functional form of the processes involved (e.g., recruitment to foraging, detoxification rate) can be modified. In what follows, we describe the algorithms underlying Bee++, with particular attention to functions and parameters that are configurable by the user. Our aim is to provide a platform that can be modified and extended to address a number of research questions. In what follows, we examine the effects of long-term pesticide exposure on the navigation abilities of foragers, primarily to illustrate the use of Bee++.

5.2 Model

Bee++ (<http://www.beeplusplus.ca>) consists of a stochastic, agent-based model for a honey bee colony and the surrounding environment. The model includes three classes of bees: hive bees, whose sub-classes consist of juveniles, nurses and maintenance work-

ers; foragers, whose sub-classes consist of scouts, nectar carriers and pollen carriers; and drones. The egg-laying function of the queen is modelled but, since Bee++ currently simulates the dynamics of a single colony, subsequent new queens produced in the hive are omitted.

Bee++ keeps track of the age of each bee, its current role, as well as any diseases it carries and its level of toxin exposure at any time. The simulation also monitors the state of the brood, the food stores in the hive (both pollen and honey, separately) and their levels of contamination by pesticides, fungicides or pathogens.

The environment external to the hive is modelled by the user as a spatial grid, in which some elements may contain nectar or pollen sources, and/or sources of pesticides or pathogens. These sources may be constant or may vary with the season as defined by the user. Within this grid, the position of each bee at each time step is tracked and updated as described in the sections to follow.

As a brief overview of the algorithm, at each time step the time-dependent parameters (e.g., environmental temperature) are updated, and then the decisions of each bee are considered. The number of brood is only updated once per day for simplicity and computational consideration. The number of brood that survive is dependent on the current food stores and amount of care available. The decisions of the hive bees depend on a number of parameters, namely temperature, infection, food stores, age and intoxication. The hive bees are able to transition between juveniles, nursing duties, maintenance duties and foraging based on the aforementioned parameters. Once recruited to foraging, the bees begin exploring the environment looking for food. In this way, they are able to transmit infection and pesticides from the environment back to the hive. They are also able to recruit new bees to particular patches of food that they have found. The navigational abilities of the foragers, along with their ability to survive, recruit and carry food are dependent mainly on the parameters mentioned above. Flow diagrams for the main program loop and for the three main classes of bees are provided in Figures 5.1 and 5.2, respectively. Details for the various processes follow.

5.2.1 Bees

Hive bees: Hive bees are modelled as agents, which, at each time step, make probabilistic decisions based on their age, the current demography of the colony and the state of the surrounding environment. The most important of these decisions is whether or not to be recruited to foraging duties. The recruitment rate increases with the age of the bee and is reduced if the temperature is not appropriate for foraging or if the fraction of bees already foraging is optimal. Specifically, a hive bee of age a begins watching a waggle dance (with the possibility of being recruited to also forage from that patch) at rate

$$p_W = \alpha \left(\frac{4(T - T_1)(T_2 - T)}{(T_1 + T_2)^2} \right) \left(\frac{a}{k + a} \right) \left(1 - \sigma \frac{F_T}{N} \right) \quad (5.1)$$

where α is the base rate of recruitment, k denotes the age at which a hive bee has a 50% chance of being recruited, F_T is the total number of bees currently foraging and N is the total working population in the colony. The factor $1/\sigma$ thus represents the fraction of foragers required to halt recruitment through social inhibition [17, 46, 72]. T_1 and T_2 are threshold temperatures such that foraging stops if the environmental temperature $T < T_1$ or $T > T_2$, and foraging peaks at $T = (T_1 + T_2)/2$. This is consistent with experimental

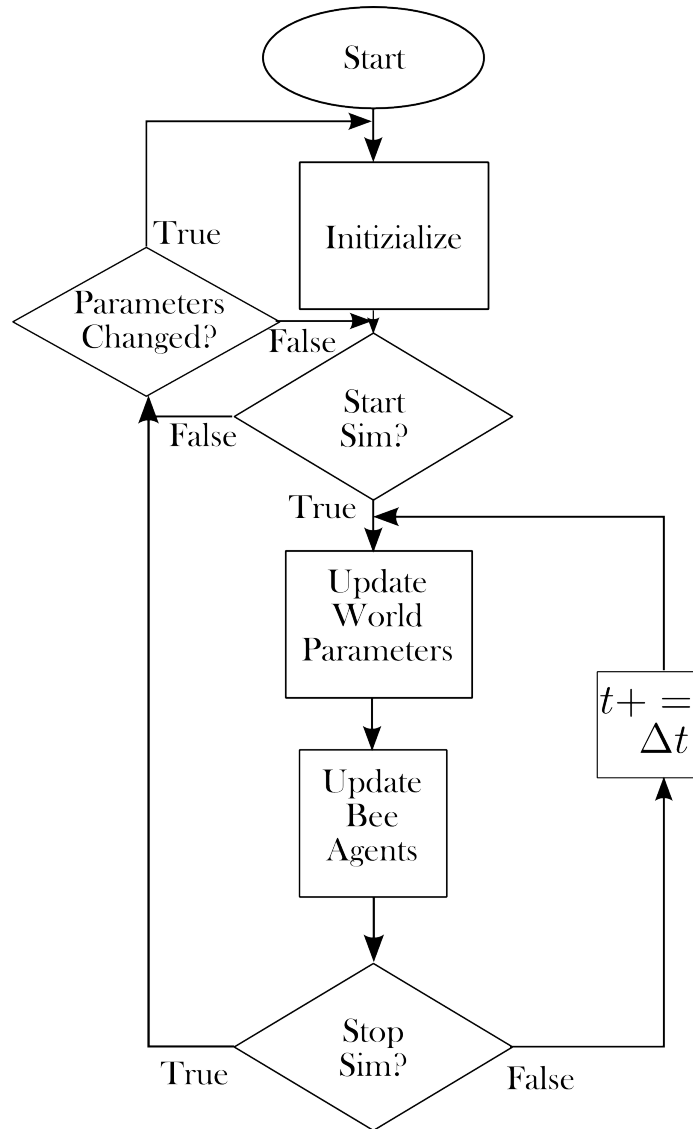


Figure 5.1: Flow diagram of the main program loop.

findings that there is a peak foraging temperature [81] and that foraging decreases away from this optimal temperature [10, 41]. Note that Equation (5.1) represents the default recruitment function in Bee++; not only can each parameter be set by the user, but the form of the function itself can be reconfigured as needed through straight-forward modifications to the open source code.

At some point a hive bee foregoes other duties and waits to watch a forager as it returns to the hive and begins a dance. The hive bee then inherits the target coordinates and carrier type (pollen or nectar) of the forager. If there is more than one forager dancing during the time that the hive bee is watching, the hive bee has equal chance of following any of the current dances, or becoming a scout.

Foragers: Foragers are divided into subclasses: scouts, recruits (working foragers), resting foragers and dancers [18]. Each forager follows the directions of a waggle dance to the

target food patch, but does not follow these directions perfectly; thus, movement is dictated by a biased random walk toward the destination.

We acknowledge that many strategies may be used by honey bees when foraging, and a number of movement models have been proposed in the literature [13, 18, 62]. Due to the resolution of the spatial grid in our model, however, we found a biased random walk sufficient. A finer grid, in which individual plants could be resolved, would be better modelled by a Lévy flight [63].

In the biased random walk, the inherent error in following directions is given by parameter ε . The probability of travelling in the correct vertical direction is given by

$$p_V = \left(\frac{d_V}{d_V + d_H} \right) (1 - \varepsilon) + \frac{\varepsilon}{4} \quad (5.2)$$

where d_V is the vertical distance between the forager and its target, and d_H is the horizontal distance between the forager and its target. In other words, if the forager is at coordinates (x_F, y_F) and the target food patch is at coordinates (x_T, y_T) , then

$$d_V = |y_T - y_F| \quad (5.3)$$

$$d_H = |x_T - x_F|. \quad (5.4)$$

Similarly, the forager travels in the correct horizontal direction with probability

$$p_H = \left(\frac{d_H}{d_V + d_H} \right) (1 - \varepsilon) + \frac{\varepsilon}{4}. \quad (5.5)$$

This leaves a probability $\frac{\varepsilon}{4}$ of travelling in each of the two wrong cardinal directions. Note that the error parameter, ε , is set by the user and can be a function of the intoxication level in an individual bee, such that pesticides that may interfere with navigation can be simulated. The parameter ε may be affected by pesticides ingested by the forager, and this is modelled explicitly as

$$\varepsilon = \varepsilon_{base} + \varphi X \quad (5.6)$$

where X is the intoxication level of the bee, φ is a configurable parameter and ε_{base} is the natural error in a honey bee's navigation.

In addition, this randomness in movement is necessary to allow foragers to find new sources of food. In fact, our simulation is set up in such a way that if a forager comes across a viable food source before reaching its target, it will update its target to the patch it has just found.

Foragers will eventually give up on their target if they are looking for too long without successfully finding the target food source [9]; this search time limit in our model is given by t_S . Furthermore, bees who have been out of the hive for time t_H will attempt to return home before death from exhaustion. Foragers are considered lost if they die a distance d_L from the hive or from any food patches.

The duty of a scout is solely to find new sources of pollen or nectar [1]. Therefore, they do not have a target, and thus, by setting $d_V = d_H = 0$, we are able to allow scouts to diffuse through the environment until they reach a viable food source. Put simply, a scout's movement is governed by a random walk. Once a food source is found, the scout will use a biased random walk to navigate back to the hive and back to the food source in the future.

We assume that a forager always carries a full load of either nectar or pollen back to the hive and that the time it takes to extract the nectar/pollen from the source depends solely on the properties of the source. When they get back to the hive, food stores are updated for both nectar, pollen and any contaminants carried, as described further in Section 2.2. Upon their return, foragers also decide to dance with (currently) fixed probability, p_{Dance} .

Drones: Our model also accounts for drones in the hive. The details of drone dynamics can be found in Appendix A.1.

The brood: The queen has substantial, if not full, control over the number of fertilized eggs she lays [59, 86]. In general, the number of eggs laid is seasonally dependent [50]. In addition, the queen's health depends on food availability, and thus we assume the number of eggs she may lay per day depends on the food available to her. Therefore, we model the number of eggs laid per day as

$$L = L_B \min\left(\frac{f_P}{f_P + b} e^{-E_1(t-\hat{t})^2}, 1\right), \quad (5.7)$$

where \hat{t} is the day of the year on which the queen lays the most eggs, and E_1 is a constant determining the egg laying season of the queen. The variable f_P is the amount of pollen available in the hive, while b is a shape parameter (amount of pollen at which the number of eggs laid is half maximum). L_B is a randomly generated number to simulate the decision-making of the queen. Specifically, L_B is Poisson-distributed with a mean value set by the user, which is the mean number of eggs laid per day at the peak of the season, if pollen stores are plentiful. After L is computed, the number of fertilized eggs is determined by a binomial random variable; the probability that an egg is fertilized is set by the user.

For computational considerations, the brood is not considered on an individual level. Instead, the number of brood cells that survive in one day is dependent on the amount of pollen available for consumption and the amount of care that can be provided by the nursing bees [43]. This fraction is denoted the survivability function, S , and is defined as

$$S = \left(\frac{f_P}{f_P + b}\right) \left(\frac{N_N}{N_N + w}\right) \quad (5.8)$$

where N_N is the number of bees currently nursing and w is a shape parameter (number of nurses for which half the brood survives). As before, we note that the functional forms of both L and S are configurable; we describe here the default functions currently implemented.

The worker brood are capped at eight days by default, a parameter value motivated by [32]. Between this day and when the pupae emerge, they survive off the food provided during their larval stage and are considered well protected. Surviving worker bee pupae emerge 21 days after egg laying [15], and surviving drone pupae after 24 days of development [54]. Three days after emerging, the workers begin their nursing duties [67]. We emphasize that we choose these values as defaults as they correspond with parameter values in the literature. All parameters can be modified to simulate different scenarios.

Intoxication: Each bee is assumed to have a level of intoxication. Intoxication increases when toxins (such as pesticides) are ingested, and decreases naturally through detoxification mechanisms. These mechanisms are poorly understood [23], but it is known that

certain fungicides hinder certain mechanisms (namely P450 detoxification) [39]. In order to simulate these particular interactions, Bee++ is configured to account for one type of pesticide, P , and one type of fungicide, \mathcal{F} , which interact in their effects on bee intoxication, such that:

$$\frac{dX}{dt} = \gamma_N C_P - x_D \frac{X}{\gamma_N C_{\mathcal{F}} + X + 1}. \quad (5.9)$$

Here, X is the intoxication level of the bee; γ_N is the amount of food ingested in one time step; C_P is the concentration of pesticide in the food stores; x_D is the base rate of detoxification in a honey bee; and $C_{\mathcal{F}}$ is the concentration of fungicide in the food stores. Thus, the detoxification rate is reduced by high levels of fungicide in the food stores. Of course, as more information becomes available this can be modified to incorporate many types of interactions between a multitude of different toxins. The concentrations C_P and $C_{\mathcal{F}}$ depend on the influx of contaminated food from different sources. Each source, i , may have a different concentration of toxin present, denoted by $\hat{C}_{P,i}$ and $\hat{C}_{\mathcal{F},i}$; these are again configurable. The parameter x_D is generally difficult to measure, but recent studies have been able to measure the half life of pesticides within a honey bee [78, 79], $t_{1/2}$, and from this value, we can calculate a metabolization rate, x_D , through the conversion $x_D = \ln(2)/t_{1/2}$.

Unlike previous agent-based models, or even general mathematical models for honey bee colony dynamics, the above method of tracking pesticides allows for exploration of the effects of toxins on the colony in both a spatially explicit and toxicologically explicit way. Previous models have simulated the effects of pesticides only by increasing the natural death rate of the foragers [6, 7, 22, 42, 43, 60, 61, 82]. Bee++ allows us, in addition, to track the effects of pesticides on, for example, a bee's ability to navigate its environment or potentially the effects on recruitment by modifying Equations (5.1), (5.2), or (5.5), or parameter α .

Death rates: The death of bees is also handled stochastically. The probability of death at any given time is dependent on many factors, and in this model we simulate death as a function of temperature, disease, intoxication, food availability and natural causes.

Bees outside the hive are subject to death rate $d_O = d_n + d_d + d_T + d_{Tox}$, where each term is defined below. The natural death rate, d_n , is given by

$$d_n = C \left(1 + \frac{K}{K + f_N} \right) \frac{(a - a_{opt})^2}{a_{opt}^2} \quad (5.10)$$

where a_{opt} is the optimal age of a forager (when it is the strongest), f_N is the amount of nectar available in the colony, and C and K are scaling parameters. Thus, the natural death rate increases quadratically for young or old bees and can be increased by a factor of two if insufficient nectar is available.

The death rate is also sensitive to the environmental temperature, T , such that:

$$d_T = \begin{cases} (1 - Ae^{-J(T-T_I)^2}) & d_T > 0 \\ 0 & \text{otherwise.} \end{cases} \quad (5.11)$$

Here, T_I is the ideal environmental temperature for honey bees; A and J are scaling parameters.

The death rate due to intoxication depends on the toxin (or combination of toxins) within the bee and is proportional to a user-defined combination of toxins

$$d_{Tox} = K_T X \quad (5.12)$$

where K_T is a scaling parameter that would depend on the specific toxin being studied and its associated LD_{50} value and X is the intoxication of the individual.

The disease-related death rate is disease dependent and configurable. If a bee suffers from multiple inflictions, we assume the effects are additive. For example, nosemosis induced by *N. cerenae* has been shown to double the death rate of honey bees [11], and thus, for this particular disease, we have

$$d_d = d_n. \quad (5.13)$$

Bees inside the hive suffer from the same natural death rate (Equation (5.10)), with a different scaling parameter C due to the safety the hive provides. They are also subject to death due to differences in temperature, although temperature affects these bees in a different way.

Specifically, bees work to keep the temperature inside the hive constant at 35 °C by either fanning their wings to cool, or expending metabolic heat to warm the hive [71]. With this information, we posit that the effects of temperature within the hive are tied to the number of bees within the hive [45]. The number of bees needed to maintain a constant temperature within the hive is thus modelled to be proportional to the difference between the ambient temperature and the target temperature. In other words, the farther away the ambient temperature is from the ideal, the more bees are required to produce the necessary metabolic heat to maintain a constant temperature. Therefore, inside the hive, we define temperature-related death as

$$d_{TH} = \frac{C_1 |T - T_I|}{C_2 + C_3 N_H} \quad (5.14)$$

where C_1 , C_2 and C_3 are constants that can be adjusted and N_H is the total number of bees within the hive.

When the temperature outside the hive drops below the threshold, T_W , all bees attempt to return to the hive and begin over-wintering behaviour (i.e. all bees act to maintain brood and control the temperature of the hive). Drones are cast out of the hive, as during winter they are a detriment to survival [88].

5.2.2 Food Stores

Bee++ keeps track of the amount of pollen, f_P , and honey (derived from nectar), f_N , at time t in the hive. The average concentrations of pesticides and fungicides, C_P and C_F , in these food stores are also tracked.

For simplicity, food stores are assumed to be consumed at a constant rate by bees that are present in the hive at any given time. This means that individual bees do not make a decision to eat, but are assumed to find time within each time step to eat, based on the consumption rate for their caste γ_j . Therefore, the amount of pollen is reduced by $\Delta t \gamma_B B_U$, while the amount of honey is reduced by $\Delta t (\gamma_H H + \gamma_F F_R)$ in each time step Δt , where B_U is the total population of uncapped brood, F_R is the number of resting foragers and H is the total hive bee population. The amount of pesticide removed from the food stores per bee,

as the bees consume pesticides with the food, is given by $C_P \gamma_j \Delta t$, where j represents the particular caste of the bee eating; fungicides are treated analogously. In its present form, Bee++ assumes that pesticides do not decay within the food stores, or in the environment.

When a forager returns to the hive from the environment, it will add its load, c_P or c_N , to the pollen or honey stores, respectively. The amount of pesticide added to the food stores from source i is $c_P \hat{C}_{P,i}$; again, fungicides are treated analogously.

The average water content of honey is approximately 20% [4], whereas the water content of nectar can vary anywhere between 20% and 95%, depending on the plant of origin [4]. This gives a median value of 57.5% water content for nectar, which is in close agreement with the water content given for alfalfa and clover (55% water concentration) given by Wilson et al. [87]. With these numbers, we can deduce that the sugar concentration of nectar is approximately 45%, and the sugar concentration of honey is approximately 80%. Using these numbers, we can convert the weight of nectar in grams to the weight of honey in grams via

$$W_h = 0.54W_n \quad (5.15)$$

where W_h is the amount of honey by weight and W_n is the amount of nectar by weight. This is necessary, as foragers collect nectar, which is then converted to honey in the hive.

5.2.3 Environment

The environment is represented by an $N \times N$ grid of space with which the bees can interact. Each element of the grid is either empty (meaning a bee may fly through it without any interactions), a pollen source, a nectar source, or a mating patch as defined by the user. One cell (typically the centre) is designated as the hive. The pollen and nectar sources have the ability to be time-dependent to model seasonality, and may be depleted as the resource is consumed by the bees. The cells may also harbour pesticides or fungicides, which are transferred to foragers who interact with the patch, who in turn contaminate the hive food stores when returning to the hive with pollen or nectar. Again, for computational tractability, we assume that the pesticides are well mixed in both the sources of food, and in the food stores in the hive.

In terms of the effects of pollination on the flowers, we track how many bees return to the same plant type for two (or more) consecutive trips. With each consecutive trip, we assume the bee is able to pollinate more flowers and thus increase the potential fruit yield for the patch. In this way, Bee++ is able to simulate not only honey bee dynamics, but also the effects of honey bee colonies on a surrounding environment.

The environmental patches are also able to harbour pathogens and pesticides, which can then be transmitted to forager bees and brought back to the hive. Moreover, in the case of certain pathogens, infected foragers may leave parasites on a plant, resulting in infection of subsequent visitors. The amount of pollen and/or nectar available at a given patch is seasonally dynamic, allowing for studies of biodiversity as a potential stressor.

The default time step of Bee++ is on the order of minutes. This gives Bee++ the ability to track the foraging trips of individuals, which, on average, last 6–7 minutes for healthy bees [1, 44]. The default spatial scale is on the order of square meters per spatial element of the grid. Because of the fixed flight speed of the bees, the spatial scale and time step are linked. Large areas can be modelled by scaling back the resolution of the map (i.e. allowing for larger cells), and in this case the time step should be adjusted to

days or weeks, such that bees travel one spatial step per time step. Clearly, scaling up the resolution comes at the cost of being able to accurately track the behaviour of individual bees.

5.2.4 Pathogens

Three types of pathogens are currently included in Bee++: *Varroa* mites, *Nosema apis* and *Nosema cerenae*. These are arguably the three most common pathogens affecting honey bee colonies [73]. They are also the three pathogens most likely to be factors in colony collapse [85]. Again, for computational reasons, it is not feasible to track these pathogens individually, but detailed pathogen-specific behaviour is feasible as described in Appendix A.2. The behaviour of these pathogens is described in detail in Appendix A.2.

5.3 Results

We illustrate the use of Bee++ by simulating a single hive, with several nectar and pollen sources, over the course of one spring/summer season. Temperature data were obtained for 2015 from London CS Station at London International Airport (YXU) in London, Ontario, Canada, as shown in Figure 5.3. Simulations were run with constant availability of pesticide-free food so as to highlight the dynamics of the bees themselves without potential environmental pressures.

Table A.1 shows the key parameter values used in the simulations. A comprehensive list of all parameter choices are given as the default values in Bee++ in the file `Parameters.cpp`.

Sensitivity analysis was performed on a subset of 17 parameters, which we believe are crucial to the function of a healthy colony. We varied these parameters by $\pm 20\%$ around the mean values given in Table A.1. The parameters used are denoted in bold in Table A.1. Given the large parameter space this creates, we use Latin hypercube sampling [49] with 10 divisions in order to obtain an illustrative sample of the parameter space. The sample sets used are represented in Table 5.2. The results of the sensitivity analysis on the total colony size, brood size, and Average Age of Recruitment to Foraging (AARF) are shown in Figures 5.4–5.6, respectively.

Figures 5.7 and 5.8 show the results of the simulation for comparison to other data from the literature, namely [6, 12, 52, 53, 69]. The data from [52] are fitted using a series of measurements related to colony size; [6] is simulated data; [53] is model data; and [12] is measured data. Given that the climate in London, Ontario, is different from that of, say, northern France in the case of [52] or Hertfordshire in the case of [6], we would like to highlight the qualitative similarities between these results and extant data.

In addition, note that Bee++ is able to capture the decreasing spring population as seen in [8]. The results suggest that this drop is caused by a combination of the increased average age of the population within the colony at the end of winter, and the temperature oscillations around the threshold temperature. The addition of time-dependent food availability would surely further exacerbate this effect.

Figures 5.9 and 5.10 show the Average Age of Recruitment to Foraging (AARF). This metric is highly variable when the temperature is close to the threshold in early spring (Figure 5.10), but stabilizes as the temperature remains above the threshold temperature, and increases steadily as the colony becomes stronger in numbers (Figure 5.9), eventually leading to a situation in which foraging is an ‘end of life’ activity. The two lines in the plot compare the AARF for a colony that is not exposed to pesticides, with one that is consistently exposed to pesticides through the local plant life. In this example, we remove all effects of pesticides except the pesticide’s ability to disrupt the navigation abilities of the foraging bees. We see that the AARF is robust against this particular effect of pesticides on a colony.

Tracking intoxication levels in bees individually allows Bee++ to explore and confirm the effects of pesticides on a colony. Figure 5.11 shows a time course of the average pesticide concentration in the foraging population as well as the number of bees who have become lost in the last 20 days as a result. As a liberal estimate, we assume that bees only die of pesticide exposure if they consume their body weight in pesticide. In Panels (b) and (c) of Figure 5.12, we introduce pesticides in the local environment which have the effect of interfering with honey bee navigation. In the third panel we note that a far more uniform distribution of honey bee deaths outside the hive results, indicating that navigation even at these short distances has been affected by consistent exposure to pesticides, even though the doses remain sub-lethal. In the case illustrated in Panel (c), parameters were set such that bees that are highly intoxicated can lose any semblance of navigational ability (i.e., $\max(\varepsilon) = 1$). In this situation, food stores become depleted as many bees cannot find their way back to the hive, and the colony goes extinct in late spring. Figure 5.12b shows a more realistic case in which $\max(\varepsilon) = 0.3$. Here, the dead bees are contained within the ‘boundary’ of the food sources, but they are more evenly distributed.

The spatial distribution of bee deaths can be easily tracked in an agent-based simulation; this distribution is of interest since a lack of dead bees around the hive is a symptom of Colony Collapse Disorder [83, 89]. Figure 5.12a shows the spatial distribution of bees that have died, while away from the hive, between February and September of the simulated year. We see that the highest concentration of dead bees is near the food sources as this is where foragers spend the majority of their time outside the hive. Note that bees tend to find their way back to the hive fairly well; although not visible in the colour resolution of the figure, fewer than 10 bees have died in each spatial cell beyond the food sources, over the course of the season.

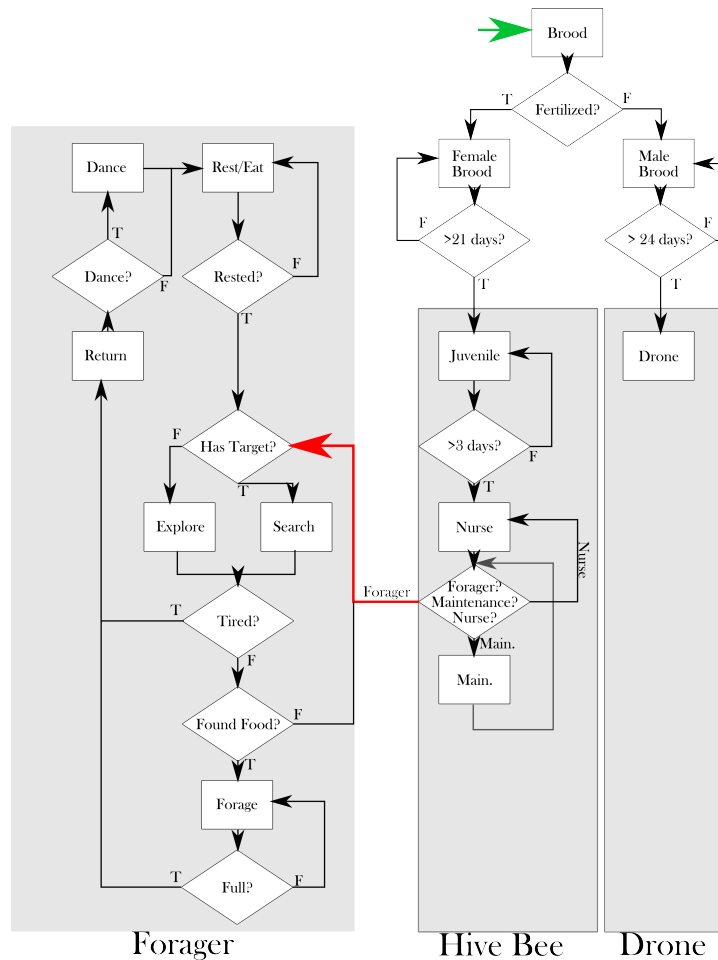


Figure 5.2: Flow diagram of the three main bee classes and their possible decisions in one time step. This diagram is not exhaustive, but intended to be illustrative of the main decision tree for each of the three main classes: **drones**, **hive bees**, and **foragers**. These classes of bees are further divided into different states, which changes the behaviours and parameters associated with each bee. The **green arrow** begins the cycle for one bee agent. The queen lays an egg, which then gets added to the **Brood**. The Brood are either fertilized (female) or not (male). After 21 days, the fertilized brood will emerge and become **juveniles**. **Hive bee:** The **juveniles** are responsible for cleaning cells. After three days, the hive bee juvenile will become a **nurse**. The nurses are responsible for caring for the brood, ensuring their survival. At each time point, the nurse will decide to become a **maintenance** bee, remain a nurse or become a **forager**. The **maintenance** bees are responsible for hive repair, security and other duties around the hive that are specifically *not* caring for brood. Maintenance bees can also revert to nurse bees if there is a need, or be recruited (**red arrow**) to the forager class. The probability of the bee choosing one of these three states is dependent on the needs of the hive, the bee's age and many other factors (pesticide exposure, disease, weather etc.). The **forager** class is typically an 'end of life' class. Bees recruited to forager will leave the hive. If they have a target, the bee will **search** out the target. If the bee does not have a target or loses its target, it will **explore**. A bee who is **tired** (i.e., runs out of energy) will **return** to the hive. If a bee has **found food**, it will begin to **forage** in that patch. When the bee is **full**, it will **return** to the hive. In the hive, the bee may decide to **dance** to relay the location of a food source to other bees. Whether or not a bee dances, she will always **rest**. Once rested, the forager will again leave the hive to forage. **Drones:** After 24 days, an unfertilized egg will develop into a drone. Currently, drones in Bee++ stay in the hive and consume resources until they die or are ejected by the females. At each state, the bee has a probability of death, which has been omitted from the diagram for clarity.

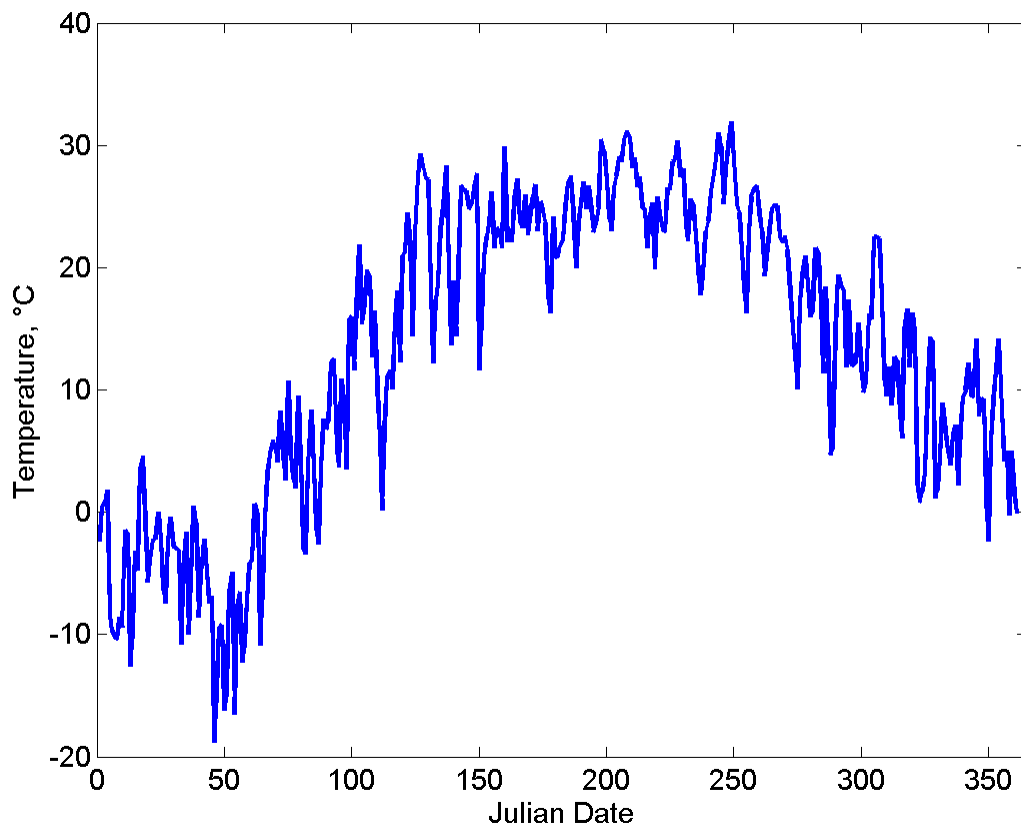


Figure 5.3: Daily temperature highs for London, Ontario, Canada, for the 2015 calendar year, measured at weather station London CS. Data provided by Environment Canada.

Table 5.1: Parameter values and source references.

L	maximum rate of egg laying	1500 eggs/day	[28]
w	number of hive bees for 50% egg survival	1000 bees	
b	mass of food stored for 50% egg survival	500 g/day	[42]
a_m	age at which hive bees begin brood care	4 days	[67]
<i>a_T</i>	age at which hive bees end brood care	16 days	[67]
a_R	minimum age of recruitment to foraging	4 days	[25]
k	age at which rate of recruitment is 50% of max.	10 days	
α	maximum rate of recruitment	1 /day	
$\frac{1}{\sigma}$	maximum fraction of colony that can be foraging	$\frac{1}{3}$	[43]
<i>d_n</i>	natural death rate of foragers outside the hive	equation (5.10)	[21]
c_n	nectar gathered per day per forager	0.03 g/day/bee	[66]
c_p	pollen gathered per day per forager	0.016 g/day/bee	[66]
γ_H	daily food requirement per hive bee	0.08 g/bee	[33, 64]
γ_F	daily food requirement per forager	0.13 g/bee	[33, 64]
γ_D	daily food requirement per drone	0.1 g/bee	[33, 64]
γ_{Bp}	daily pollen requirement per uncapped brood cell	0.067 g/bee	[33, 64]
γ_{Bn}	daily nectar requirement per uncapped brood cell	0.018 g/bee	[33, 64]
K	Shape parameter for exit probability of forager	30 min	
t_R	Minimum time in hive	1 h	
t_E	Time forager spends searching for target	15 min	
t_H	Maximum flight time	45 min	
<i>T_W</i>	Temperature at which foraging begins	10 °C	[41, 81]
<i>T_I</i>	Ideal ambient temperature *	25 °C	[41, 71, 81]
<i>T₁</i>	Minimum foraging temperature	10 °C	[41, 71, 81]
<i>T₂</i>	Maximum foraging temperature	40 °C	[10]
<i>x_D</i>	Rate at which pesticides are metabolised	3.33 /day	[78, 79]
\hat{C}_P	Concentration of pesticide in nectar	1.9 ng/g	[75, 77]
ϵ_{base}	Error in forager navigation	0.1	
φ	Scaling of pesticide effect on navigation	10	

* Bee++ assumes there is always some metabolic heat being generated by the bees; therefore, we set the ideal temperature lower than the measured ideal hive temperature in [71]. Bold indicates parameters for which sensitivity analysis was performed.

Table 5.2: Parameters used in 10 simulations for sensitivity analysis. Each column represents one simulation. Mean values provided in Table A.1.

	% Change from Mean									
k	1.152	-5.9516	13.53	11.145	-10.583	-1.5224	-12.415	6.49	-17.051	19.035
w	-14.492	-18.092	2.3472	15.129	16.566	-11.444	6.8644	-2.4616	-7.118	8.1808
b	12.322	-17.539	7.3496	-15.187	-4.4552	-8.6352	10.577	16.609	-2.3312	1.6552
K	16.297	13.7	7.96	-11.238	9.5648	-17.92	-5.0736	-13.032	-1.924	3.0908
d_R	19.806	-12.677	-5.0336	7.2084	1.5772	-11.295	8.7576	12.791	-18.832	-3.4376
d_m	-19.124	3.1848	-3.9732	15.626	-14.602	7.1392	-4.9756	18.641	11.208	-10.027
t_H	-3.8032	-9.5784	17.662	-6.426	-14.858	2.394	12.565	8.318	4.9968	-17.142
γ_F	-7.1872	15.429	-10.018	1.5572	-14.815	-17.533	-2.9148	4.4508	19.777	11.447
γ_H	-19.452	-1.6868	-9.6452	-7.8364	16.999	0.076	7.066	11.615	-13.538	13.999
γ_D	-18.281	12.094	10.028	6.3964	-15.98	-9.044	-6.6612	-3.8572	17.315	2.8032
γ_{Bp}	13.876	-0.006	16.465	-17.618	2.7952	-11.802	-5.8424	10.85	-12.338	5.6712
γ_{Bn}	7.3876	15.708	-10.322	-13.148	18.552	-2.8992	-7.4332	2.6084	-19.847	8.1856
t_E	-4.824	12.927	9.538	0.3244	-14.41	-2.8084	17.025	-9.5404	-17.006	7.8528
t_H	-5.8884	-10.58	6.884	13.928	11.017	-17.19	-14.602	-3.5656	16.556	3.1604
c_N	10.404	12.448	-5.026	-19.867	1.5232	7.3388	-11.305	-2.6228	-14.186	18.995
c_P	-0.1608	3.0664	-5.4444	-14.534	-19.944	15.171	8.9716	-11.545	18.111	7.3644
L	8.7564	18.094	-16.465	-7.5028	-2.5408	7.6108	-11.634	15.86	-12.159	0.0456

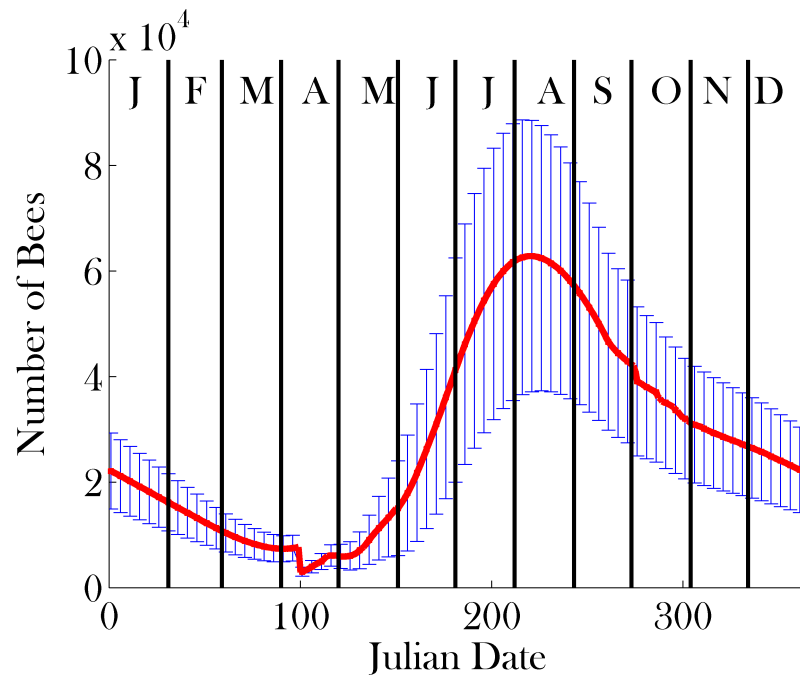


Figure 5.4: Results of sensitivity analysis on total colony size: mean (red line) \pm one standard deviation (error bars). Parameter sets were sampled using Latin hypercube sampling [49] with 10 divisions from the mean values provided in Table A.1, ranging $\pm 20\%$. The parameters on which sensitivity analysis was performed appear in bold in Table A.1.

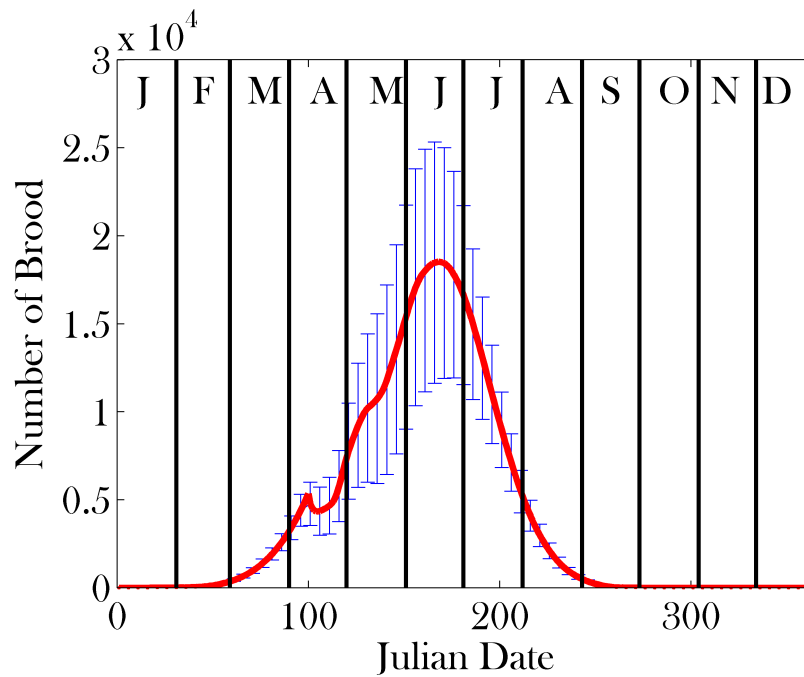


Figure 5.5: Results of sensitivity analysis on brood size: mean (red line) \pm one standard deviation (error bars). Parameter sets were sampled using Latin hypercube sampling [49] with 10 divisions from the mean values provided in Table A.1, ranging $\pm 20\%$. The parameters on which sensitivity analysis was performed appear in bold in Table A.1.

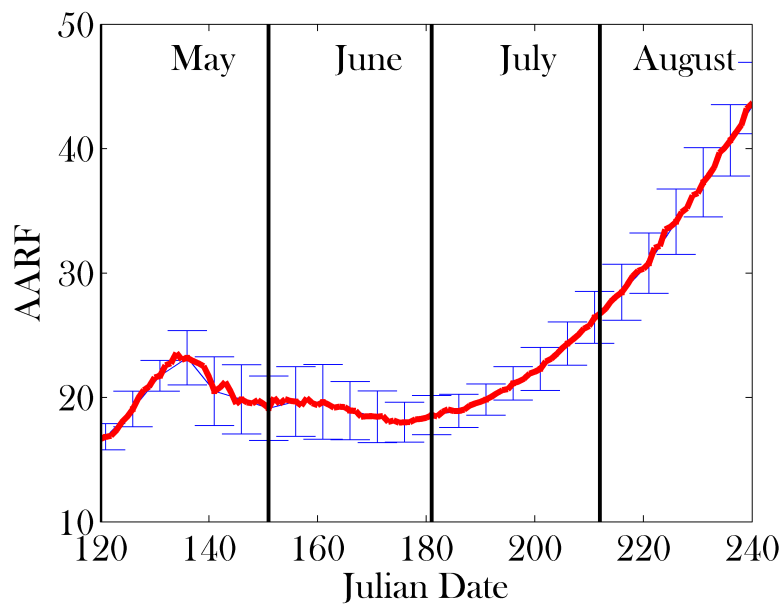


Figure 5.6: Results of sensitivity analysis on Average Age of Recruitment to Foraging (AARF): mean (red line) \pm one standard deviation (error bars). Parameter sets were sampled using Latin hypercube sampling [49] with 10 divisions from the mean values provided in Table A.1, ranging $\pm 20\%$. The parameters on which sensitivity analysis was performed appear in bold in Table A.1.

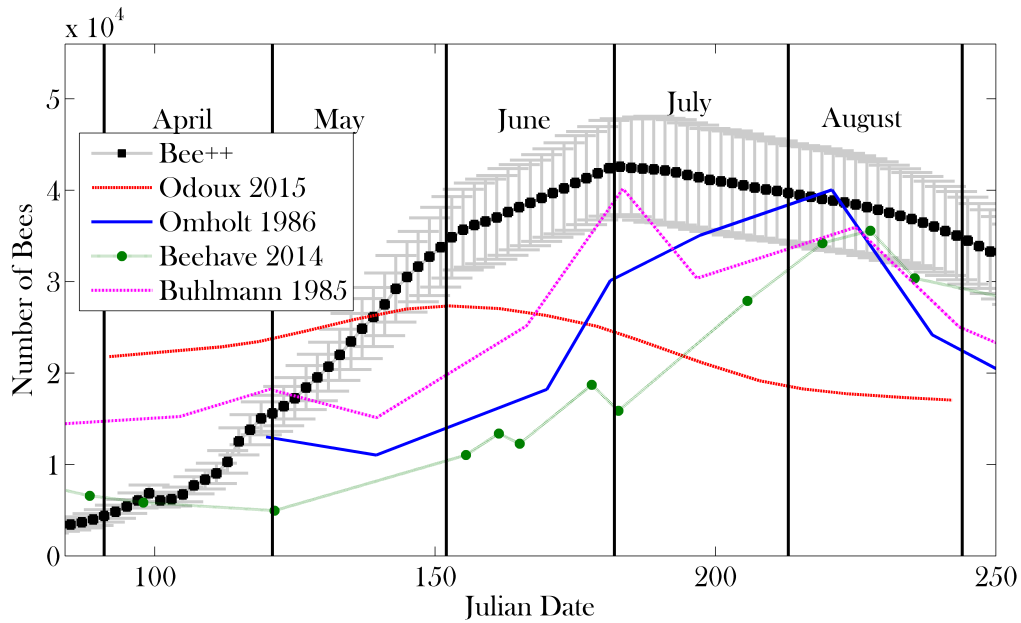


Figure 5.7: Total bee population from early spring to late summer using data from 10 simulations with the same parameter set (mean in black circles, grey error bars show \pm one standard deviation). These 10 simulations begin after the model has simulated 12 years of data, thereby representing the colony size and distribution of a well established colony. Results from the model are compared with those of other studies [6, 12, 52, 53]. The simulation agrees qualitatively with previous models (Omholt) [53], observation (Buhlmann) [12], and simulation (Beehave) [6]. Data from Odoux [52] were obtained by model fitting, using measurements from many colonies. In the Bee++ example we have assumed constant availability of food in the environment and therefore we see a larger peak population.

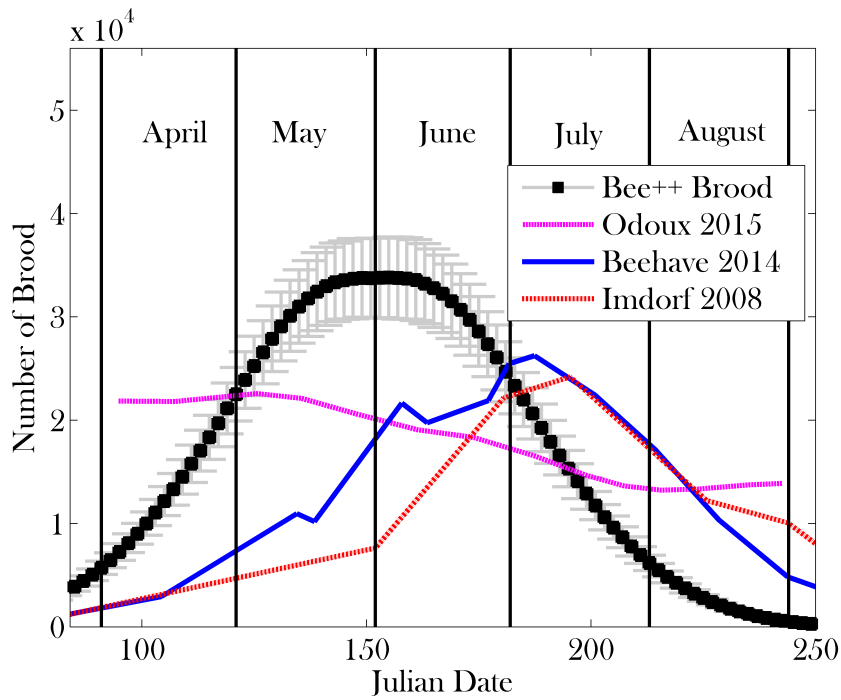


Figure 5.8: A comparison of brood size obtained using 10 simulations of Bee++ with simulation [6], observed data (Imdorf) [38], and fitted data (Odoux) [52]. Again we have simulated data for a well established colony, and note that the temporal distribution of brood size is influenced largely by the function used to model the laying rate of the queen. As in Figure 5.7, we see consistent qualitative agreement in all cases except in comparison to [52], which represents fitted data averaged over many colonies. Given the 21 day development time of the brood, the peak in the brood appears roughly 21 days before the peak in adult bee numbers. The simulation in Bee++ assumed constant availability of food throughout the spring and summer. Since brood survival depends in part on the available food, we see a much smoother curve.

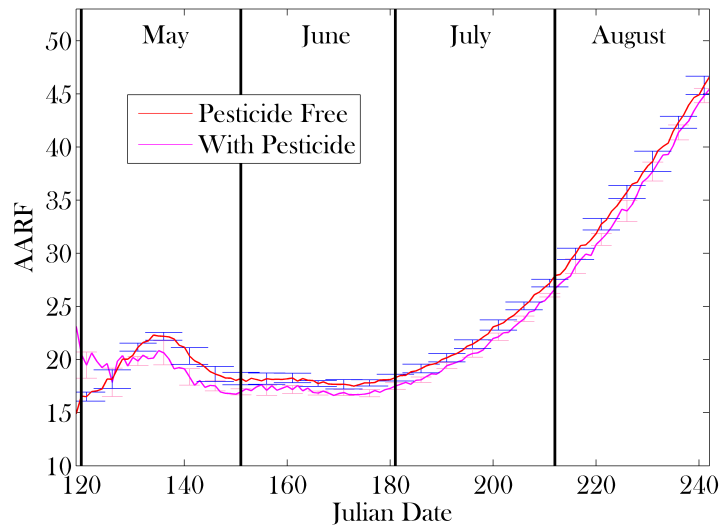


Figure 5.9: The average age of recruitment to foraging calculated in 7 simulations without pesticides (red line) and a simulation with pesticide treated plants (magenta line) through the summer months. Error bars represent one standard deviation. As mentioned in the text, pesticide exposure in this example affects the navigation abilities of the foragers but does not affect their lifespan, or the age at which they are recruited, thus it may be studied independently from other confounding effects. We see that the AARF is robust against pesticide exposure. We also see that an age of recruitment between 20–30 days corresponds to a healthy colony. An AARF that is above this range could indicate a lack of new brood or problem in the brood, as the increase in the AARF corresponds to the decrease in the brood population in Figure 5.8. An AARF below this range (as seen in [7, 43, 56]) can indicate an external stressor (in this case the added stress of early spring on the colony).

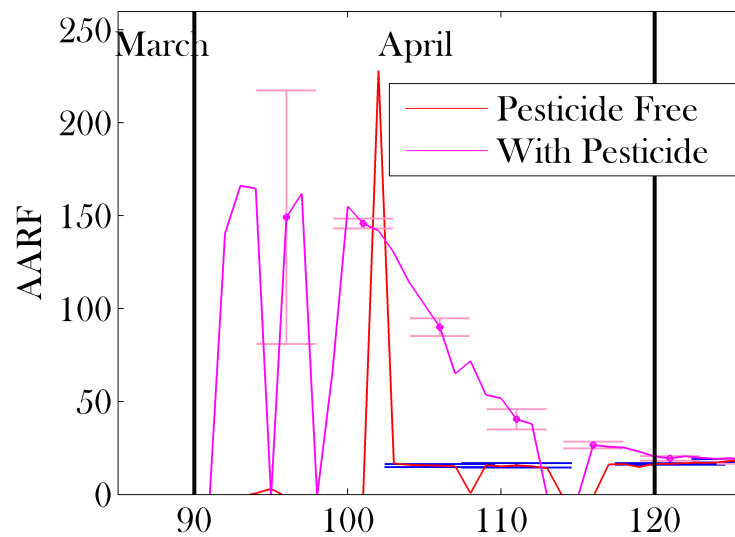


Figure 5.10: The average age of recruitment to foraging calculated in 7 simulations without pesticides (red line) and a simulation with pesticide treated plants (magenta line) through spring. Error bars, blue and pink respectively, represent one standard deviation. Compared with the results in Figure 5.9, the value of AARF is here seen to be generally higher and highly volatile in April. This is caused by large swings in the ambient temperature during this time, the ageing of bees and the absence of new bees during winter. Thus AARF is not a useful metric of the health of the colony during early spring.

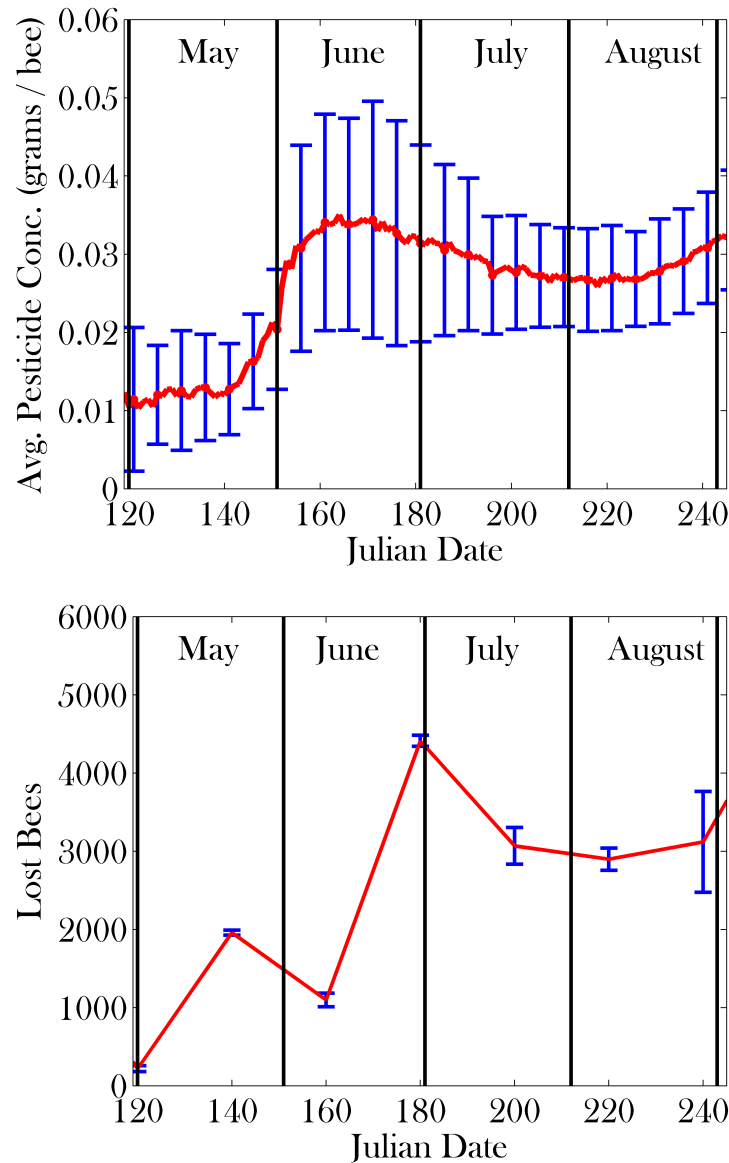


Figure 5.11: Intoxication of foragers and its effect on navigation over time. Seven simulations were used. Error bars represent one standard deviation. The top plot shows the metabolic efforts of the bees are not enough to completely flush the pesticides from their system. We see that once pesticide concentration in a bee is high enough to force higher metabolic effort, there is a decrease to a more stable concentration. The bottom plot shows the correlation between pesticide exposure and its effects on navigation. Plotted is the current date versus the number of bees lost in the previous 20 days. Bees are considered lost if they die outside a radius of nine patches from the hive (food is at most nine patches away). This plot highlights the functionality of Bee++ as well as how pesticide exposure may explain one possible symptom of CCD.

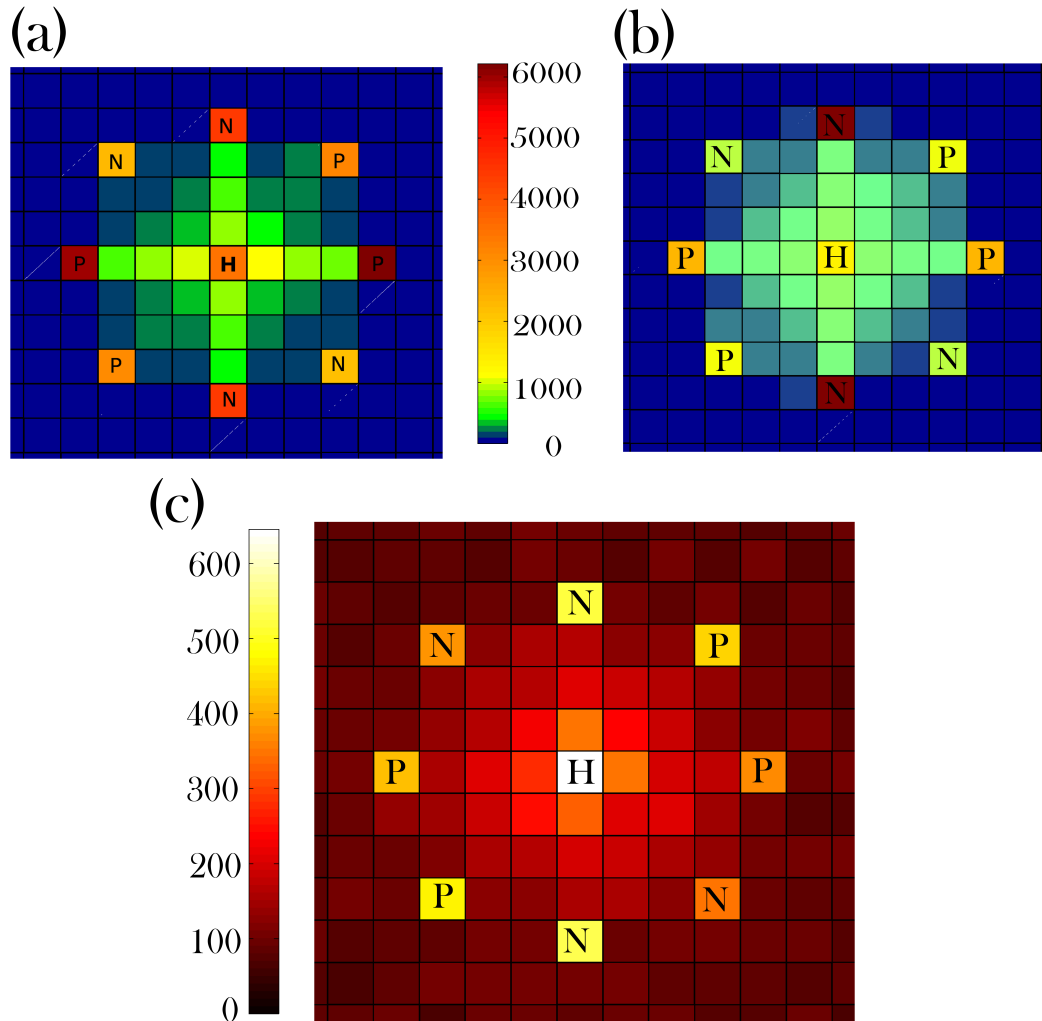


Figure 5.12: Number of dead foragers found in each patch of a 25×25 grid of $4\text{m} \times 4\text{m}$ patches totalled between February and September. The total number of dead foragers in this time is 55,283, 55,592 and 56,426 in (a,b,c) respectively. The pollen and nectar sources (in patches labelled P and N, respectively) are assumed to be constant throughout the year. The hive itself is labelled H. The colour resolution is roughly 100 bees in Panels (a,b) and 10 bees in Panel (c). Panel (a) shows a simulation with no pesticide exposure but with normal navigation error $\varepsilon = 0.1$. In Panels (b,c), this navigation error is increased because of pesticide exposure to a maximum of 0.35 and 1.0, respectively. In Panel (a), there are fewer than 10 bees in each blue cell, and in Panel (b), there are between 10 and 30 bees in each blue cell. The effect of pesticide on the bees is cumulative. In early spring, there is less build up of toxins within individual bees and thus their navigation is better than it is in late summer.

5.4 Discussion

We present a detailed, agent-based simulation package for honey bee colony dynamics, which is broadly configurable and can be adapted to address a wide range of investigations. In the Results, we demonstrate the behaviour of the model at default parameter values, predicting colony dynamics that are comparable to those predicted by other models and simulations [6, 43, 69]. The larger peak population size obtained in our simulations is due to the idealized condition that food is plentiful and constant, allowing bees to successfully forage from early spring through late fall; this is configurable in the model. Moreover, the peak population predicted by Bee++ is well within the range of realistic managed colonies [58]. In the simulated data, this peak appears in mid-summer, consistent with observed bee behaviour [16]. Field observations indicate that variation in the timing of this peak is quite large, with some honey bee populations peaking as early as late spring [29], depending on the local climate.

Sensitivity analysis shows that the model behaves as expected under a range of biologically reasonable conditions. Parameters not tested here, such as those associated with intoxication and the transmission rates for different parasites, will clearly also affect the dynamics of the colony. Sensitivity analyses for these can be carried out by individual researchers after their default environmental and colony parameters have been chosen. The framework for sensitivity analysis is built into the source code and can easily be modified to accommodate a detailed sensitivity study for each research question.

The flight patterns of honey bees, and the factors impacting their navigation are complex and quite involved [31]. The navigation used for the bees in Bee++ is macro scale navigation, given the size of the patches intended for use ($\geq 1m^2$). This means that the bees are moving toward a general target, and their individual movements between flowers is not modelled here. Models of movement between individual flowers have been well studied [13]. Future work entails optimizing the model so that navigation between individual flowers can be included. Moreover, displaced or lost honey bees have been shown to use a number of mechanisms to search for the hive, which can be modelled as a Lévy flight [62]. These mechanisms could also be considered in future extensions of the flight mechanisms in Bee++.

Figure 5.8 shows that the brood population of a healthy colony peaks in early June, consistent again with experimental findings [3]. Qualitatively, we see the same brood-rearing dynamics as predicted by other models. The measurements provided by [52] differ qualitatively from the other data presented in Figure 5.8. One potential explanation for this discrepancy is that the results of [52] are calculated using 208 different colonies, over four years. Different weather patterns over the 4 years and across the different locales may force the colonies to peak at different times of the year, potentially obfuscating the peak experienced by any one colony.

Figure 5.9 predicts that, when the pesticide-free colony population is at its strongest, the average age of recruitment to foraging is between approximately 20 and 30 days old. This is in full agreement with previous results [11, 42, 43, 56]. Furthermore, in early spring, when the colony is under increased stress, we see a lower AARF, consistent with the predictions of [43], which correlate the AARF and colony health. Our simulations also show that as the number of eggs laid by the queen diminishes in late summer, the AARF increases substantially. This behaviour seems to benefit the colony, as the younger, stronger bees are left in the hive for the incoming winter.

The results shown in Figure 5.9 indicate that while the AARF can be used to determine

certain aspects of colony health (i.e. a high AARF in the fall corresponds to dwindling numbers of the brood, or as an indication of infection [7]), the AARF is *not* a strong metric for the effects of pesticides on the navigational abilities of the worker bees. Results such as those in [56] (accelerated maturation of bees) can also be added to Bee++, further compounding the effects of pesticides on the age of foragers, with likely detrimental results. While the AARF has been previously proposed as a measure of colony health [7, 42, 43], the source of any change to the AARF is hard to extract from this metric, as many stresses will change its value. Therefore, it is important to know what will and will not effect this metric as some stresses (such as degrading navigational ability) can be detrimental to the colony, but asymptomatic without invasive tests on the bees (such as determining intoxication levels within the bees). In future work, we would like to study the compounding effects of pesticides, and also investigate the use of time-dependent AARF and other metrics to potentially identify which source of stress is causing the most harm to the bees. One preliminary hypothesis is that high AARF may indicate a problem in the brood, as AARF indeed increases in our model as the brood population decreases.

One of the key benefits of Bee++ is the ability to explicitly track toxins within individual bees, a feature that has not been included in previous studies. With this mechanism, we are able to explore explicit effects of sub-lethal doses of pesticides on honey bees without approximating these effects as an increased death rate. In particular, our model explicitly allows for pesticide exposure to interfere with foragers' navigational abilities, as has been demonstrated experimentally [34]. When comparing the panels of Figure 5.12, we see that as pesticides affect navigation more strongly, more bees die at distances further from the hive. Importantly, a lack of dead bees around the hive is one of the symptoms of Colony Collapse Disorder (CCD) [83, 89]; our model predicts that an encumbrance on foragers' navigation ability can help explain this phenomenon. In other words, a loss of navigation ability is one potential explanation for the lack of bee corpses reported in CCD. This inability to navigate in turn causes a reduction in the amount of food in the hive, and thus an increased death rate as the bees are generally weaker.

Given the recent proposal by the U.S. Fish and Wildlife service to declare the rusty-patched bumble bee as an endangered species [90], an accurate, parameter-rich model of bumble bee dynamics may be crucial in developing policies to protect this species. The source code of Bee++ can be modified to perform such a task, as bumble bee populations share a very similar social structure to honey bees. We hope to do so in the near future.

As well, our future work includes plans to modify the model to run on parallel processing architectures. With the exception of the waggle dances, each bee makes a decision at each time step independent of other bees, thus it should be possible to create a more efficient code by allowing (ideally) all bees to make decisions simultaneously.

Overall, Bee++ has the ability to create realistic simulations of honey bee colonies by incorporating a wide range of parameters and potential interactions. The object-oriented nature of the model implementation in C++ allows for easy modification of the source code so that the model can easily be improved and expanded as more experimental data become available. The simulations of Bee++ can be used to study the potential underlying causes of honey bee colony decline such as the effects of biodiversity, disease, predation and intoxication on colony dynamics. The effects of preventive measures (such as optimal plant diversity, crop density or anti-viral treatments) or recovery plans (such as manual feeding or colony transplant) can thus be studied before costly implementation.

Appendix 5.A.

Appendix 5.A.1. Drone Dynamics

Drones are born of the unfertilized eggs laid by the queen [88]. Their main duty in life is procreation with a queen of another hive. Upon success, the drone dies [88]. The drones make two decisions in their lifetime. With probability

$$p_L = \max(e^{t-t^*}, 1) \quad (5.16)$$

the drones will leave the hive in search of a mate. Here, t^* represents the optimal time of year for mating. The drones then move in much the same fashion as foragers, with their target being the mating area. Those that become lost will return to the hive, and those that reach the mating area will successfully mate with a queen with probability

$$p_M = \min\left(\frac{N_Q}{N_D}, 1\right) \quad (5.17)$$

where N_Q is the number of queens present in the mating area and N_D is the number of drones present. The drones do not mate with their own queen (as they are genetic clones of the queen). The mating process is built into Bee++ so that realistic numbers of drones can be modelled (since mating is followed by death of the drone). As well, having this functionality is the first step to creating a model and simulation package with interacting colonies. At present, multiple colonies are not implemented in the model and therefore the position of any mating sites and the number of queens present at any given time must be set manually by the user. Nonetheless the drones are an important part of a honey bee colony, as they can be a source of pathogens as well as a drain on the food stores and can account for up to 15% of the total population [70].

Appendix 5.A.2. Pathogen Dynamics

Both sub-types of the microsporidian *Nosema* reproduce within the epithelial cells of live bees, which in turn causes dysentery, forcing bees to expel waste within hive cells where spores will be picked up by bees, which clean contaminated cells [27]. *Nosema ceranae* is reported to affect foragers disproportionately, killing them away from the hive at an unsustainable rate [35]. There is also evidence that spores can be transmitted to bees through food stores [73]. With this in mind, we posit that bees that clean cells (i.e., nurses) are most likely to be infected, while secondary mechanisms may exist through direct bee to bee transmission and food stores. Therefore, we constrain the rates of transmission of either type of *Nosema* spore to foragers, drones, maintenance bees and nurses ($\beta_F, \beta_D, \beta_M$ and β_N respectively) through the condition

$$\beta_F \approx \beta_D \approx \beta_M < \beta_N. \quad (5.18)$$

Since hive cells are often soiled during the winter, when honey bees cannot leave the hive to defecate, the transmission of *Nosema* spores is temperature dependent. Presently Bee++ does not consider a spatially explicit interior to the hive, therefore we cannot track individual brood/food cells and instead treat the pathogen populations and bee populations as well mixed.

Each infection rate will then depend on the number of spores in the environment (which in turn depends on the number of infected bees), as well as susceptibility of a particular

bee to infection (pesticide exposure may increase susceptibility [84]). In other words, we define the time-dependent infection rates, p_I , as

$$p_{I,i,j} = \beta_i(P, \vec{I}, i) \frac{S_j}{s + S_j} \quad (5.19)$$

where β_i is a function dependent on the intoxication level P of the bee, the number of infections I it has acquired that may be compromising its immune system, and the caste of the bee, i . S_j is the number of free *Nosema* spores of type j (*apis* or *ceranae*) and s is a shape parameter. This infection through free spores is the main transmission method for both types of *Nosema*, and the one that our model currently considers. Of course, future work can expand the model to include secondary transmission routes.

The population of free spores of type j , S_j , is governed by the differential equation,

$$\frac{dS_j}{dt} = \sum_i B_{S,i,j} I_i - CN_N. \quad (5.20)$$

where $B_{S,i,j}$ is the shedding rate of *Nosema* spores of type j by one infected bee of type i and I_i is the number of infected bees of type i , C is the rate at which nurses can clean the cells, and N_N is once again the total number of nurses.

There is evidence that the fungicide, which prevents *Nosema apis* infection within honey bee colonies, may actually allow *Nosema ceranae* to thrive [37]. Therefore we thought it imperative to include both possible infections in our model, as well as the *N. apis* treatment, fumagillin, as a toxin. In this way, our model allows one to explore the trade-offs between these three very important, and evidently lethal stressors.

Varroa mites on the other hand, reproduce in the sealed brood cells [47]. Within the cell, the mite will lay female and male eggs (usually one male and five female [80]). The mites mate within the sealed brood cell [48], and the female mites emerge with the larvae, and attach themselves to nearby adult worker bees [47]. The mites feed on the blood of the adult worker bees, and use them as a means to disperse to new brood cells where they may reproduce [68].

Varroa has been observed to act as a vector for viruses such as Deformed Wing Virus (DWV) and Acute Paralysis Virus (APV) [20, 48]. Therefore, our *Varroa* mites are modelled as three types, V_i , depending on whether they do not carry any virus, are carriers of DWV, or carriers of APV.

Varroa mites feed on adult bees for approximately 4 to 5 days [68] before entering a brood cell that is about to be capped. Therefore, we keep track of the number of days a bee has had a mite attached. When a mite has reached reproductive maturity, with probability $p_E(t)$ the mite will enter a viable brood cell. Once the mite enters a brood cell, the adult bee is no longer considered infested with a mite. The number of mites that leave their adult bee hosts are exactly the number of brood cells that end up inhabited by a *Varroa* mite. We recognize that this assumes that more than one mite cannot occupy the same brood cell. We use this assumption first on the basis of empirical data [68] and, second, in order to make the problem tractable without explicitly tracking the spatial movement of the bees within the hive. We further assume that all mites either enter a brood cell or die after 5 days of attaching to a host.

The number of new *Varroa* mites created by one infected brood cell as the new bee emerges is

$$V_{new} = r_V B_I \quad (5.21)$$

where r_V is the average number of female mites produced by one foundress (i.e., an egg-laying mite), and B_I is the number of infected brood cells. We further assume that upon hatching, the new female mites find a host bee or die. Therefore the number of infected bees is directly proportional to the number of surviving emerging mites.

Bibliography

- [1] ABOU-SHAARA, H., ET AL. The foraging behaviour of honey bees, *Apis mellifera*: a review. *Vet Med (Praha)* 59, 1 (2014), 1–10.
- [2] AUFUVRE, J., BIRON, D. G., VIDAU, C., FONTBONNE, R., ROUDEL, M., DIOGON, M., VIGUÈS, B., BELZUNCES, L. P., DELBAC, F., AND BLOT, N. Parasite-insecticide interactions: a case study of *Nosema ceranae* and fipronil synergy on honeybee. *Scientific reports* 2 (2012).
- [3] BALL, B., AND ALLEN, M. The prevalence of pathogens in honey bee (*Apis mellifera*) colonies infested with the parasitic mite *Varroa jacobsoni*. *Annals of applied biology* 113, 2 (1988), 237–244.
- [4] BALL, D. W. The chemical composition of honey. *J. Chem. Educ* 84, 10 (2007), 1643.
- [5] BECHER, M. A., GRIMM, V., THORBEC, P., HORN, J., KENNEDY, P. J., AND OSBORNE, J. L. BEEHAVE: a systems model of honeybee colony dynamics and foraging to explore multifactorial causes of colony failure. *Journal of applied ecology* 51, 2 (2014), 470–482.
- [6] BECHER, M. A., OSBORNE, J. L., THORBEC, P., KENNEDY, P. J., AND GRIMM, V. Review: Towards a systems approach for understanding honeybee decline: a stocktaking and synthesis of existing models. *Journal of Applied Ecology* 50, 4 (2013), 868–880.
- [7] BETTI, M. I., WAHL, L. M., AND ZAMIR, M. Effects of infection on honey bee population dynamics: A model. *PLOS ONE* 9, 10 (2014), e110237.
- [8] BETTI, M. I., WAHL, L. M., AND ZAMIR, M. Age structure is critical to the population dynamics and survival of honeybee colonies. *Royal Society Open Science* 3, 11 (2016), 160444.
- [9] BIESMEIJER, J. C., AND DE VRIES, H. Exploration and exploitation of food sources by social insect colonies: a revision of the scout-recruit concept. *Behavioral Ecology and Sociobiology* 49, 2-3 (2001), 89–99.
- [10] BLAŽYTĖ-ČEREŠKIENĖ, L., VAITKEVIČIENĖ, G., VENSKUTONYTĖ, S., AND BŪDA, V. Honey bee foraging in spring oilseed rape crops under high ambient temperature conditions. *Žemdirbystė Agriculture* 97, 1 (2010), 61–70.
- [11] BOTIAS, C., MARTIN-HERNANDEZ, R., BARRIOS, L., MEANA, A., AND HIGES, M. *Nosema* spp. infection and its negative effects on honey bees (*Apis mellifera iberiensis*) at the colony level. *Veterinary research* 44, 1 (2013), 1–15.
- [12] BÜHLMANN, G. Assessing population dynamics in a honeybee colony. *Mitteilungen der Deutschen Gesellschaft fuer Allgemeine und Angewandte Entomologie (Germany, FR)* (1985).

- [13] BUKOVAC, Z., DORIN, A., AND DYER, A. A-bees see: a simulation to assess social bee visual attention during complex search tasks. In *Proceedings of the 12th European Conference on Artificial Life (ECAL 2013)* (2013), MIT Press Taormina, pp. 276–283.
- [14] CALDERONE, N. W. Insect pollinated crops, insect pollinators and US agriculture: Trend analysis of aggregate data for the period 1992-2009. *PLOS ONE* 7, 5 (05 2012), e37235.
- [15] CAMAZINE, S. Self-organizing pattern formation on the combs of honey bee colonies. *Behavioral ecology and sociobiology* 28, 1 (1991), 61–76.
- [16] CAPINERA, J. L. *Encyclopedia of entomology*, vol. 4. Springer Science & Business Media, 2008.
- [17] CASTILLO, C., CHEN, H., GRAVES, C., MAISONNASSE, A., LE CONTE, Y., AND PLETTNER, E. Biosynthesis of ethyl oleate, a primer pheromone, in the honey bee (*Apis mellifera* L.). *Insect biochemistry and molecular biology* 42, 6 (2012), 404–416.
- [18] DE VRIES, H., AND BIESMEIJER, J. C. Modelling collective foraging by means of individual behaviour rules in honey-bees. *Behavioral Ecology and Sociobiology* 44, 2 (1998), 109–124.
- [19] DEVILLERS, J. The ecological importance of honey bees and their relevance to ecotoxicology. In *Honey Bees: Estimating the Environmental Impact of Chemicals*, J. Devillers and M. Pham-Delègue, Eds. Taylor and Francis London, London, 2002, pp. 1–11.
- [20] DI PRISCO, G., PENNACCHIO, F., CAPRIO, E., BONCRISTIANI JR, H. F., EVANS, J. D., AND CHEN, Y. *Varroa destructor* is an effective vector of Israeli acute paralysis virus in the honeybee, *Apis mellifera*. *Journal of General Virology* 92, 1 (2011), 151–155.
- [21] DUKAS, R. Mortality rates of honey bees in the wild. *Insectes Sociaux* 55, 3 (2008), 252–255.
- [22] EBERL, H. J., FREDERICK, M. R., AND KEVAN, P. G. Importance of brood maintenance terms in simple models of the honeybee - *Varroa destructor* - Acute Bee Paralysis Virus complex. *Electronic Journal of Differential Equations (EJDE) [electronic only]* 2010 (2010), 85–98.
- [23] ESTHER, E., SMIT, S., BEUKES, M., APOSTOLIDES, Z., PIRK, C. W., AND NICOLSON, S. W. Detoxification mechanisms of honey bees (*Apis mellifera*) resulting in tolerance of dietary nicotine. *Scientific reports* 5 (2015).
- [24] EVANS, J. D., AND SCHWARZ, R. S. Bees brought to their knees: microbes affecting honey bee health. *Trends in microbiology* 19, 12 (2011), 614–620.
- [25] FAHRBACH, S., AND ROBINSON, G. Juvenile hormone, behavioral maturation and brain structure in the honey bee. *Developmental Neuroscience* 18 (1996), 102–114.
- [26] FAVRE, D. Mobile phone-induced honeybee worker piping. *Apidologie* 42, 3 (2011), 270–279.
- [27] FRIES, I. *Nosema apis* parasite in the honey bee colony. *Bee World* 74, 1 (1993), 5–19.
- [28] GARY, N. E. Activities and behavior of honey bees. *The hive and the honey bee* (1992), 269–373.

- [29] GINSBERG, H. S. Foraging ecology of bees in an old field. *Ecology* 64, 1 (1983), 165–175.
- [30] GOULSON, D., NICHOLLS, E., BOTÍAS, C., AND ROTHERAY, E. L. Bee declines driven by combined stress from parasites, pesticides, and lack of flowers. *Science* 347, 6229 (2015), 1255957.
- [31] GRIMM, V., REVILLA, E., BERGER, U., JELTSCH, F., MOOIJ, W. M., RAILSBACK, S. F., THULKE, H.-H., WEINER, J., WIEGAND, T., AND DEANGELIS, D. L. Pattern-oriented modeling of agent-based complex systems: lessons from ecology. *science* 310, 5750 (2005), 987–991.
- [32] HARBO, J. R. Effect of population size on brood production, worker survival and honey gain in colonies of honeybees. *Journal of Apicultural Research* 25, 1 (1986), 22–29.
- [33] HAYDAK, M. H. Honey bee nutrition. *Annual review of entomology* 15, 1 (1970), 143–156.
- [34] HENRY, M., BEGUIN, M., REQUIER, F., ROLLIN, O., ODOUX, J.-F., AUPINEL, P., APTEL, J., TCHAMITCHIAN, S., AND DECOURTYE, A. A common pesticide decreases foraging success and survival in honey bees. *Science* 336, 6079 (2012), 348–350.
- [35] HIGES, M., MARTIN-HERNANDEZ, R., GARRIDO-BAILON, E., GONZALEZ-PORTO, A. V., GARCIA-PALENCIA, P., AND MEANA, A. Honeybee colony collapse due to *Nosema ceranae* in professional apiaries. *Environmental Microbiology Reports* 1, 2 (2009), 110–113.
- [36] HO, M.-W., AND CUMMINS, J. Mystery of disappearing honeybees. *Science in Society* 34 (2007), 35–36.
- [37] HUANG, W.-F., SOLTER, L. F., YAU, P. M., AND IMAI, B. S. *Nosema ceranae* escapes fumagillin control in honey bees. *PLOS Pathog* 9, 3 (2013), e1003185.
- [38] IMDORF, A., RUOFF, K., AND FLURI, P. Volksentwicklung bei der honigbiene. In *ALP forum* (2008), vol. 68, pp. 1–88.
- [39] JOHNSON, R. M., DAHLGREN, L., SIEGFRIED, B. D., AND ELLIS, M. D. Acaricide, fungicide and drug interactions in honey bees (*Apis mellifera*). *PLOS ONE* 8, 1 (2013), e54092.
- [40] JOHNSON, R. M., WEN, Z., SCHULER, M. A., AND BERENBAUM, M. R. Mediation of pyrethroid insecticide toxicity to honey bees (*Hymenoptera: Apidae*) by cytochrome p450 monooxygenases. *Journal of economic entomology* 99, 4 (2006), 1046–1050.
- [41] JOSHI, N. C., AND JOSHI, P. Foraging behaviour of *Apis* spp. on apple flowers in a subtropical environment. *New York Science Journal* 3, 3 (2010), 71–76.
- [42] KHOURY, D. S., BARRON, A. B., AND MYERSCOUGH, M. R. Modelling food and population dynamics in honey bee colonies. *PLOS ONE* 8, 5 (05 2013), e59084.
- [43] KHOURY, D. S., MYERSCOUGH, M. R., AND BARRON, A. B. A quantitative model of honey bee colony population dynamics. *PLOS ONE* 6, 4 (04 2011), e18491.
- [44] KRALJ, J., AND FUCHS, S. Parasitic *Varroa destructor* mites influence flight duration and homing ability of infested *Apis mellifera* foragers. *Apidologie* 37, 5 (2006), 577.
- [45] KRONENBERG, F. Colonial thermoregulation in honey bees. *Journal of Comparative Physiology B* 148 (1979), 65–78.

- [46] LEONCINI, I., LE CONTE, Y., COSTAGLIOLA, G., PLETTNER, E., TOTH, A. L., AND WANG, M. Regulation of behavioral maturation by a primer pheromone produced by adult worker honey bees. *Proceedings of the National Academy of Sciences of the United States of America* 101, 50 (2004), 17559–17564.
- [47] MARTIN, S. Hygienic behaviour: an alternative view. *Bee Improvement* 7 (2000), 6–7.
- [48] MARTIN, S. Biology and life-history of *Varroa* mites. *Mites of the honey bee*. Dadant & Sons, Hamilton, IL (2001), 131–148.
- [49] MCKAY, M. D., BECKMAN, R. J., AND CONOVER, W. J. A comparison of three methods for selecting values of input variables in the analysis of output from a computer code. *Technometrics* 42, 1 (2000), 55–61.
- [50] McLELLAN, A. Growth and decline of honeybee colonies and inter-relationships of adult bees, brood, honey and pollen. *Journal of Applied Ecology* (1978), 155–161.
- [51] NEUMANN, P., AND CARRECK, N. L. Honey bee colony losses. *Journal of Apicultural Research* 49, 1 (2010), 1–6.
- [52] ODOUX, J.-F., AUPINEL, P., GATEFF, S., REQUIER, F., HENRY, M., AND BRETAGNOLLE, V. ECOBEE: a tool for long-term honey bee colony monitoring at the landscape scale in West European intensive agroecosystems. *Journal of Apicultural Research* 53, 1 (2014), 57–66.
- [53] OMHOLT, S. W. A model for intracolony population dynamics of the honeybee in temperate zones. *Journal of Apicultural Research* 25, 1 (1986), 9–21.
- [54] PAGE, R. E., AND PENG, C. Y.-S. Aging and development in social insects with emphasis on the honey bee, *apis mellifera* l. *Experimental gerontology* 36, 4 (2001), 695–711.
- [55] PAXTON, R. J., KLEE, J., KORPELA, S., AND FRIES, I. *Nosema ceranae* has infected *Apis mellifera* in Europe since at least 1998 and may be more virulent than *Nosema apis*. *Apidologie* 38, 6 (2007), 558–565.
- [56] PERRY, C. J., SØVIK, E., MYERSCOUGH, M. R., AND BARRON, A. B. Rapid behavioral maturation accelerates failure of stressed honey bee colonies. *Proceedings of the National Academy of Sciences* 112, 11 (2015), 3427–3432.
- [57] PETTIS, J. S., LICHTENBERG, E. M., ANDREE, M., STITZINGER, J., ROSE, R., VANENGELSDORP, D., ET AL. Crop pollination exposes honey bees to pesticides which alters their susceptibility to the gut pathogen *Nosema ceranae*. *PLOS ONE* 8, 7 (2013), e70182.
- [58] RATNIEKS, F. L. Egg-laying, egg-removal, and ovary development by workers in queenright honey bee colonies. *Behavioral Ecology and Sociobiology* 32, 3 (1993), 191–198.
- [59] RATNIEKS, F. L., AND KELLER, L. Queen control of egg fertilization in the honey bee. *Behavioral Ecology and Sociobiology* 44, 1 (1998), 57–61.
- [60] RATTI, V., KEVAN, P. G., AND EBERL, H. J. A mathematical model for population dynamics in honeybee colonies infested with *Varroa destructor* and the Acute Bee Paralysis Virus. *Canadian Applied Mathematics Quarterly* 21, 1 (2013), 63–93.
- [61] RATTI, V., KEVAN, P. G., AND EBERL, H. J. A mathematical model of the honeybee-*Varroa destructor*-Acute Bee Paralysis Virus complex with seasonal effects. *Bulletin of Mathematical Biology* (2015).

- [62] REYNOLDS, A. M., SMITH, A. D., MENZEL, R., GREGGERS, U., REYNOLDS, D. R., AND RILEY, J. R. Displaced honey bees perform optimal scale-free search flights. *Ecology* 88, 8 (2007), 1955–1961.
- [63] REYNOLDS, A. M., SMITH, A. D., REYNOLDS, D. R., CARRECK, N. L., AND OSBORNE, J. L. Honeybees perform optimal scale-free searching flights when attempting to locate a food source. *Journal of Experimental Biology* 210, 21 (2007), 3763–3770.
- [64] RORTAIS, A., ARNOLD, G., HALM, M.-P., AND TOUFFET-BRIENS, F. Modes of honeybees exposure to systemic insecticides: estimated amounts of contaminated pollen and nectar consumed by different categories of bees. *Apidologie* 36, 1 (2005), 71–83.
- [65] ROUBIK, D. W., AND WOLDA, H. Do competing honey bees matter? Dynamics and abundance of native bees before and after honey bee invasion. *Population Ecology* 43, 1 (2001), 53–62.
- [66] RUSSELL, S., BARRON, A. B., AND HARRIS, D. Dynamic modelling of honey bee (*Apis mellifera*) colony growth and failure. *Ecological Modelling* 265, 0 (2013), 158 – 169.
- [67] SAKAGAMI, S., AND FUKUDA, H. Life tables for worker honeybees. *Researches on Population Ecology* 10, 2 (1968), 127–139.
- [68] SAMMATARO, D., GERSON, U., AND NEEDHAM, G. Parasitic mites of honey bees: life history, implications, and impact. *Annual review of entomology* 45, 1 (2000), 519–548.
- [69] SCHMICKL, T., AND CRAILSHEIM, K. Hopomo: A model of honeybee intracolony population dynamics and resource management. *Ecological modelling* 204, 1 (2007), 219–245.
- [70] SEELEY, T. D. *The wisdom of the hive: the social physiology of honey bee colonies*. Harvard University Press, 2009.
- [71] SEELEY, T. D. *Honeybee ecology: a study of adaptation in social life*. Princeton University Press, 2014.
- [72] SLESSOR, K. N., WINSTON, M. L., AND LE CONTE, Y. Pheromone communication in the honeybee (*Apis mellifera* L.). *Journal of chemical ecology* 31, 11 (2005), 2731–2745.
- [73] SMITH, M. L. The honey bee parasite *Nosema ceranae*: Transmissible via food exchange? *PLOS ONE* 7, 8 (08 2012), e43319.
- [74] SOUTHWICK, E. E., AND SOUTHWICK JR, L. Estimating the economic value of honey bees (*Hymenoptera: Apidae*) as agricultural pollinators in the United States. *Journal of Economic Entomology* 85, 3 (1992), 621–633.
- [75] STANLEY, J., AND PREETHA, G. *Pesticide Toxicity to Non-target Organisms: Exposure, Toxicity and Risk Assessment Methodologies*. Springer, 2016.
- [76] STILLMAN, R. A., RAILSBACK, S. F., GISKE, J., BERGER, U., AND GRIMM, V. Making predictions in a changing world: the benefits of individual-based ecology. *BioScience* 65, 2 (2015), 140–150.
- [77] STONER, K. A., AND EITZER, B. D. Movement of soil-applied imidacloprid and thiamethoxam into nectar and pollen of squash (*Cucurbita pepo*). *PLOS ONE* 7, 6 (2012), e39114.

- [78] SUCHAIL, S., DE SOUSA, G., RAHMANI, R., AND BELZUNCES, L. P. In vivo distribution and metabolisation of ¹⁴C-imidacloprid in different compartments of *Apis mellifera* L. *Pest management science* 60, 11 (2004), 1056–1062.
- [79] SUCHAIL, S., DEBRAUWER, L., AND BELZUNCES, L. P. Metabolism of imidacloprid in *Apis mellifera*. *Pest management science* 60, 3 (2004), 291–296.
- [80] SUMPTER, D. J. T., AND MARTIN, S. J. The dynamics of virus epidemics in *Varroa*-infested honey bee colonies. *Journal of Animal Ecology* 73, 1 (2004), 51–63.
- [81] TAN, K., YANG, S., WANG, Z.-W., RADLOFF, S. E., AND OLDROYD, B. P. Differences in foraging and broodnest temperature in the honey bees *Apis cerana* and *A. mellifera*. *Apidologie* 43, 6 (2012), 618–623.
- [82] THORBEC, P., CAMPBELL, P. J., SWEENEY, P. J., AND THOMPSON, H. M. Using BEEHAVE to explore pesticide protection goals for European honeybee (*Apis mellifera* L.) worker losses at different forage qualities. *Environmental Toxicology and Chemistry* (2016).
- [83] VANĒNGELSDORP, D., EVANS, J. D., SAEGERMAN, C., MULLIN, C., HAUBRUGE, E., NGUYEN, B. K., FRAZIER, M., FRAZIER, J., COX-FOSTER, D., CHEN, Y., UNDERWOOD, R., TARPY, D. R., AND PETTIS, J. S. Colony collapse disorder: A descriptive study. *PLOS ONE* 4, 8 (08 2009), e6481.
- [84] VIDAU, C., DIOGON, M., AUFUUVRE, J., FONTBONNE, R., VIGUÈS, B., BRUNET, J.-L., TEXIER, C., BIRON, D. G., BLOT, N., EL ALAOU, H., ET AL. Exposure to sublethal doses of fipronil and thiacloprid highly increases mortality of honeybees previously infected by *Nosema ceranae*. *PLOS ONE* 6, 6 (2011), e21550.
- [85] WATANABE, M. E. Colony collapse disorder: Many suspects, no smoking gun. *BioScience* 58, 5 (2008), 384–388.
- [86] WHARTON, K. E., DYER, F. C., HUANG, Z. Y., AND GETTY, T. The honeybee queen influences the regulation of colony drone production. *Behavioral Ecology* 18, 6 (2007), 1092–1099.
- [87] WILSON, W. T., MOFFETT, J. O., HARRINGTON, H. D., ET AL. Nectar and pollen plants of Colorado. *Colorado State University, Experiment Station Bulletin* (1958), 503–S.
- [88] WINSTON, M. *The biology of the honey bee*. Harvard University Press, 1987.
- [89] YAMADA, T., ET AL. Honeybee colony collapse disorder. *Emerging Biological Threats: A Reference Guide* 13 (2009), 141.
- [90] ZUCKERMAN, L. Rusty patched bumble bee proposed for U.S. endangered species status.

Chapter 6

Discrete and continuum operators for the spread of disease: A closed-form next generation operator for reaction-diffusion systems

Abstract

The next generation operator (NGO) is a clear analog to the next generation matrix (NGM) for disease models. However, the NGO has been derived independently of the NGM and the quantifiable connection between the two approaches remains an open question. Here, we demonstrate that the NGO can be directly obtained as the limit of the NGM, as the number of discrete classes approaches infinity. In the case of continuous age-structured disease models, this approach recovers the NGO as previously defined for both separable and non-separable interaction terms. For reaction-diffusion systems, we present a new, closed-form formulation for the NGO for disease spread. The Fourier methods illustrated here present a new approach for formulating a closed-form next generation operator, which can then be used to provide a reproduction number for more complex models, including the fractional derivatives used to describe Lévy flight.

6.1 Introduction

At the core of modeling the progression of disease within a population is the basic reproduction number, R_0 . This key parameter determines whether a disease will spread in a population, and allows for quantitative estimates of the strength of control measures required to contain this spread [20, 27].

The next generation matrix (NGM) [35] offers an intuitively elegant and well-studied method for calculating R_0 for a disease affecting a population of N discrete classes, that is, for disease dynamics described by a system of

ordinary differential equations. The NGM is arguably the most widely used approach for estimating the basic reproduction number in either discrete or continuous time (as evidenced by the number of studies that rely on the method [20]), equating the basic reproduction number to the spectral radius of a closed-form matrix with a clear biological meaning. In recent work, Diekmann *et al.* proposed a method of deriving the NGM directly from model parameters for general epidemic models in discrete compartments [16]. A still more recent study by Roberts and Heesterbeek characterizes the next generation matrix and basic reproduction number, R_0 , for a variety of ecological models [32], while Cushing and Diekmann explore how different physical interpretations of the same model can result in different formulations of the NGM, by essentially counting infections in different units [11]. Throughout this paper, for models with discrete classes we will adopt the definition of the basic reproduction number as the dominant positive eigenvalue with non-negative eigenvector of the NGM [11, 34, 35].

In recent years, a number of extensions and alternatives to the NGM have been proposed. For example, in discrete time models, Li and Schneider take the novel approach of defining the projection matrix as a matrix sum [25], which can then be used to calculate R_0 . In [31], Roberts *et al.* extend the idea of the next generation matrix to develop new estimates of control efforts for infectious disease. These estimates have the same threshold behaviour as R_0 , but each estimate is applicable to one host type. Roberts *et al.* have also recently proposed methods of extending and relating ecological dynamics to R_0 in predator-prey systems [32]. In [22], Hyman and Li derive an explicit expression for R_0 for an HIV model, demonstrating an equivalence between the next generation matrix and the Jacobian of the system. R_0 can also be calculated in randomly fluctuating environments, for discrete population classes in either discrete or continuous time [4].

In many model formulations, however, it is more intuitive to assume that populations are structured along a continuum, as opposed to having discrete classes. In the case of periodic infectibility, that is, assuming an interaction term that depends both on continuous infection age and time, an expression for R_0 has also been obtained as the spectral radius of a matrix closely related to the NGM [3, 12]. Other examples include models with continuous age structure or spatially heterogeneous populations, that is, models described by systems of partial differential equations. The basic reproduction number has been determined for such infinite-dimensional models in a number of disease-specific cases, as for example in dengue [10], nosocomial infections [9] and infections in honey bee colonies [5]. Wang and Zhao [38] developed an elegant method for determining the spectral radius of the next generation operator for the special case of a reaction-diffusion system.

More generally, Greenhalgh first conjectured that the spectral radius of an integral operator would provide a threshold criterion, R_0 , in the case of infinite-dimensional population structure [17, 18]. This conjecture was confirmed by Inaba [23], and in parallel work, the Next Generation Operator (NGO) was defined by Diekmann *et al.* [15]. The connection between R_0 , defined as the spectral radius of a positive bounded linear operator, and the spectral bound

of a related linear operator, has also been elucidated in some detail by Thieme [34].

Although the NGO is clearly the continuous analog of the NGM, the derivation of the NGO has typically proceeded either by defining the contribution of infectious individuals to the “next generation” of infectious individuals [14], or by deriving an operator whose spectral radius has the necessary threshold behaviour [34]. Here, we take a different approach, explicitly demonstrating the connection between the NGO and the NGM by taking the limit of the NGM as the number of discrete classes approaches infinity. This approach allows us to derive the NGO for a class of well-studied reaction-diffusion disease models. Specifically, we derive a new, closed-form expression for the NGO in the case of a diffusing infected population with constant death rate, as well as conjecture an operator for a diffusing population with general death rate.

The importance of reaction-diffusion models in mathematical biology cannot be overstated. The construction and analysis of reaction-diffusion systems are central to modelling and understanding the complex interactions of mobile individuals, as elucidated in standard reference texts in mathematical biology ([1, 2, 7, 8, 26, 29], see [30, 36] for review). In 2012, Wang and Zhao proved that the next-generation operator exists for reaction-diffusion systems [38]. These authors also proved that the spectral radius of the operator does indeed yield the basic reproduction number. In an illustrative example, Wang and Zhao consider an SEIR model with diffusion [38]. While a framework to determine R_0 is provided in this example, the exact closed-form expression for the next generation operator, both generally and in the illustrative example, remains open. The difficulty in determining such an operator lies in the inversion of the non-infection related terms. These terms often involve explicit spatial dependence as well as second derivative terms which complicate inversion. The derivation of a closed-form solution, as we illustrate below, could lead to a richer understanding of the dynamics and stability of this central class of disease models.

In Section 2, we extend the next generation matrix into the continuum for a general age-structured disease model, first with a separable interaction term and then in a more general case. In Section 3, we consider a spatial reaction-diffusion model, and present a closed form next generation operator in the case of constant diffusion and constant disease-related death. We conjecture an extension of this operator to models with spatially-dependent death. Section 4 applies these methods to a broader set of equations which include the fractional derivative operators used to model Lévy flights. In Section 5 we extend the methods used in [6] to derive an upper bound for R_0 in the case of a general interaction term for age-structured models.

6.2 The limit of the Next Generation Matrix

Consider an outbreak of infection in an age-structured population in which the susceptible class, $S(a, t)$, and infected class, $I(a, t)$, both functions of age, a ,

and time, t , are governed by

$$\frac{\partial S(a, t)}{\partial a} + \frac{\partial S(a, t)}{\partial t} = -f_S(a)S(a, t) - S(a, t) \int_0^\infty \beta(a, a')I(a', t)da' \quad (6.1)$$

$$\frac{\partial I(a, t)}{\partial a} + \frac{\partial I(a, t)}{\partial t} = -f_I(a)I(a, t) + S(a, t) \int_0^\infty \beta(a, a')I(a', t)da' \quad (6.2)$$

$$S(0, t) = B_S \quad (6.3)$$

$$I(0, t) = 0 \quad (6.4)$$

The function $\beta(a, a')$ is the infection term, allowing for localized or distant interactions in age space, while the terms $f_S(a)$ and $f_I(a)$ are the flux through each age class (assumed to be bounded and eventually positive, i.e. there exists an $A \in \mathbb{R}^+$ such that $f(a) > 0$ for all $a > A$), and B_S is the constant birth rate of new individuals into the population. This simple model assumes that no individuals are born infected.

6.2.1 Separable Interaction Term

In many cases, the term $\beta(a, a')$ creates difficulties in analyzing equations (6.1), (6.2), (6.3), and (6.4). If a disease can be modeled via a separable interaction term, i.e. $\beta(a, a') = \alpha(a)\gamma(a')$, the governing equations can be simplified to

$$\frac{\partial S(a, t)}{\partial a} + \frac{\partial S(a, t)}{\partial t} = -f_S(a)S(a, t) - \alpha(a)S(a, t) \int_0^\infty \gamma(a')I(a', t)da' \quad (6.5)$$

$$\frac{\partial I(a, t)}{\partial a} + \frac{\partial I(a, t)}{\partial t} = -f_I(a)I(a, t) + \alpha(a)S(a, t) \int_0^\infty \gamma(a')I(a', t)da' \quad (6.6)$$

$$S(0, t) = B \quad (6.7)$$

$$I(0, t) = 0 \quad (6.8)$$

where $\gamma(a')$ represents the *infectiousness* of an infected individual of age a' , while $\alpha(a)$ is proportional to the *susceptibility* of susceptible individuals of age a to infection.

The disease-free equilibrium for equations (6.5), (6.6), (6.7), and (6.8) is given as the solution to the simple ordinary differential equation

$$\frac{dS(a)}{da} = -f_S(a)S(a) \quad (6.9)$$

with initial condition

$$S(0) = B_S \quad (6.10)$$

$$(6.11)$$

The equilibrium (obtained as a solution to equation (6.9) by separation of variables) is

$$S^*(a) = B_S \exp\left(-\int_0^a f_S(\bar{a})d\bar{a}\right). \quad (6.12)$$

Brauer derives an expression for R_0 in [6] for equations (6.6) and (6.8):

$$R_0 = \int_0^\infty \gamma(a)e^{-\Gamma(a)} \left\{ \int_0^a \alpha(s)S^*(s)e^{\Gamma(s)} ds \right\} da \quad (6.13)$$

where

$$\Gamma(a) = \int_0^a f_I(\tilde{a})d\tilde{a}. \quad (6.14)$$

However, the method developed in [6] does not elucidate the relationship between this expression and the next generation matrix. Here, we will discretize equations (6.5), (6.6) and (6.8) into N distinct age classes so that we may use the next generation matrix to find R_0 . We will then show that the limit of this expression is indeed equation (6.13).

Consider an age-structured ODE model with N age classes, each of size Δa :

$$\begin{aligned} \frac{dS_1}{dt} &= B_S - \alpha_1 S_1 \sum_{j=1}^N \gamma_j I_j - \frac{S_1}{\Delta a} \\ \frac{dS_i}{dt} &= -f_{S,i} S_i - \alpha_i S_i \sum_{j=1}^N \gamma_j I_j + \frac{S_{i-1} - S_i}{\Delta a} \quad 2 \leq i \leq N \\ \frac{dI_1}{dt} &= -f_{I,i} I_1 + \alpha_i S_1 \sum_{j=1}^N \gamma_j I_j + \frac{-I_1}{\Delta a} \\ \frac{dI_i}{dt} &= -f_{I,i} I_i + \alpha_i S_i \sum_{j=1}^N \gamma_j I_j + \frac{I_{i-1} - I_i}{\Delta a} \quad 2 \leq i \leq N \end{aligned} \quad (6.15)$$

where B_S is some birth rate, and, as above, f_i is the total rate of flux through a particular age class. The last term in each equation specifically represents the aging process. The number of classes, N , is directly related to the discretization, Δa , through

$$N = \frac{a_{max}}{\Delta a}. \quad (6.16)$$

Therefore, the limit $\Delta a \rightarrow 0$ implies $N \rightarrow \infty$.

The disease-free equilibrium for System (6.15) is given by

$$S_1^* = \Delta a B_S, \quad (6.17)$$

$$S_i^* = \frac{S_{i-1}^*}{\Delta a} \left(\frac{1}{\Delta a} - f_{S,i} \right)^{-1}, \quad i \in [2, N]. \quad (6.18)$$

Note here, as it will come into play when taking the limit as $\Delta a \rightarrow 0$, that Δa is implicit in the S_i^* terms. This means that in order to transition smoothly from the discrete to the continuous disease free equilibrium, we take the limit as

$$\lim_{\Delta a \rightarrow 0} S_i^* = \hat{S}_i^* = S(a). \quad (6.19)$$

We can use the above to find the next generation matrix, FV^{-1} , where the components of F are given by

$$F_{ij} = \alpha_i \gamma_j S_i^* \quad 1 \leq i, j \leq N \quad (6.20)$$

and those of V are given by

$$V_{ij} = \begin{cases} f_{I,i} + \frac{1}{\Delta a} & \text{if } i = j \\ -\frac{1}{\Delta a} & \text{if } i = j + 1 \\ 0 & \text{otherwise} \end{cases} \quad (6.21)$$

We note here that F is of rank 1 since the columns are all multiples of one another, therefore the product FV^{-1} must also be of rank 1 [28]. This means the eigenvalues of the next generation matrix are $\lambda_1 = 0$ with multiplicity $N - 1$ and $\lambda_2 = \text{Trace}(FV^{-1})$. It follows immediately that $R_0 = \lambda_2$. The expression for R_0 is then

$$\hat{R}_0 = \sum_{i=1}^N \Delta a \gamma_i \left(\prod_{k=1}^i \frac{1}{f_{I,k} \Delta a + 1} \right) \sum_{j=1}^i \alpha_j S_j^* \prod_{l=1}^{j-1} (f_{I,l} \Delta a + 1). \quad (6.22)$$

We can recover equation (6.13) by taking the limit of equation (6.22) as $\Delta a \rightarrow 0$. In doing so, we use a result from product integration [33]:

$$\lim_{\Delta x \rightarrow 0} \prod_{i=a}^b (1 + f_i \Delta x) = \prod_{i=a}^b (1 + f(x) dx) = e^{\int_a^b f(x) dx}. \quad (6.23)$$

In the limit as Δa approaches 0, the sums in equation (6.22) become integrals, and using equation (6.23) yields

$$\lim_{\Delta a \rightarrow 0} \hat{R}_0 = \int_0^{\infty} \gamma(a) e^{-\Gamma(a)} \left\{ \int_0^a \alpha(s) S^*(s) e^{\Gamma(s)} ds \right\} da = R_0. \quad (6.24)$$

The trace of the FV^{-1} can equivalently be written as

$$\hat{R}_0 = \sum_{i=1}^N \alpha_i S_i^* \Delta a \left(\prod_{k=1}^{i-1} f_k \Delta a + 1 \right) \sum_{j=i}^N \gamma_j \prod_{l=1}^j \frac{1}{f_l \Delta a + 1} \quad (6.25)$$

and again, taking the limit we find that

$$\lim_{\Delta a \rightarrow 0} \hat{R}_0 = \int_0^{\infty} S^*(a) e^{\Gamma(a)} \left\{ \int_a^{\infty} \gamma(s) e^{-\Gamma(s)} ds \right\} da = R_0. \quad (6.26)$$

We thus directly recover Brauer's expression for R_0 in a continuous age-structured disease model [6], as the limit of the NGM as the number of age classes approaches infinity.

6.2.2 Non-separable Interaction Term

The next generation operator can also be recovered from the next generation matrix in the more general case of an arbitrary interaction function $\beta(a, a')$. In this case, we find that in the next generation matrix for a model with N age classes, each of size Δa , the components of F and V are given by

$$F_{ij} = \beta_{ij} S_i^* \quad i, j \in [1, N] \quad (6.27)$$

and those of V are as in equation (6.21).

We seek a vector, \vec{I} , with components I_i , where $i \in [1, N]$ such that

$$\lambda \vec{I} = FV^{-1} \vec{I} \quad (6.28)$$

and $\lambda = \rho(FV^{-1})$. As is, (6.28) gives us N equations. If we sum these equations, the result is one equation of the form

$$\lambda \sum_{i=1}^N I_i = \sum_{i=1}^N C_i I_i \quad (6.29)$$

where

$$C_i = \Delta a \prod_{l=1}^i (f_l \Delta a + 1) \sum_{j=1}^N S_j^* \sum_{k=i}^N \frac{\beta_{jk}}{\prod_{m=1}^k (f_m \Delta a + 1)}. \quad (6.30)$$

Multiplying both sides of (6.29) by Δa and, as in Section 2.1, letting $\Delta a \rightarrow 0$ and making use of equation (6.23) allows us to rewrite equation (6.29) in the limit as

$$\lambda \int_0^\infty I(a) da = \int_0^\infty S^*(a) \int_0^\infty I(a') e^{\Gamma(a')} \int_{a'}^\infty \beta(a, s) e^{-\Gamma(s)} ds da' da. \quad (6.31)$$

This makes it possible to extract the next generation operator

$$N_a \{I(a)\} = S^*(a) \int_0^\infty I(a') e^{\Gamma(a')} \int_{a'}^\infty \beta(a, s) e^{-\Gamma(s)} ds da' \quad (6.32)$$

thus we recover the operator proposed in [15] and [18]. The method demonstrated here, however, offers the additional insight that the NGO is the continuous limit of the NGM. We note that iterative methods for recovering the value of R_0 from such integral operators are well known [24].

6.3 Reaction-Diffusion System

Consider a spatial reaction-diffusion system:

$$\frac{\partial S}{\partial t} + L_x S(x, t) = -S(x, t) \int_{-\infty}^\infty \beta(x, y) I(y, t) dy \quad (6.33)$$

$$\frac{\partial I}{\partial t} = \frac{d}{dx} \left(D(x) \frac{dI}{dx} \right) - f_I(x) I(x, t) + S(x, t) \int_{-\infty}^\infty \beta(x, y) I(y, t) dy \quad (6.34)$$

where $D(x)$ is the rate of diffusion of the infected population, and L_x is some linear operator in x such as $L_x = -\frac{\partial^2 S(x, t)}{\partial x^2} + S(x, t)$ which would represent a population diffusing at a constant rate, while dying at rate 1 individual per unit time. Note that S and I are time-dependent functions, but the time argument has been suppressed in equations (6.33) and (6.34) for the sake of readability.

In the special case of constant diffusion, $D(x) = D$, constant flux, $f_I(x) = f$, and an interaction term that depends on the distance between two individuals, $\beta(x, y) = \beta(x - y)$, an operator for the basic reproduction number can be obtained as follows. Making these substitutions, we obtain

$$\frac{\partial S}{\partial t} + L_x S(x, t) = -S(x, t) \int_{-\infty}^{\infty} \beta(x - y) I(y, t) dy \quad (6.35)$$

$$\frac{\partial I}{\partial t} = D \frac{\partial^2 I}{\partial x^2} - f I(x, t) + S(x, t) \int_{-\infty}^{\infty} \beta(x - y) I(y, t) dy. \quad (6.36)$$

The disease-free equilibrium is once again denoted $S^*(x)$, and we use this to linearize equation (6.36) about $S^*(x)$:

$$\frac{\partial I}{\partial t} = D \frac{\partial^2 I}{\partial x^2} - f I(x, t) + S^*(x) \int_{-\infty}^{\infty} \beta(x - y) I(y, t) dy. \quad (6.37)$$

Discretizing equations (6.37) in x allows us to directly compute the NGM which, as in Section 2, will allow us to recover the NGO. To do so, we approximate equation (6.37) as a series of N ODEs, each of spatial resolution Δx . This yields the matrices

$$F_{x_{ij}} = \Delta x \beta_{i-j} S_i^* \quad (6.38)$$

and

$$B_{ij} = \begin{cases} f + \frac{2D}{\Delta x^2} & i = j \\ -\frac{D}{\Delta x^2} & i = j \pm 1 \\ 0 & \text{otherwise} \end{cases}. \quad (6.39)$$

Matrix B is a tri-diagonal, symmetric matrix and its inverse can be found analytically [21], but it is unclear how to proceed in taking the limit of FB^{-1} . Here we proceed by taking the Fourier transform, $\mathcal{F}[\cdot]$ of equation (6.37), from x -space to s -space to obtain,

$$\frac{\partial \mathcal{I}}{\partial t} = -Ds^2 \mathcal{I}(s, t) - f \mathcal{I}(s, t) + \int_{-\infty}^{\infty} \mathcal{S}^*(s - l) \mathcal{B}(l) \mathcal{I}(l, t) dl \quad (6.40)$$

where $\mathcal{I}(s, t) = \mathcal{F}[I]$, $\mathcal{B}(s) = \mathcal{F}[\beta]$ and $\mathcal{S}^*(s) = \mathcal{F}[S^*]$.

As in [38], we assume that near the disease-free equilibrium, the eigenfunction $i(x)$ will evolve in time according to $T(t)$. In other words, near the disease-free equilibrium, we have $I(x, t) = T(t)i(x)$, and consequently $\mathcal{I}(s, t) = T(t)\mathcal{F}\{i(x)\}(s)$. From here, we can affirm that if $T'(t) > 0$ the infected population $I(x, t)$ is growing. Since $\mathcal{I}(s, t)$ grows at the same rate as $I(x, t)$ it is clear that $\mathcal{I}(s, t)$ is also growing under this conditions, whereas if $T'(t) < 0$ both $I(x, t)$ and $\mathcal{I}(s, t)$ will approach 0 as t tends to infinity. Therefore, near

the disease-free equilibrium, the exponential growth parameter of the infected population is preserved under the Fourier transform. This will allow us to determine a reproduction number in Fourier space which has the same threshold behaviour as R_0 .

From Theorem 3.1 in [38], if we define $\sigma(\cdot)$ as the spectral radius of an operator and define operators F_x and B as

$$F_x[I] = S^*(x) \int_{-\infty}^{\infty} \beta(x-y)I(y)dy \quad (6.41)$$

and

$$B[I] = D \frac{\partial^2 I}{\partial x^2} - fI(x) \quad (6.42)$$

then $\sigma(-F_x B^{-1}) - 1$ and $\sigma(A = B + F_x)$, and the exponential growth bound of the eigenfunction $I(x)$ all have the same sign.

Accordingly, in Fourier space, we define $\mathcal{V}[I] = -Ds^2I - fI$, $\hat{\mathcal{F}}[I] = \int_{-\infty}^{\infty} S^*(s-l)\mathcal{B}(l)I(l)dl$ and $\mathcal{A} = \hat{\mathcal{F}} + \mathcal{V}$, and appeal to Theorems 2.3 and 3.14 in [34] to conclude that $\sigma(\mathcal{A})$, $\sigma(-\hat{\mathcal{F}}\mathcal{V}^{-1}) - 1$ and the exponential growth bound of $I(s)$ all have the same sign. Since we have already shown that the exponential growth bound is preserved under Fourier transform, it follows that both systems will have the same threshold value $R_0 = 1$, such that the disease-free equilibrium is asymptotically stable for $R_0 < 1$.

Discretizing equation (6.40) into N equations of the form,

$$\frac{dI_i}{dt} = -Ds_i^2 I_i - fI_i + \sum_{j=0}^N S_{i-j}^* \mathcal{B}_j I_j \Delta l \quad (6.43)$$

permits the use of the next generation matrix where

$$\hat{\mathcal{F}}_{ij} = S_{i-j}^* \mathcal{B}_j \Delta l \quad (6.44)$$

and

$$\mathcal{V}_{ij} = \begin{cases} f + Ds_i^2, & i = j \\ 0, & i \neq j \end{cases} \quad (6.45)$$

for $i, j \in [0, N]$.

Using the same techniques as described in Section 2.2, in the limit as $\Delta s \rightarrow 0$ we obtain the operator

$$N_s[I] = \int_{-\infty}^{\infty} S^*(s-l) \frac{\mathcal{B}(l)}{f + Dl^2} I(l) dl. \quad (6.46)$$

Since this equation is the limit of the next generation matrix as the number of classes approaches infinity, the spectral radius of operator N_s can be interpreted as the basic reproduction number, \mathcal{R}_0 for equations (6.35) and (6.40). Given the above arguments, \mathcal{R}_0 has the same threshold behaviour as the basic reproduction number, R_0 , for equations (6.35) and (6.36). Figure 6.1 shows numerically that not only are the threshold values the same for the spectral

radii \mathcal{R}_0 and R_0 , but that indeed there are cases when $R_0 = \mathcal{R}_0$. Elucidating the conditions for equivalence is a clear avenue for future work.

Moreover, taking the inverse Fourier transform of equation (6.46) will bring the problem back to real space, x .

$$\mathcal{F}\{N_s[I]\} = \mathcal{F}\{S^*\} \mathcal{F}\left\{\frac{\mathcal{B}I}{Ds^2 + f}\right\} \quad (6.47)$$

$$= S^*(x) \int_{-\infty}^{\infty} \mathcal{F}\left\{\frac{1}{Ds^2 + f}\right\}(x-y) \mathcal{F}\{\mathcal{B}I\}(y) dy \quad (6.48)$$

$$= \frac{S^*(x)}{2\sqrt{Df}} \int_{-\infty}^{\infty} L(x-y) \int_{-\infty}^{\infty} \beta(y-z)I(z) dz dy \quad (6.49)$$

where

$$L(x-y) = e^{-\sqrt{|D|}|x-y|} \quad (6.50)$$

Thus, we can define the operator

$$N_x[I] = \frac{S^*(x)}{2\sqrt{Df}} \int_{-\infty}^{\infty} L(x-y) \int_{-\infty}^{\infty} \beta(y-z)I(z) dz dy. \quad (6.51)$$

Let λ be the spectral radius of $N_s[I]$, then

$$N_x[I] = \mathcal{F}[N_s[I]] = \lambda \mathcal{F}[I] = \lambda I \quad (6.52)$$

Therefore, λ is also the spectral radius of $N_x[I]$.

The spectral radius of $N_x[I]$ (denoted $\sigma(N_x)$) will again have the same threshold behaviour as R_0 .

6.3.1 Inversion Formula: the expected infectious occupation time

We can use Fubini's Theorem to rewrite equation (6.51) as

$$N_x[I] = \int_{-\infty}^{\infty} \int_{-\infty}^{\infty} \frac{S^*(x)}{2\sqrt{Df}} \beta(y-z) L(x-y) I(z) dy dz. \quad (6.53)$$

Numerically, estimates of the spectral radius of $-FB^{-1}$ as defined in equations (6.41) and (6.42) are in perfect agreement with the spectral radius of operator $N_x[I]$ in equation (6.51). Here, we show that for $B[I(x)] = \frac{\partial^2 I}{\partial x^2} - fI$,

$$B^{-1}[I](x) = \left(\frac{d^2 I}{dx^2} - fI\right)^{-1} \quad (6.54)$$

$$= \frac{-1}{2\sqrt{Df}} \int_{-\infty}^{\infty} L(x-y) I(y) dy \quad (6.55)$$

$$= \frac{-1}{2\sqrt{Df}} \int_{-\infty}^{\infty} e^{-\sqrt{|D|}|x-y|} I(y) dy, \quad (6.56)$$

provided the integral exists.

This can be shown in a straightforward manner by considering the expression

$$-\frac{1}{2\sqrt{Df}} \int_{-\infty}^{\infty} e^{-\sqrt{f/D}|x-y|} (Dw''(y) - fw(y)) dy \quad (6.57)$$

where $w(y)$ is any smooth function for which

$$\int_{-\infty}^{\infty} L(x-y)w(y) dy$$

exists. We split this into two integrals, which we can compute:

$$-\frac{1}{2\sqrt{Df}} \int_{-\infty}^{\infty} e^{-\sqrt{f/D}|x-y|} (Dw''(y) - fw(y)) dy = I_L + I_R \quad (6.58)$$

where

$$I_L = -\frac{1}{2\sqrt{Df}} \int_{-\infty}^x e^{-\sqrt{f/D}(x-y)} (Dw''(y) - fw(y)) dy \quad (6.59)$$

and

$$I_R = -\frac{1}{2\sqrt{Df}} \int_x^{\infty} e^{-\sqrt{f/D}(y-x)} (Dw''(y) - fw(y)) dy. \quad (6.60)$$

The result

$$-\frac{1}{2\sqrt{Df}} \int_{-\infty}^{\infty} e^{-\sqrt{f/D}|x-y|} (Dw''(y) - fw(y)) dy = w(x) \quad (6.61)$$

comes from integrating by parts. When working with integrals of the form

$$-\frac{1}{2\sqrt{Df}} \int e^{\pm\sqrt{f/D}(x-y)} Dw''(y) dy$$

we choose $u = \exp(\pm\sqrt{f/D}(x-y))$ and $dv = w''(y)$ and for integrals of the form

$$-\frac{1}{2\sqrt{Df}} \int e^{\pm\sqrt{f/D}(x-y)} (-fw(y)) dy$$

we choose $u = fw(y)$ and $dv = \exp(\pm\sqrt{f/D}(x-y))$. From here, equation (6.61) follows easily.

Figure 6.3 shows some test functions which illustrate this inversion formula. The functions are chosen to highlight three possible classes of functions: those that decay as $x \rightarrow \pm\infty$, those that are periodic and measurable, and finally those that are not integrable on $(-\infty, \infty)$, but are less than exponential order. In analogy with the previous sections, we interpret $B^{-1}[I](x)$ as the expected length of time an individual will be at position x before either dying or moving to a new position.

6.3.2 Conjecture

We conjecture that equation (6.56) can be extended to the case of a spatially variable death rate. In this case, we have

$$B^{-1}[I](x) = \left(\frac{d^2 I}{dx^2} - f(x)I \right)^{-1} \quad (6.62)$$

$$= \frac{-1}{2\sqrt{Df(x)}} \int_{-\infty}^{\infty} M(x-y)I(y)dy \quad (6.63)$$

where

$$M(x-y) = e^{-\sqrt{f(x)/D}|x-y|}. \quad (6.64)$$

Of course, this requires $f(x) \neq 0$.

Figure 6.4 shows some test functions that support this conjecture. Numerical exploration suggests that equation (6.63) may hold for periodic functions, monotonically increasing functions that are less than exponential order, and those that are bounded but not integrable; we show one example of each case.

6.4 Lévy Flight

The above methods can be generalized to other movement patterns including Lévy flights [13]. The generalized system makes use of fractional derivatives:

$$\frac{\partial S}{\partial t} + L_x S(x, t) = -S(x, t) \int_{-\infty}^{\infty} \beta(x, y)I(y, t)dy \quad (6.65)$$

$$\frac{\partial I}{\partial t} = \gamma \frac{\partial^\alpha I}{\partial x^\alpha} - f_I(x)I(x, t) + S(x, t) \int_{-\infty}^{\infty} \beta(x, y)I(y, t)dy \quad (6.66)$$

where $0 < \alpha \leq 2$, γ is a movement constant and the fractional derivative is defined through the Fourier transform, \mathcal{F} as

$$\mathcal{F} \left[\frac{\partial^\alpha I}{\partial x^\alpha} \right] = -|s|^\alpha \mathcal{F}[I(x)]. \quad (6.67)$$

Using the same methods and arguments as Section 3, we assume the disease-free equilibrium exists and is denoted by $S^*(x)$, and that we may linearize around $S^*(x)$, and apply a Fourier transform to equation (6.66). Doing so allows us to write out a generalized next generation operator in Fourier space:

$$N_L[I] = \int_{-\infty}^{\infty} S^*(s-l) \frac{\mathcal{B}(l)}{f_I + |\gamma l|^\alpha} \mathcal{I}(l)dl \quad (6.68)$$

where \mathcal{B} , S^* and \mathcal{I} are defined as in Section 3 (below equation (6.40)).

The largest eigenvalue of this operator will have the same threshold behaviour as R_0 . Reverting to real space, x , is difficult and needs further investigation.

6.5 Approximating the Spectral Radius of the Next Generation Operator

In order to obtain the basic reproduction number for a continuously age-structured population, it is required to solve

$$R_0 I(a) = S^*(a) \int_0^\infty I(a') e^{\Gamma(a')} \int_{a'}^\infty \beta(a, s) e^{-\Gamma(s)} ds da' \quad (6.69)$$

such that $I(a) > 0$ for all a . This problem may be intractable because of the arbitrary nature of both β and Γ . Therefore, in the following section, we attempt to find a closed-form approximation to R_0 .

We begin by adapting Brauer's method [6] for the case of a separable interaction term to a general interaction term. To do so, we linearize equation (6.2) about $S^*(x)$,

$$\frac{\partial I}{\partial a} + \frac{\partial I}{\partial t} = S^*(a) \int_0^\infty \beta(a, a') I(a', t) da' - (f_I(a)) I(a, t) \quad (6.70)$$

and again use the ansatz that near the disease-free equilibrium, the infected population, $I(a, t)$ grows exponentially in time, proportional to the eigenfunction $i(a)$ [6], that is

$$I(a, t) = e^{\rho t} i(a) . \quad (6.71)$$

This yields

$$\frac{di}{da} = S^*(a) W(a) - (f_I(a) + \rho) i(a) \quad (6.72)$$

where

$$W(a) = \int_0^\infty \beta(a, a') i(a') da' . \quad (6.73)$$

Solving equation (6.72) gives

$$i(a) = e^{-\rho a - \Gamma(a)} \int_0^a S^*(s) W(s) e^{\Gamma(s) + \rho s} ds . \quad (6.74)$$

Substituting (6.74) into (6.73) gives

$$W(a) = \int_0^\infty \beta(a, a') e^{-\rho a' - \Gamma(a')} \left\{ \int_0^{a'} S^*(s) W(s) e^{\Gamma(s) + \rho s} ds \right\} da' \quad (6.75)$$

and rewriting the integral yields

$$W(a) = \int_0^\infty S^*(a') e^{\Gamma(a') + \rho a'} \left\{ \int_{a'}^\infty \beta(a, s) e^{-\rho s - \Gamma(s)} ds \right\} W(a') da' . \quad (6.76)$$

This is a homogeneous Fredholm equation of the second kind for the function $W(a)$ [39]. A non-trivial solution to equation (6.76) exists if $W(a)$ is an eigenfunction of the kernel, that is

$$K(a, a', \rho) = S^*(a') e^{\Gamma(a') + \rho a'} \left\{ \int_{a'}^\infty \beta(a, s) e^{-\rho s - \Gamma(s)} ds \right\} \quad (6.77)$$

with associated eigenvalue $\lambda = 1$ [39].

Following the proof in [39], squaring equation (6.76) yields

$$W(a)^2 = \left[\int_0^\infty K(a, a', \rho) W(a') da' \right]^2 \quad (6.78)$$

and we may then use the Cauchy-Schwarz inequality to write

$$W(a)^2 \leq \int_0^\infty K(a, a', \rho)^2 da' \int_0^\infty W(a')^2 da'. \quad (6.79)$$

Integrating both sides of equation (6.79) with respect to variable a , we find:

$$\int_0^\infty W(a)^2 da \leq \int_0^\infty K(a, a', \rho)^2 da' \int_0^\infty W(a')^2 da'. \quad (6.80)$$

Therefore, a non-trivial solution to equation (6.76) exists only if the value of the growth parameter ρ is such that

$$\|K\|_2 \geq 1. \quad (6.81)$$

Since $K(a, a', \rho)$ is a decreasing function of ρ , we know that if $\|K(a, a', 0)\|_2 < 1$ then the only ρ values which satisfy equation (6.81) must be negative. Therefore near the disease-free equilibrium, $I(a, t)$ is a decreasing function of t as per equation (6.71). In contrast, if $\|K(a, a', 0)\|_2 > 1$ then by continuity there must exist a $\rho^* > 0$ such that $\|K(a, a', \rho^*)\|_2 = 1$. In this case, every $\rho < \rho^*$ will also satisfy condition (6.81). Therefore, the actual growth parameter ρ may be positive or negative. Thus $\|K(a, a', 0)\|_2$ is only an upper bound on the basic reproduction number, R_0 . This differs from the case of a separable interaction term in which the analogous condition is $\|K(a, a', \rho)\|_1 = 1$ (see [6] for details), and a unique ρ satisfies this condition, hence $\|K(a, a', 0)\|_1 = R_0$.

6.6 Discussion

Arguably among the most well-studied tools in disease modelling are the next generation matrix of discrete systems [2, 3, 16, 32, 35] and the next generation operators used in continuum models [3, 15, 17, 18, 22, 34, 37, 38]. While the two formulations are clear analogs of one another, in this study we show that the NGO can be directly obtained as the limit of the NGM, as the number of classes approaches infinity. This approach allows us to extend these limit arguments to disease models described by reaction-diffusion equations, and to derive a closed-form next generation operator for these well-known systems.

The relationship between the next generation matrix of discrete dynamics and the next generation operator of continuum dynamics is critical to the biological interpretation of these operators. The next generation matrix is understood easily as the force of infection, F , multiplied by the expected lifetime in each compartment of an infected individual, V^{-1} [11]. When moving to the continuum, these interpretations can be confounded by either the techniques used to determine the operator [6] or by the more complicated nature of the

mathematics involved (such as the convolution and exponential terms appearing in equation (6.32)).

This equivalence between the discrete and continuum approaches makes it possible to manipulate a simple reaction-diffusion model with non-local infectibility to determine a closed-form next generation operator whose spectral radius can be guaranteed to have the same threshold dynamics as R_0 , by connecting theorems found in [34, 38] and taking advantage of the linear properties of the Fourier transform. While the existence of such an operator has previously been proven [34, 38], and while similar results have been applied to various systems such as a dengue fever model [37] and a general model with fixed latent period and nonlocal infection [19], a closed-form operator for R_0 has remained elusive. Since in the present study the next generation operator is derived as the limit of a discrete operator, this derivation provides an avenue toward a threshold parameter in both the discrete and continuum models.

Our study also suggests that the Fourier transform may be a more natural setting for computation of R_0 . We see that a closed-form integral operator with the same threshold characteristics as the next generation operator can be derived for both diffusion and Lévy flight equations, and can be trivially extended to higher dimensions. A next step would be to generalize this method to work with spatially-dependent death rates, in such a way that the validity of the operator can be proven. Here, we provide such an operator as a conjecture.

Moreover, we offer a novel, closed-form expression for inversion of the operator $B[I] = \frac{d^2 I}{dx^2} - fI$. The ubiquity of reaction-diffusion operators in mathematical biology indicates both the need for, and potential importance of, such a closed-form inversion. The inversion operator gives the expected time an individual will occupy position x before either dying or moving to a new position. Biologically this is relevant to many spatial models in ecology, and can potentially be extended to an inversion formula for the expected ‘occupation time’ of migrating populations. Mathematically, this formula makes it possible to turn a reaction-diffusion equation into an eigenvalue problem, which allows a wide range of techniques for solving a reaction-diffusion system analytically and numerically.

We conclude with a technique to find a closed-form upper bound for the basic reproduction number using the operators derived herein. This expression may be useful for understanding the spread of disease in the context of continuous age or space, and for deriving quantitative estimates of control measures. While we show the approximation for the age-structured model, the method can also be applied to equation (6.46) to determine a closed-form approximation for the upper bound of R_0 for a spatially-explicit model.

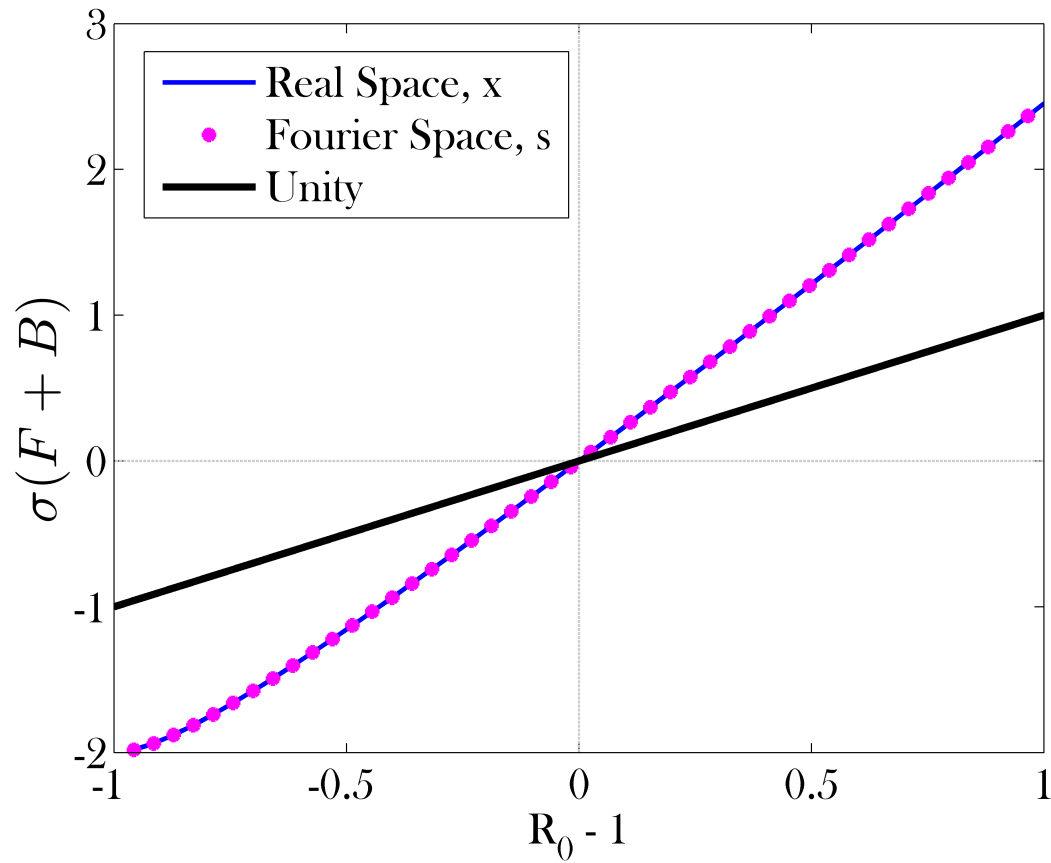


Figure 6.1: R_0 and $\sigma(A)$ calculated in both real space, x , (blue solid line) using FB^{-1} (as defined in equations (6.38) and (6.39), with $\Delta x = 0.1001$ and $N = 2000$), and Fourier space s (magenta points) using equation (6.46) with $\Delta s = 0.1001$. The interaction term used here is $\beta(x - y) = C \exp(-k(x - y)^2)$, $C \in [0.01, 0.5]$, and $L_x[S^*] = xS^{*''}(x) + S^{*'}(x) + 4x^3S^*(x)$. The diffusion rate is set to $D = 1$ and the infected death rate, $f = 1$. We see that not only does the system in Fourier space have the same threshold behaviour as the system in real space, but in fact the values for R_0 are identical.

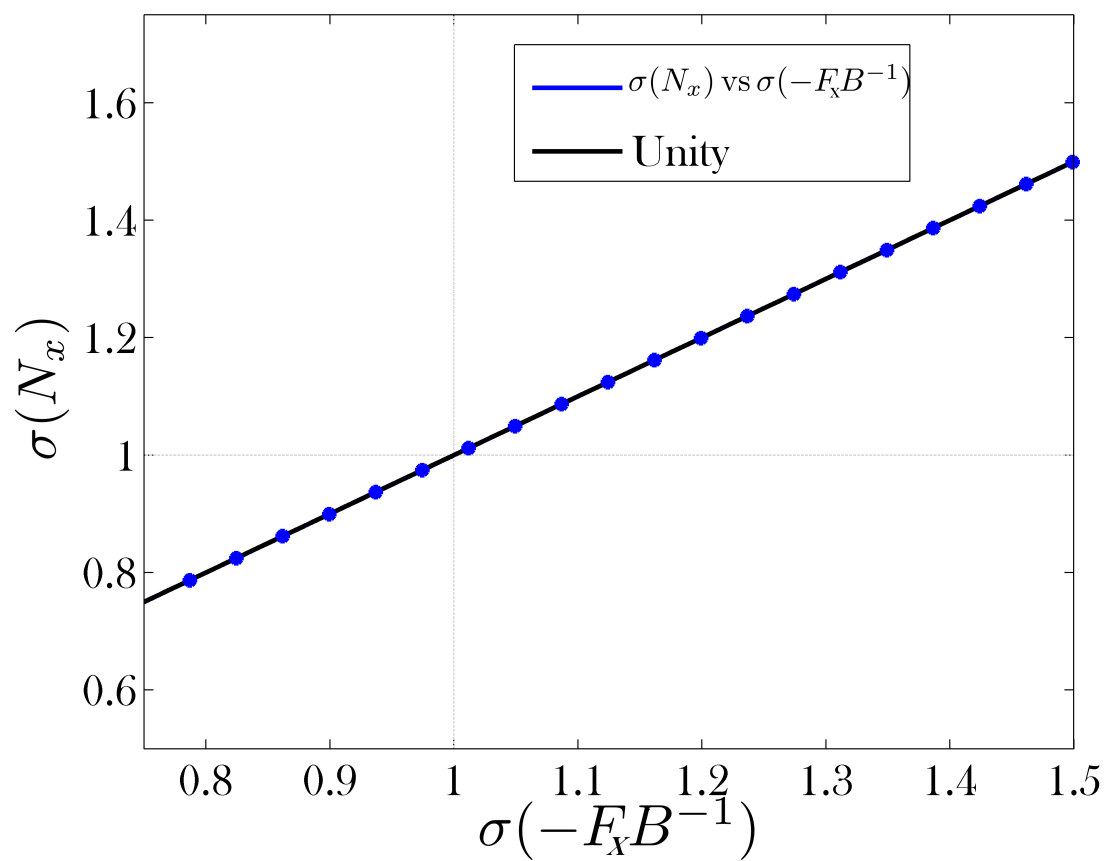


Figure 6.2: $\sigma(-F_x B^{-1})$ vs. $\sigma(N_x)$. $\sigma(-F_x B^{-1})$ is calculated using equations (6.38) and (6.39), with $\Delta x = 0.1001$ and $N = 2000$. $\sigma(N_x)$ is calculated using equation (6.51) with $\Delta x = 0.1001$.

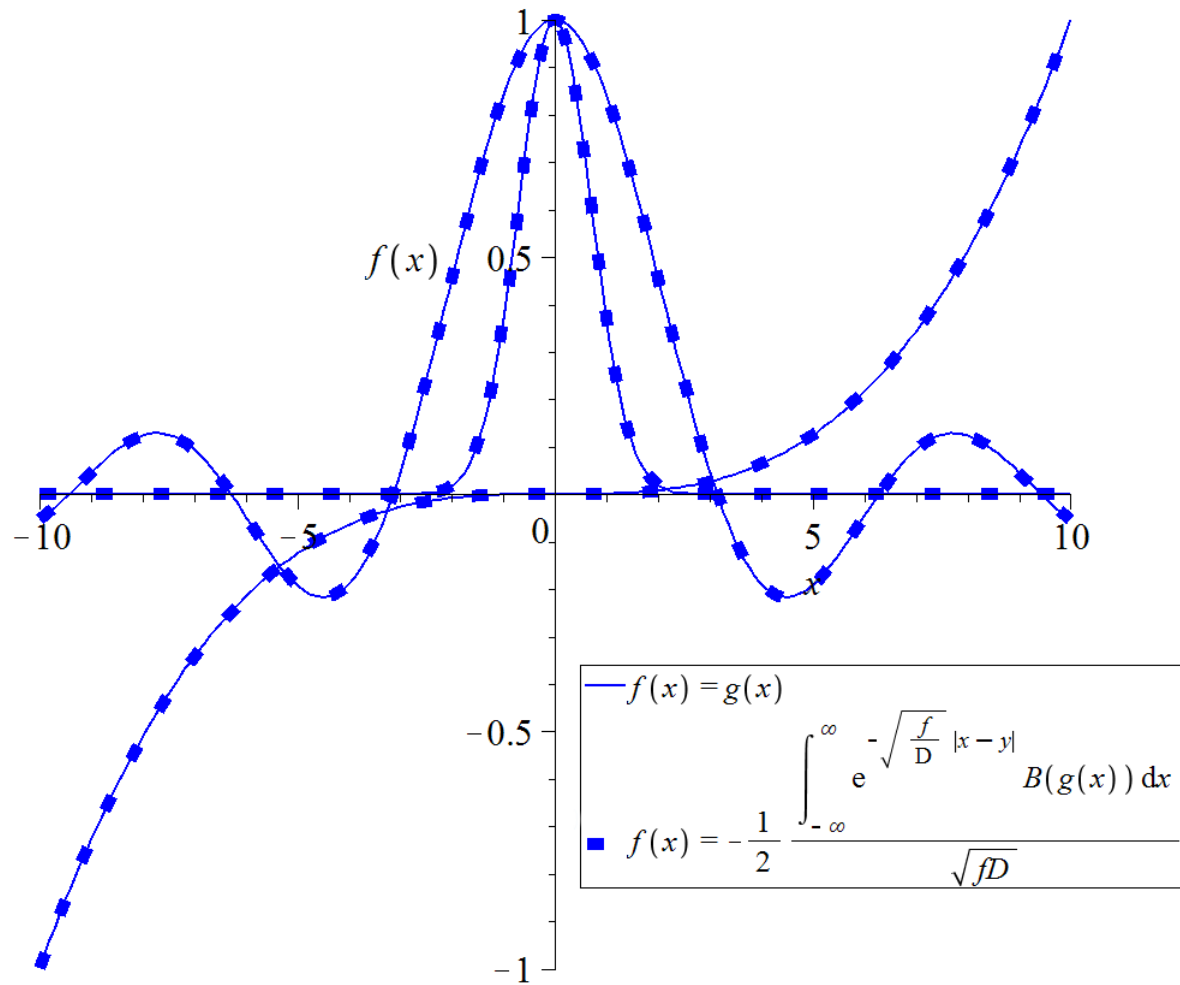


Figure 6.3: Plots of several test functions to illustrate the validity of equation (6.61) in Section 3.1, namely equation (6.56). The test functions used are $g(x) = \exp(-x^2)$, $g(x) = (x/10)^3$, $g(x) = \sin(x)/x$.

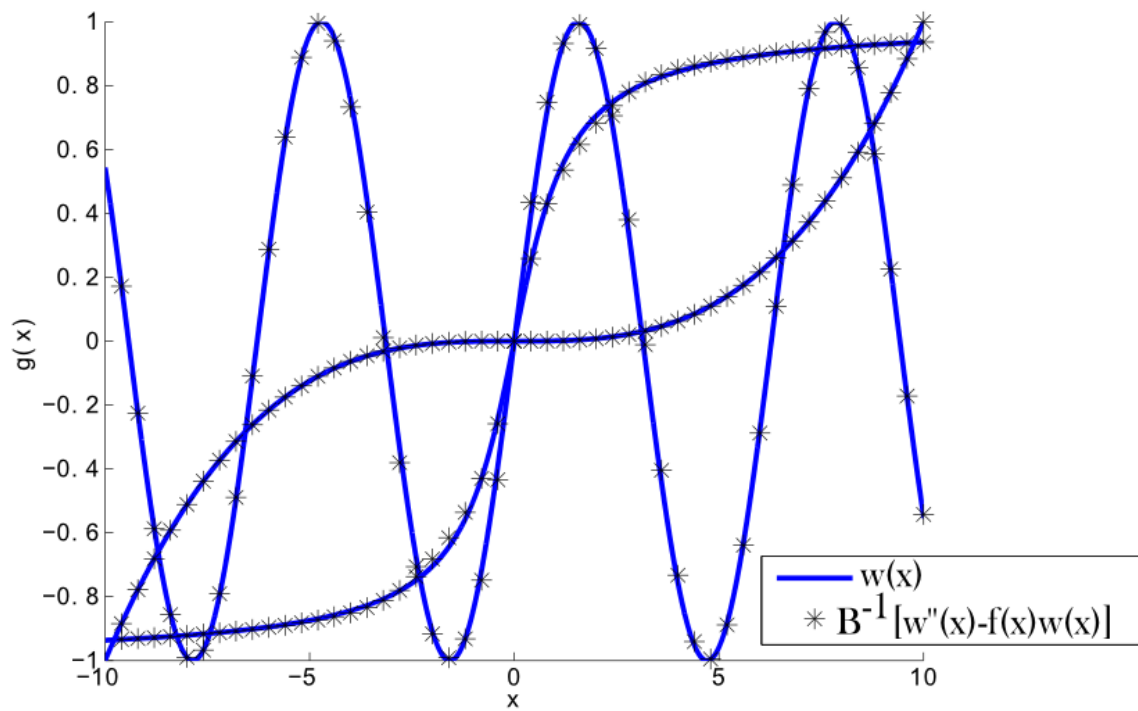


Figure 6.4: Plots of several test functions to illustrate the accuracy of equation (6.63) in Section 3.2, with $f(x) = x^2 + 1$ to ensure smoothness everywhere. The test functions used are $w(x) = \frac{2}{\pi} \arctan(x)$, $w(x) = x^3/10^3$, $w(x) = \sin(x)$.

Bibliography

- [1] ALLEN, L. J. *Introduction to mathematical biology*. Pearson/Prentice Hall, 2007.
- [2] ALLEN, L. J., AND VAN DEN DRIESSCHE, P. The basic reproduction number in some discrete-time epidemic models. *Journal of Difference Equations and Applications* 14, 10-11 (2008), 1127–1147.
- [3] BACAËR, N. Approximation of the basic reproduction number R_0 for vector-borne diseases with a periodic vector population. *Bulletin of mathematical biology* 69, 3 (2007), 1067–1091.
- [4] BACAËR, N., AND KHALADI, M. On the basic reproduction number in a random environment. *Journal of mathematical biology* 67, 6-7 (2013), 1729–1739.
- [5] BETTI, M. I., WAHL, L. M., AND ZAMIR, M. Reproduction number and asymptotic stability for a model with continuous age structure: An application to honey bee dynamics. *Bulletin of Mathematical Biology* (2016). submitted.
- [6] BRAUER, F., AND CASTILLO-CHAVEZ, C. *Mathematical models in population biology and epidemiology*, vol. 1. Springer, 2001.
- [7] BRITTON, N. *Essential mathematical biology*. Springer Science & Business Media, 2012.
- [8] BRITTON, N. F. *Reaction-diffusion equations and their applications to biology*. Academic Press, 1986.
- [9] BROWNE, C., AND WEBB, G. F. A nosocomial epidemic model with infection of patients due to contaminated rooms. *Mathematical Biosciences and Engineering* 12, 4 (2015), 761–787.
- [10] CHOWELL, G., FUENTES, R., OLEA, A., AGUILERA, X., NESSE, H., AND HYMAN, J. The basic reproduction number R_0 and effectiveness of reactive interventions during dengue epidemics: The 2002 dengue outbreak in Easter Island, Chile. *Mathematical biosciences and engineering: MBE* 10 (2013), 1455.
- [11] CUSHING, J., AND DIEKMANN, O. The many guises of R_0 (a didactic note). *Journal of Theoretical Biology* 404 (2016), 295–302.
- [12] CUSHING, J. M., AND ACKLEH, A. A net reproductive number for periodic matrix models. *Journal of biological dynamics* 6, 2 (2012), 166–188.
- [13] DEL CASTILLO-NEGRETE, D., CARRERAS, B., AND LYNCH, V. Front dynamics in reaction-diffusion systems with Lévy flights: a fractional diffusion approach. *Physical Review Letters* 91, 1 (2003), 018302.

- [14] DIEKMANN, O., AND HEESTERBEEK, J. *Mathematical epidemiology of infectious diseases: model building, analysis and interpretation*, vol. 5. John Wiley & Sons, 2000.
- [15] DIEKMANN, O., HEESTERBEEK, J., AND METZ, J. A. On the definition and the computation of the basic reproduction ratio R_0 in models for infectious diseases in heterogeneous populations. *Journal of mathematical biology* 28, 4 (1990), 365–382.
- [16] DIEKMANN, O., HEESTERBEEK, J., AND ROBERTS, M. The construction of next-generation matrices for compartmental epidemic models. *Journal of the Royal Society Interface* (2009), rsif20090386.
- [17] GREENHALGH, D. Analytical results on the stability of age-structured recurrent epidemic models. *Mathematical Medicine and Biology* 4, 2 (1987), 109–144.
- [18] GREENHALGH, D. Threshold and stability results for an epidemic model with an age-structured meeting rate. *Mathematical Medicine and Biology* 5, 2 (1988), 81–100.
- [19] GUO, Z., WANG, F.-B., AND ZOU, X. Threshold dynamics of an infective disease model with a fixed latent period and non-local infections. *Journal of mathematical biology* 65, 6-7 (2012), 1387–1410.
- [20] HEFFERNAN, J., SMITH, R., AND WAHL, L. M. Perspectives on the basic reproductive ratio. *Journal of the Royal Society Interface* 2, 4 (2005), 281–293.
- [21] HU, G., AND O’CONNELL, R. F. Analytical inversion of symmetric tridiagonal matrices. *Journal of Physics A: Mathematical and General* 29, 7 (1996), 1511.
- [22] HYMAN, J. M., AND LI, J. The reproductive number for an HIV model with differential infectivity and staged progression. *Linear algebra and its applications* 398 (2005), 101–116.
- [23] INABA, H. Threshold and stability results for an age-structured epidemic model. *Journal of mathematical biology* 28, 4 (1990), 411–434.
- [24] LANCZOS, C. An iteration method for the solution of the eigenvalue problem of linear differential and integral operators. *Journal of Research or the National Bureau of Standards* 45, 4 (1950), 255–282.
- [25] LI, C.-K., AND SCHNEIDER, H. Applications of Perron–Frobenius theory to population dynamics. *Journal of Mathematical Biology* 44, 5 (2002), 450–462.
- [26] MURRAY, J. D. *Mathematical Biology. II Spatial Models and Biomedical Applications {Interdisciplinary Applied Mathematics V. 18}*. Springer-Verlag New York Incorporated, 2001.
- [27] MURRAY, J. D. *Mathematical Biology: I An Introduction {Interdisciplinary Applied Mathematics V. 17}*. Springer, New York, NY, USA, 2002.
- [28] NOBLE, B., AND DANIEL, J. W. *Applied linear algebra*, vol. 3. Prentice-Hall New Jersey, 1988.
- [29] OTTO, S. P., AND DAY, T. *A biologist’s guide to mathematical modeling in ecology and evolution*, vol. 13. Princeton University Press, 2007.

- [30] PASTOR-SATORRAS, R., CASTELLANO, C., VAN MIEGHEM, P., AND VESPIGNANI, A. Epidemic processes in complex networks. *Reviews of modern physics* 87, 3 (2015), 925.
- [31] ROBERTS, M., AND HEESTERBEEK, J. A new method for estimating the effort required to control an infectious disease. *Proceedings of the Royal Society of London B: Biological Sciences* 270, 1522 (2003), 1359–1364.
- [32] ROBERTS, M. G., AND HEESTERBEEK, J. Characterizing the next-generation matrix and basic reproduction number in ecological epidemiology. *Journal of mathematical biology* 66, 4-5 (2013), 1045–1064.
- [33] SLAVÍK, A. *Product integration, its history and applications*. Matfyzpress Prague, 2007.
- [34] THIEME, H. R. Spectral bound and reproduction number for infinite-dimensional population structure and time heterogeneity. *SIAM Journal on Applied Mathematics* 70, 1 (2009), 188–211.
- [35] VAN DEN DRIESSCHE, P., AND WATMOUGH, J. Reproduction numbers and sub-threshold endemic equilibria for compartmental models of disease transmission. *Mathematical biosciences* 180, 1 (2002), 29–48.
- [36] VOLPERT, V., AND PETROVSKII, S. Reaction–diffusion waves in biology. *Physics of life reviews* 6, 4 (2009), 267–310.
- [37] WANG, W., AND ZHAO, X.-Q. A nonlocal and time-delayed reaction-diffusion model of dengue transmission. *SIAM Journal on Applied Mathematics* 71, 1 (2011), 147–168.
- [38] WANG, W., AND ZHAO, X.-Q. Basic reproduction numbers for reaction-diffusion epidemic models. *SIAM Journal on Applied Dynamical Systems* 11, 4 (2012), 1652–1673.
- [39] ZEMYAN, S. M. Fredholm integral equations of the second kind (general kernel). In *The Classical Theory of Integral Equations*. Springer, 2012, pp. 31–84.

Chapter 7

Discussion & Conclusions

The aim of this dissertation was to study models of honey bee colony dynamics. Building upon the work of others, [10, 11, 15], I have developed and analyzed three separate models of honey bee colony dynamics. Each extension to the model has allowed for new predictions or captured new behaviours which were not within the scope of other models.

The first such model, as discussed in Chapter 2, was developed to incorporate high-level seasonality and disease dynamics into honey bee models. Two key predictions came from this model. The first is the use of the Average Age of Recruitment to Foraging (AARF) as an indicator of a diseased colony and, ultimately, as a herald of colony extinction. The second is the role of the onset of winter in the severity of disease. The model shows that diseases that occur in late fall are predicted to have more severe long term effects on colony health than an infection that is introduced in, say, early summer. This model, as a first pass, was developed to be very general. The main aim was to highlight predictors and nonlinear dynamics that arise from the interplay between infection and seasonality, and how a diseased colony can exhibit symptoms of colony collapse.

Age structure was later added to the model and the dynamics were quite different. In Chapter 3, we show the age demography of a healthy colony, conditions for stability of the disease-free equilibrium as well as derive the basic reproduction number, R_0 , for an age-structured model of honey bee colony dynamics. This expression for R_0 is consistent with the expression derived in an age-independent model, and is found to differ significantly from the latter as the number of age classes is increased toward a continuum. Analysis of the model also gives insights into the sensitivity of honey bee colonies to the inherent age polyethism in their societies. The time spent nursing is critical to the survival of honey bee colonies.

In Chapter 4, we perform numerical simulations on the age-structured model to extract more biological insights from the model. It is found that an age-structured model successfully captures the phenomenon known as ‘spring dwindle’ without explicitly building it into the model. The age-structured model also refines the predictions of critical times for onset of infection in a honey bee colony. The introduction of age structure into the model shows that early spring and late fall are especially vulnerable times for honey bee

colonies. Moreover, the model predicts that there is a compounding effect when disease and seasonality are both considered. The model shows that an endemic disease in a honey bee colony may cause destruction of the colony many years later. This implies that the causes of honey bee declines, at least locally on a colony-by-colony basis, may not be immediate.

The agent-based model in Chapter 5 further builds upon the previous models to incorporate environmental hazards and explicit space dependence. The aim here was to develop an accurate model of honey bee dynamics which could be used in order to help guide policy and conservation efforts. The model is in good agreement with experimental data from the literature [4, 6, 14] and behaves as expected in a range of biologically reasonable parameters. In particular, the AARF extracted from simulations is consistent with previous results [2, 10, 11, 13]. The model does show that sub-lethal pesticides are hidden from the AARF, even though the mortality of bees is increased indirectly through, for example, hindered navigation. This particular example of a sub-lethal pesticide effects is simulated and shows that this alone may contribute to Colony Collapse Disorder, as many bees will die quite far away from the hive.

Currently, there is much work being done on honey bee genomics and selectively breeding queens that are able to thrive in the current ecological landscape [7, 9, 12, 16]. With all the new data coming from these studies, and the fact that honey bees are haploid-diploid, a model for the persistence of beneficial mutations in honey bee colonies can help guide efforts to create colonies that thrive, without disrupting the genetic diversity of managed honey bees. It is in this direction that I will continue my work on models of honey bees. Insights can be gained through dynamical systems models and through agent-based simulations. The groundwork has been laid herein to then later study the phenotypical responses at the colony level to genomic changes.

Of course, there is also much much to be done in the way of modeling honey bee colony dynamics. The models herein take a simplified approach to modeling the effect of temperature on forager dynamics. Honey bees are not able generate enough heat in their muscles at low temperatures in order to achieve flight [5]. As well, temperature of the brood has been shown to influence the behaviour of an adult honey bee [18]. Moreover, higher temperatures will evaporate some of the water content in nectar, thus making it more difficult to extract [8]. Also, higher temperatures correlate to increases in flower visiting speed and simultaneous decreases in the number of flowers visited [1]. These observed phenomena will greatly influence not only the dynamics of a honey bee colony, but as well the bee-plant interactions within the ecosystem. The importance of these temperature effects on the longterm health of honey bees is particularly pertinent in the face of global warming [17].

Chapter 6 investigates the connections between the basic reproduction number for compartmental models and partial differential equation models. This work was motivated by the similarities and differences found in the analysis of R_0 in Chapter 3. For general models, R_0 is often difficult – if not impossible – to write down analytically and so we focus on the connection between the next generation matrix (NGM) and its continuous counterpart: the next generation operator (NGO). The basic reproduction number, R_0 , is then the spectral

radius of the defined matrix/operator. We show that for age-structured models, while other techniques exist for defining the NGO [3], one can also recover the NGO as the limit of the NGM. This allows for an algorithmic way to determine the next generation operators for a wide class of advection models as well as allows the techniques and tools developed in the context of compartmental models to be used on models for which one parameter exists on a continuum.

In the case of reaction-diffusion models, we use the above technique to develop a closed-form next generation operator which can be used to extract R_0 . Some implications here are that R_0 has the same threshold behaviour in Fourier space as in real space, and often the NGO is easier to derive in Fourier space. We are also able to recover an inverse for the operator $\frac{\partial^2}{\partial x^2} - f$ and conjecture that this inverse can be extended to operators of the form $D(x)\frac{\partial^2}{\partial x^2} - f(x)$.

The proof of the conjecture is open, and I believe can be of great value both mathematically and biologically if proved. Moreover, there are many ways to modify the simple exploratory models for which the NGOs above have been derived. Future work would entail either developing the NGO for more complex models using the above framework, or showing how perturbations to the simple models will change the NGO.

Bibliography

- [1] BENEDEK, P., AND PRENNER, J. Effect of temperature on the behaviour and pollinating efficiency of honeybees on winter rape flowers. *Journal of Applied Entomology* 71, 1-4 (1972), 120–124.
- [2] BOTIAS, C., MARTIN-HERNANDEZ, R., BARRIOS, L., MEANA, A., AND HIGES, M. *Nosema* spp. infection and its negative effects on honey bees (*Apis mellifera iberiensis*) at the colony level. *Veterinary research* 44, 1 (2013), 1–15.
- [3] BRAUER, F., AND CASTILLO-CHAVEZ, C. *Mathematical models in population biology and epidemiology*, vol. 1. Springer, 2001.
- [4] CAPINERA, J. L. *Encyclopedia of entomology*, vol. 4. Springer Science & Business Media, 2008.
- [5] ESCH, H. Body temperature and flight performance of honey bees in a servo-mechanically controlled wind tunnel. *Journal of comparative physiology* 109, 3 (1976), 265–277.
- [6] GINSBERG, H. S. Foraging ecology of bees in an old field. *Ecology* 64, 1 (1983), 165–175.
- [7] HARPUR, B. A., KENT, C. F., MOLODTSOVA, D., LEBON, J. M., ALQARNI, A. S., OWAYSS, A. A., AND ZAYED, A. Population genomics of the honey bee reveals strong signatures of positive selection on worker traits. *Proceedings of the National Academy of Sciences* 111, 7 (2014), 2614–2619.
- [8] HAYDAK, M. H. Honey bee nutrition. *Annual review of entomology* 15, 1 (1970), 143–156.
- [9] IBRAHIM, A., REUTER, G. S., AND SPIVAK, M. Field trial of honey bee colonies bred for mechanisms of resistance against *Varroa destructor*. *Apidologie* 38, 1 (2007), 67–76.
- [10] KHOURY, D. S., BARRON, A. B., AND MYERSCOUGH, M. R. Modelling food and population dynamics in honey bee colonies. *PLOS ONE* 8, 5 (05 2013), e59084.
- [11] KHOURY, D. S., MYERSCOUGH, M. R., AND BARRON, A. B. A quantitative model of honey bee colony population dynamics. *PLOS ONE* 6, 4 (04 2011), e18491.
- [12] MEIXNER, M. D., COSTA, C., KRYGER, P., HATJINA, F., BOUGA, M., IVANOVA, E., AND BÜCHLER, R. Conserving diversity and vitality for honey bee breeding. *Journal of Apicultural Research* 49, 1 (2010), 85–92.
- [13] PERRY, C. J., SØVIK, E., MYERSCOUGH, M. R., AND BARRON, A. B. Rapid behavioral maturation accelerates failure of stressed honey bee colonies.

- Proceedings of the National Academy of Sciences* 112, 11 (2015), 3427–3432.
- [14] RATNIEKS, F. L. Egg-laying, egg-removal, and ovary development by workers in queenright honey bee colonies. *Behavioral Ecology and Sociobiology* 32, 3 (1993), 191–198.
- [15] RATTI, V., KEVAN, P. G., AND EBERL, H. J. A mathematical model of the honeybee-*Varroa destructor*-Acute Bee Paralysis Virus complex with seasonal effects. *Bulletin of Mathematical Biology* (2015).
- [16] RINDERER, T. E., GUZMAN, L. I. D., FRAKE, A. M., TARVER, M. R., AND KHONGPHINITBUNJONG, K. An evaluation of the associations of parameters related to the fall of *Varroa destructor* (*Acari: Varroidae*) from commercial honey bee (*Hymenoptera: Apidae*) colonies as tools for selective breeding for mite resistance. *Journal of economic entomology* 107, 2 (2014), 516–522.
- [17] STOCKER, T. *Climate change 2013: the physical science basis: Working Group I contribution to the Fifth assessment report of the Intergovernmental Panel on Climate Change*. Cambridge University Press, 2014.
- [18] TAUTZ, J., MAIER, S., GROH, C., RÖSSLER, W., AND BROCKMANN, A. Behavioral performance in adult honey bees is influenced by the temperature experienced during their pupal development. *Proceedings of the National Academy of Sciences* 100, 12 (2003), 7343–7347.

Appendix A

Age structure is Critical to the Population Dynamics and Survival of Honey Bee Colonies – Supplementary Material

Table A.1: Parameter values and source references.

L	maximum rate of egg laying	2000 eggs/day	[5]
w	number of hive bees for 50% egg survival	5000 bees	[5]
a_m	age at which hive bees begin brood care	3 days	[7]
a_T	age at which hive bees end brood care	11 days	[7]
a_R	minimum recruitment age	4 days	[2]
k	age at which rate of recruitment is 25% of max.	10 days	
α	maximum rate of recruitment	1 /day	
$\frac{1}{\sigma}$	maximum fraction of colony that can be foraging	$\frac{1}{3}$	[5]
$\mu(a)$	natural death rate of foragers (summer)	Figure 1	[1]
μ_w	natural death rate of foragers and hive bees (winter)	1/180 /day	[7]
b	mass of food stored for 50% egg survival	500 g	[4]
c	food gathered per day per forager	0.1 g /day / bee	[6]
γ	daily food requirement per adult bee	0.007 g /bee	[4]
$d_H(a)$	death rate of hive bees due to infection	0.14 /day or Figure 1	[3]
$d_F(a)$	death rate of hive bees due to infection	0.14 /day or Figure 1	[3]
β	disease transmission rate	variable	

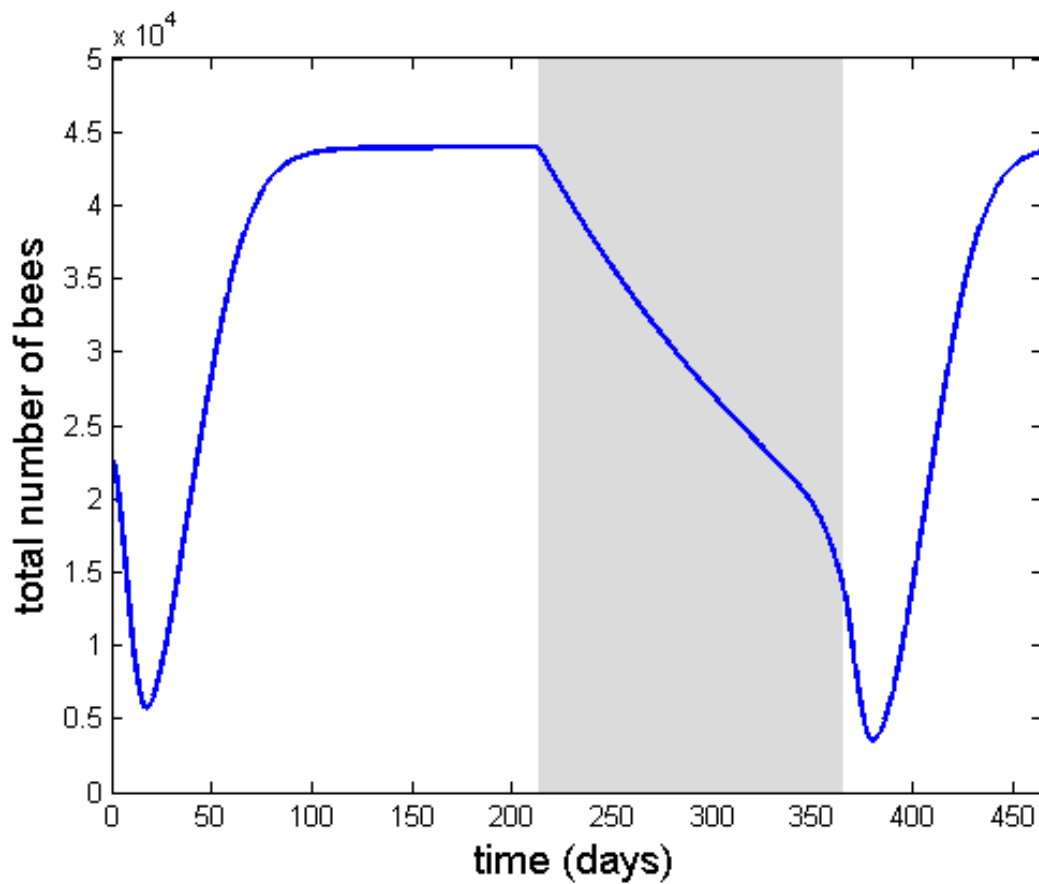


Figure A.1: Time course of total bee population in a disease-free colony. Shaded area denotes winter, during which no new hive bees are produced. Here we use more realistic food intake $c = 0.5$ and consumption rates, $\gamma = 0.07$ [37]. We see that the dynamics of the colony are not sensitive to the food intake and consumption rates.

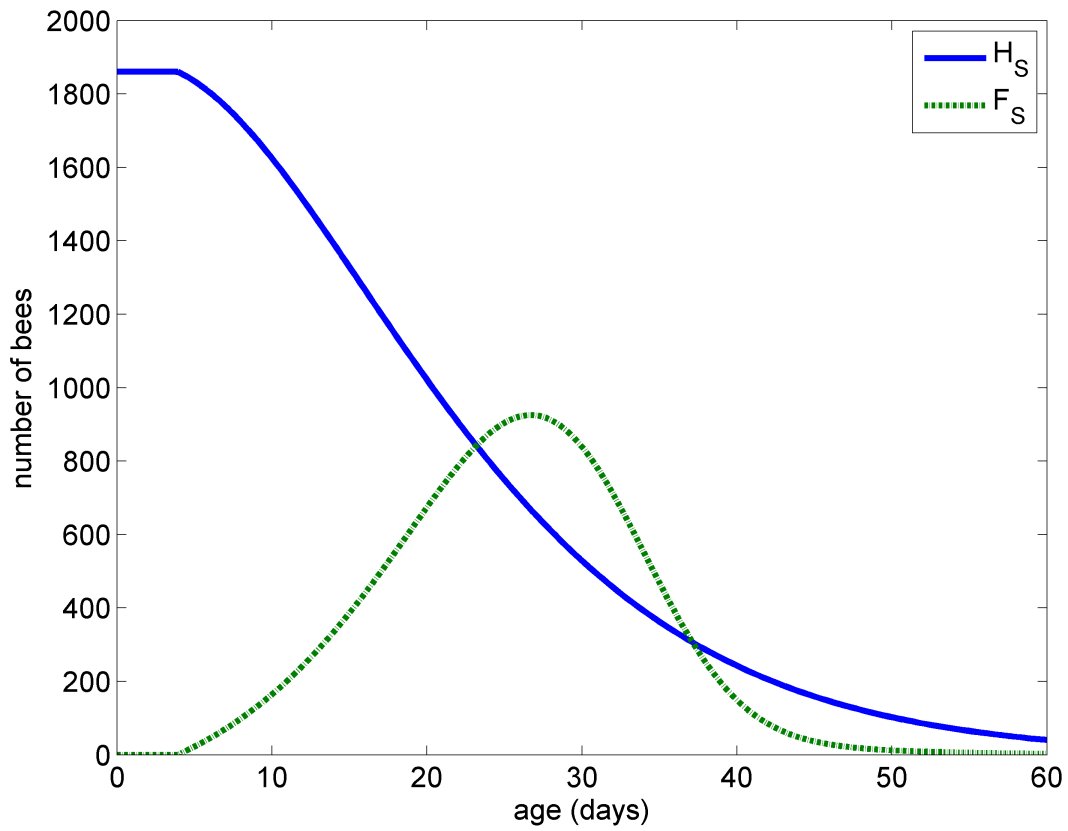


Figure A.2: Age distribution of a healthy colony at equilibrium during the active season, based on the natural death rate, $\mu(a)$ presented in Figure 1.

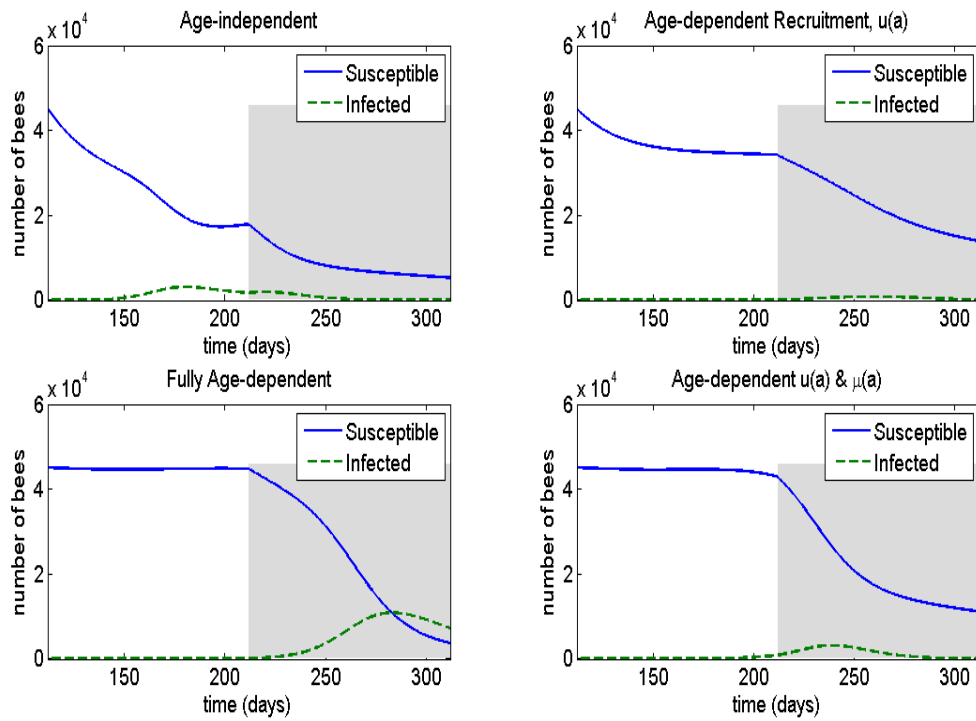


Figure A.3: Population dynamics with increasing effects of age-dependent parameters: clockwise from top-left (age-independent model) to bottom-left (fully age-dependent model).

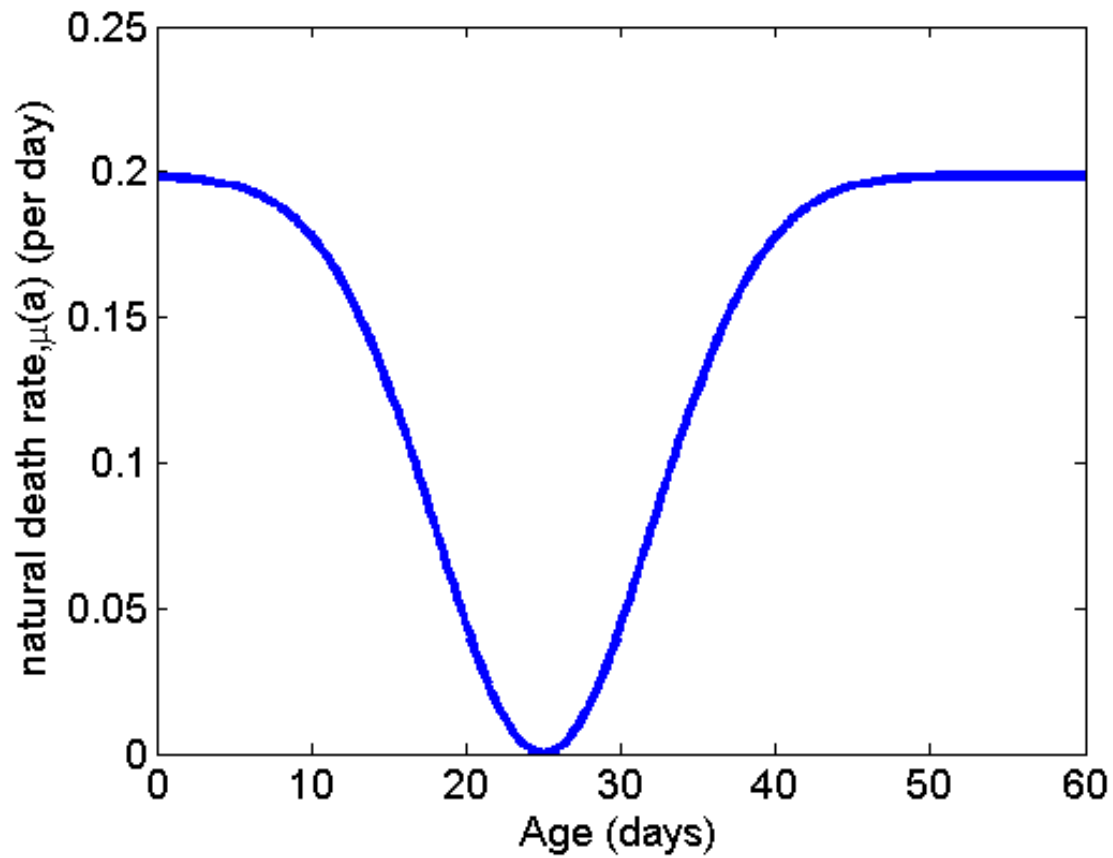


Figure A.4: An inverted Gaussian natural death rate, $\mu(a) = Ae^{-(a-25)^2/B}$ where A and B are chosen such that the average death rate is $\mu_{avg} = 0.14$ per day. Results based on this death rate are shown below.

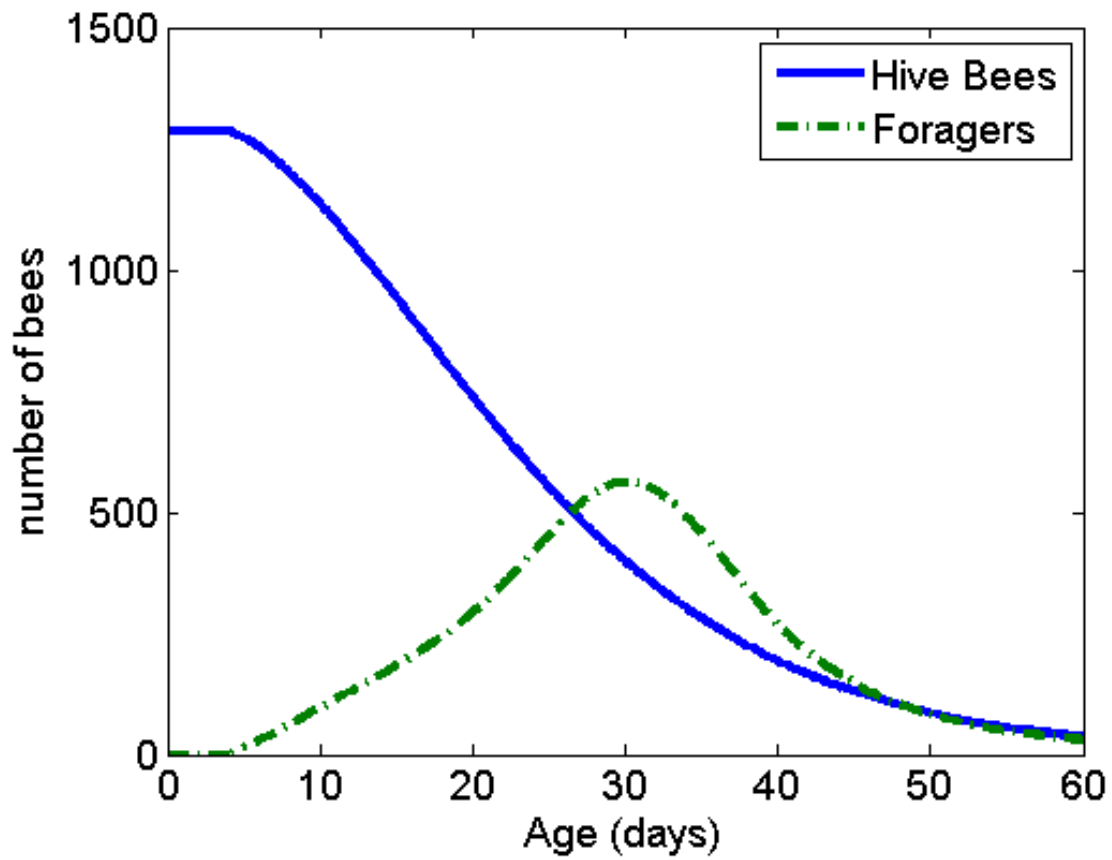


Figure A.5: Equilibrium age distribution of healthy colony under the natural death rate shown in Figure A.4.

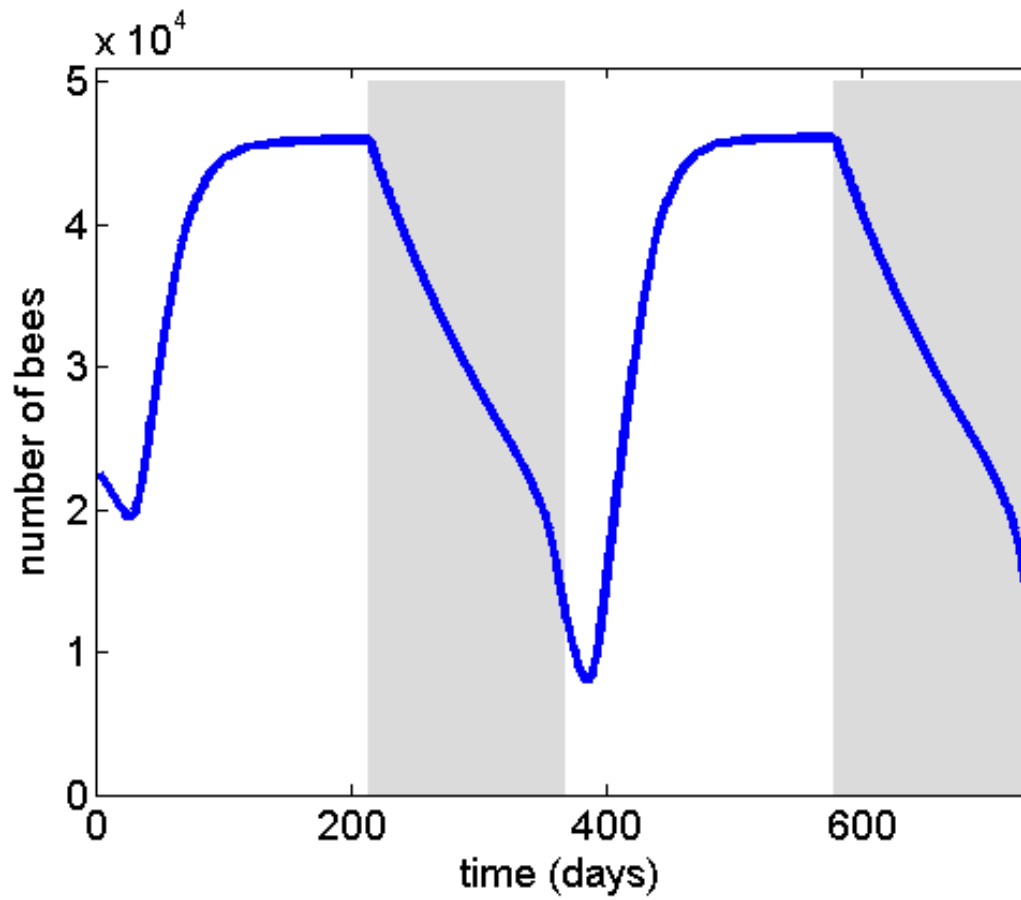


Figure A.6: Time course of disease-free colony based on natural death rate $\mu(a)$ shown in Figure A.4.

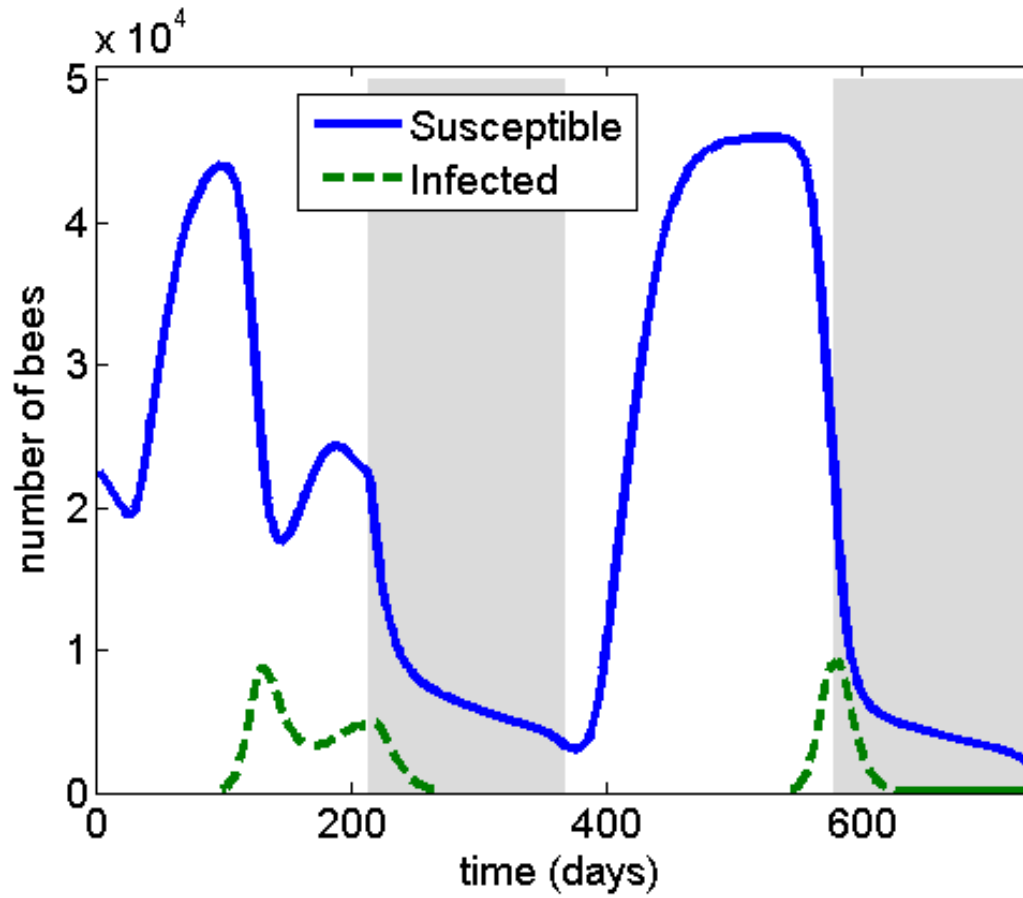


Figure A.7: Time course of infected colony based on natural death rate $\mu(a)$ shown in Figure A.4 and a constant disease death rate $d(a) = d = 0.14$ per day.

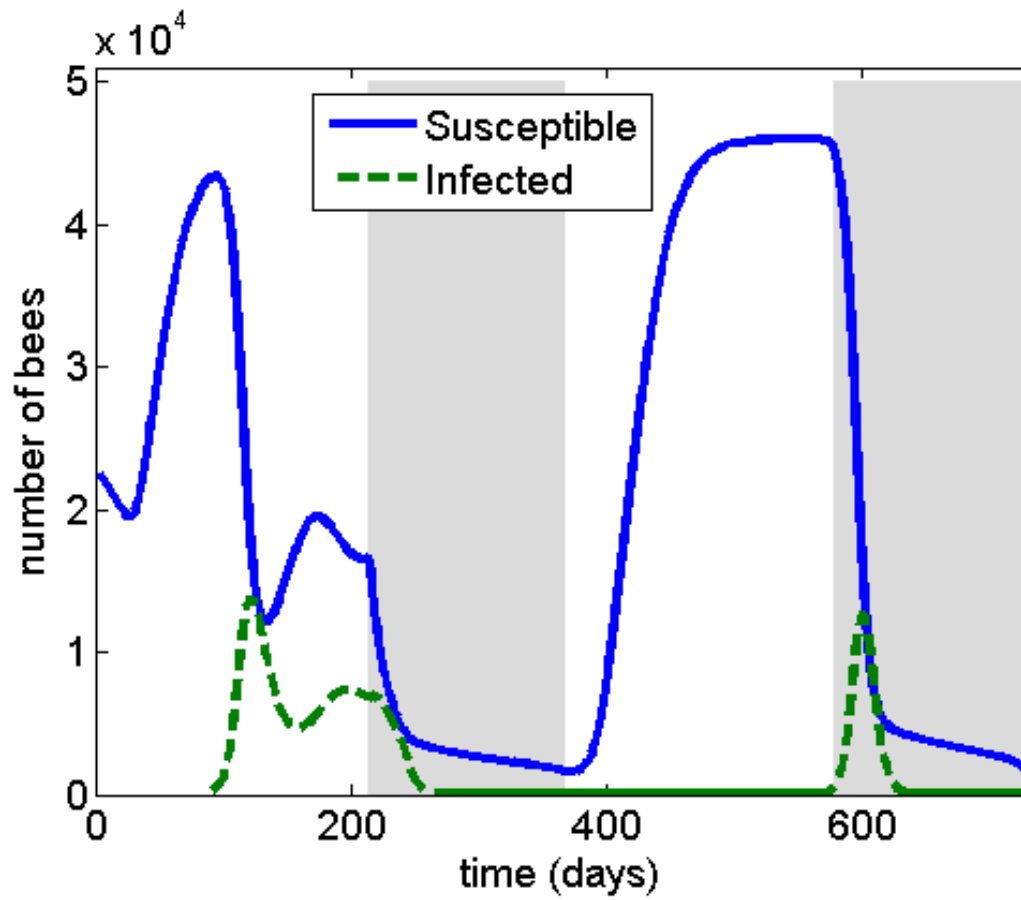


Figure A.8: Time course of infected colony based on natural death rate $\mu(a)$ shown in Figure A.4 and a disease death rate $d(a) = \mu(a)$.

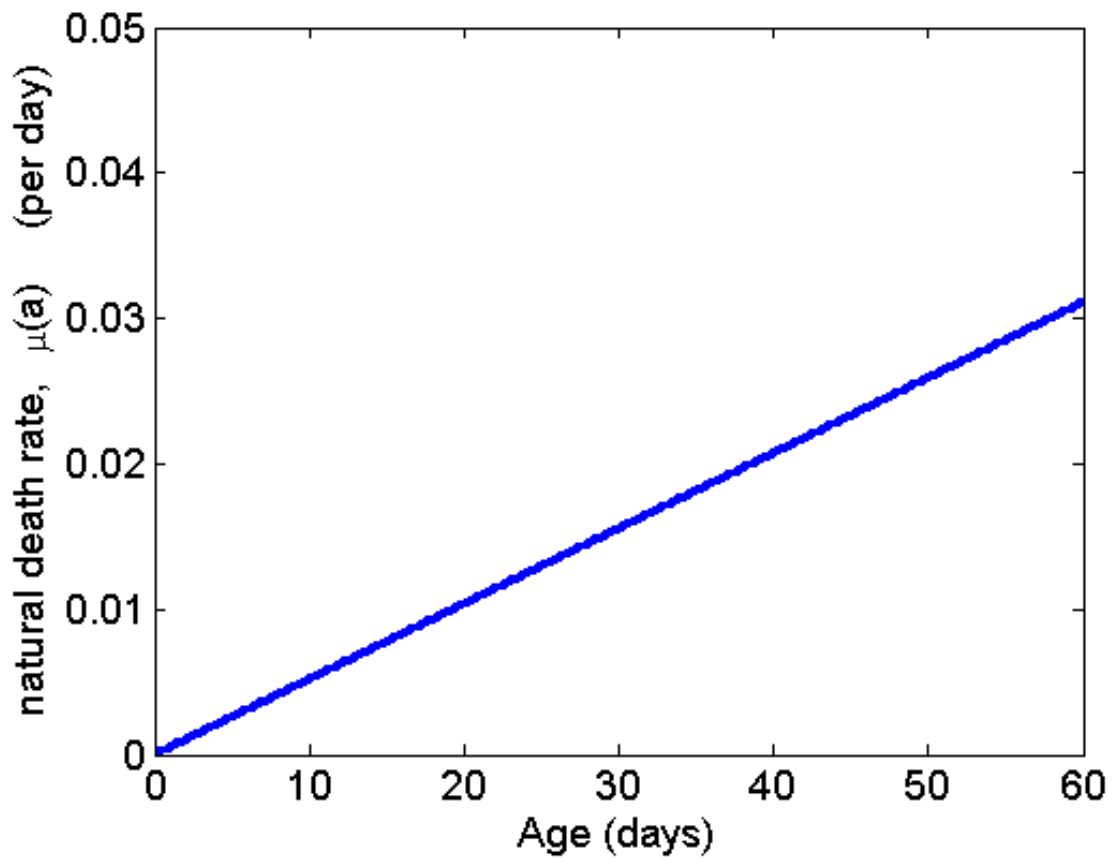


Figure A.9: An admittedly unrealistic linear natural death rate $\mu(a) = Aa$ where A is chosen so once again the average is 0.14 per day. We show this death rate to illustrate that the qualitative results of our model hold in even with drastically different parameter choices.

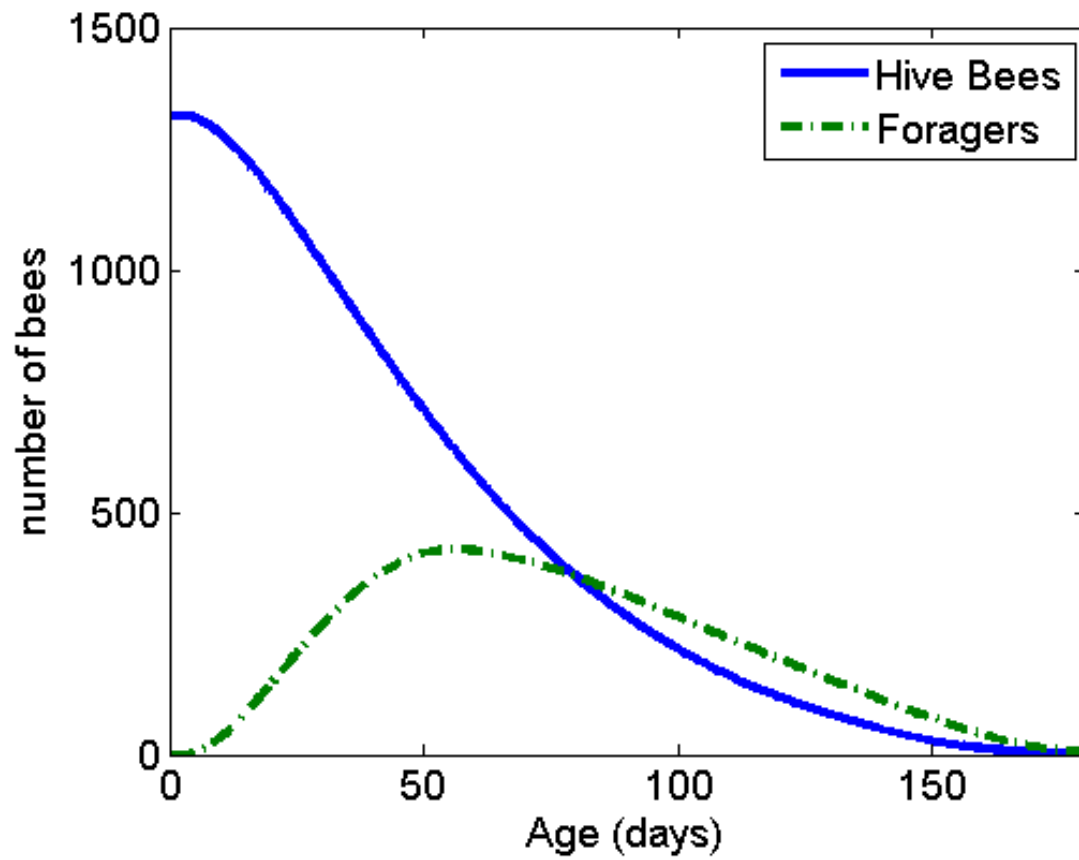


Figure A.10: Equilibrium age distribution of healthy colony under the natural death rate shown in Figure A.9. Note that the linear death rate leads to an unrealistically long lifespan.

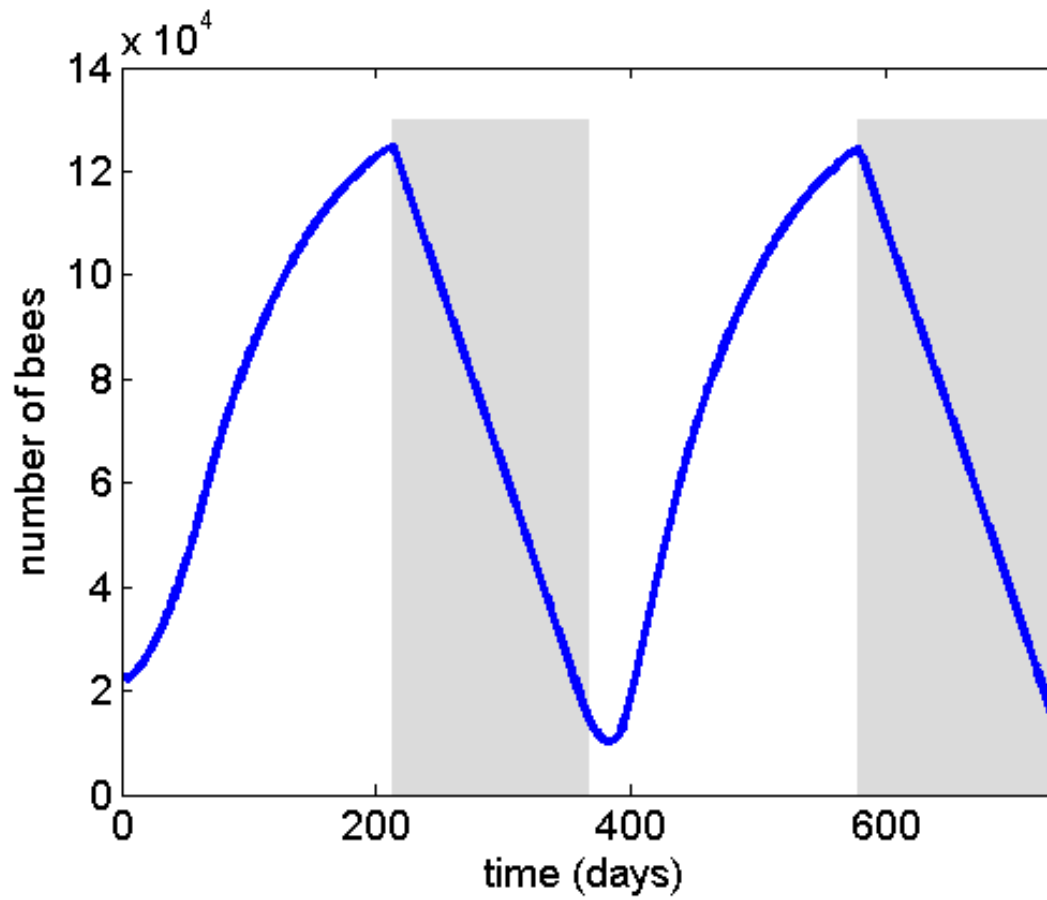


Figure A.11: Time course of disease-free colony based on natural death rate $\mu(a)$ shown in Figure A.9. Despite the unrealistically large colony size and absurdly long lifetime of a bee, we still observe the spring dwindle as a natural phenomena.

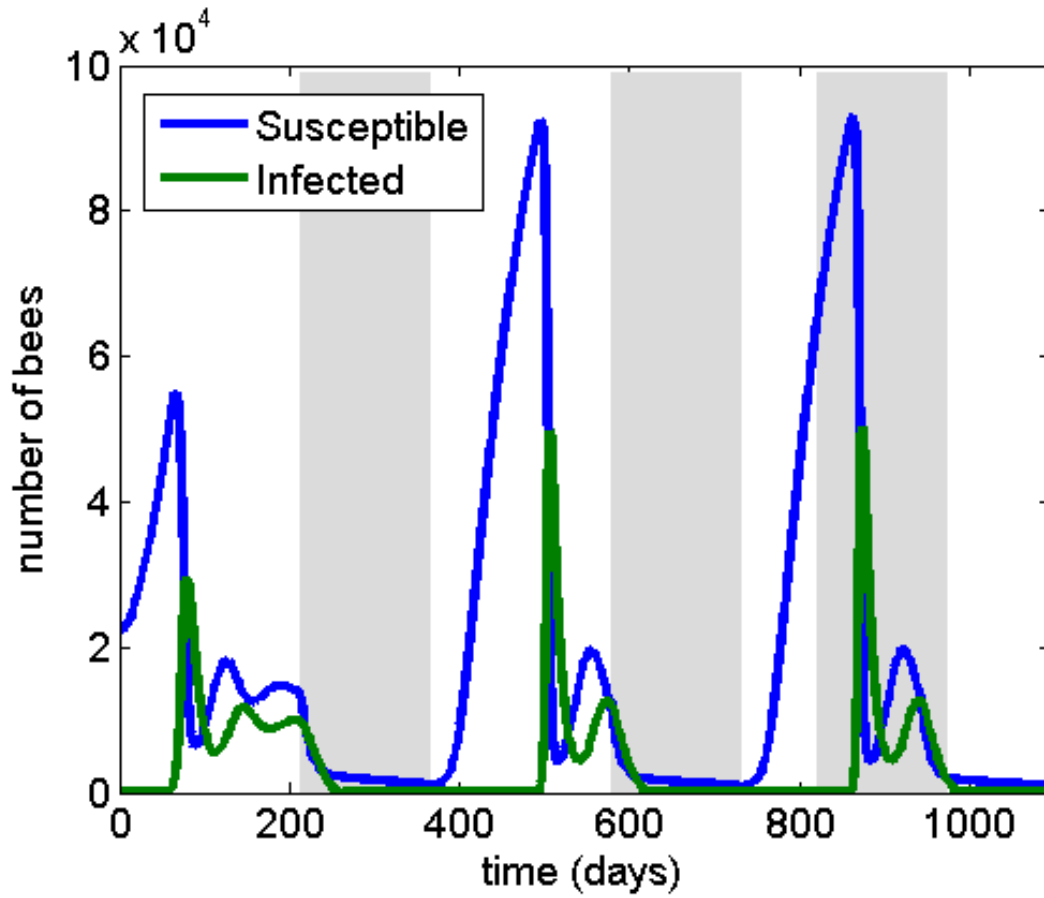


Figure A.12: Time course of infected colony based on natural death rate $\mu(a)$ shown in Figure A.9 and a Gaussian disease-related death rate, $d(a)$. Note that the infection continues to spike years after the initial infection.

Bibliography

- [1] R. DUKAS, *Mortality rates of honey bees in the wild*, *Insectes Sociaux*, 55 (2008), pp. 252–255.
- [2] S. FAHRBACH AND G. ROBINSON, *Juvenile hormone, behavioral maturation and brain structure in the honey bee*, *Developmental Neuroscience*, 18 (1996), pp. 102–114.
- [3] M. GOBLIRSCH, Z. Y. HUANG, AND M. SPIVAK, *Physiological and behavioral changes in honey bees (*Apis mellifera*) induced by *Nosema ceranae* infection*, *PLOS ONE*, 8 (2013), p. e58165.
- [4] D. S. KHOURY, A. B. BARRON, AND M. R. MYERSCOUGH, *Modelling food and population dynamics in honey bee colonies*, *PLOS ONE*, 8 (2013), p. e59084.
- [5] D. S. KHOURY, M. R. MYERSCOUGH, AND A. B. BARRON, *A quantitative model of honey bee colony population dynamics*, *PLOS ONE*, 6 (2011), p. e18491.
- [6] S. RUSSELL, A. B. BARRON, AND D. HARRIS, *Dynamic modelling of honey bee (*Apis mellifera*) colony growth and failure*, *Ecological Modelling*, 265 (2013), pp. 158 – 169.
- [7] S. SAKAGAMI AND H. FUKUDA, *Life tables for worker honeybees*, *Researches on Population Ecology*, 10 (1968), pp. 127–139.

Curriculum Vitae

Matthew Betti, Ph.D.

Areas of specialization

Mathematical Biology, Epidemiology, Population Dynamics, Partial Differential Equations.

Education

- 2006–2010 BSc in Mathematics and Physics, McMaster University, Hamilton, ON
- 2010–2012 MSc in Mathematics, McMaster University, Hamilton, ON
- 2013–2017 PhD in Applied Mathematics, Western University, London, ON

Grants, Honors and Awards

- 2014–2017 NSERC PGS, NSERC
- 2016–2017 Doctoral Research Excellence Research Award, Western University
- 2016 Best Graduate Talk, Ontario Ecology, Evolution and Ethology Conference
University of Toronto
- 2015 Fallona Family Interdisciplinary Poster Session - First Place, Western University
- 2015 Graduate Student Teaching Award, Faculty of Science, Western University
- 2015 Graduate Student Teaching Award, School of Graduate and Postdoctoral Studies,
Western University
- 2009 Dr. Harry Lyman Hooker Scholarship, McMaster University
- 2006–2010 Entrance Scholarship, McMaster University

Publications

REFEREED JOURNAL ARTICLES

- 2009 Wilson, Patrick R, Roschuk, Tyler, Dunn, Kayne, Betti, Matthew, Wojcik, Jacek and Mascher, P (2009), “The Influence of Structural Ordering on Luminescence from Nitride-and Oxynitride-Passivated Silicon Nanoclusters”, *ECS Transactions* 19:8 19–28
- 2013 Sprung, DWL, Betti, MI and van Dijk, W(2013), “Finite Fourier transforms computed by a modified Filon–Euler–Maclaurin method” *Computer Physics Communications*, 184:3 607-616
- 2013b Betti, Matthew and Pelinovsky, Dmitry E (2013), “Periodic traveling waves in diatomic granular chains”, *Journal of Nonlinear Science* 23:5 689–730.
- 2014 Betti, Matt I, Wahl, Lindi M and Zamir, Mair (2014), “Effects of infection on honey bee population dynamics: a model”, *PLoS one* 9:10 e110237.
- 2016 Betti, Matt I, Wahl, Lindi M and Zamir, Mair (2016), “Reproduction Number And Asymptotic Stability For The Dynamics of a Honey Bee Colony with Continuous Age Structure”, *Bull. of Math. Bio.* 79(7) 1586-1611.
- 2016 Betti, Matt I, Wahl, Lindi M and Zamir, Mair (2016), “Age structure is Critical to the Population Dynamics and Survival of Honey Bee Colonies”, *Royal Society Open Science* 3:11 160444.
- 2017 Betti, Matt I, LeClair, Josh, Wahl, Lindi M and Zamir, Mair (2016), “Bee++: An Object-Oriented, Agent-Based Simulator for Honey Bee Colonies”, *Insects* 8(1):31; doi:10.3390/insects8010031
- 2017 Betti, Matt I, LeClair, Josh, Wahl, Lindi M and Zamir, Mair (2016), “ A closed form next generation operator for reaction-diffusion systems and the connection between discrete and continuum disease models”, *In review*

TALKS AND POSTERS

- 2012 Betti, Matthew and Pelinovsky, Dmitry E (2012), “Periodic Travelling Waves in Diatomic Granular Chains”, *SIAM Annual Meeting*, Seattle
- 2015 Betti, Matthew I, Wahl, Lindi M and Zamir, Mair (2015), “Population Dynamics and Infections in Honey Bees”, *CAIMS Annual Meeting*, Waterloo
- 2015 Betti, Matthew I, Wahl, Lindi M and Zamir, Mair (2015), “Age Before Bee-auty: An Age-structured Honey Bee model”, *ICMA-V*, London
- 2015 Betti, Matthew I, Wahl, Lindi M and Zamir, Mair (2015), “Temperature, Disease and the Death of Honey Bees”, *Fallona Family Interdisciplinary Symposium*, London
- 2016 Betti, Matthew I, Wahl, Lindi M and Zamir, Mair (2016), “Effects of Infection on Honey Bee Population Dynamics”, *Ontario Ecology, Evolution and Ethology Conference*, Toronto
- 2016 Betti, Matthew I, Wahl, Lindi M and Zamir, Mair (2016), “Population Dynamics and Infections in Honey Bees”, *CAIMS Annual Meeting*, Edmonton
- 2017 Betti, Matthew I, Wahl, LeClair, Josh, Lindi M and Zamir, Mair (2017), “Honey

- bees in Silica”, *Fallona Family Interdisciplinary Symposium*, London
- 2017 Betti, Matthew I, LeClair, Josh, Wahl, Lindi M and Zamir, Mair (2017), “ A Novel Closed-Form Next Generation Operator for Reaction-Diffusion Systems and A Natural Environment For Modeling Movement” *AMMCS International Meeting*, Waterloo

INVITED TALKS

- 2015 Betti, Matthew I, Wahl, Lindi M and Zamir, Mair (2015), “Honey Bee Population Dynamics in the Presence of Infection”, *Southern Ontario Bee Conference*, Toronto
- 2015 Betti, Matthew I, Wahl, Lindi M and Zamir, Mair(2015), “Effects of Infection on Honey Bee Population Dynamics”, *Ontario Ecology, Evolution and Ethology Conference*, Toronto
- 2016 Betti, Matthew I (2016), “The Calculus of Honey Bees”, *Western Biology Undergraduate Soceity Seminar*, London
- 2017 Betti, Matthew I, LeClair, Josh, Wahl, Lindi M and Zamir, Mair (2017), “Modeling honey bee-plant symbiosis in the presence of environmental toxins”, *AAAS Annual Meeting*, Boston
- 2017 Betti, Matthew I, LeClair, Josh, Wahl, Lindi M and Zamir, Mair (2017), “ The Symbiotic Relationship of Mathematics and Biology”, *Undergraduate Conference of Mathematical Sciences*, London (Plenary Speaker)
- 2017 Betti, Matthew I, LeClair, Josh, Wahl, Lindi M and Zamir, Mair (2017), “Mathematical Biology: Why Math Can Be Useful”, *SHAD Western, Summer Program*, London
- 2017 Betti, Matthew I, LeClair, Josh, Wahl, Lindi M and Zamir, Mair (2017), “Honey bee dynamics in an ever-changing environment”, *SMB Annual Meeting*, Salt Lake City

PRESS

- 2015 Wain, Jennifer (April 2, 2015), “Calculating a new version of pi(e)” *Western News*
- 2015 (April 22, 2015), “Can Math Save the Honeybees?”, *Toronto/Vancouver Metro*
- 2015 (April 23, 2015), “Afternoon Drive”, *CBC Radio One*
- 2015 Montanini, Chris (April 30, 2015), “How math can help us understand bee colony collapse”, *The Londoner*.
- 2017 Buck, Genna (March 16, 2017), “Canadian mathematicians create Sims-like program to save bees”, *Toronto Metro News*.

Teaching

- 2008-2010 Teaching Assistant, *Introduction to Electrostatics*, Department of Physics, McMaster University.
- 2010 Teaching Assistant, *Multivariate Calculus*, Department of Mathematics Statistics, McMaster University

- 2011 Teaching Assistant, *Advanced Mathematics for Engineers (PDEs and Probability)*, Department of Mathematics Statistics, McMaster University
- 2011 Teaching Assistant, *Multivariate Calculus*, Department of Mathematics Statistics, McMaster University
- 2012 Teaching Assistant, *Multivariate Calculus*, Department of Mathematics Statistics, McMaster University
- 2012 Instructor, *Mathematics*, Department of Mathematics, Humber College
- 2013 Teaching Assistant, *Partial Differential Equations for Engineers*, Department of Applied Mathematics, Western University
- 2014 Teaching Assistant, *Advanced Partial Differential Equations*, Department of Applied Mathematics, Western University
- 2014 Teaching Assistant, *Ordinary Differential Equations*, Department of Applied Mathematics, Western University
- 2015 Teaching Assistant, *Differential Equations Probability for Life Sciences*, Department of Applied Mathematics, Western University
- 2015 Teaching Assistant, *Ordinary Differential Equations for Engineers*, Department of Applied Mathematics, Western University
- 2016 Teaching Assistant, *Differential Equations Probability for Life Sciences*, Department of Applied Mathematics, Western University
- 2016 Teaching Assistant, *Ordinary Differential Equations for Engineers*, Department of Applied Mathematics, Western University
- 2017 Instructor, *Vector Calculus for Engineers*, Department of Applied Mathematics, Western University

Software Packages

- 2016 *Bee++*: A comprehensive, open source simulator for honey bee dynamics over spatially explicit landscapes.